SCHOOL OF
CIVIL ENGINEERING

INDIANA
DEPARTMENT OF HIGHWAYS

JOINT HIGHWAY RESEARCH PROJECT

FHWA/IN/JHRP-86/7

Final Report

DRILLED PIERS USED FOR SLOPE STABILIZATION

M. W. Oakland
J. L. Chameau

PURDUE UNIVERSITY

JOINT HIGHWAY RESEARCH PROJECT

FHWA/IN/JHRP-86/7

Final Report

DRILLED PIERS USED FOR SLOPE STABILIZATION

M. W. Oakland
J. L. Chameau

Final Report

DRILLED PIERS USED FOR SLOPE STABILIZATION

TO: Harold L. Michael, Director
Joint Highway Research Project

March 27, 1986
Revised September 12, 1986
Project: C-36-360

FROM: J. L. Chameau
Joint Highway Research Project

File: 6-14-15

Please find enclosed a Final Report entitled "Drilled Piers Used for Slope Stabilization" by M. W. Oakland and J. L. Chameau. This is the final report on the HPR project entitled "Design of Laterally Loaded Drilled-in-Piers for Landslide Correction Anchored within Sedimentary Rocks". It complements the interim report entitled "Stabilization of Slopes Using Piles" by Hassiotis and Chameau (1984).

The report presents a three dimensional finite element model for slopes stabilized by drilled piers which are socketed in bedrock. The computer program is able to model construction sequences, the interaction between the piers and soil, weak seams in the soil profile, and remolded areas around the piers. The primary output of the program is composed of displacement, strain and stress fields. The stresses are used in a post processing analysis to estimate the factor of safety of the slope.

Two two analysis packages which were developed during this research project complement each other. The 2-D approach presented in the interim report provides "easy to use" programs which are applicable to many conditions for designing the piles or piers and estimating the safety factor of the slope. The 3-D approach can be used to determine stresses and deformations in the soil, and to assess the safety of the slope for more complex situations such as cases involving construction sequences or surface loads.

This report is presented for review and approval as evidence of partial fulfillment of the objectives of this project.

Respectfully submitted,

J. L. Chameau
Associate Professor of
Civil Engineering

cc:

A.G. Altschaeffl	D.E. Hancher	K.M. Mellinger	J.R. Skinner
J.M. Bell	J.A. Havers	R.D. Miles	C.A. Venable
M.E. Cantrall	K.R. Hoover	P.L. Owens	E.W. Walters
W.F. Chen	M.K. Hunter	B.K. Partridge	T.D. White
Sidney Diamond	J.P. Isenbarger	G.T. Satterly	L.E. Wood
W.L. Dolch	G.A. Leonards	C.F. Scholer	
R.L. Eskew	R.H. Lucas	L.R. Scott	
J.D. Fricker	J.F. McLaughlin	K.C. Sinha	

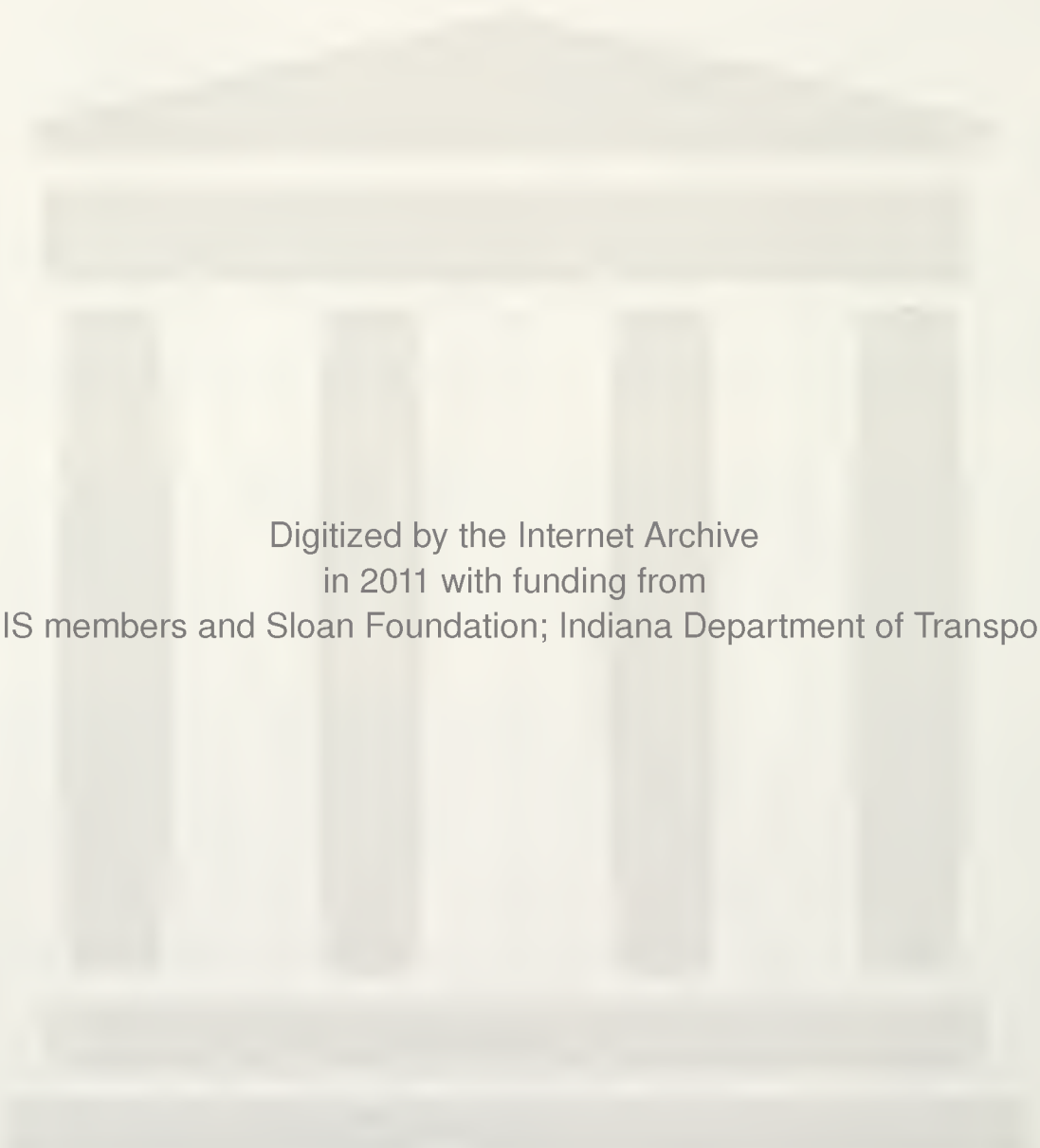

Final Report

DRILLED PIERS USED FOR SLOPE STABILIZATION

by

M. W. Oakland
Graduate Research Assistant

J. L. Chameau
Associate Professor of Civil Engineering

Joint Highway Research Project

Project No.: C-36-360

File No.: 6-14-15

Prepared as Part of an Investigation

Conducted by

Joint Highway Research Project
Engineering Experiment Station
Purdue University

in cooperation with

Indiana Department of Highways

and the

U.S. Department of Transportation
Federal Highway Administration

Purdue University
West Lafayette, Indiana
March 27, 1986
Revised September 12, 1986

TECHNICAL REPORT STANDARD TITLE PAGE

1. Report No.	2. Government Accession No.	3. Recipient's Catalog No.
FHWA/IN/JHRP-86/7		

4. Title and Subtitle	5. Report Date
Drilled Piers Used for Slope Stabilization	March 27, 1986 Revised September 12, 1986
	6. Performing Organization Code

7. Author(s)	8. Performing Organization Report No.
M. W. Oakland and J. L. Chameau	JHRP-86-7

9. Performing Organization Name and Address	10. Work Unit No.
Joint Highway Research Project Civil Engineering Building Purdue University West Lafayette, IN 47907	11. Contract or Grant No. HPR-1(24), Part II
	13. Type of Report and Period Covered
12. Sponsoring Agency Name and Address Indiana Department of Highways State Office Building 100 N. Senate Avenue Indianapolis, IN 46204	Final Report
	14. Sponsoring Agency Code

15. Supplementary Notes

Prepared in cooperation with the U.S. Department of Transportation, Federal Highway Administration. Study title is "Design of Laterally Loaded Drilled-In Piers for Landslide Correction Anchored Within Sedimentary Rocks."

16. Abstract

A three dimensional model for slopes stabilized by drilled piers has been developed. This model includes provisions for mesh generation, finite element analysis and stability analysis. The finite element analysis involves nonlinear soil behavior, construction sequences and remolded surfaces around the piers. A two dimensional, limiting equilibrium analysis uses the stress field output from the finite element model to estimate the factor of safety of the slope.

A number of cases are explored to give insight into the slope/pier interaction mechanisms, and to evaluate the efficiency of the piers as retaining structures. Several conditions have been considered during the course of this study: surcharge loading, excavation, cutslope and self weight loading.

The soil arching was found to provide an effective barrier against soil movement even though the piers do not form a continuous wall. The piers add lateral support to a stressed slope, however, a significant amount of soil support is also found to be provided in clay soils by the vertical support of the piers.

17. Key Words	18. Distribution Statement
Piers; Piles; Slope Stability; Reinforcement; finite element method	No restrictions. This document is available to the public through the National Technical Information Service, Springfield, VA 22161

19. Security Classif. (of this report)	20. Security Classif. (of this page)	21. No. of Pages	22. Price
Unclassified	Unclassified	305	

Form DOT F 1700.7 (8-69)

ACKNOWLEDGMENTS

The financial support for this research was provided by The Indiana Department of Highways and The Federal Highways Administration. The research was administered through The Joint Highway Research Project, Purdue University, West Lafayette, Indiana.

Professors C. William Lovell, W. F. Chen, Terry R. West and David A. Dunavant served on the first author's Ph.D. committee. Their help in reviewing the manuscript is greatly appreciated.

The authors would also like to recognize Sophia Hassiotis who conducted a parallel study on this research project.

TABLE OF CONTENTS

LIST OF TABLES

LIST OF FIGURES

LIST OF ABBREVIATIONS AND SYMBOLS

A_n: hyperelastic model constants

AASHTO: American Association of State Highway and Transportation Officials

B: element width

B_n: hyperelastic model constants

C: elasticity matrix

D: Duncan-Chang model constant

E: modulus of elasticity (Young's modulus)

E_i: initial modulus of elasticity

E_p: plastic modulus of elasticity

E_r: range of modulus of elasticity

E_t: tangent modulus of elasticity

E_{ur}: unload-reload modulus of elasticity

F: Duncan-Chang model constant

F_h: horizontal nodal load

F_v: vertical nodal load

FE: finite element

G: shear modulus or Duncan-Chang model constant

G_{max}: maximum shear modulus

G_s: secant shear modulus

H_n: horizontal span across element

I:	bending moment of inertia
J_i:	effective stress invariants
K:	bulk modulus or Duncan-Chang model constant
K_b:	modified Duncan-Chang model constant
K_o:	initial stress ratio
K_t:	tangent bulk modulus
K_{ur}:	Duncan-Chang model constant
L:	length
M:	constrained modulus
P_a:	atmospheric pressure
R_f:	Duncan-Chang model constant
RC:	relative compaction
V_n:	vertical span across element
W:	strain energy density function
a:	Hardin model constant or pier stiffness matrix
a_i:	spline function constants
b_i:	spline function constants
c:	cohesion
c_i:	spline function constants
d:	nodal displacements
d_c:	nodal displacements at constrained degrees of freedom
d_i:	spline function constants
d_u:	nodal displacements at unconstrained degrees of freedom
deg:	degrees
dia.	diameter

ft: foot

h: depth below surface

h_i: strain difference

in: inches

k: kilopounds

lbs: pounds

m: modified Duncan-Chang model constant or Ramberg-Osgood model constant

mm: millimeter

n: Duncan-Chang model constant

p: Ramberg-Osgood model constant or Richard and Abbott model constant

pcf: pounds per cubic foot

psf: pounds per square foot

psi: pounds per square inch

q: extended Hardin model constant

r: nodal forces

r_c: nodal forces at constrained degrees of freedom

r_u: nodal forces at unconstrained degrees of freedom

sk_{cc}: totally constrained stiffness matrix

$sk_{uc} = sk_{cu}$: partially constrained stiffness matrix

sk_{uu}: totally unconstrained stiffness matrix

t: element thickness

w: element width

x: global coordinate

x_1: length of toe

x_2: distance from toe to pier

x_3: distance from pier to crest

x_4: length of crest

y: global coordinate

y_1: depth to foundation under toe

y_2: depth to foundation at the pier

y_3: depth to foundation under crest

z: global coordinate

Δ: change in

Ω: complimentary energy density function

α: angle of slope

$\gamma = \gamma_m$: unit weight of soil or accumulated shear strain

δ: kronecker function or partial derivative

ε: strain or local coordinate direction

$\dot{\varepsilon}$: strain rate

ε_1: major principle strain

ε_a: axial strain

ε_f: final strain

ε_i: initial strain

ε_v: volumetric strain

ζ: local coordinate direction

η: local coordinate direction

λ: Lame parameter

ν: Poisson's ratio

ν_{max}: Poisson's ratio at failure

ν_{min}: Poisson's ratio at zero strain

ν_s: secant Poisson's ratio

ν_t: tangent Poisson's ratio

σ: stress vector or normal stress

σ': effective stress

$\dot{\sigma}$: stress rate

σ_1: major principle stress

σ_3: minor principle stress

$\sigma_1 - \sigma_3$: deviator stress

$(\sigma_1 - \sigma_3)_f$: deviator stress at failure

$(\sigma_1 - \sigma_3)_{ult}$: ultimate deviator stress

σ_f: final stress

σ_i: initial stress

σ_m: Ramberg-Osgood stress constant

σ_x horizontal normal stress

σ_y: yield stress or vertical normal stress

τ: shear stress

τ_m: maximum shear stress

τ_{xy}: vertical or horizontal shear stress

ϕ: friction angle

ϕ_o: initial friction angle

ψ: error in strain

HIGHLIGHT SUMMARY

Large diameter drilled piers discretely placed so that some clear space exists between the piers can take advantage of the arching action of the soil to form a continuous barrier. The drilled piers improve the stability of the slope in two ways: by transmission of the driving stresses to more stable foundation layers, and by redistribution of the stress patterns in the slope.

A three dimensional model for slopes stabilized by drilled piers has been developed for this study. This model includes provisions for mesh generation, finite element analysis and stability analysis. The finite element analysis involves nonlinear soil behavior, construction sequences and remolded surfaces around the piers. A two dimensional, limiting equilibrium analysis uses the stress field output from the finite element model to estimate the factor of safety of the slope.

A number of cases are explored to give insight into the slope/pier interaction mechanisms, and to evaluate the efficiency of the piers as retaining structures. Several conditions have been considered during the course of this

study: surcharge loading, excavation, cutslope and self weight loading.

The soil arching was found to provide an effective barrier against soil movement even though the piers do not form a continuous wall. The piers added lateral support to a stresses slope as has been the commonly used situation of these piers in practice. However, a significant amount of soil support was also found to be provided in clay soils by the vertical support of the piers. Previous studies have found the piers to be ineffective if allowed to rotate. This study examines cases of piers firmly socketted in bedrock or stiff foundation materials. Other constraints, such as tiebacks and caps, which ease the structural demands on the piers, can also be modelled. In general, the effectiveness of the piers increases for increased pier stiffness, increased pier diameter and decreased pier spacing. The position of the piers in the slope can be related to the failure mode with a trade-off between overall stability and volume of the slide. In general, the optimum position of the piers is at the point of maximum displacement for the unreinforced case.

CHAPTER 1: INTRODUCTION

During the past two decades innovative soil reinforcement techniques, such as reinforced earth, stone columns, soil anchors and cast-in-place piers have been developed to solve many slope stability problems. These techniques, when compared to the more traditional building of berms and/or dewatering, can provide cost-effective solutions for a variety of situations. In Sweden, battered timber piles are used to increase the slope stability in very soft clays (figure 1.1). The angle of the piles allows them to act partially in compression rather than relying totally on their shear strength. Steel pipe piles have been used for the same purpose in Japan (Taniguchi, 1967). Large diameter cast-in-place reinforced concrete piers have been used to stabilize active landslide areas in stiff clays and shales through dowel action (Merriam, 1960; Andrews and Klasell, 1964; Bulley, 1965; Gould, 1970; Offenberger, 1981; Mathis, 1981; De Paepe and Wallays, 1984; Leadbeater, 1985; Gudehus and Schwarz, 1985). The diameters of these piers can be as large as 1.5 meters (figure 1.2). These piers have often been used side by side to form a continuous wall. The Fondedile reticulated root pile method (figure 1.3) takes

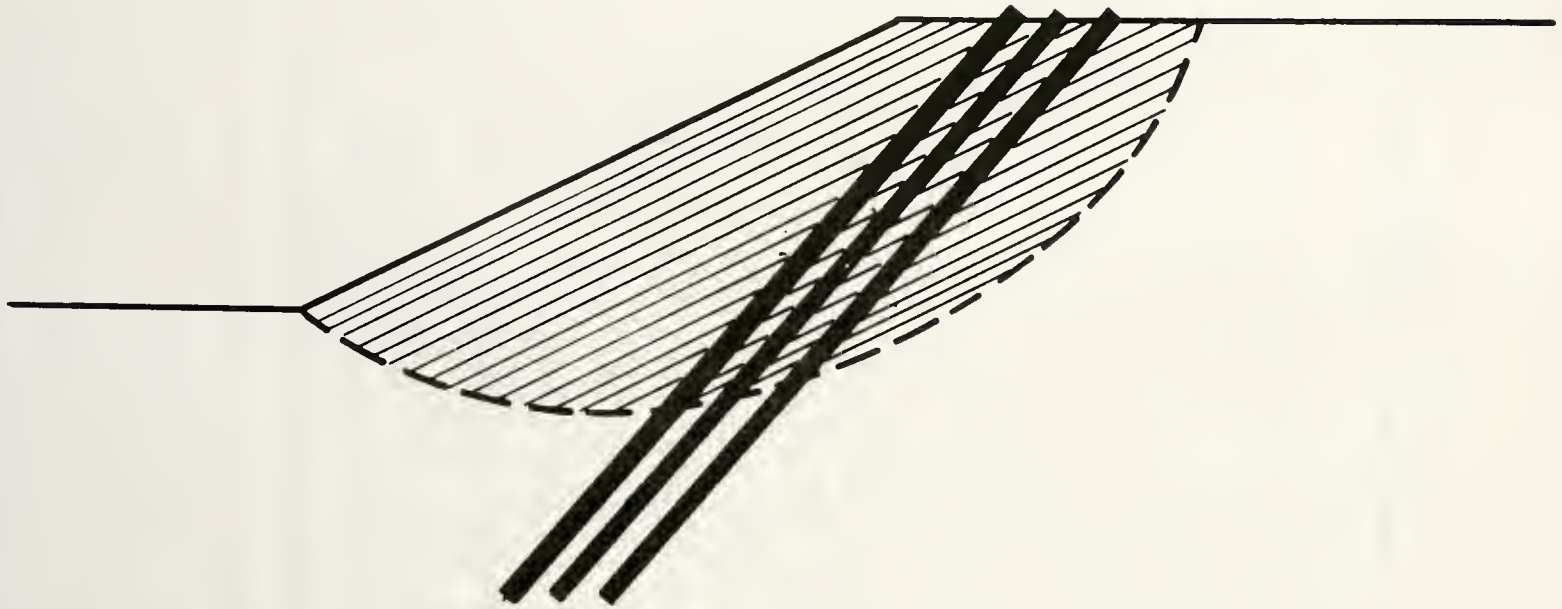

Figure 1.1: Battered Timber Piles Used to Stabilize Slopes

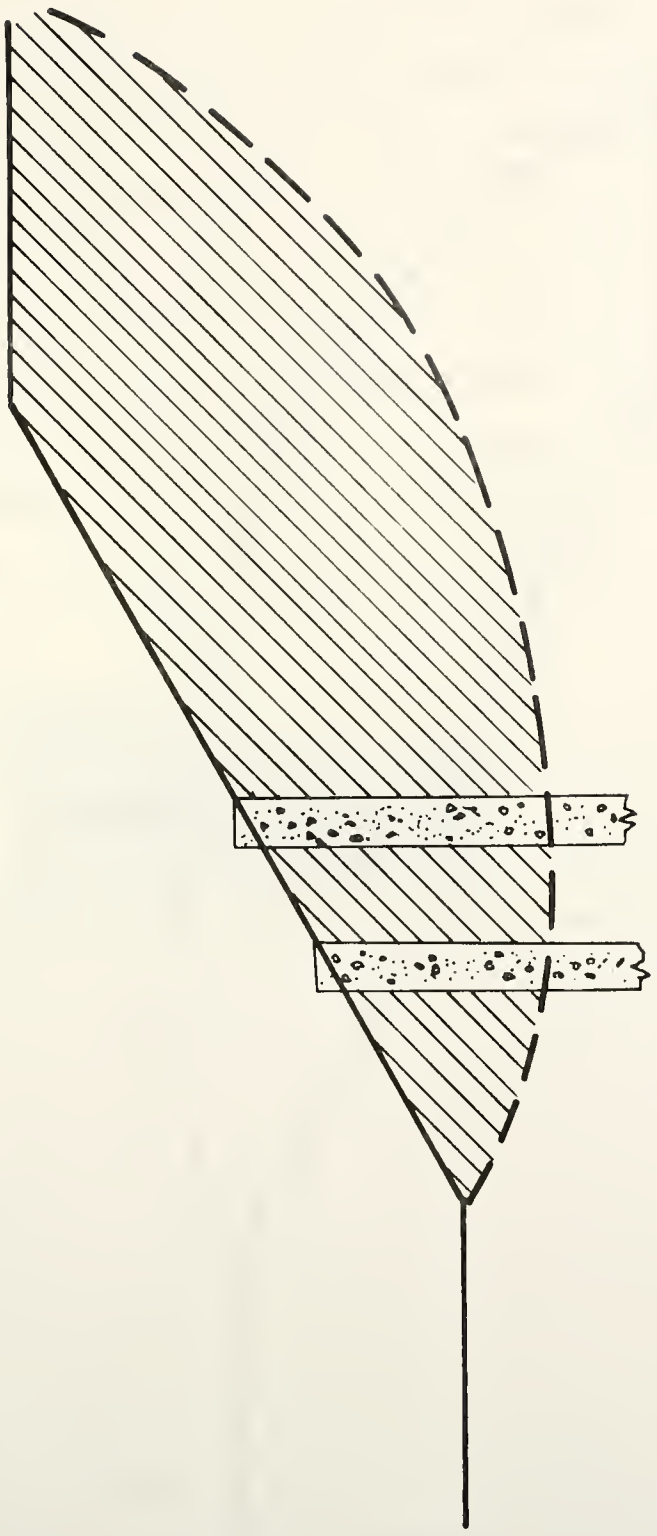

Figure 1.2: Reinforced Concrete Piers Used to Stabilize Slopes

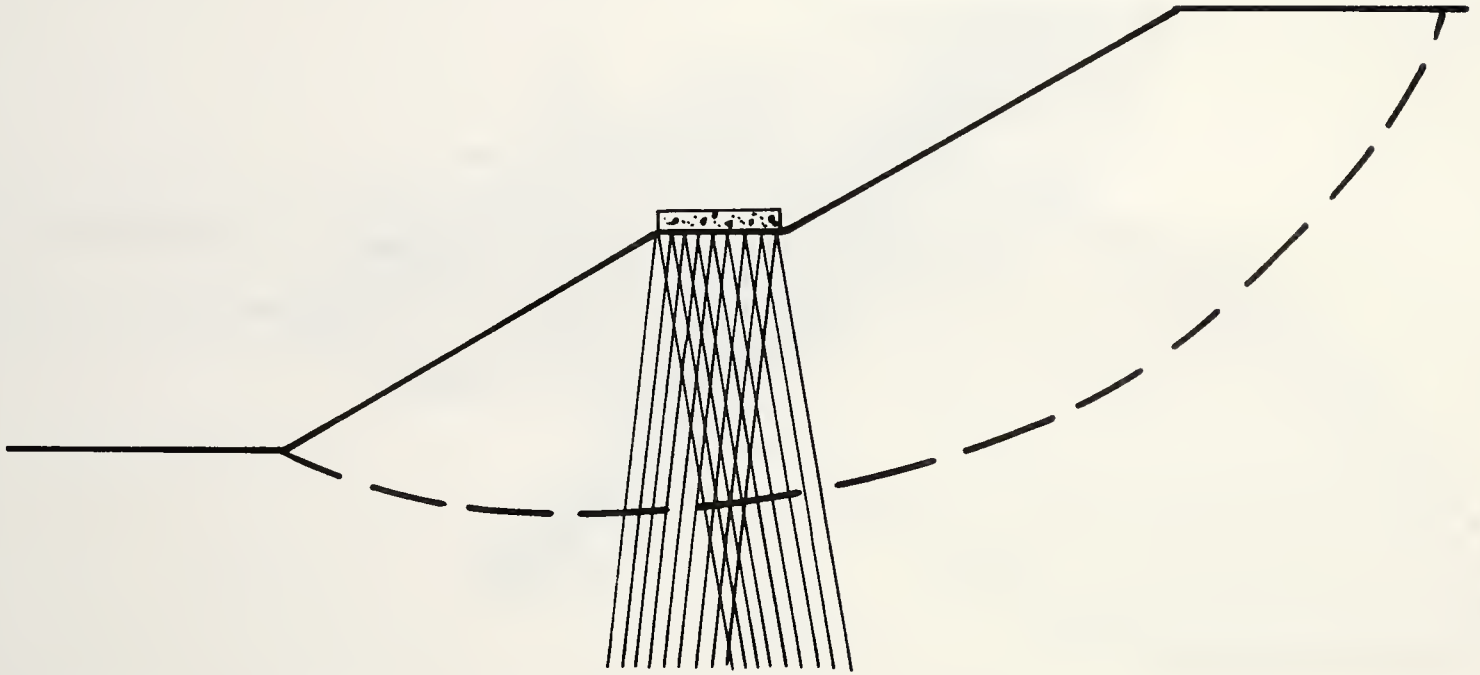

Figure 1.3: Fondedile Root Piles Used to Stabilize Slopes

advantage of the soil strengthened by small diameter drilled piles to form a barrier against further movement or stress transfer downslope (Dash and Jovino, 1980). Stone columns (figure 1.4), although relatively new within the United States, have been proven to be quite effective in Europe (Goughnour and DiMaggio, 1978; Barksdale and Bachus, 1983; Bachus and Barksdale, 1985). The stone columns are positioned to take advantage of their high shear strength across the failure surface as well as their high modulus of elasticity to transfer vertical loads directly to the more stable foundation layers below.

Large diameter drilled piers discretely placed so that some clear space exists between the piers can take advantage of many of the strong points of the techniques described above. The piers have the advantage of being installed quickly while not requiring large excavations which would create an extra load on a slope sometimes already distressed. This makes drilled piers an ideal remedial measure to slow or halt the progress of failing slopes (Mathis, 1981). A second advantage of not requiring large excavations is to preserve the in-situ strength of the soil when strain softening may occur. The piers are able to improve the shearing resistance across existing failure surfaces as can be achieved with drilled pier walls. However, by proper positioning, the piers can also absorb vertical forces and transmit them directly to the

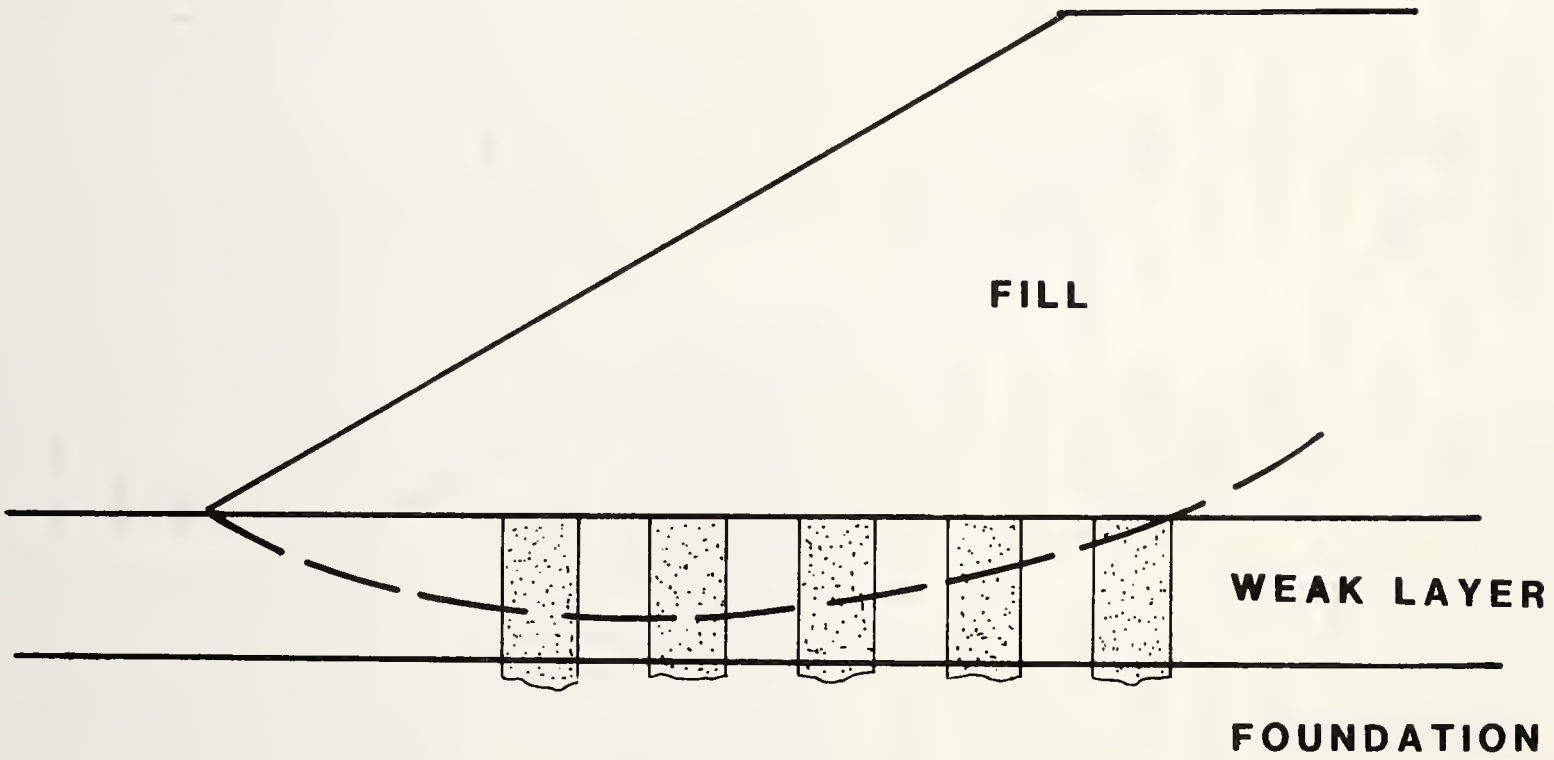

Figure 1.4: Stone Columns Used to Stabilize an Embankment

foundation as can be done with stone columns and inclined timber piles. Greater efficiency can be achieved in the vertical mode by discrete placement of the piers, rather than continuous placement, by increasing the surface area which interacts with the soil. Cost savings also result because of the reduced number of piers which are required. The lateral effectiveness is not sacrificed because the piers rely upon soil arching, as would root piles, to form a continuous barrier.

Analysis techniques have been developed to predict the forces against the piers when used as reinforcement in slopes (Poulos, 1973; Ito and Matsui, 1975; Baguelin, et al., 1976; Viggiani, 1981; Winter, et al., 1983; De Paepe and Wallays, 1984; Gudehus and Schwarz, 1985). The technique developed by Ito and Matsui (1975) was incorporated in a limiting equilibrium solution by Hassiotis (1984). While these techniques are sufficient to design the reinforcing system for lateral loads, they can not model the behavior of the slope itself. Loading under the complex boundary conditions of a slope stabilized by drilled piers will dramatically alter the stress field in the slope. An application of the finite element method is proposed herein to improve the analysis of this problem.

This study will develop a three dimensional finite element model for slopes stabilized by drilled piers which

are socketed in bedrock. The model will include quadratic strain soil elements which are capable of modelling the curved surfaces of the piers. Cubic strain one dimensional spar elements will model the piers. A hyperbolic stress-strain relationship will be used to model the soil. The program will be able to model construction sequences, the interaction between the piers and soil, weak seams in the soil profile, and remolded areas around the piers. The primary output of the program will be displacement, strain and stress fields. The stresses will be used in a post processing analysis to estimate the factor of safety of the slope.

CHAPTER 2: REVIEW OF CASE STUDIES

Introduction

A complete review of analysis techniques to predict the lateral load against drilled piers to stabilize slopes was conducted by Hassiotis (1984). Hence, the purpose of this chapter is to update the review by Hassiotis (1984) with regard to case studies and numerical modelling of drilled piers used to reinforce slopes. The models reviewed will be either physical or numerical in nature.

Physical Modelling

Physical models include scale modelling and observations of actual cases.

Scale Modelling

To check the validity of their theoretical derivation of the lateral pressures on passive piles in a row, Matsui et al. (1982) used scale modelling. An apparatus using air pistons pushed a block of soil through a row of model piles. In general, their theory was satisfactory in predicting lateral loads over a wide variety of cases.

However, this modelling is not exactly applicable to real slopes since the soil was pushed perpendicularly to the piles. A more realistic model must allow for both the vertical and rotational movements of the failing mass. These are the factors which will have a significant effect on the stresses along a potential failure surface and must be accounted for when analyzing the stability of the slope.

Observations of Actual Cases

Several case histories of attempts to stabilize slopes using drilled piers, successful and unsuccessful, can be found in the literature.

1) Portuguese Bend Landslide, Palos Verde Hills, California (Merriam, 1960). An attempt was made to stop a 300 to 400 acre sliding landmass. The vertical relief of the sliding mass was about 1000 feet with a maximum length of about 6000 feet. Horizontal movements as large as 68 feet were measured at some points. Twenty-five 4 foot diameter, 20 feet long precast caissons, were placed at discrete points (not in a row) along the toe of the slide. The piers were designed such that the lower 10 feet were in a stationary shale formation. The caissons did not provide any measurable effect on the movement of the landmass even though, in some cases, twice the design lateral force developed against the piers. The soil mass flowed

around the piers, eventually tilting or shearing them off at the failure surface.

2) U.S. 421, Harlan Kentucky (Mathis, 1981). Drilled piers constructed of railroad rails and gravel backfill placed on 4 foot centers in 2 staggered rows, were used as a temporary measure to slow landslide movement until permanent corrective measures could be implemented. The temporary measures were to prevent the breakage of a 10 inch water line which supplied a hospital. The slide was shallow and approximately 200 feet long. The piers where used primarily as lateral supports near the middle of the profile of the sliding mass. No monitoring systems were installed during the period when the piers held the slope, however, the support was viewed as successful. The temporary measures supported the slope for about three weeks.

3) Snake Pass remedial work (Leadbeater, 1985). Drilled piers were used as a remedial measure to stabilize a long term landslide which threatened to close a 120 meter section of Road A57 (Snake Pass), the principal route between Manchester and Sheffield, England. The piers were used at the top of a 50 meter block slide to absorb stresses in the vertical and lateral directions. The support consisted of 1.2 meter diameter piers with a center to center distance of 2.0 meters. Two staggered

pier rows were used with a 1.2 meter distance between the centers of each row. The staggered formation was used so that a cap slab could be placed over the piers. The slab could develop some moment, thus reducing the structural demands on the piers. This system was completed by the Spring of 1981 and has not developed any problem since then.

4) Oudenberg Hill, Geraardsbergen, Belgium (De Paepe and Wallays, 1984). In order to repair a slumped portion of roadway and stabilize a distressed slope, drilled piers served two purposes. First, to support a viaduct so that fill material would not be needed to bring the embankment up to its original level, thus adding weight to the failing slope. Second, to act as "nails" to stabilize the slope. The sliding area consisted of two primary slip surfaces, totaling 135 meters in length. The piers were placed at the top of the upper surface, absorbing both vertical and lateral stresses. Three rows of piers spaced 4.3 meters apart consisting of 1.5 meter diameter piers were used to support the viaduct which reestablished traffic. The piers also successfully stopped any additional slope movement.

5) Dautemheim (Gudehus and Schwaz, 1985). An 8 meter high fill was stabilized after showing creep movement as high as 0.1 to 0.15 cm/day over several years.

Two staggered rows of piers, 3 meters apart, 1.5 meters in diameter, with a spacing of 7.6 meters were used to stabilize a sliding mass approximately 40 meters in cross sectional length. The piers were placed in the middle of the slip surface, absorbing primarily lateral loads. No measurable movement occurred over the following few months while observations continued.

6) Unspecified Railway Cut (Gudehus and Schwaz, 1985). A large scale field testing program was conducted while stabilizing a 100 year old cut in stiff fissured clay. Two rows of 0.4 meter piers reduced the movement from 4.7 mm/month to 1.3 mm/month. The slide was a block type approximately 45 meters in length and 7 meters deep. No information was gathered regarding the long term performance of the piers due to the termination of funding. Also tested on an experimental basis were predrilled grouted piers made of steel pipe casings of 1.5 and 2.0 foot diameters sealed with a mixture of cement and silica. Several test patterns were tried in 10 meter by 10 meter plots. All patterns initially reduced the movement with the denser patterns and bigger piers working better, but all of them eventually failed under the progressive movement.

Numerical Modelling

Numerical modelling provides an opportunity to study a great number of cases. The problem of discretely placed piers is clearly one involving three dimensional effects, however, two dimensional approximations can be made which are quite useful.

Two Dimensional Model

Rowe and Poulos (1979) developed a two dimensional model which approximates the three dimensional problem by making allowances for the soil "flowing through" the row of piers. Separate solution routines were used to analysis the movements in the soil and displacement of the piers. The study dealt primarily with the effect of the slope movement on the piers. A limited parametric study was conducted for three rows of piers, spaced 2.0 meters apart with 0.5 and 1.0 meter diameters, placed at the crest of a small slope. The conclusions were:

1) Improvement of slope deformation and stability increases very slowly with increasing pier stiffness. It may be necessary to use very rigid piers.

2) Effectiveness is enhanced by restraining the pier tip. However, this combined with increased stiffness of the piers, drastically increases the bending moments in the piers.

3) Increasing soil stiffness and strength with depth has a positive effect on reducing the moments in the piers.

Three Dimensional Model

Oakland and Chameau (1984) conducted a finite element study of drilled piers used for slope stabilization in the case of a surcharge loading at the embankment crest. Three dimensional finite elements (eight node, linear strain) were used to model the soil movement around the piers. The loading scheme used was a surcharge loading at the embankment crest. The piers were modelled as rectangular columns. In this study, surface displacements were evaluated for a variety of cases using different pier variables of position, spacing, size and stiffness. The conclusions were:

1) To be most effective the position of the piers should be at the location of the maximum potential movement (identified in the case without a pier).

2) Both increasing the diameter and reducing the spacing of the piers have similar effects in reducing the surface displacements.

3) The effect of increasing the stiffness of the pier is to uniformly decrease the displacements over the entire profile.

This simplified model (i.e. rectangular piers, no slip elements, linear soil model, etc.) was used to establish a rough estimate of the feasability of a drilled pier reinforcing system. In reevaluating the results of this pilot study, it can be seen that many of the later conclusions were evident then, such as the effects of the vertical support of the piers. A redrafted version of this paper is given in the Appendix of this study.

CHAPTER 3: SOIL MODELLING

Part I: Constitutive Relations

Introduction

Three sets of equations must be met when relating loads to displacements (figure 3.1): first the loads must be transformed into stresses, then the stresses related to strains, and finally, the strains are transformed into displacements. The respective equations involved are:

1) Equations of equilibrium
2) Compatibility of strains and displacements
3) Material constitutive equations

The first two sets of equations can be formulated by a numerical technique such as the finite element method. The accuracy of their solution can usually be improved by increasing the number of integration points, the order of elements, or the number of elements. For geotechnical problems, it is usually the third set of equations, the constitutive relations, which are the weakest link in the chain.

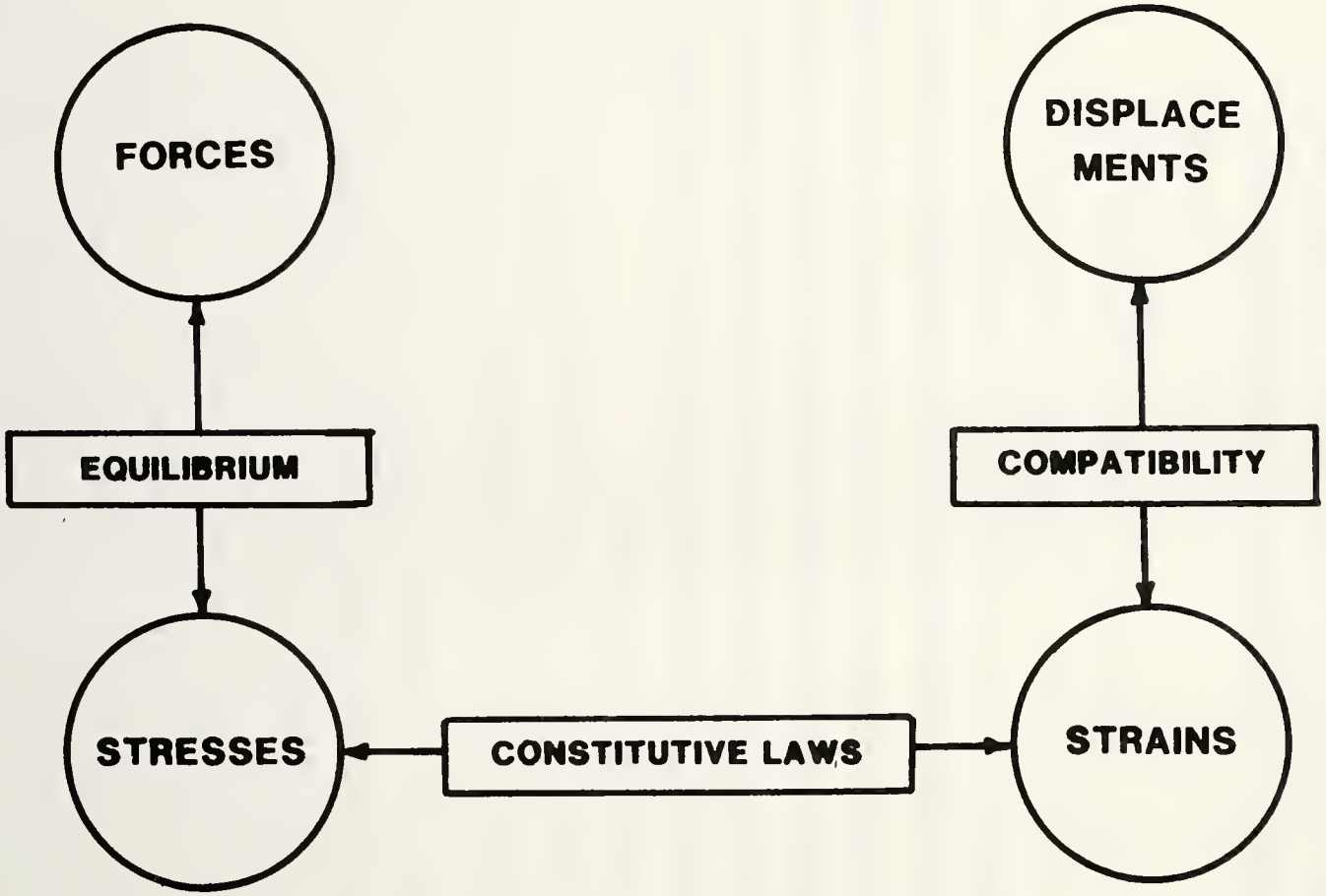

Figure 3.1: Equations Relating Loads to Displacements
(From Chen and Saleeb, 1982)

The multiphase nature of soils, consisting of solids, water and air, as well as often being highly inhomogeneous and anisotropic, creates difficulty in predicting their stress-strain curves. Some of the major variables are minerological composition, void ratio, stress level, stress or strain history, temperature, time, and degree of saturation (Leonards et al, 1982, pg 8). Since each factor is complex in itself, writing a universal equation is virtually impossible. To keep the model within practicality and testing capability, many simplified models have been developed based on phenomenological observations. These are models which try to duplicate observed behavior, but are not necessarily based on the fundamentals of soil mechanics.

The constitutive equations commonly used in geotechnical engineering can be divided into three main catagories: elastic solutions, plastic solutions and variable modulus solutions. A material is elastic if upon release of applied stresses it returns to its original size and shape (Chen and Saleeb, 1982, pg. 147). Elastic behavior is reversible and path independent, i.e. memoryless. Plastic behavior on the other hand is generally not reversible, i.e. permanent strains exist after unloading. Finally, variable modulus techniques offer "hybrid" solutions between elastic and plastic models. The equations on which they are based are elastic in origin, however,

different functions are used in loading and unloading so that permanent deformations can be modelled.

This chapter will present a variety of soil models and implementation schemes which will be considered for use in the finite element program developed for this study. The specific models discussed in this chapter could be interchanged with the models which are used in the finite element program with relative ease. While plasticity models are conceptually superior, the computational effort needed to utilize them combined with the effort necessary to create the three dimensional model was beyond the scope of this study. Furthermore, one of the requirements of the research project was to select parameters and approaches which can be implemented efficiently by the sponsoring agency. For these reasons plasticity models are not considered in this chapter.

Elastic Solutions

Tabular Form

Tabulating the stress-strain data is a non-mathematical way of expressing constitutive relationships, and although it is not unique to elastic solutions, the tabular format is able to represent elastic behavior. The curves are input as data points into computer memory and

soil parameters are found by interpolation and numerical differentiation (Clough and Woodward, 1967; Girijavallabahan and Reese, 1968; Desai, 1968). As long as enough data points are stored, the deformations can be modelled accurately. The model will follow the test curve to any degree desired, including odd dips and bends. The main shortcoming of this approach is the impossibility of predicting soil behavior, i.e. each soil must be fully tested under the conditions expected in the analysis. Other disadvantages include the amount of required computer storage and the cumbersomeness to input and use the data.

Cauchy

A Cauchy material has no stress or strain behavior dependency on the stress or strain histories followed to reach the current state of stress or strain (e.g., Eringen, 1962; Malvern, 1969). Stresses are a unique function of the strains (generalized Hooke's law):

$$\sigma_{ij} = C_{ijkl}\ \varepsilon_{kl} \qquad 3.1$$

where: C_{ijkl} = fourth-order tensor,

σ_{ij} = second order tensor of stresses, and

ε_{kl} = second order tensor of strains.

As indicated above, this relation indicates a behavior

which is both reversible and path independent. Reversibility is following the same path in loading and unloading (figure 3.2a). There is no hysteresis or plastic strain. Path independence implies that whichever strain path is followed, the final state of stress in the material depends only on the final state of strain (figure 3.2b).

The Cauchy elastic model is very attractive because of its simplicity. It is usually only a matter of finding a mathematical function which approximates the actual stress-strain behavior. Many of these functions have been proposed and a few are mentioned below.

Linear Models

The most simple constitutive relation is the linear elastic Cauchy model. For a linear material, the C_{ijkl} tensor is composed of 81 constants, but if complete isotropy is assumed the number of constants is reduced to 2. Any of the sets of two independent constants given in table 3.1 can be used in the formulation. For example, the modulus of elasticity and Poisson's ratio are often used, thus the generalized Hooke's equation becomes:

$$\sigma_{ij} = \frac{E}{1+\nu}\epsilon_{ij} + \frac{\nu E}{(1+\nu)(1-2\nu)}\epsilon_{kk}\delta_{ij} \qquad 3.2$$

where: E = modulus of elasticity,

ν = Poisson's ratio, and

δ_{ij} = kronecker function.

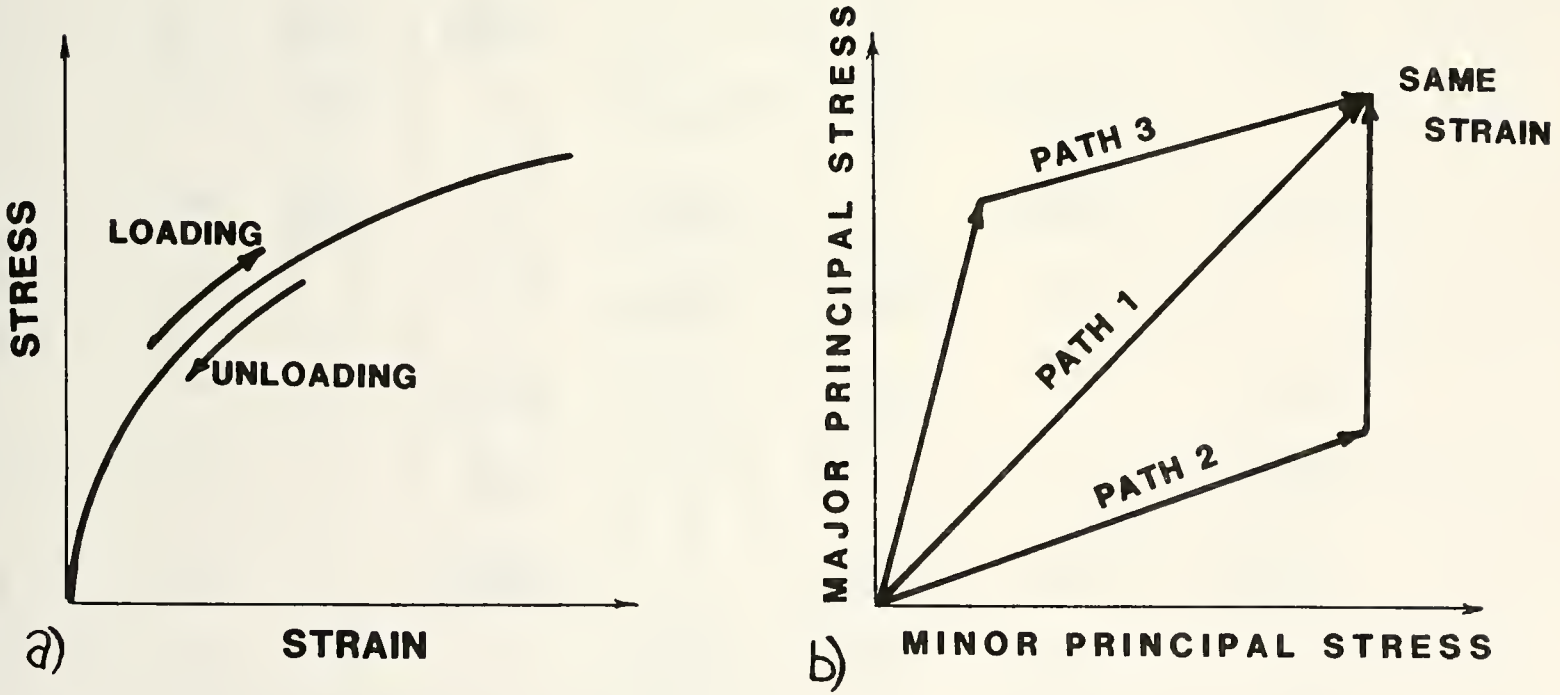

Figure 3.2: Material Behavior
a) Reversibility
b) Path Independence

Table 3.1: Relationships Among Elastic Moduli (From Chen and Saleeb, 1982)

	Shear Modulus, G	Young's Modulus, E	Constrained Modulus, M	Bulk Modulus, K	Lame Parameter, λ	Poisson's Ratio ν
G,E	G	E	$\frac{G(4G-E)}{3G-E}$	$\frac{GE}{9G-3E}$	$\frac{G(E-2G)}{3G-E}$	$\frac{E-2G}{2G}$
G,M	G	$\frac{G(3M-4G)}{M-G}$	M	$M-\frac{4}{3}G$	$M-2G$	$\frac{M-2G}{2(M-G)}$
G,K	G	$\frac{9GK}{3K+G}$	$K+\frac{4}{3}G$	K	$K-\frac{2G}{3}$	$\frac{3K-2G}{2(3K+G)}$
G,λ	G	$\frac{G(3\lambda+2G)}{\lambda+G}$	$\lambda+2G$	$\lambda+\frac{2G}{3}$	λ	$\frac{\lambda}{2(\lambda+G)}$
G,ν	G	$2G(1+\nu)$	$\frac{2G(1-\nu)}{1-2\nu}$	$\frac{2G(1+\nu)}{3(1-2\nu)}$	$\frac{2G\nu}{1-2\nu}$	ν
E,K	$\frac{3KE}{9K-E}$	E	$\frac{K(9K+3E)}{9K-E}$	K	$\frac{K(9K-3E)}{9K-E}$	$\frac{3K-E}{6K}$
E,ν	$\frac{E}{2(1+\nu)}$	E	$\frac{E(1-\nu)}{(1+\nu)(1-2\nu)}$	$\frac{E}{3(1-2\nu)}$	$\frac{\nu E}{(1+\nu)(1-2\nu)}$	ν
K,λ	$\frac{3(K-\lambda)}{2}$	$\frac{9K(K-\lambda)}{3K-\lambda}$	$3K-2\lambda$	K	λ	$\frac{\lambda}{3K-\lambda}$
K,M	$\frac{3(M-K)}{4}$	$\frac{9K(M-K)}{3K+M}$	M	K	$\frac{3K-M}{2}$	$\frac{3K(2M-1)+M}{3K(2M+1)-M}$
K,ν	$\frac{3K(1-2\nu)}{2(1+\nu)}$	$3K(1-2\nu)$	$\frac{3K(1-\nu)}{1+\nu}$	K	$\frac{3K\nu}{1+\nu}$	ν

Classically, it has been assumed that many materials display linear behavior when stressed below the yield point. This is probably more valid for metals than soils, but is commonly used in the latter for simplicity. Typical geotechnical materials are, however, often stressed beyond the yield point where they become highly nonlinear. The program "SPILES" includes an option to utilize linear elastic behavior.

Nonlinear Models

Nonlinear models are often referred to as functional relationships because they assume a mathematical function to express the nonlinear stress-strain relationships. A number of functions are commonly used, such as: hyperbolic, parabolic, interpolation, spline, and others.

Hyperbolic Relationships. Kondner (1963) showed that the stress-strain curve of a number of soils could be adequately represented by a hyperbola. This function is convenient because the parameters in the hyperbolic equation have physical significance, and they can be easily determined from test data by transforming the equation into a linear relationship. Several forms of this model are used in practice.

Duncan-Chang Model. The most widely used hyperbolic relationship is the model developed by Duncan and Chang

(1970). Following the approach of Kondner, the stress-strain relation can be expressed as:

$$\sigma_1-\sigma_3 = \frac{\varepsilon_1}{(\frac{1}{E_i}) + \frac{1}{(\sigma_1-\sigma_3)_{ult}}\varepsilon_1} \qquad 3.3$$

where: $\sigma_1-\sigma_3$ = deviator stress,

$(\sigma_1-\sigma_3)_{ult}$ = ultimate deviator stress,

ε_1 = maximum principal strain, and

E_i = initial modulus of elasticity.

The hyperbolic relation is plotted in figures 3.3a and 3.3b in the original and transformed (linear) versions, respectively. Note that the values of E_i and $(\sigma_1-\sigma_3)_{ult}$ have physical interpretation as well as being parameters in the hyperbolic equation; they can be obtained from laboratory experiments on representative soil samples.

Janbu (1963) found that the initial modulus of elasticity is dependent on the confining pressure for all but totally saturated soils. In general, the modulus increases proportionally with confining pressure (represented by σ_3 in a triaxial test) as:

$$E_i = K\, P_a(\sigma_3/P_a)^n \qquad 3.4$$

where: E_i = initial modulus of elasticity,

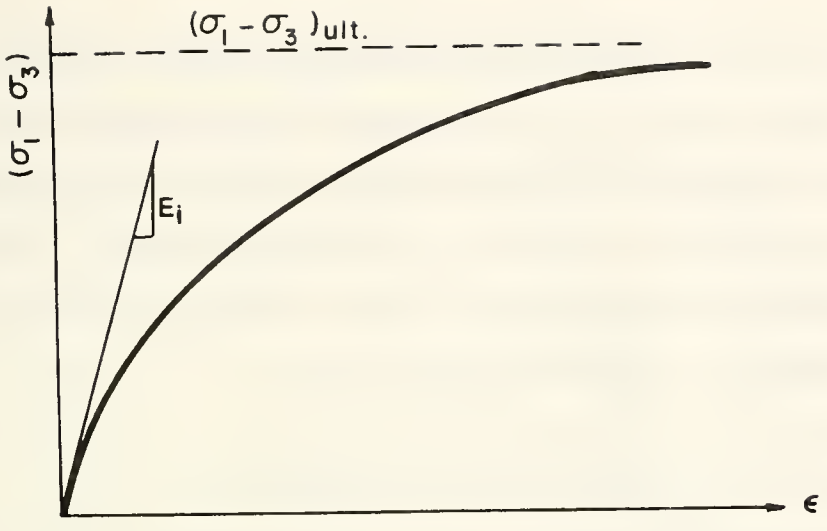

a)

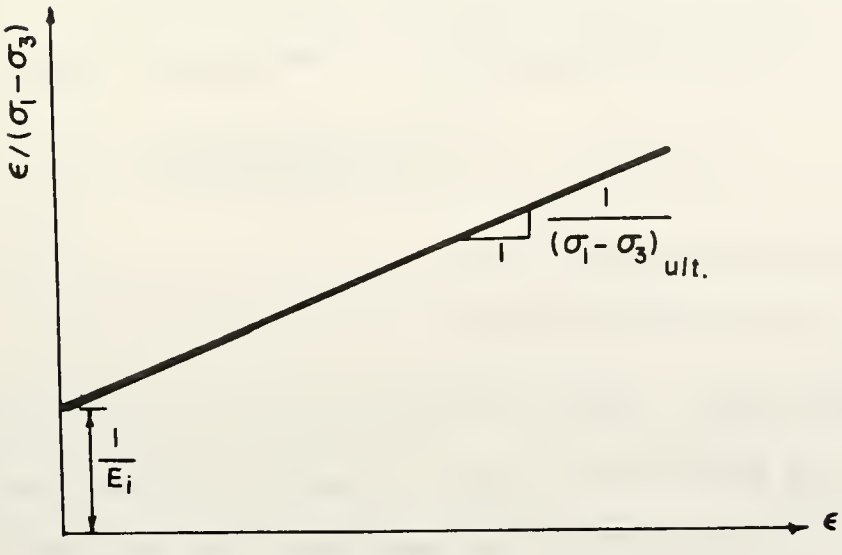

b)

Figure 3.3: Duncan-Chang Model
a) Real
b) Transformed

P_a = atmospheric pressure,

σ_3 = minor principal stress, and

K, n = constants.

To account for strain softening effects after the yield point, $(\sigma_1-\sigma_3)_{ult}$, is related to the confining stress by the Mohr-Coulomb strength equation through the value of $(\sigma_1-\sigma_3)$ at failure. That is, a failure point is chosen below the ultimate strength as a ratio of the ultimate strength. The relationship is:

$$(\sigma_1-\sigma_3)_f = R_f(\sigma_1-\sigma_3)_{ult} \qquad 3.5$$

where: $(\sigma_1-\sigma_3)_f$ = deviator stress at failure, and

R_f = constant.

Typical values of R_f range from 0.5 to 0.9.

The Mohr-Coulomb equation can be expressed as:

$$(\sigma_1-\sigma_3)_f = \frac{2c\cos\phi + 2\sigma_3\sin\phi}{1-\sin\phi} \qquad 3.6$$

where: c = cohesion, and

ϕ = friction angle.

The tangent modulus of elasticity, E_t, is obtained by taking the derivative of the stress-strain relation (equation 3.3), and substituting equations 3.4, 3.5, and 3.6:

$$E_t = \left(1-\frac{R_f(1-\sin\phi)(\sigma_1-\sigma_3)}{2c\cos\phi + 2\sigma_3\sin\phi}\right)^2 KP_a\left(\frac{\sigma_3}{P_a}\right)^n \qquad 3.7$$

This is the nonlinear soil modelling option provided in the program "SPILES".

Another complication in the modelling of soils is nonlinear volume change characteristics (figure 3.4). Kulhawy et al. (1969) approached this problem in a similar manner to the Duncan-Chang approach of the nonlinear modulus of elasticity. It is assumed that the volume change curves also have a hyperbolic shape and that the initial Poisson's ratio is a function of confining pressure. The tangent Poisson's ratio, ν_t, can be obtained following a similar procedure as that used to determine E_t:

$$\nu_t = \frac{G - F\log(\sigma_3/P_a)}{\left(1 - \frac{D(\sigma_1-\sigma_3)}{K\,P_a(\frac{\sigma_3}{P_a})^n\,(1 - \frac{R_f\,(\sigma_1-\sigma_3)(1-\sin\phi)}{2c\,\cos\phi + 2\sigma_3\,\sin\phi})}\right)^2} \qquad 3.8$$

where: D, F, G = constants

Typical values of the parameters required for the determination of E_t and ν_t are given in Wong and Duncan (1974). The program developed for this study has an option to include a variable Poisson's ratio as specified above in addition to using the variable modulus of elasticity.

Modified Duncan Model. In a parallel approach to account for nonlinear volume change, Duncan, et al. (1978) proposed using a tangent bulk modulus which depends only on

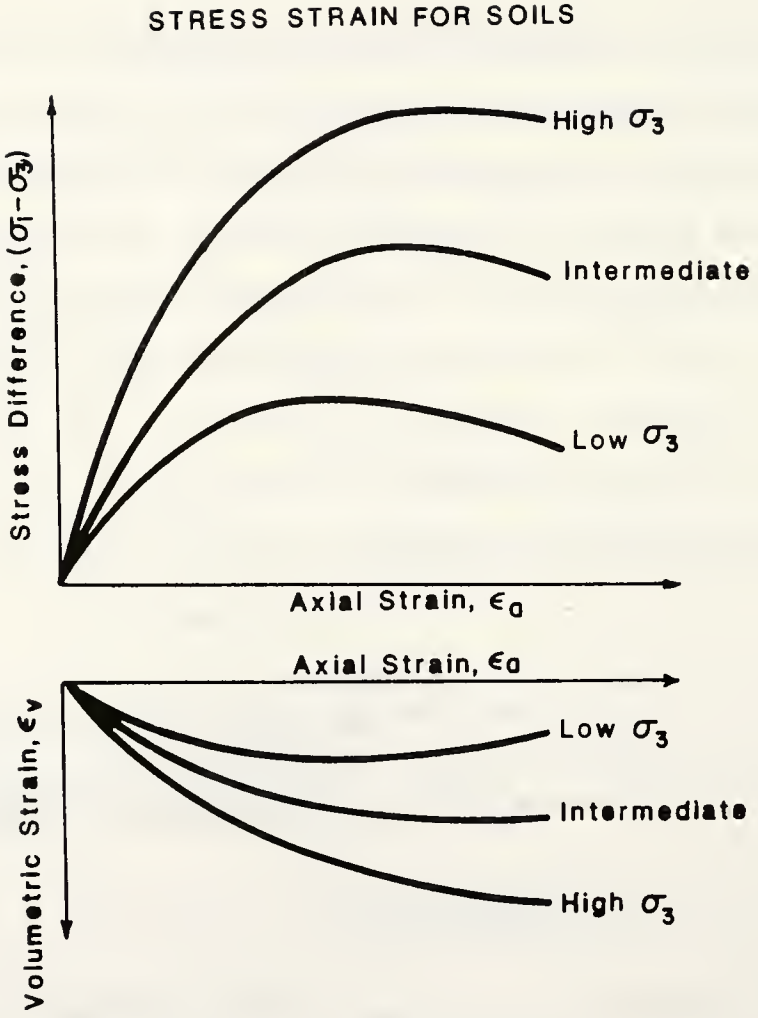

Figure 3.4: Nonlinear Volume Change Characteristics of Soils (From Duncan, 1980)

confining pressure as follows:

$$K_t = K_b P_a (\sigma_3 / P_a)^m \qquad 3.9$$

where: K_t = bulk modulus, and

K_b, m = constants.

Typical values of the parameters required for the determination of E_t and ν_t are given in table 3.2.

In this alternate formulation of the hyperbolic model, E_t and ν_t are replaced by E_t and K_t. A numerical problem arises, however, when values of the bulk modulus approaches a value which corresponds to the Poisson's ratio approaching zero. Similarly, it is possible for the tangent bulk modulus to correspond to a Poisson's ratio exceeding 0.50. Limits must be placed on the range of the bulk modulus to prevent this.

Extended Hardin Model. Another commonly used model based on hyperbolic relationships is the Hardin model (Hardin, 1970; Hardin and Drnevich, 1972). This model was originally developed for soil dynamics problems to relate shear strains to earthquake loading, but it can be used for static cases. The secant shear modulus is expressed in hyperbolic form as:

$$G_s = \frac{G_{max}}{1 + \frac{\gamma G_{max}}{\tau_{max}}\left(1 + \frac{a}{\exp\left(\left(\frac{\gamma G_{max}}{\tau_{max}}\right)^{0.4}\right)}\right)} \qquad 3.10$$

Table 3.2: Representative Parameter Values of the Modified Duncan Model (From Duncan, 1979)

Unified Soil Classification	RC* Stand. AASHTO	γ_m k/ft^3	ϕ_o deg	$\Delta\phi$ deg	c k/ft^2	K	n	R_f	k_b	m
GW, GP SW, SP	105	0.150	42	9	0	600	0.4	0.7	175	0.2
	100	0.145	39	7	0	450	0.4	0.7	125	0.2
	95	0.140	36	5	0	300	0.4	0.7	75	0.2
	90	0.135	33	3	0	200	0.4	0.7	50	0.2
SM	100	0.135	36	8	0	600	0.25	0.7	450	0.0
	95	0.130	34	6	0	450	0.25	0.7	350	0.0
	90	0.125	32	4	0	300	0.25	0.7	250	0.0
	85	0.120	30	2	0	150	0.25	0.7	150	0.0
SM-SC	100	0.135	33	0	0.5	400	0.6	0.7	200	0.5
	95	0.130	33	0	0.4	200	0.6	0.7	100	0.5
	90	0.125	33	0	0.3	150	0.6	0.7	75	0.5
	85	0.120	33	0	0.2	100	0.6	0.7	50	0.5
CL	100	0.135	30	0	0.4	150	0.45	0.7	140	0.2
	95	0.130	30	0	0.3	120	0.45	0.7	110	0.2
	90	0.125	30	0	0.2	90	0.45	0.7	80	0.2
	85	0.120	30	0	0.1	60	0.45	0.7	50	0.2

* RC = relative compaction, in percent

where: G_s = secant shear modulus,

G_{max} = maximum shear modulus,

γ = accumulated shear strain,

τ_{max} = maximum shear strain, and

a = constant function of for soil type,

To account for nonlinear volume changes, Katona, et al. (1976) extended Hardin's work to develop a nonlinear Poisson's ratio function as a hyperbolic curve.

$$\nu_s = \frac{\nu_{min} + q \frac{\gamma G_{max}}{\tau_{max}} \nu_{max}}{1 + q \frac{\gamma G_{max}}{\tau_{max}}} \qquad 3.11$$

where: ν_s = secant Poisson's ratio,

ν_{min} = Poisson's ratio at zero strain,

ν_{max} = Poisson's ratio at failure, and

q = constant.

These two equations form the Extended Hardin model.

Higher Order Mathematical Functions. Higher order mathematical functions provide a more versatile model to follow the actual stress-strain curve more accurately. The disadvantage is that more parameters are required to define the model. Some of these models are summarized in the following.

Ramberg-Osgood Model. The higher order curve in this model (Ramberg and Osgood, 1943; Jennings, 1964; Idriss et al., 1978). is the following three parameter function (figure 3.5):

$$\varepsilon = \frac{\sigma}{E_i} + k\left(\frac{\sigma}{E_i}\right)^p \qquad 3.12$$

with

$$k = (1/m-1)\left(\frac{\sigma_m}{E_i}\right)^{1-p} \qquad 3.13$$

where: E_i = initial modulus of elasticity,

σ_m = stress corresponding to the intersection of the stress-strain curve with the line mE_i, and

m, p = constants,

Richard and Abbott Model. A similar three parameter model proposed by Richard and Abbott (Richard, 1961; Richard and Abbott, 1975) takes the form:

$$\sigma = \frac{E_r \varepsilon}{\left(1 + \left|\frac{E_r \varepsilon}{\sigma_y}\right|^p\right)^{1/p}} + E_p \varepsilon \qquad 3.14$$

where: $E_r = E_i - E_p$,

E_i = initial modulus of elasticity,

E_p = plastic modulus of elasticity,

σ_y = yield stress,

p = constant which can account for confining pressure and stress path by iteration scheme (Desai and Wu, 1976)

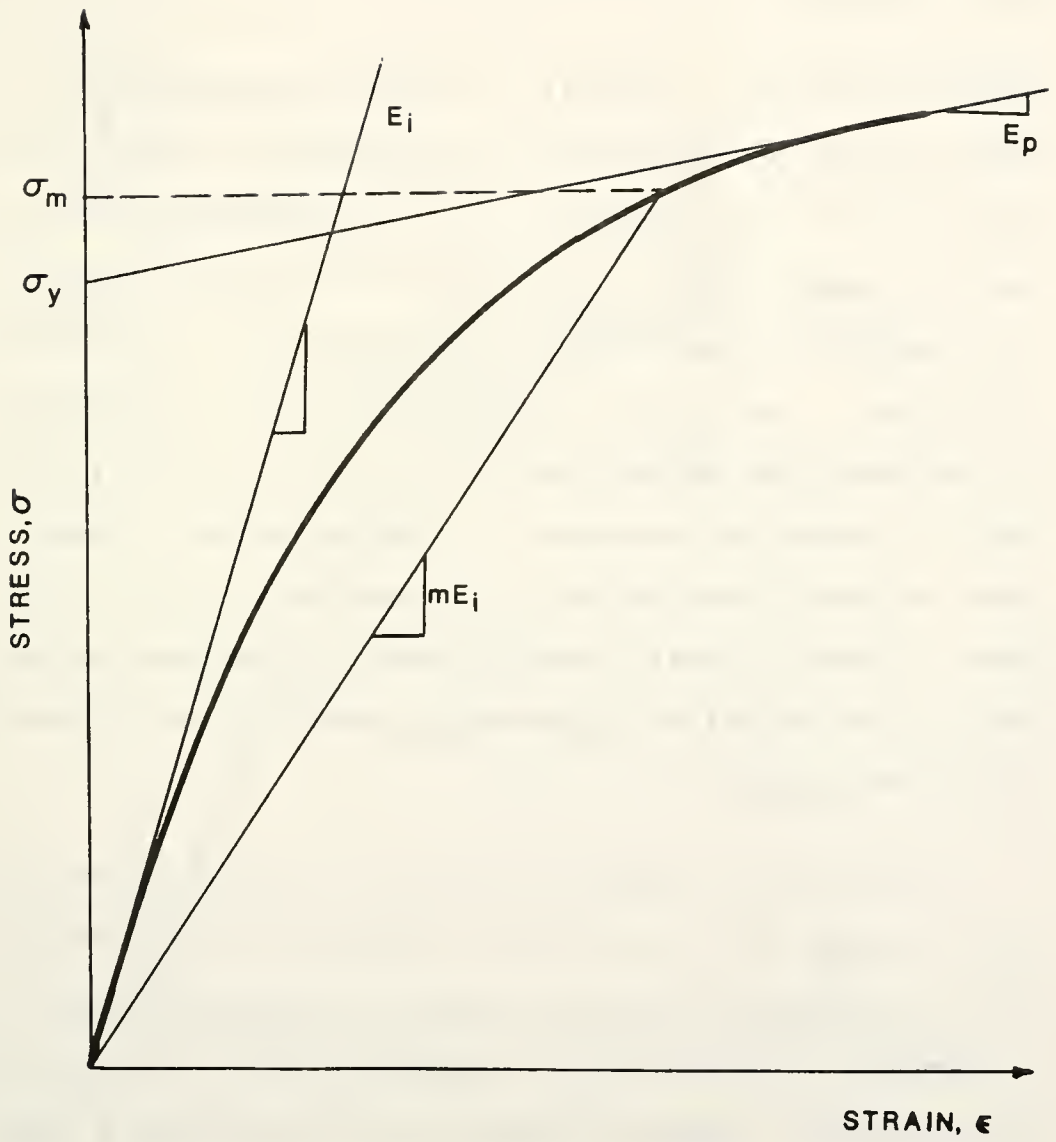

Figure 3.5: Ramberg-Osgood Model

This model reduces to the hyperbolic form for $E_p=0$ and $p=1$. Because the strain variable is present in both the denominator and numerator of the first term, this model can exhibit strain softening, while the Ramberg-Osgood model can not.

Spline Functions. Generally, the known conditions to define spline functions are the location and slope of the line at each point (figure 3.6). If a separate curve is used to connect each pair of sequential points, then the curve must be of cubic order to satisfy the four boundary conditions. The entire curve is continuous with respect to the first two derivatives. The third derivative, the rate of change of curvature, is discontinuous. Higher order splines could be used to connect points, but the cubic spline is usually satisfactory for engineering purposes. The detail of the overall curve can be improved by using more points.

Desai (1971) proposed the use of a cubic spline function to model the stress-strain behavior of soils because of its increased flexibility over the hyperbolic function. It provides a better model, especially in the initial part of the curve. Singh and Sandler (1975) proposed a function expressed in terms of strains as:

$$\sigma = a_i(\varepsilon-\varepsilon_i)^3+b_i(\varepsilon-\varepsilon_i)^2+c_i(\varepsilon-\varepsilon_i)+d_i \qquad 3.15$$

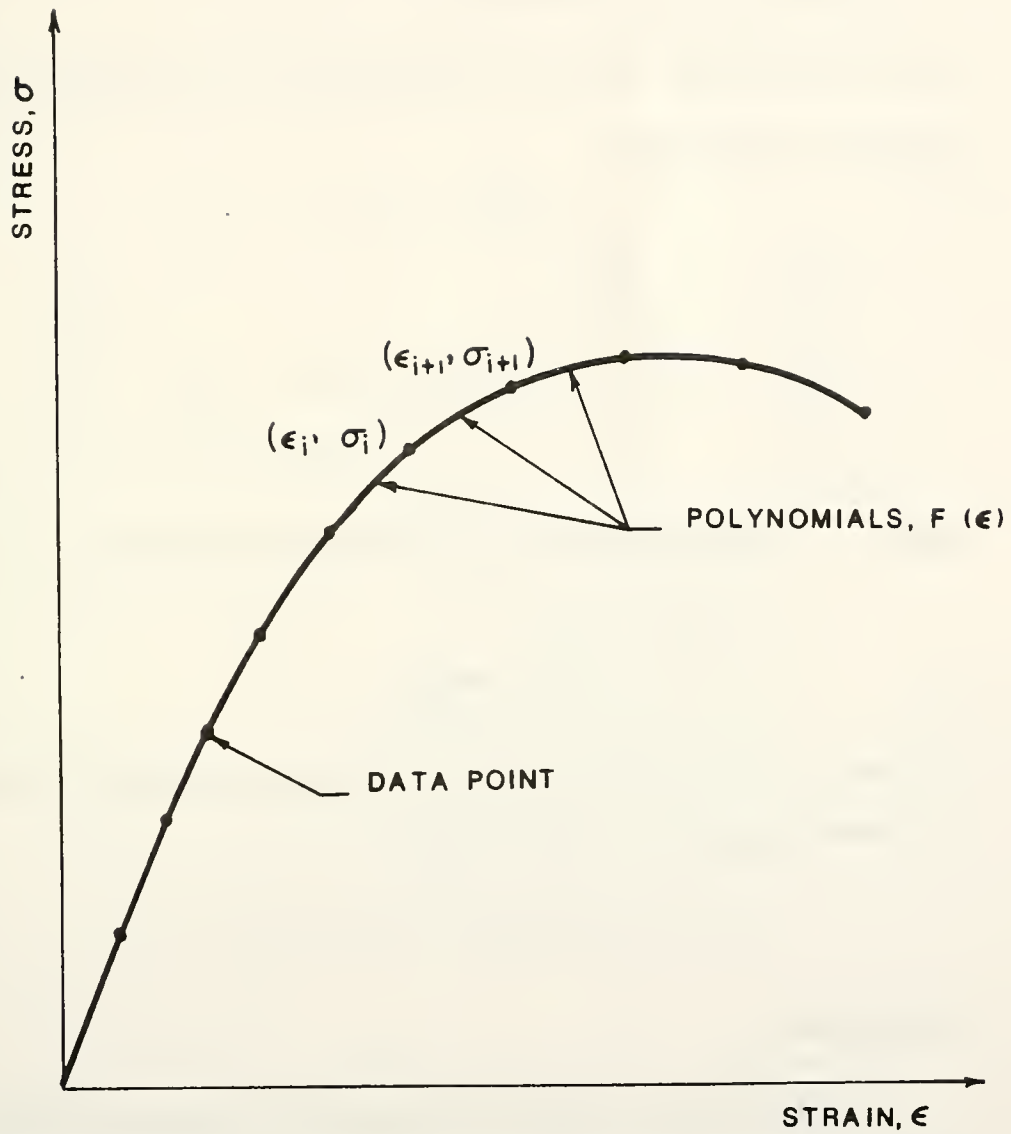

Figure 3.6: Spline Function

where: ε_i = strain at ith point,

ε = strain,

σ = stress, and

a_i, b_i, c_i, d_i = constants.

The coefficients for each segment can be found from the boundary conditions.

$$\begin{vmatrix} a_i \\ b_i \\ c_i \\ d_i \end{vmatrix} = \frac{1}{12h_i^2} \begin{vmatrix} -2h_i & 2h_i & 0 & 0 \\ 6h_i^2 & 0 & 0 & 0 \\ -4h_i^3 & -2h_i^3 & -12h_i & 12h_i \\ 0 & 2 & 12h_i & 0 \end{vmatrix} \begin{vmatrix} E_i \\ E_{i+1} \\ \sigma_i \\ \sigma_{i+1} \end{vmatrix} \qquad 3.16$$

where: E_i = modulus of elasticity at ith point,

$h_i = \varepsilon_{i+1} - \varepsilon_i$, and

σ_i = stress at ith point.

The derivative of the spline which is the tangent modulus of elasticity, E_t, is defined as:

$$E_t = 3a_i(\varepsilon-\varepsilon_i)^2 + 2b_i(\varepsilon-\varepsilon_i) + c_i \qquad 3.17$$

Hyperelastic

Cauchy type elastic materials can generate energy under certain loading-unloading cycles (Chen and Saleeb, 1982, pg. 148). This is a violation of the laws of thermodynamics. For this reason hyperelastic models are sometimes used.

Hyperelastic models, sometimes referred to as Green elastic models (e.g., Feng, 1965; Eringen, 1962; Green and Zerna, 1954; and Malvern, 1969), ensure that no energy is generated in the load-unload cycle. The stress-strain relationship is given as:

$$\sigma_{ij} = \frac{\partial W}{\partial \varepsilon_{ij}} \qquad 3.18$$

or

$$\varepsilon_{ij} = \frac{\partial \Omega}{\partial \sigma_{ij}} \qquad 3.19$$

The strain energy density function, W, and the complementary energy density function, Ω, are represented in figure 3.7. For the linear case:

$$W = \Omega = 1/2\ \sigma_{ij}\varepsilon_{ij} \qquad 3.20$$

where: W = strain energy density function,

Ω = complimentary energy density function,

σ_{ij} = stresses, and

ε_{ij} = strains.

For the nonlinear case, where the density function is dependent on strain (or stress) level, the equations can be written in terms of the three strain or stress invariants. These invariants can be in terms of total or effective values, or can be a combination of both.

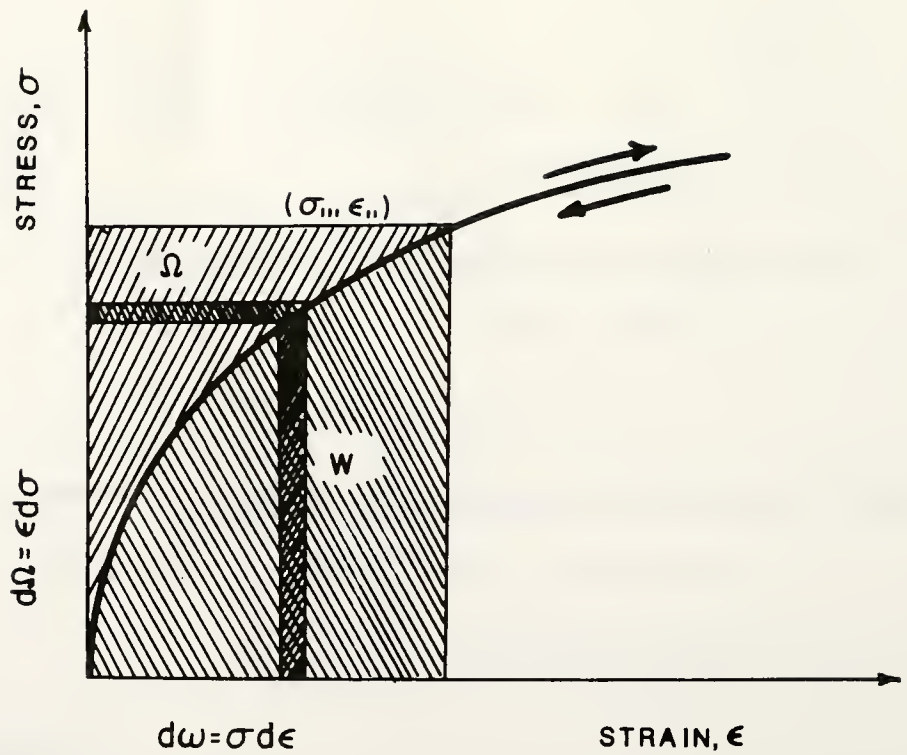

Figure 3.7: Strain and Complementary Energy Density Functions

If the effective stress invariants are used:

$$J_1 = \sigma'_{kk}$$

$$J_2 = 1/2\ \sigma'_{km}\sigma'_{km}$$

$$J_3 = 1/3\ \sigma'_{km}\sigma'_{kn}\sigma'_{mn}$$

then the constitutive law in terms of the complementary energy density function would be:

$$\varepsilon_{ij} = \frac{\partial \Omega}{\partial J_1}\frac{\partial J_1}{\partial \sigma'_{ij}} + \frac{\partial \Omega}{\partial J_2}\frac{\partial J_2}{\partial \sigma'_{ij}} + \frac{\partial \Omega}{\partial J_3}\frac{\partial J_3}{\partial \sigma'_{ij}} \qquad 3.21$$

where: J_i = effective stress invariants,

Ω = complementary energy density function,

σ'_{ij} = effective stresses, and

ε_{ij} = strains.

Again, this model is reversible and path independent. This means it can not account for stress history. Unlike the Cauchy model, however, this model can account for dilation (volume change under pure shear).

Ko and Masson (1976) suggested using a third order hyperelastic model developed by Evans and Pister (1966). The following complementary energy density function is based on the three effective stress invariants. The third order function has the form:

$$\Omega = A_o + A_1 J_1 + 1/2\ B_1 J_1^2 + 1/3\ B_2 J_1^3 + B_3 J_1 J_2 + B_4 J_2 B_5 J_2 + 1/4\ B_6 J_1^4 + B_7 J_1^2 J_2 + 1/2\ B_8 J_2^2 + B_9 J_1 J_3 \qquad 3.22$$

where: J_n = effective stress invariants,

Ω = complementary energy function, and

A_n, B_n = constants.

If there is no initial strain, the constitutive relation is:

$$\varepsilon_{ij} = [B_1 J_1 + B_2 J_2^2 + B_3 J_2 + B_6 J_1^3 + 2B_7 J_1 J_2 + B_9 J_3]\delta_{ij} + [B_3 J_1 + B_4 + B_7 J_1^2 + B_8 J_2]\sigma_{ij} + [B_5 + B_9 J_1]\sigma_{im}\sigma_{jm} \quad 3.23$$

Where: J_n = effective stress invariants,

σ_{ij} = stresses,

ε_{ij} = strains,

δ_{ij} = delta function, and

B_n = constants.

The constants B_1-B_9 are determined by a series of tests.

Odd order relationships are found to be most efficient because they best model shearing in triaxial compression and extension tests (Saleeb and Chen, 1980[1]). Even terms add little to the accuracy for the additional parameters which must be solved. A third order relationship was used because a fifth order involved more parameters than could practically be determined.

If the parameters are determined by tests which are close to the field stress path, then the general hyperelastic

model is satisfactory in all respects including strain hardening and dilation in sands (Chen and Saleeb, 1980[2]).

Saleeb and Chen (1980[2]) used the general third order hyperelastic model to predict the stress-strain relationship of two clays and a sand for several stress paths. In a critical review of these predictions (Christian, 1980), it was found that the model does well for the stress paths similar to those which the parameters where determined from, but may not be accurate for other cases. The model seems also to deviate from experimental results near failure.

Hypoelastic

The previous two models were total stress models. Because they are path independent, the final state of strains could be calculated from the final state of stress. Hypoelastic models (e.g., Malvern, 1969; and Truesdell, 1955) are part of a group which are path dependent. The final state of strain is found by applying the stress state in increments following a specific stress path.

In its most general form the hypoelastic equations can be written as:

$$F(\sigma_{ij}, \dot{\sigma}_{kl}, \varepsilon_{mn}, \dot{\varepsilon}_{pq}) = 0 \qquad 3.24$$

where: σ_{ij} = stresses,

$\dot{\sigma}_{kl}$ = stress rate,

ε_{mn} = strains, and

$\dot{\varepsilon}_{pq}$ = strain rate.

The strain and stress rates are not actually functions of time since time occurs to the same order in all terms and therefore can be eliminated (Saleeb and Chen, 1980[1]). The parameters then become stress and strain increments.

This model has the advantage of being path dependent. That is, a different state of strain will result from the same stress state achieved by separate stress paths. However, this model is only incrementally reversible. Elasticity is only valid within an increment and it is generally not possible to retrace the stress path and arrive at the initial state of strains. Another disadvantage is that in its most general form, 12 response parameters are needed to describe the C_{ijkl} constants (Leonards et al., 1982). These must be obtained from test data and curve fitting.

Variable Modulus Solutions

Variable modulus models are not in themselves an independent category, but rather an hybrid form of the previous models to allow for permanent strains upon

unloading. This involves using different stress-strain relations for loading and unloading (or reloading) behavior.

A common assumption is that the unloading-reloading part of the stress-strain curve displays linear elastic Cauchy properties. The unloading-reloading modulus can be approximated by the initial modulus. Credibility is given to this since the rebound portion of a oedometer test curve is roughly parallel to the virgin portion of the curve (figure 3.8). At high stresses, however, hysteresis becomes an important factor and the paths become distinctly nonlinear (Chen and Saleeb, 1982) (figure 3.9). The linear elastic assumptions will no longer provide a very good approximation and stress dependent model may have to be considered.

Duncan (1980) incorporates a linear elastic approximation in the Duncan-Chang and Modified Duncan models by defining an unloading-reloading modulus of elasticity as (figure 3.8):

$$E_{ur} = K_{ur} P_a \left(\frac{\sigma_3}{P_a}\right)^n \qquad 3.25$$

where: E_{ur} = unload-reload modulus of elasticity,

K_{ur}, n = constants.

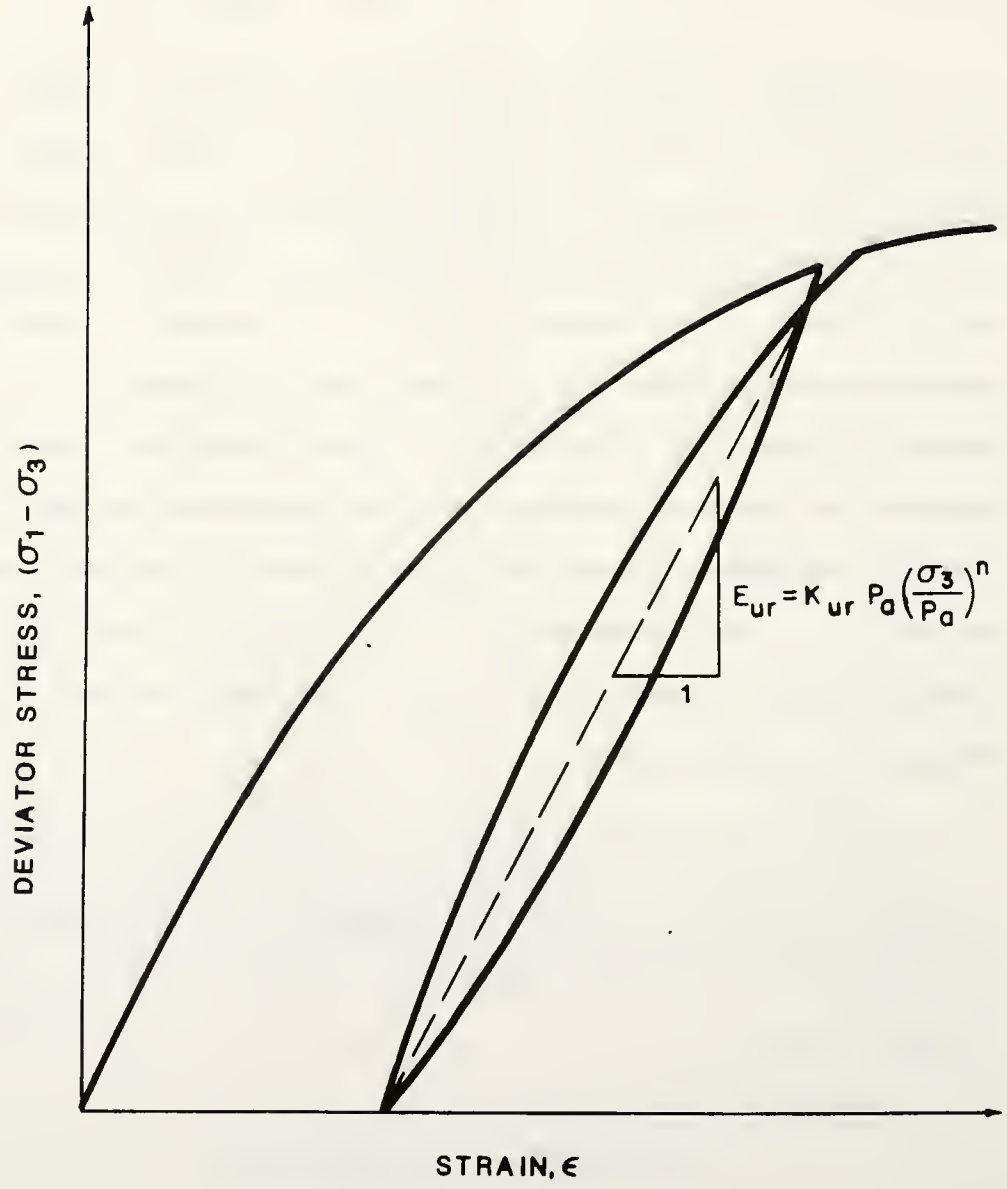

Figure 3.8: Unloading - Reloading Linear Elastic Approximation

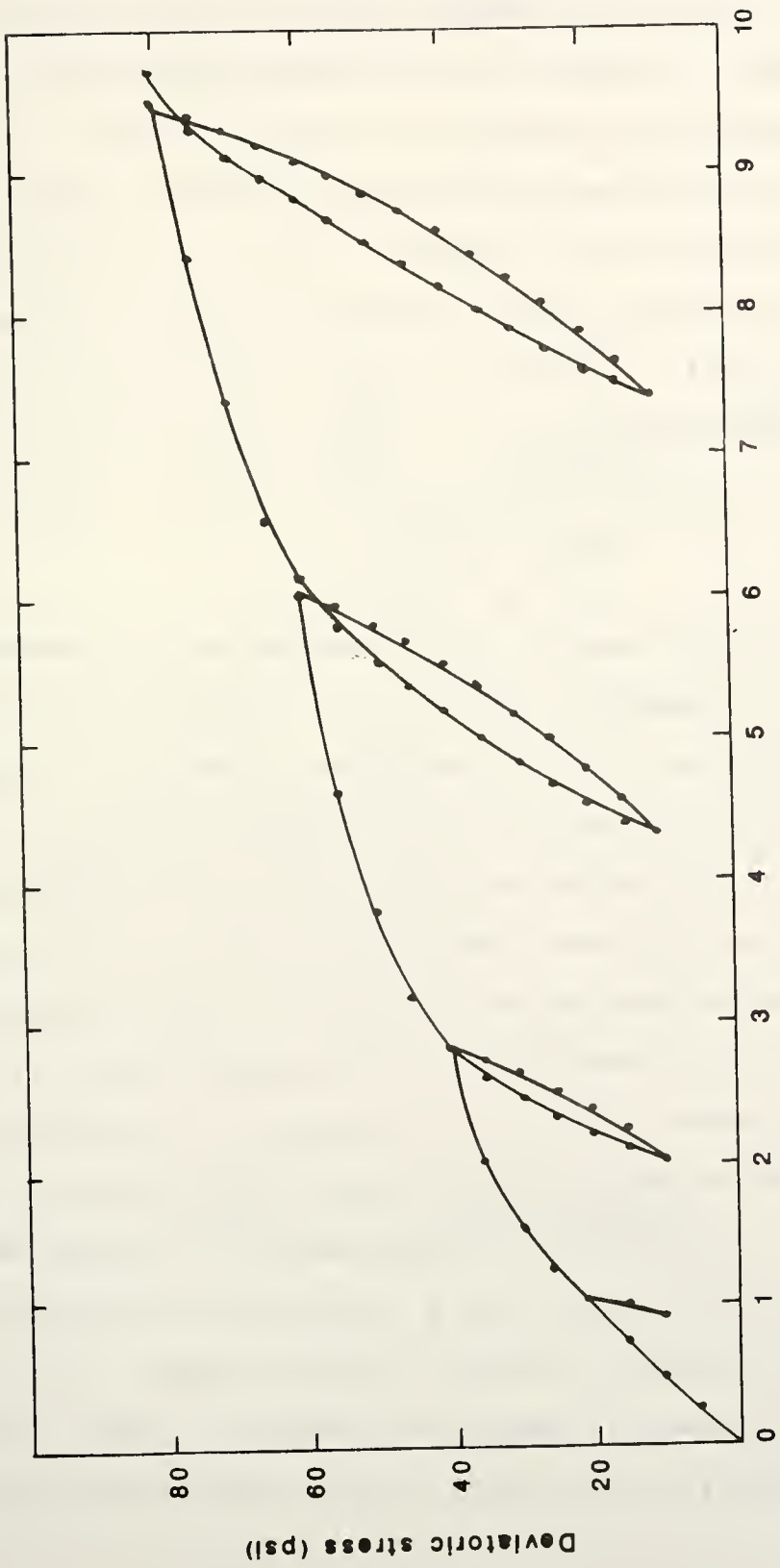

Figure 3.9: Hysteresis

The Masing criteria (Kavazanjian and Hadj-Hamou, 1980) is also used to model behavior during unloading and reloading. It states that the unloading-reloading curve will have the same shape as the virgin loading curve with the origin centered at the point of stress reversal and a scaling factor of two applied to the axis. This accounts for the hysteresis and nonlinearity at higher stresses. A complete cycle of loading returns to the point of reversal, then loading beyond the reversal strain will continue along the original virgin loading curve also called the backbone curve (figure 3.10).

The determination of when unloading or reloading begins is simple only in the case of uniaxial loading. For generalized loading conditions, there may be loading in one direction while unloading in the others, and the definition of loading may also depend on the coordinate system. In this case, the loading conditions and unloading criterion need to be expressed in terms of stress invariants. A discussion of this approach was given by Chen and Saleeb (1982). As indicated by these authors, this leads to the loading function in the theory of plasticity. A simplified technique may be to monitor the modulus of elasticity, and a decrease in the modulus from the last increment indicates further loading. If, however, the modulus attempts to increase in value, indicating a condition of unloading, the unloading-reloading

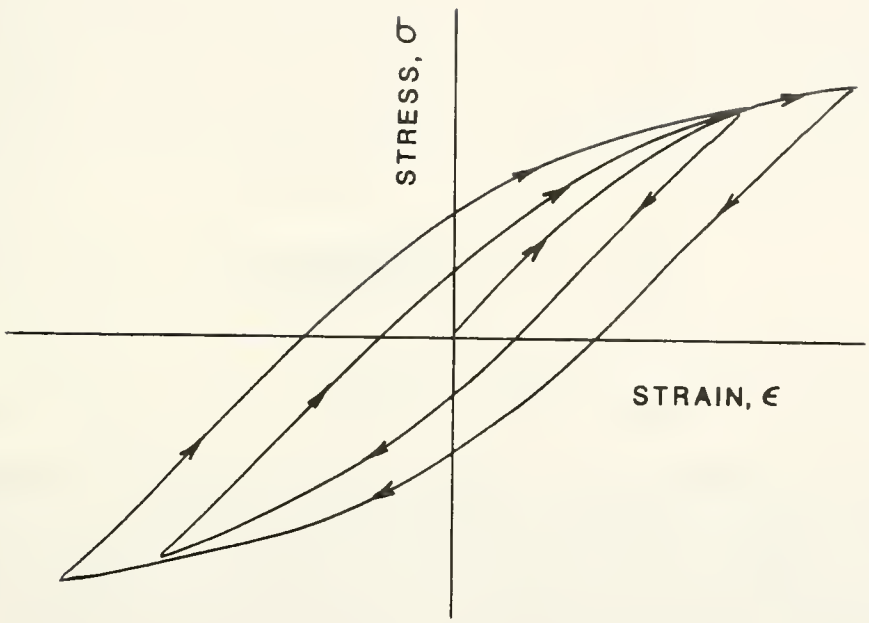

Figure 3.10: Masing Criteria

modulus can be used to simulate the near elastic behavior of this state. If, during a later increment, the modulus, as indicated by the model, decreases below the lowest previous value, the soil is beyond the reloading state and the modulus indicated by the model can again be used. This is the procedure used in the program "SPILES". The unloading-reloading modulus is approximated by the initial modulus of the soil. The approach used in this study is consistent with the approach followed by Duncan (1980).

Part II: Implementation

Introduction

Most finite element procedures are based on the solution of linear equations. Hence, special allowances have to be made to model nonlinear stress-strain behavior. Four techniques are often used: linear approximations, iterative, incremental, and mixed procedures.

Linear Approximations

These methods use only one set of moduli to compute the displacements under the total load applied to the system. No adjustment is made for error.

The most popular method is simply to use the initial moduli, that is, the moduli which exist before the load is

applied. Thus, the calculated values of strain will be less, i.e. unconservative, than the real values (figure 3.11).

To obtain conservative values, some investigators have used the moduli which exist at the final or loaded stage. Then, the calculated strains, as shown in figure 3.11, will be greater than the real strains. This method involves either estimating the final stresses before starting, or performing an additional increment (with assumed moduli) to establish them.

To reduce the errors, a third method establishes the moduli between the initial and final moduli. Additional increments are needed to establish the moduli. Often a modulus is chosen at some percentage of the final stress. The Runge-Kutta method uses the moduli at 50% of the stress difference. Although these methods will be more accurate, it is unknown if the solution is conservative or not.

These methods have the advantage of being simple and computationally efficient. They are best for stress-strain curves which are close to being linear. With highly nonlinear models, they may result in large errors.

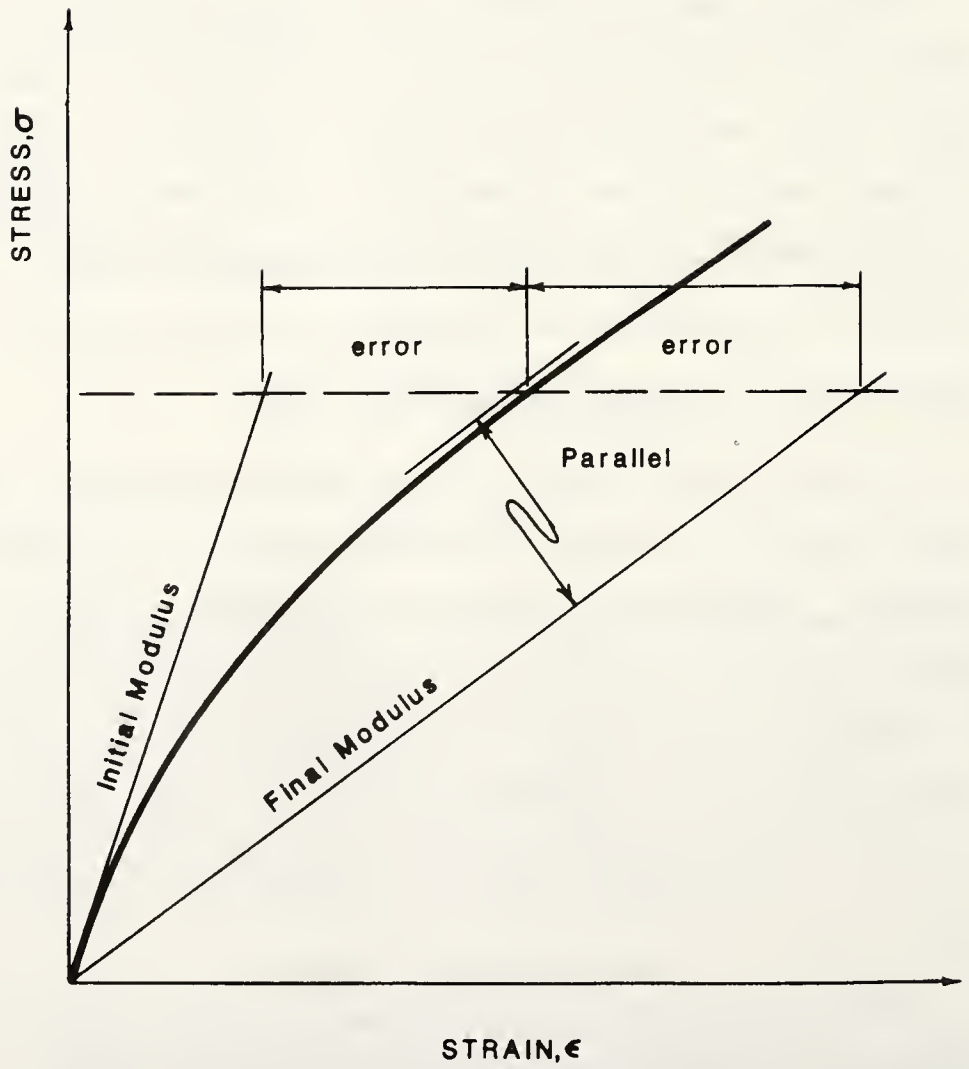

Figure 3.11: Linear Approximations

Iterative Methods

Iterative methods have the advantage of being able to converge towards the exact solution to any desired degree of accuracy. They can be divided into the constant and variable moduli approaches.

Constant Moduli Approach

These methods use only one set of moduli so that the total stiffness matrix is constructed only once. The most common method is the equivalent load method, often implemented as follows:

1. Assemble the total stiffness matrix using the initial moduli.
2. Compute the corresponding displacements.
3. Using the strains in each element, calculate the corresponding stresses from the constitutive relationship.
4. Integrate over each element to convert the stresses into nodal loads.
5. Consider these loads and corresponding stresses ($\Delta\sigma_1$ in figure 3.12) as the portion of the total load vector under equilibrium, and subtract them from the total loads to get the portion of the load and

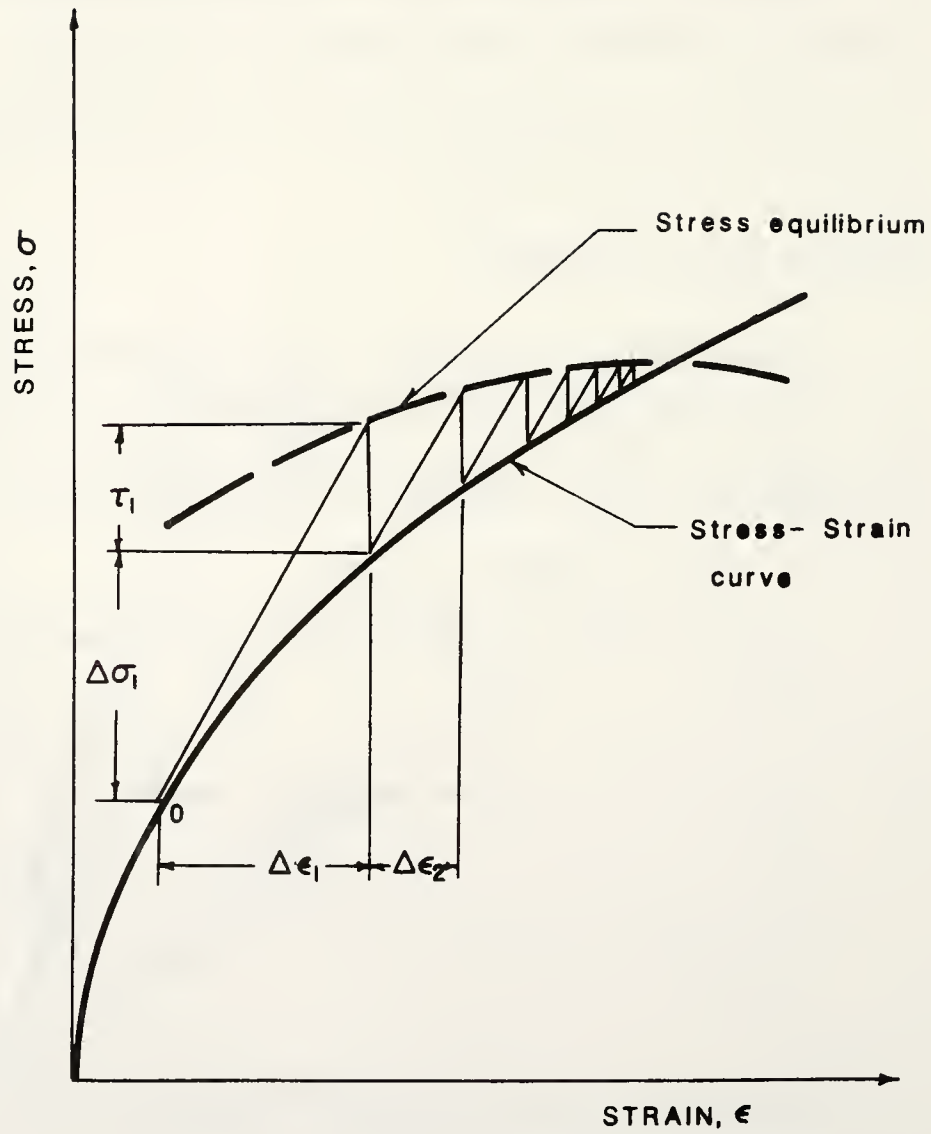

Figure 3.12: Constant Moduli Iterative Approach

corresponding stresses (τ_1 in figure 3.12) not in equilibrium.

6. Reapply the portion of the load not in equilibrium and repeat the procedure while making a summation of the corresponding displacements and strains ($\Delta\varepsilon_1$ in figure 3.12).

Several criteria have been suggested to monitor the convergence of this process. Naylor et. al. (1982) recommended the use of the square root of the sum of the squares of the errors:

$$\psi = \sqrt{\psi_1^2 + \psi_2^2 + \ldots + \psi_n^2} \qquad 3.26$$

where: ψ_i = error in strain for the ith degree of freedom,

n = number of degrees of freedom.

The process is stopped when ψ falls below a specified level.

An acceleration factor can be introduced to achieve convergence in fewer iterations. It is applied as a multiplier greater than 1.0 to the portion of the load which is not in equilibrium. In some cases, however, these multipliers will cause the load to go beyond its asymptotic value and numerical instabilities can occur.

A similar method uses the "correct" and "non-correct" portions of strain rather than stress to converge on the

correct solution. This latter technique is not always numerically stable.

Variable Moduli Approach

Convergence can often be achieved in fewer steps if the moduli can vary and the total stiffness matrix is rebuilt for each iteration. The new moduli are chosen as the tangent moduli at the stress level of the portion of the load which is in equilibrium.

Direct Iteration Approach

Sometimes referred to as the secant stiffness method, direct iteration only involves changing the moduli until convergence is achieved. The procedure is as follows:

1. Calculate the strains corresponding to the final loading state using the initial moduli. Calculate the stresses corresponding to this state of strain.

2. Determine the "correct" strain corresponding to this final stress state for the model with nonlinear stress-strain behavior. Determine the error between the calculated strain and the "correct" strain.

3. If the error is unacceptable, use the "correct" point on the nonlinear stress-strain curve to compute new values of moduli and repeat the process.

Graphical representations of the direct iteration method are shown in figure 3.13 for three iterations.

Newton-Raphson Method

This method is identical to the constant moduli approach with the exception that each new iteration involves recomputing the moduli and reforming the total stiffness matrix (figure 3.14). The constant moduli approach is sometimes referred to as the modified Newton-Raphson Method.

Advantages and Disadvantages

The greatest advantage of the iterative procedures are that they can converge to any desired degree of accuracy. There are, however, several disadvantages. One is that the technique may be divergent for some models, especially if the material is strain hardening. An example of a non-converging iteration is shown in figure 3.15. Non-convergence problems may also be encountered if a negative slope occurs in the material stress-strain curve for all cases, except the direct iteration method. Another problem is that it may take many iterations to converge towards the correct solution, especially if the material is highly non-linear. The number of iterations is reduced if the variable moduli techniques are used; however, more computer time is required to continuously rebuild the total stiffness matrix.

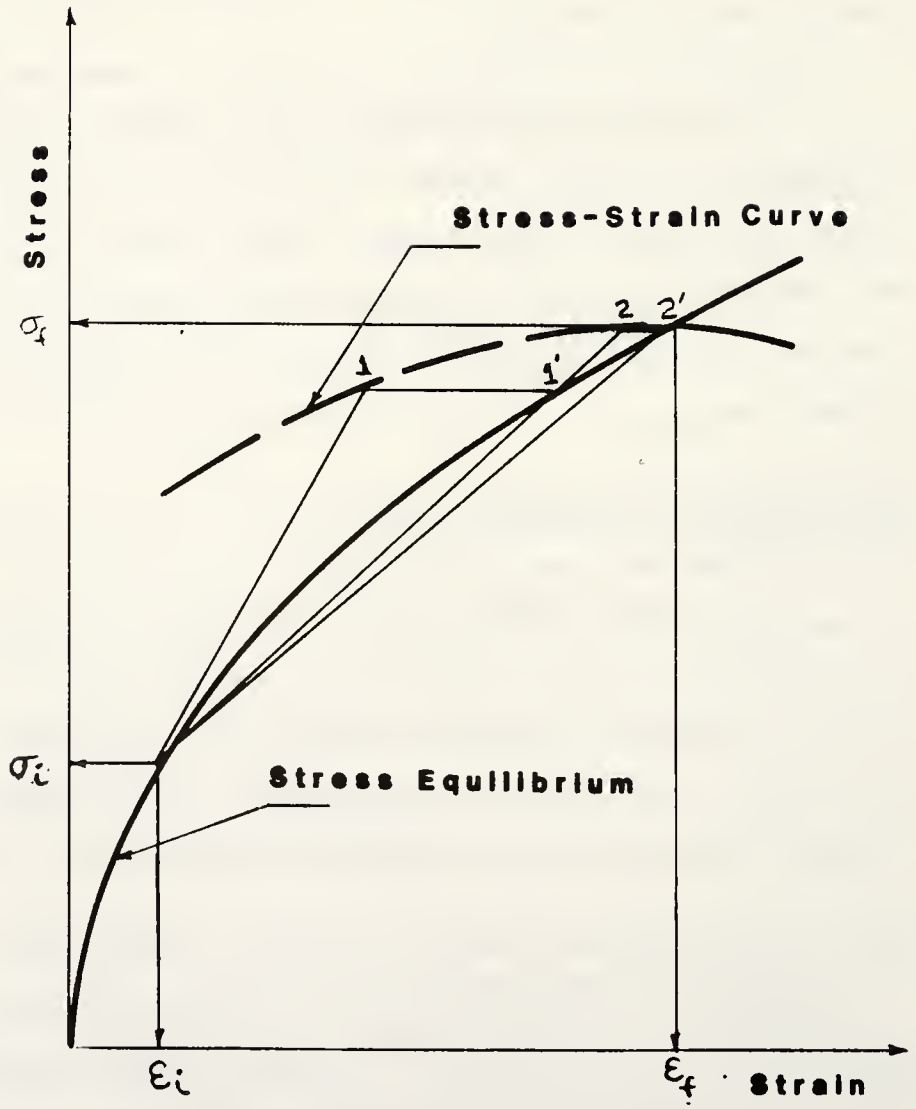

Figure 3.13: Direct Iterative Approach

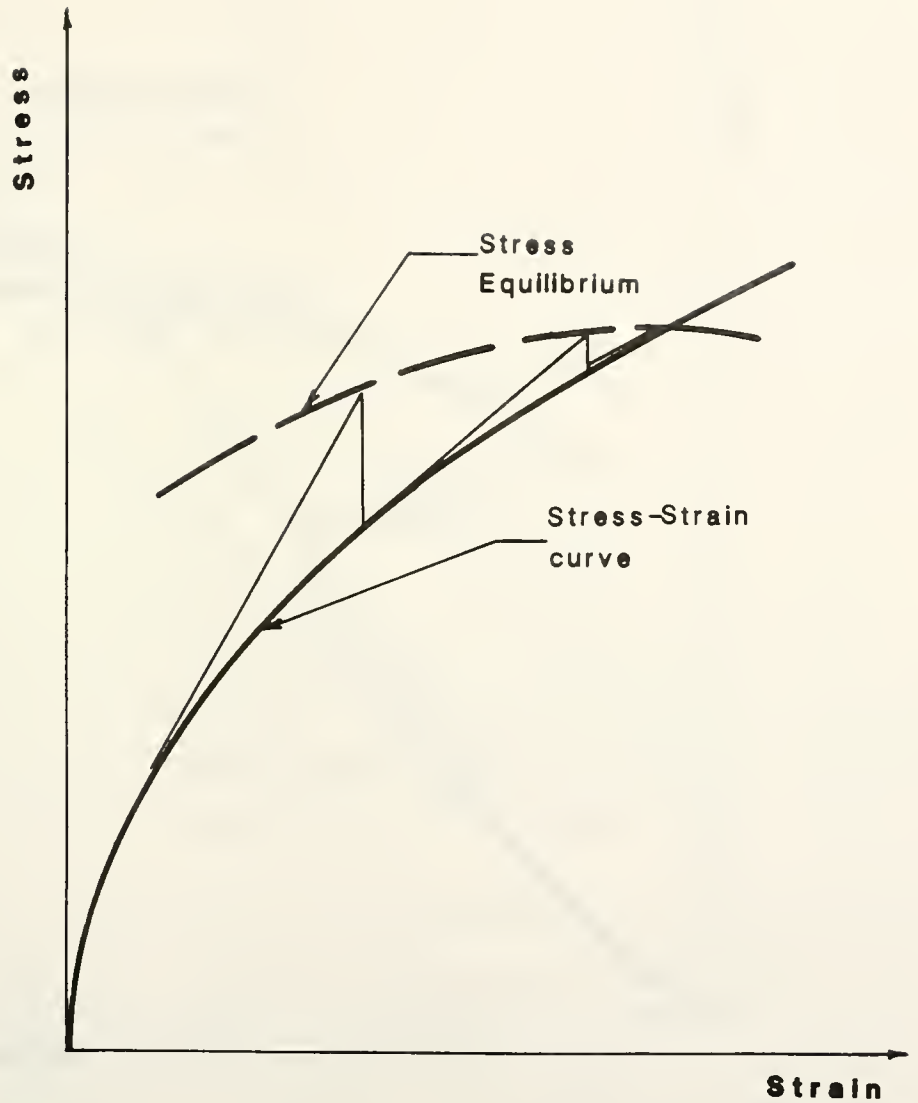

Figure 3.14: Newton-Raphson Method

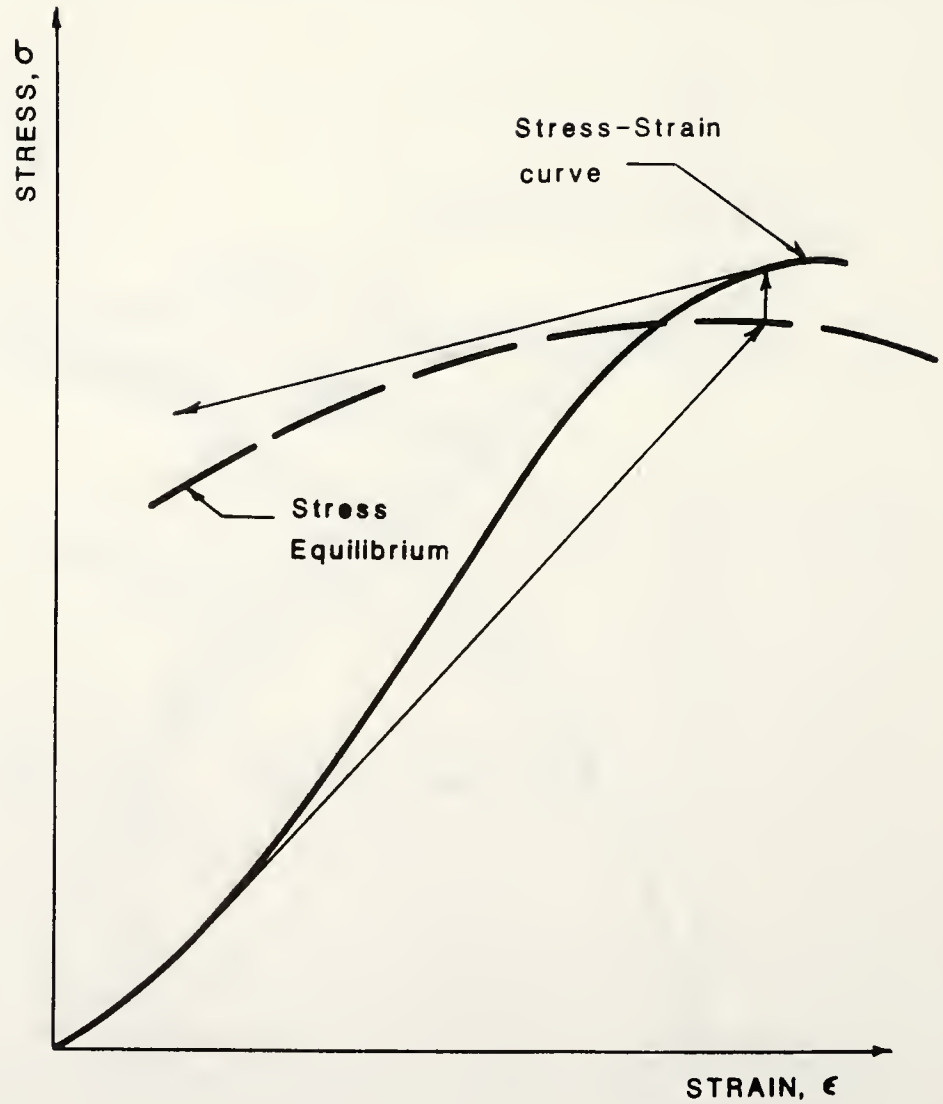

Figure 3.15: Nonconvergent Iterations

Incremental Method

A third technique to model a nonlinear stress-strain behavior is to represent the curve as a series of linear elements. Each of these linear portions is an increment. Each increment represents a portion of the total load or can model a phase in a construction sequence. The typical procedure is to compute an initial tangent modulus based on the initial stress state of the element, apply a portion of the load, recompute a new modulus and keep repeating the process until the final stress state is achieved. As indicated before, using the initial moduli of each increment to represent the increment will yield a non-conservative solution, whereas using the final moduli to represent each increment will give a conservative solution (figure 3.16). Moduli between these values will yield a curve somewhere between the two extremes.

The advantages of the incremental technique are that it is simple to use and computationally efficient; often, only a few increments are needed to achieve a tolerable error. Also, the increments can be used to represent construction sequences such as building up an embankment or making an excavation. The disadvantage is that it is not possible to specify a limiting error, the error can only be checked at the end. Errors can be reduced by using

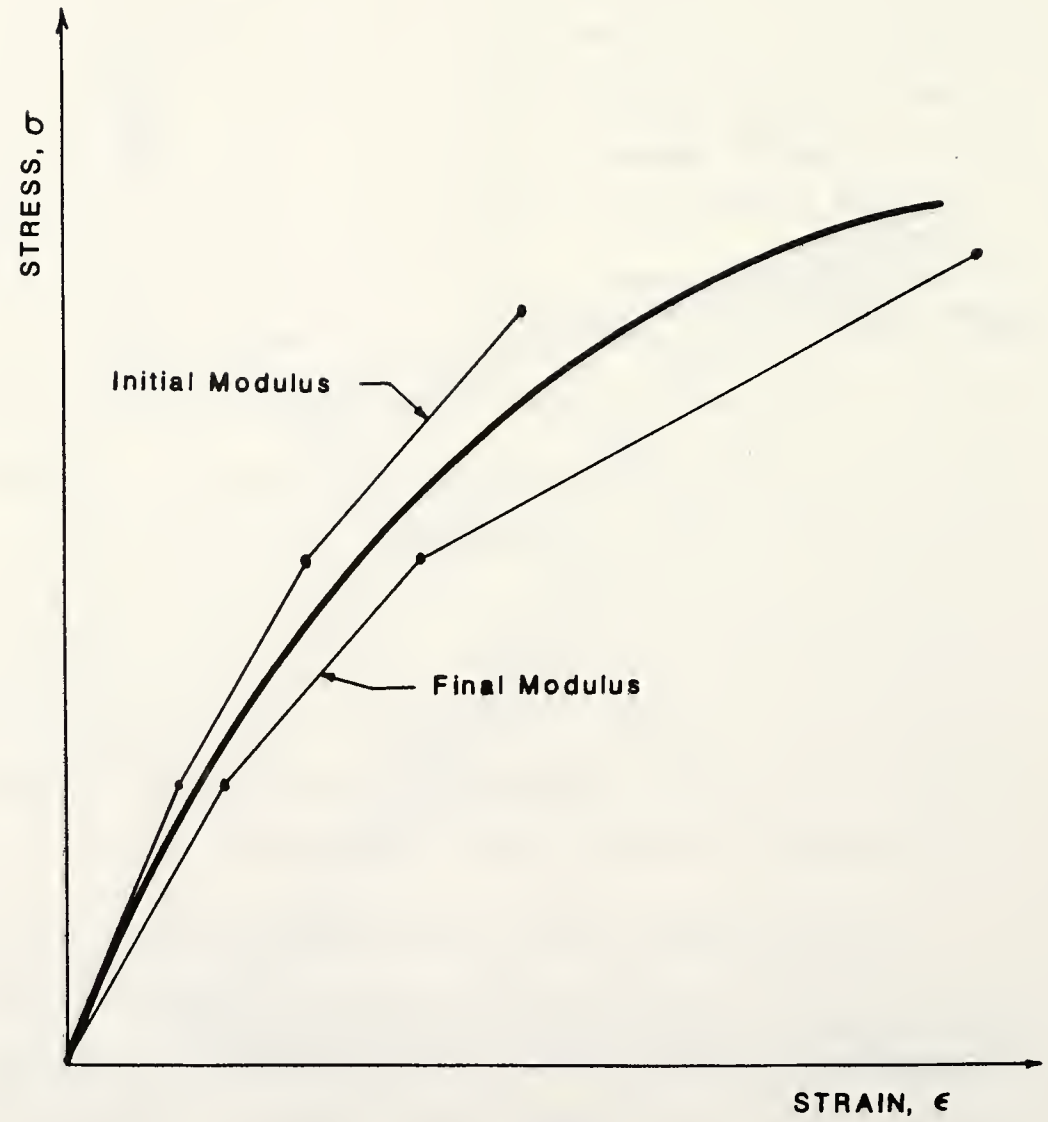

Figure 3.16: Incremental Method

more increments. If the change in stress can be estimated, it is possible to calculate the error involved beforehand as a function of the number of increments. A test of the errors involved for a typical nonlinear soil model which is to be used in this study was conducted. The results are shown in figure 3.17.

It is an incremental technique using the initial moduli approach which is used in this study.

Mixed Method

As a final note, it is possible to combine the iterative and incremental approaches to utilize the advantages of each. By adjusting the number of increments and the error tolerance during iterations, an optimum solution scheme can be found. The technique uses an iterative process within each increment (figure 3.18).

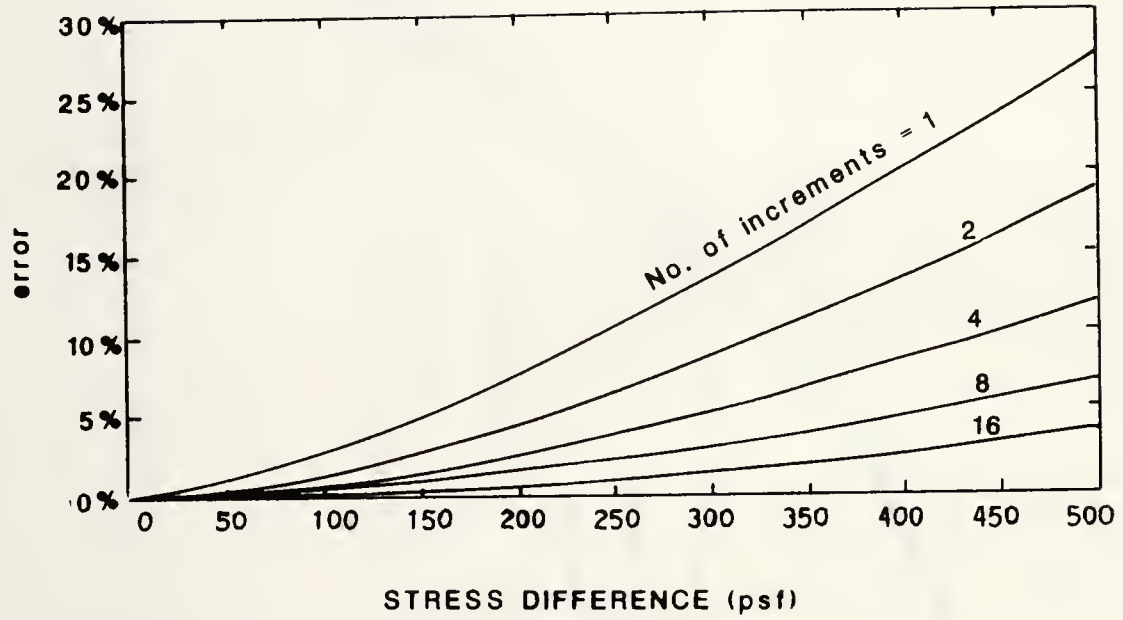

Figure 3.17: Errors Involved in the Incremental Method for a Specific Nonlinear Soil

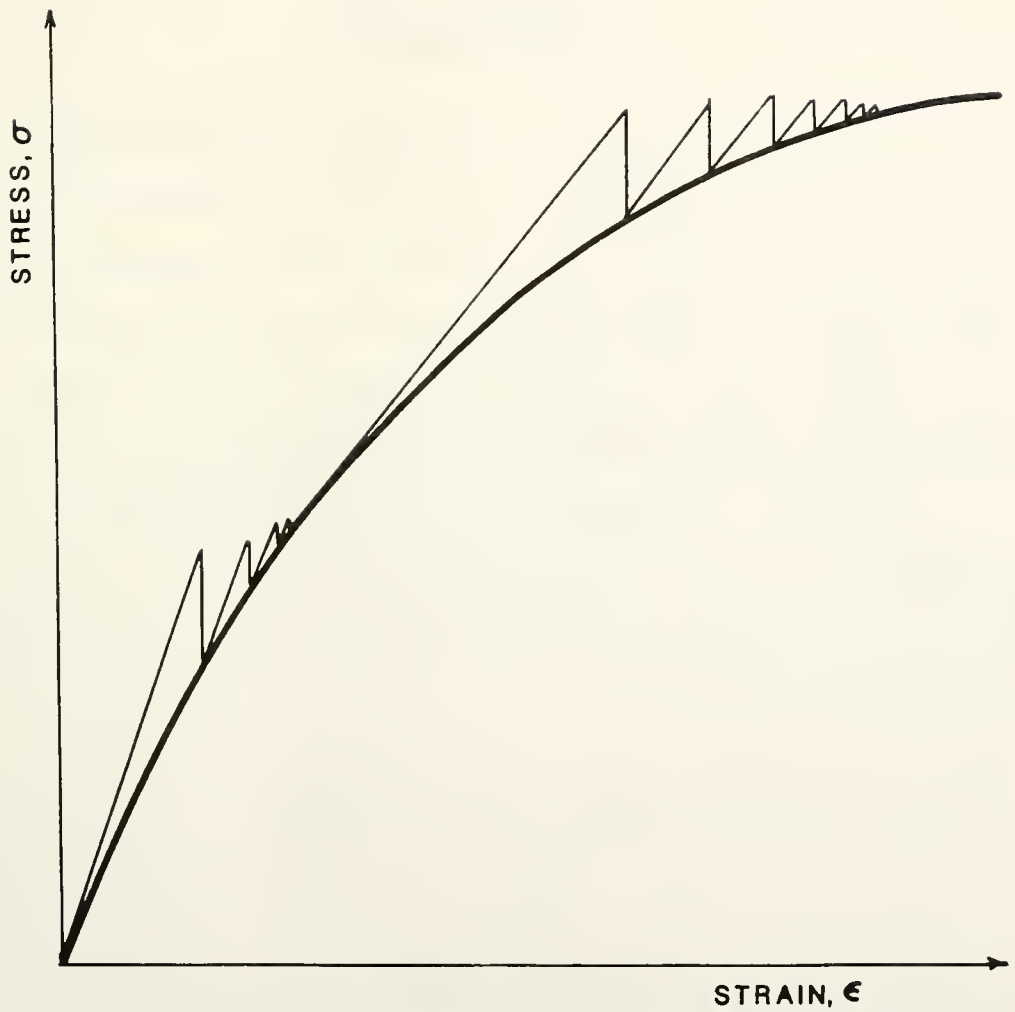

Figure 3.18: Mixed Approach

CHAPTER 4: FINITE ELEMENT MODEL

Introduction

As described in the introduction to this report, a very important aspect of the research program on the stability of reinforced slopes was to develop a finite element computer program which makes allowance for the three dimensional characteristics of the soil-pier system. The computer package "SPILES" and a number of related programs were developed to achieve this objective. The main features of these programs are presented in this chapter. Applications of the method are given in Chapters 5, 6 and in the Appendix to this report. The documentation of the computer programs developed for this study can be obtained from the Joint Highway Research Project, Purdue University, West Lafayette, IN.

This chapter is divided in three sections. The first section deals with the input parameters required by the programs and the mesh generators. Several mesh generators were developed to cover most of the cases which can be encountered in practice. The characteristics of the program "SPILES" (i.e., types of elements, material models,

initial stresses, and solution techniques) are discussed in the second section. Finally, the post-processing of the finite element results with respect to stability analysis is presented in the last section.

Part I: Input

Four types of variables are discussed in this section: loading conditions, slip surfaces, geometry and soil properties, and pier characteristics. Mesh generators were developed to provide an efficient input system by digitizing a soil mass into degrees of freedom, nodes, and elements. The geometric and loading conditions covered by these mesh generators are also presented in this section.

Variables

Loading

Three cases of loading are considered in this study: surcharge, cut slope, including an excavation from a horizontal ground surface, and self weight (figure 4.1). A surcharge loading is applied downward above the crest of the slope when either the embankment height is raised or a structure is built above the slope. A cut slope is modelled as upward forces along the slope and toe of the slope. For example, these forces may be caused by

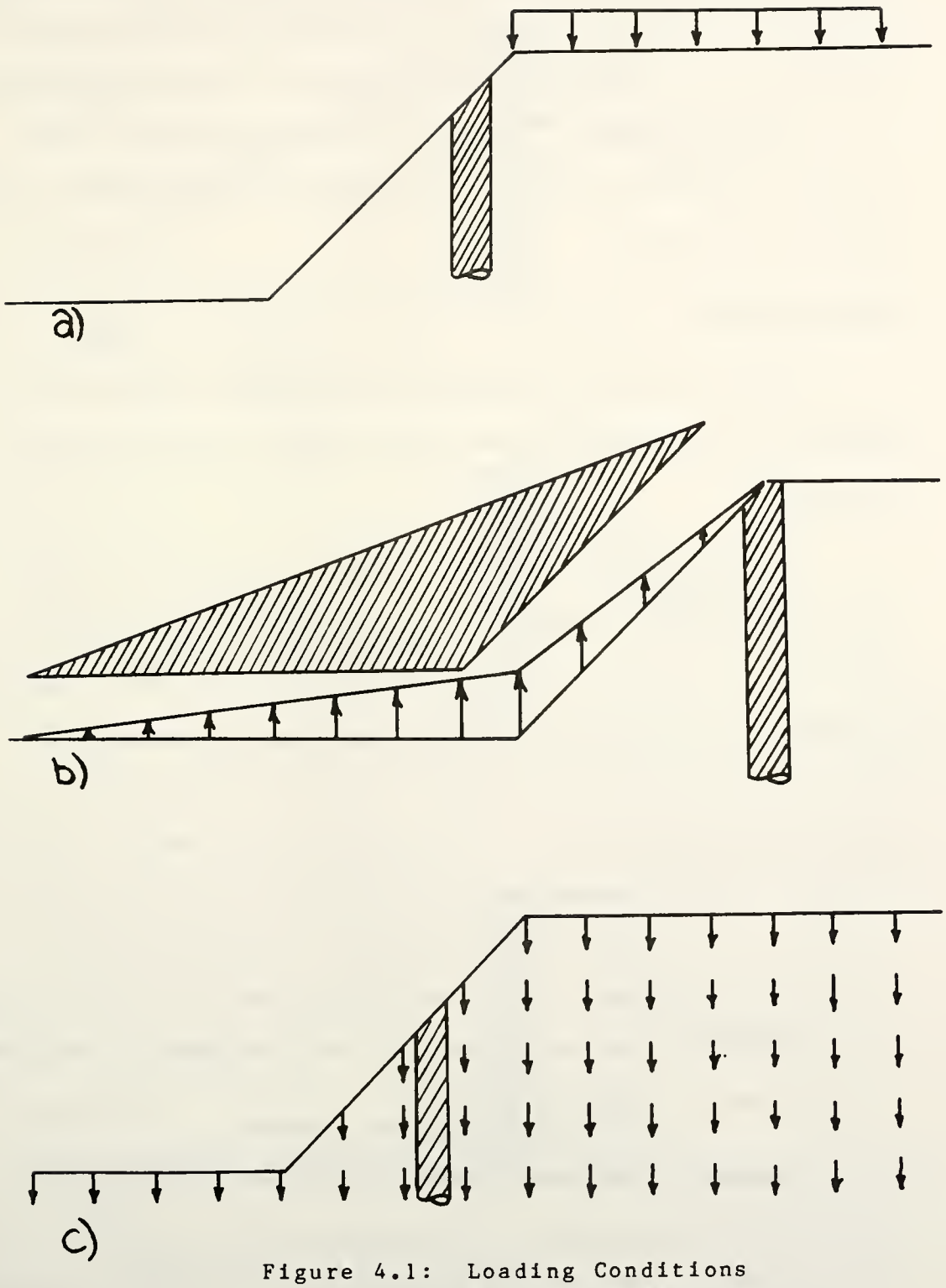

Figure 4.1: Loading Conditions
a) Surcharge
b) Cut Slope
c) Selfweight

excavating material from the toe to provide a wider roadway. Increasing the self weight of the material in the slope is modelled by increasing the unit weight of all the elements in the same proportion and calculating equivalent nodal loads. This can provide an assessment of the general stability of a slope.

Slip Surfaces

Slip surfaces containing slip elements are used to model the presence of a weak soil layer or the soil-pier interface.

Slip elements are not used when it can be assumed that good bonding exists between the pier and the soil. This will usually correspond to a mode of failure in bending with large pressures transmitted to the pier. The pressure will increase towards the top of the pier to produce a large moment in the cantilever type member (figure 4.2a). Slip elements can be introduced around the pier to assess the possibility that a "flow" type failure will occur: in this case, less pressure is exerted on the pier as the soil contact is broken and soil movement is allowed around the pier (figure 4.2b).

Commonly, weak seams will develop along the bedrock/soil interface as groundwater tends to move along this boundary. This may be especially prevalent in poorly

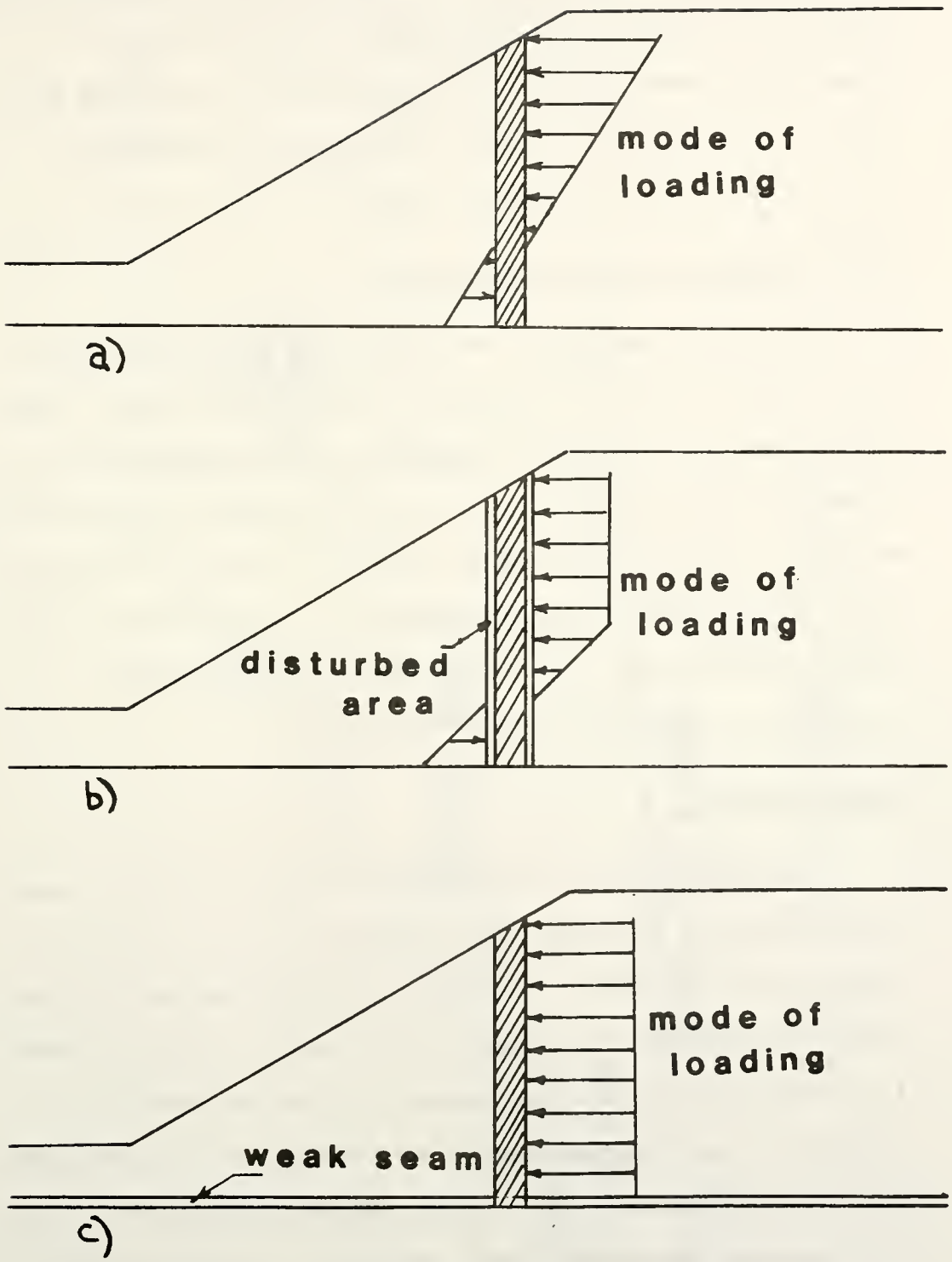

Figure 4.2: Slip Surfaces
a) No Slip Surfaces
b) Disturbed Area Around the Pier
c) Weak Seam Along the Bedrock

constructed side-hill fills. The same slip elements used around the piers can be used along this boundary. If these weak seams play a significant role, the slope will move as a rigid mass which could lead to a shearing failure of the pier (figure 4.2c).

Slope Geometry and Soil Parameters

The basic geometric variables are the slope angle, slope height, depth to bedrock, and bedrock angle (figure 4.3). The soil parameters depend on the model which is chosen for the analysis. The linear elastic system uses a modulus of elasticity and a Poisson's ratio. The Duncan-Chang model requires five parameters to represent a non-linear modulus and three additional parameters to represent a variable Poisson's ratio.

Pier Parameters

The relevant pier characteristics are the pier spacing, diameter, position with respect to the toe of the slope, and stiffness. The spacing is defined as the distance between the centroids of the piers. The stiffness is introduced through the product EI of the modulus of elasticity and bending moment of inertia of the pier (figure 4.4). Additional variables can be introduced to take into account the effect of a staggered formation, that is the use of multiple rows of piers.

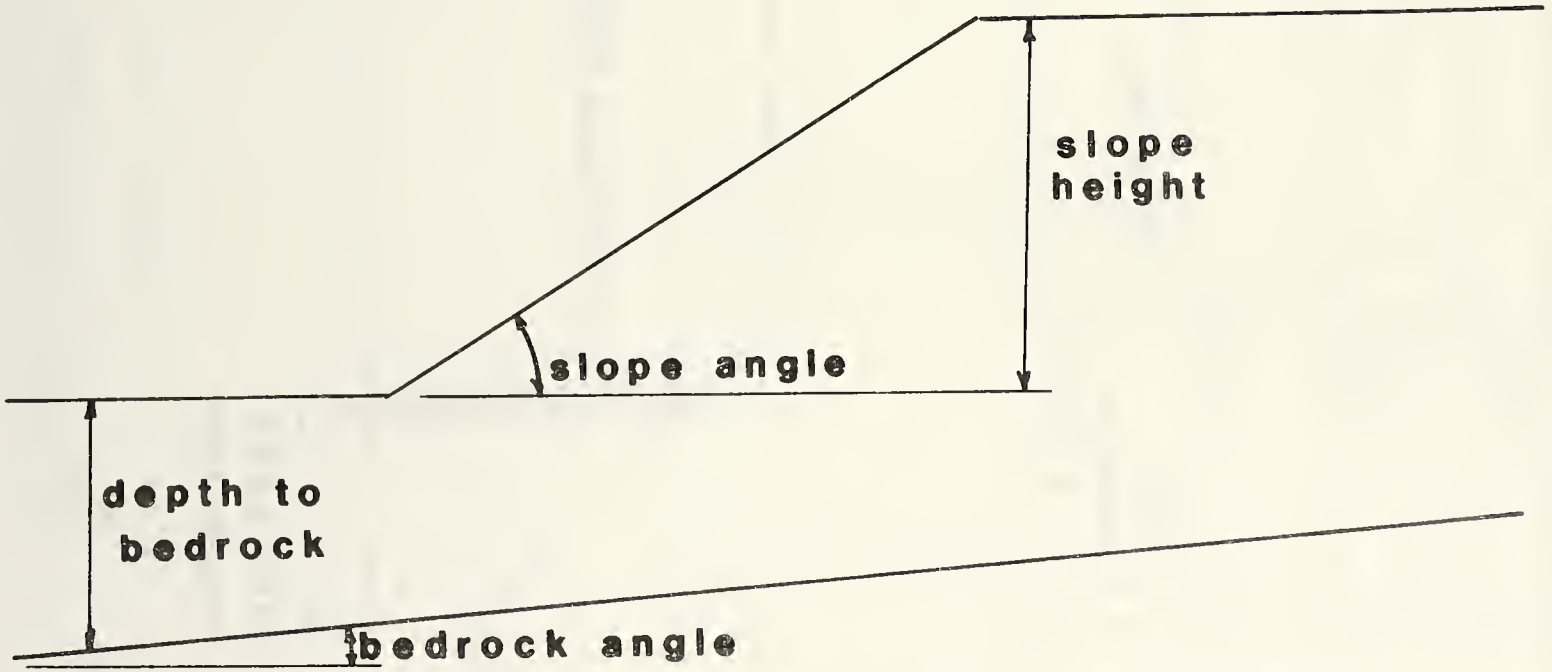

Figure 4.3: Basic Geometric Parameters

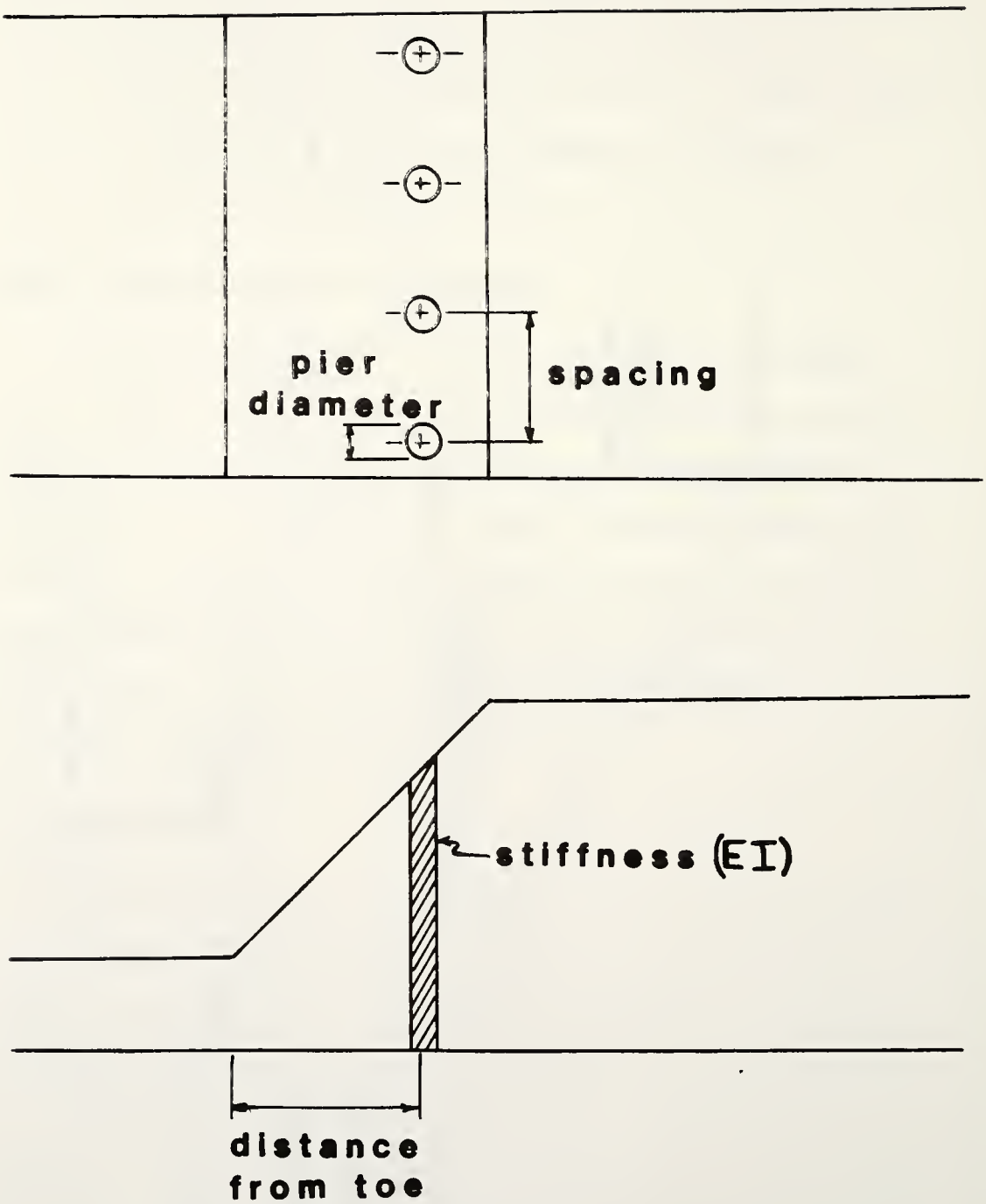

Figure 4.4: Pier Parameters

Mesh Generation

To accommodate for all the different variables described above and the different types of analysis, it was necessary to develop several independent mesh generators.

These mesh generators have several features in common: (1) Each mesh represents a slice of the slope bounded by lines of symmetry going between the center of a pier and the midpoint between piers; (2) The ends of each slice are represented by vertical rollers, the sides are horizontal rollers and the bottom is fixed; (3) The pier provides an elastic boundary against the soil mass (figure 4.5). Each generator allows for a bilinear slope, broken at the pier, connected to horizontal surfaces above and below the slope.

In general, the variables for all of the mesh generators are the same. The input consists of the spacing between the piers, the size of the piers, the number of elements across the width of each slice, the geometry of the slope and the soil parameters. The generators also allow for a sloping bedrock. The geometric input parameters are shown in figure 4.6. Additional control variables are used to control the fineness of the mesh and the concentration of elements in critical areas.

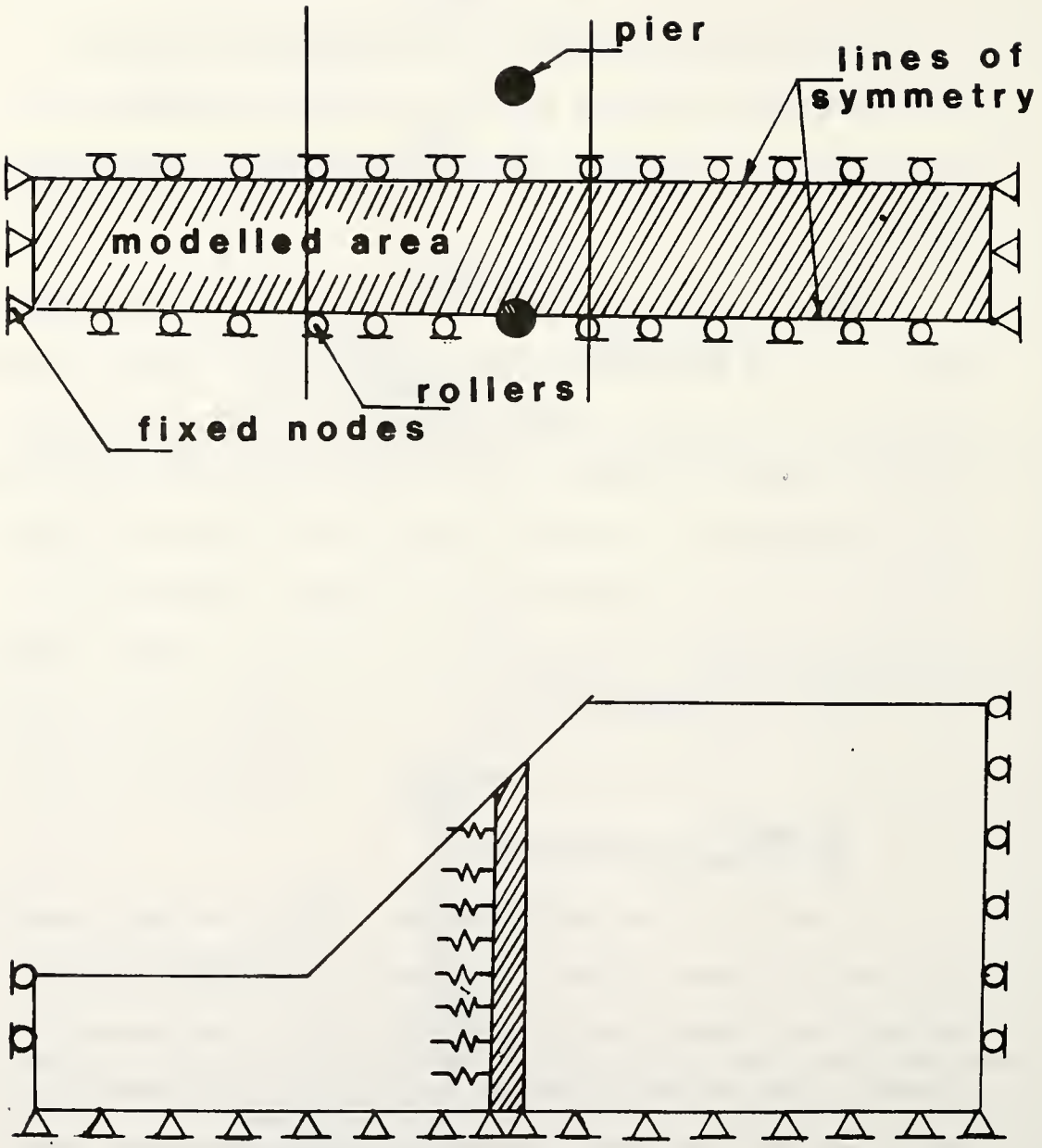

Figure 4.5: Finite Element Model

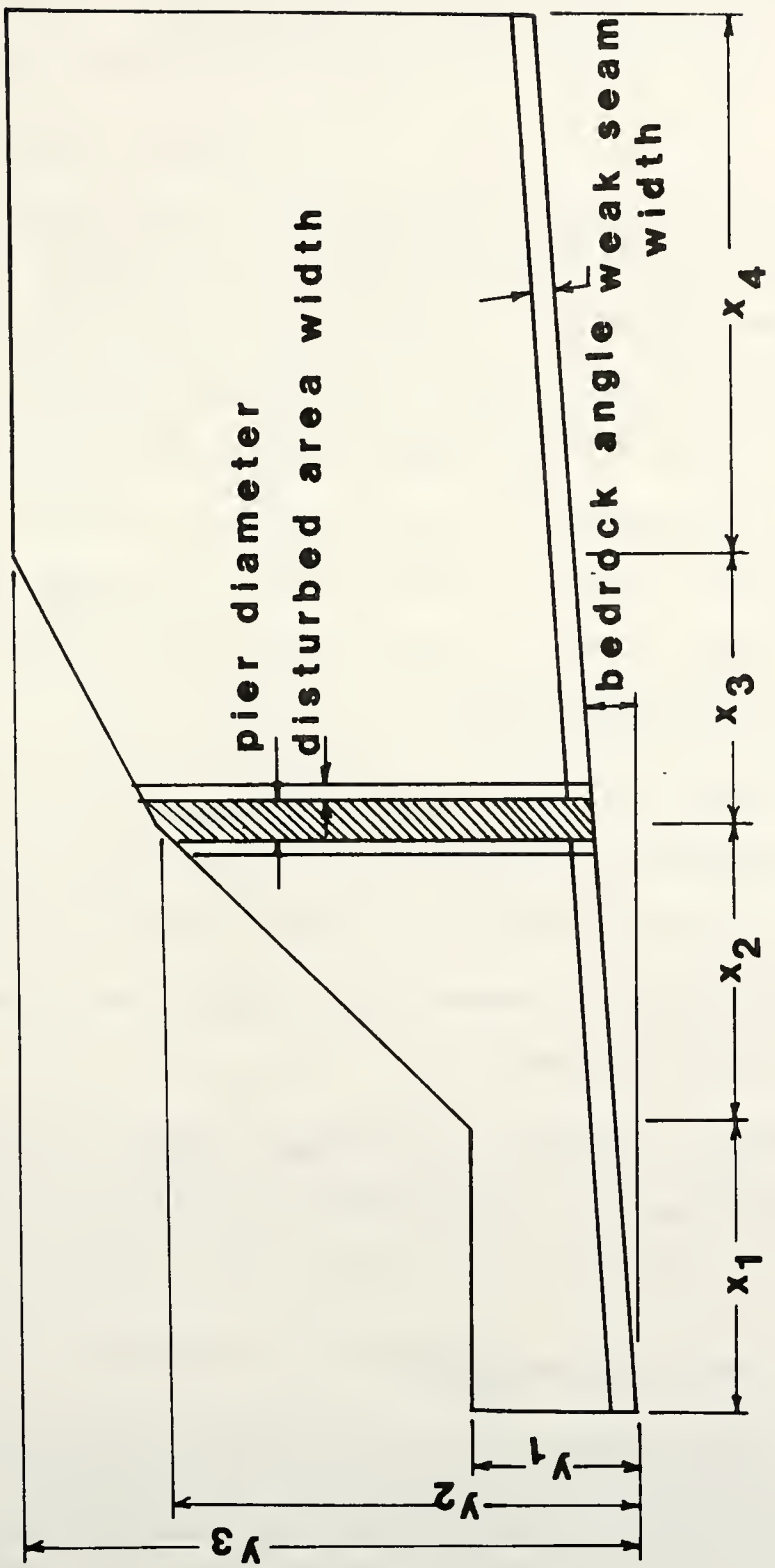

Figure 4.6: Geometric Input Parameters

The particular characteristics of each of the mesh generators are described in the following:

No Pier

The finite element mesh without piers actually represents a two dimensional case. This case is solved using three dimensional finite elements so that it retains consistency with the shape functions and integration techniques used for the other cases, and so that the initial stresses corresponding to this case can be easily transferred to cases involving a pier. Although there is no pier present, the "no pier" case retains the ability to solve for a bilinear slope.

The primary purpose of solving the case of an unreinforced slope is to establish the initial stress condition for cases involving piers. A second reason is to provide a reference point to assess the effectiveness of the piers in retaining the slope.

This mesh generator has two main options corresponding to the absence or presence of weak seams, respectively.

No Pier Without Slip Elements

This represents a case where no weak seam has developed between the bedrock and the soil material. A

rotational type of slide is expected to be most prevalent in these situations.

No Pier With Weak Seams

In cases where a weak seam has developed between the bedrock and the soil material, a second mesh generator which incorporates thin, weak (i.e., low modulus) elements along the bedrock is used. Block type sliding is expected in this model.

One Row of Piers

Three mesh generators have been developed to address the most important problem in this study, that is the case of one row of piers within the slope.

One Row of Piers Without Slip Elements

This is the most simple condition for a single row of piers (figure 4.4). The basic mesh is the same as the case above (No Pier Without Slip Elements), except that the three dimensional capabilities of the program will be needed to model the movement of soil around the pier.

One Row of Piers With Weak Seams

The same model used to describe weak seams in the case of "no pier" is incorporated in a mesh with one row of piers. The piers extend through the weak seam into the bedrock.

One Row of Piers With a Disturbed Area

The weak elements used in the mesh with weak seams are introduced around the pier to simulate a weak adhesion between the piers and the soil or a softer material due to disturbance from drilling.

Note that an extension of these generators would be to develop a mesh generator which accounts for both the effects of a weak seam along the bedrock boundary and a disturbed area around the piers.

Two Piers

This mesh is used to model two rows of piers in a staggered formation. This configuration may have an advantage from a constructional point of view, allowing more space between the piers.

Excavated Slopes

Additional features are provided to solve problems which involve incremental excavations to form slopes. A special generator produces a wedge shaped soil mass which can be excavated in increments (figure 4.7). Stresses during excavation of this wedge shaped mass are transmitted to the slope as nodal loads. Displacements due to unloading the final slope are transferred back to the wedge to simulate the unloading process.

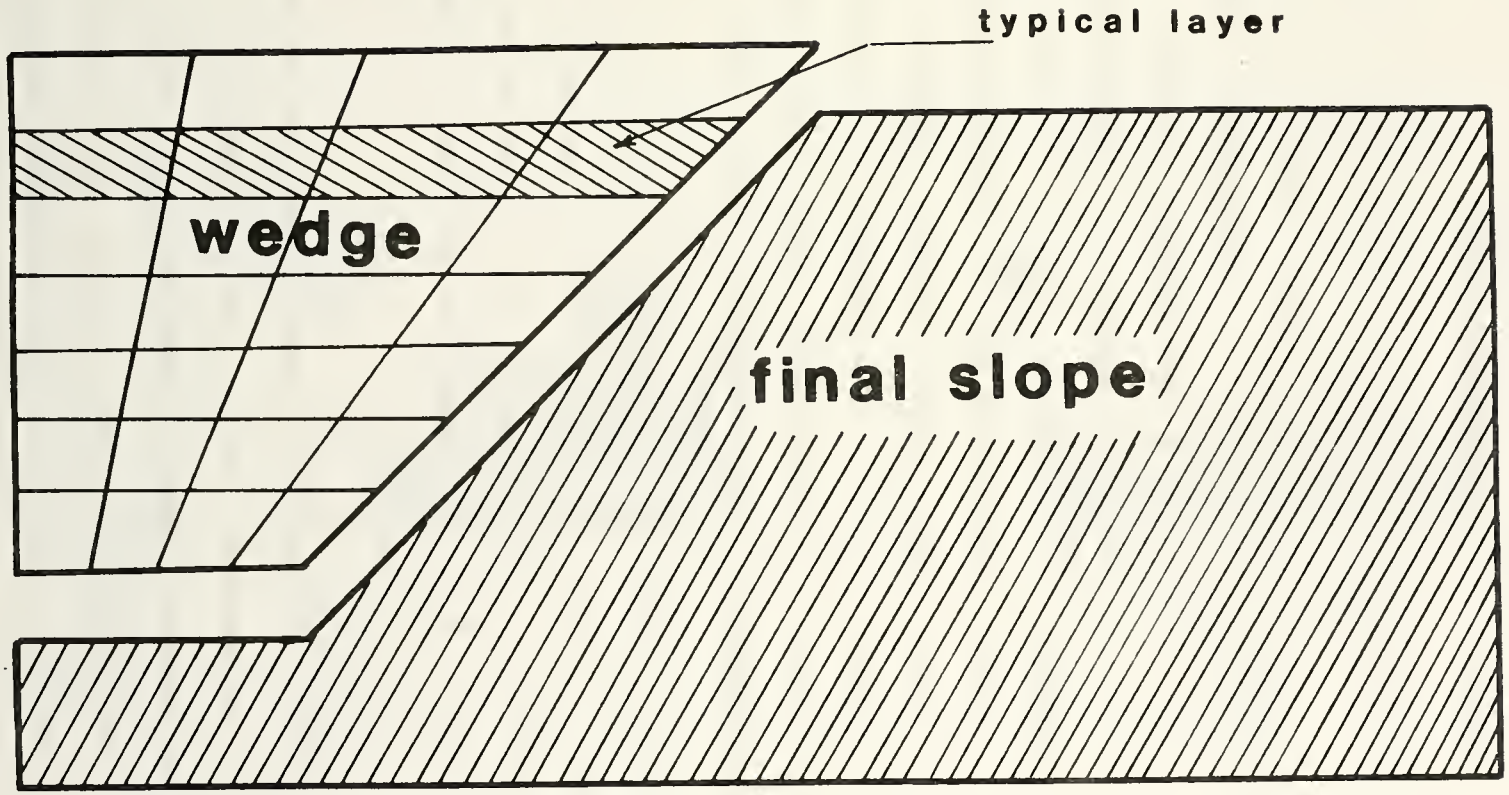

Figure 4.7: Mesh Generator for Excavated Slopes

Part II: The Program "SPILES"

The program "SPILES" is a user-oriented finite element program to calculate the resistance offered by passive, laterally loaded piers and the displacement of the surrounding soil. The common active loading on piles occurs when an external force is applied to the pier and the soil is resisting the movement. This is the case of piers used to support a retaining wall or structures subjected to wind loads (figure 4.8a). Passive loading is defined as the forces caused by the movement of the soil around the piers such as piles used to resist slope movements (figure 4.8b).

The program is dedicated to solving this problem and, thus, is simple to use and easy to modify. The number of options is limited but sufficient to solve most actual problems. Efficient mesh generators are provided to limit the number of input parameters.

The program is divided into several sections which are completely independent. Hence, the program can be easily modified; as an example, a new soil model could be introduced in the program without changing the integration technique or the output section. Each variable is used

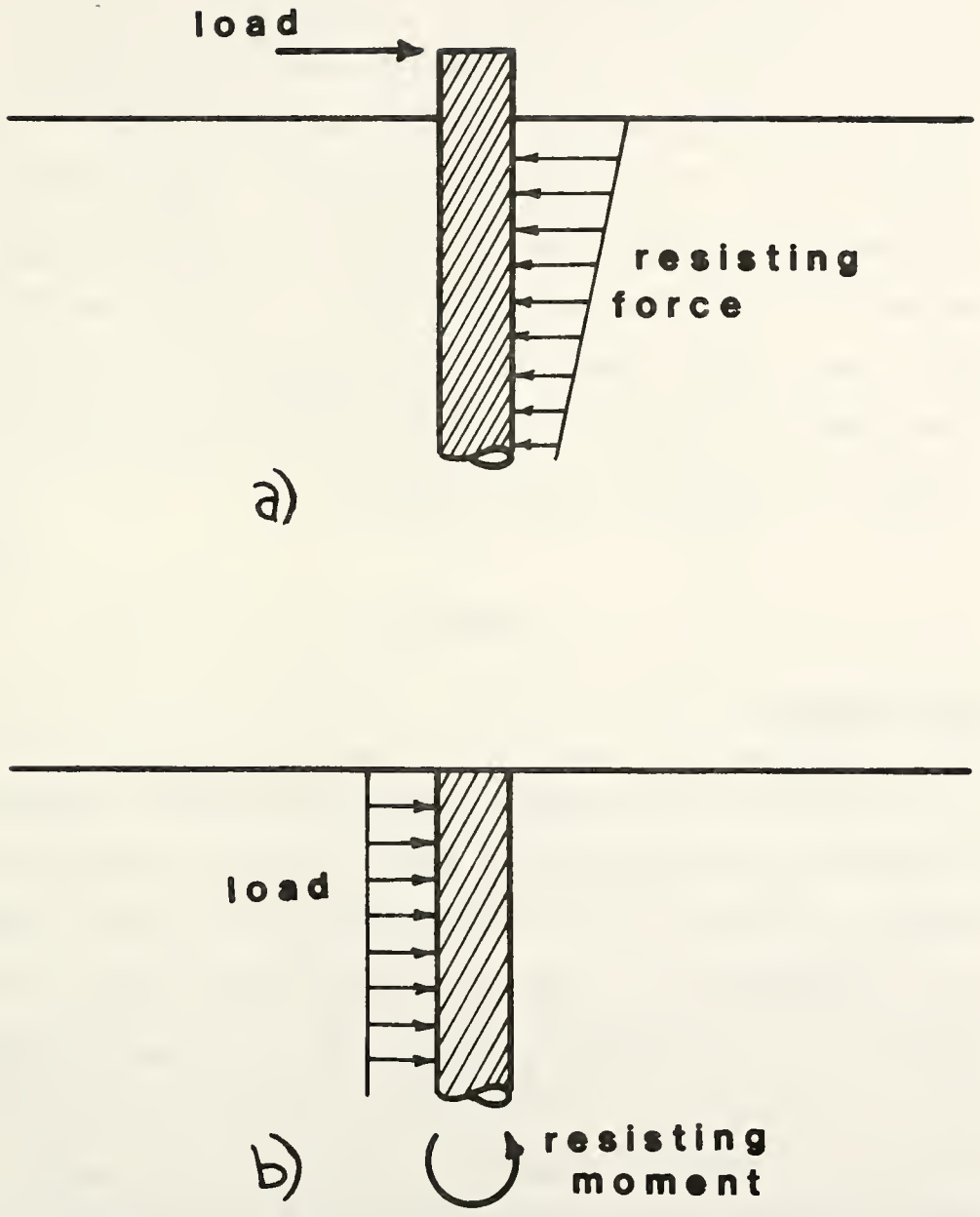

Figure 4.8: Laterally Loaded Piers
a) Active Case
b) Passive Case

for only one purpose, which allows for easy recall from any location in the program. Furthermore, the program does not require system subroutines for its execution, and can be easily implemented on any computer system. It was used at Purdue on the Vax 11, Gould, CDC 6500, Cyber 205, and IBM 3083. Because of the large storage requirements, the size of the problems solved on the CDC 6500 was limited. The program does not take advantage of the vectorization options available on the Cyber 205 and so does not operate efficiently on that machine.

Elements

Soil Elements

The basic soil element is a linear strain eight node isoparametric parallelepiped which has the capability of adding a mid-side node to one or more of its sides; thus, it is expandable to a quadratic strain twenty node isoparametric parellelepiped. These "brick" shaped elements have the advantage of being simple to visualize when the elements are stacked together to form the total model. Elements, such as the tetrahedra, which are composed of diagonal boundaries are often difficult to conceptualize in three dimensional space. This could lead to errors in nodal numbering (Zienkiewicz, 1977, pg. 14).

The additional nodes are necessary to define the circular cross section of the piles and useful in subdividing the mesh in critical areas to improve numerical accuracy. A typical element is shown in figure 4.9a. The process of adding midside nodes at will is achieved by modifying and adding to the basic eight node shape functions. This process was introduced by Cook (1981, pg. 127) for two dimensional cases, and extended here to the three dimensional case. The variable shape functions developed for this study to account for midside nodes are given in table 4.1.

A second order Gauss quadrature (eight Gauss points for the three dimensional element) is used to integrate over the shape functions to determine the stiffness coefficients. The second order Gauss quadrature is accurate for quadratic three dimensional elements (Irons, 1971; Hellen, 1972; Zienkiewicz, 1977, pg. 203). For simplicity, the Gauss points are assigned the same number as the closest corner node in the local coordinate system (figure 4.9b).

As the mesh is generated, going from the toe to the crest of the slope (left to right in figure 4.10), the increased depth calls for more elements to be used. To account for this, several elements have one of their sides divided by a midside node (figure 4.11a). The lower side of each of the two elements adjacent to an element with a

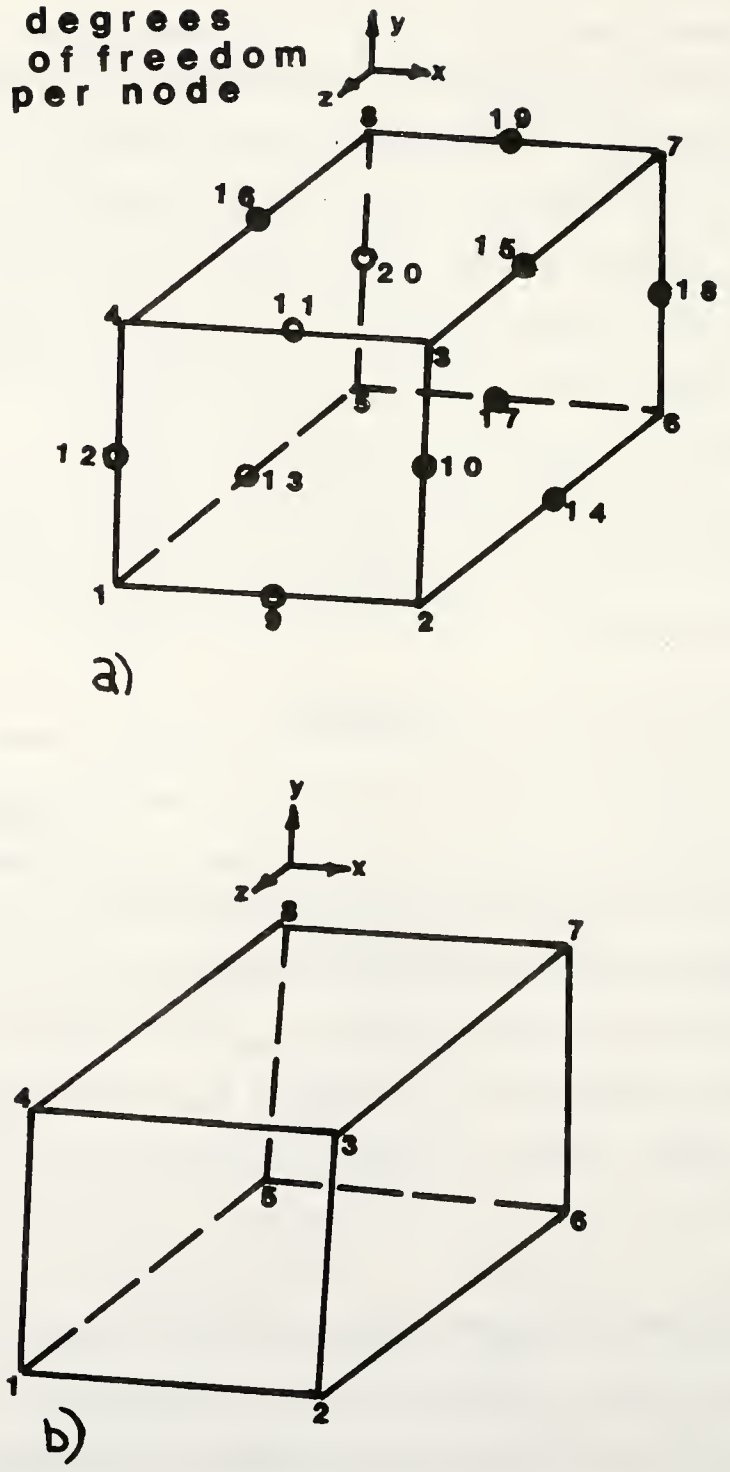

Figure 4.9: Typical Soil Element
a) Nodal Coding
b) Gauss Point Coding

Table 4.1: Variable Mode Shape Functions

Shape Function	Primary Shape Functions	Add 9	Add 10	Add 11	Add 12
N_1	$1/8\ (1+\varepsilon)(1-\eta)(1+\xi)$	$-N_9/2$			$-N_{12}/2$
N_2	$1/8\ (1+\varepsilon)(1-\eta)(1-\xi)$	$-N_9/2$	$-N_{10}/2$		
N_3	$1/8\ (1+\varepsilon)(1+\eta)(1-\xi)$		$-N_{10}/2$	$-N_{11}/2$	
N_4	$1/8\ (1+\varepsilon)(1+\eta)(1+\xi)$			$-N_{11}/2$	$-N_{12}/2$
N_5	$1/8\ (1-\varepsilon)(1-\eta)(1+\xi)$				
N_6	$1/8\ (1-\varepsilon)(1-\eta)(1-\xi)$				
N_7	$1/8\ (1-\varepsilon)(1+\eta)(1-\xi)$				
N_8	$1/8\ (1-\varepsilon)(1+\eta)(1+\xi)$				
N_9		$1/4(1+\varepsilon)(1-\eta)(1-\xi^2)$			
N_{10}			$1/4(1+\varepsilon)(1-\eta^2)(1-\xi)$		
N_{11}				$1/4(1+\varepsilon)(1+\eta)(1-\xi^2)$	
N_{12}					$1/4(1+\varepsilon)(1-\eta^2)(1+\xi)$
N_{13}					
N_{14}					
N_{15}					
N_{16}					
N_{17}					
N_{18}					
N_{19}					
N_{20}					

	Add 13	Add 14	Add 15	Add 16
N_1	$-N_{13}/2$			
N_2		$-N_{14}/2$		
N_3			$-N_{15}/2$	
N_4				$-N_{16}/2$
N_5	$-N_{13}/2$			
N_6		$-N_{14}/2$		
N_7			$-N_{15}/2$	
N_8				$-N_{16}/2$
N_9				
N_{10}				
N_{11}				
N_{12}				
N_{13}	$1/4(1-\varepsilon^2)(1-\eta)(1+\xi)$			
N_{14}		$1/4(1-\varepsilon^2)(1-\eta)(1-\xi)$		
N_{15}			$1/4(1-\varepsilon^2)(1+\eta)(1-\xi)$	
N_{16}				$1/4(1-\varepsilon^2)(1+\eta)(1+\xi)$
N_{17}				
N_{18}				
N_{19}				
N_{20}				

	Add 17	Add 18	Add 19	Add 20
N_1				
N_2				
N_3				
N_4				
N_5	$-N_{17}/2$			$-N_{20}/2$
N_6	$-N_{17}/2$	$-N_{18}/2$		
N_7		$-N_{18}/2$	$-N_{19}/2$	
N_8			$-N_{19}/2$	$-N_{20}/2$
N_9				
N_{10}				
N_{11}				
N_{12}				
N_{13}				
N_{14}				
N_{15}				
N_{16}				
N_{17}	$1/4(1-\varepsilon)(1-\eta)(1-\xi^2)$			
N_{18}		$1/4(1-\varepsilon)(1-\eta^2)(1+\xi)$		
N_{19}			$1/4(1-\varepsilon)(1+\eta)(1-\xi^2)$	
N_{20}				$1/4(1-\varepsilon)(1-\eta^2)(1+\xi)$

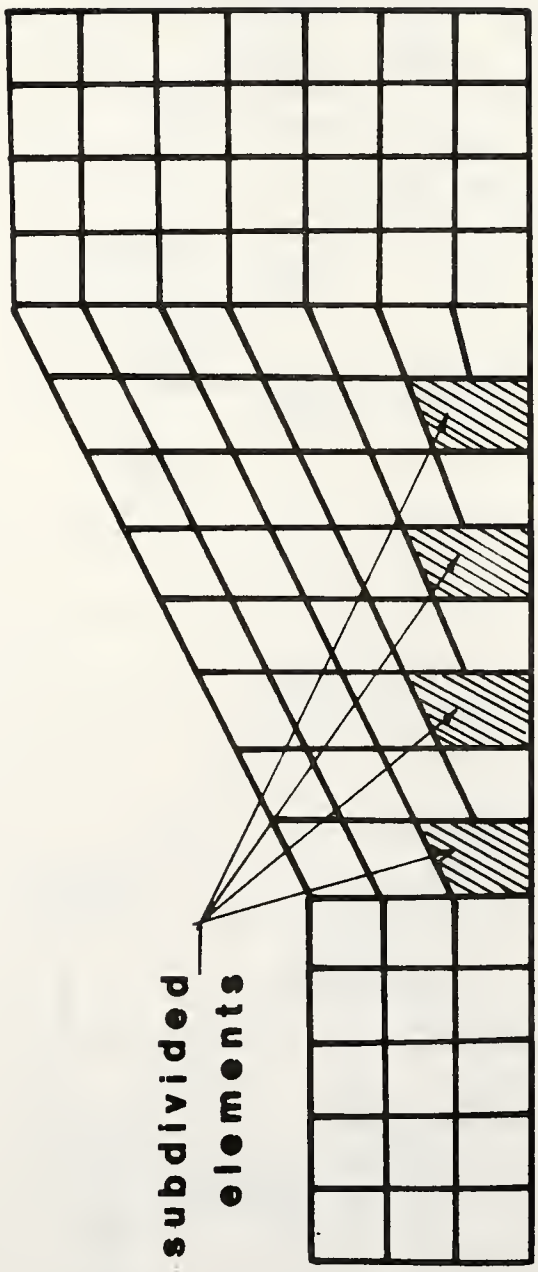

Figure 4.10: Location of Subdivided Elements

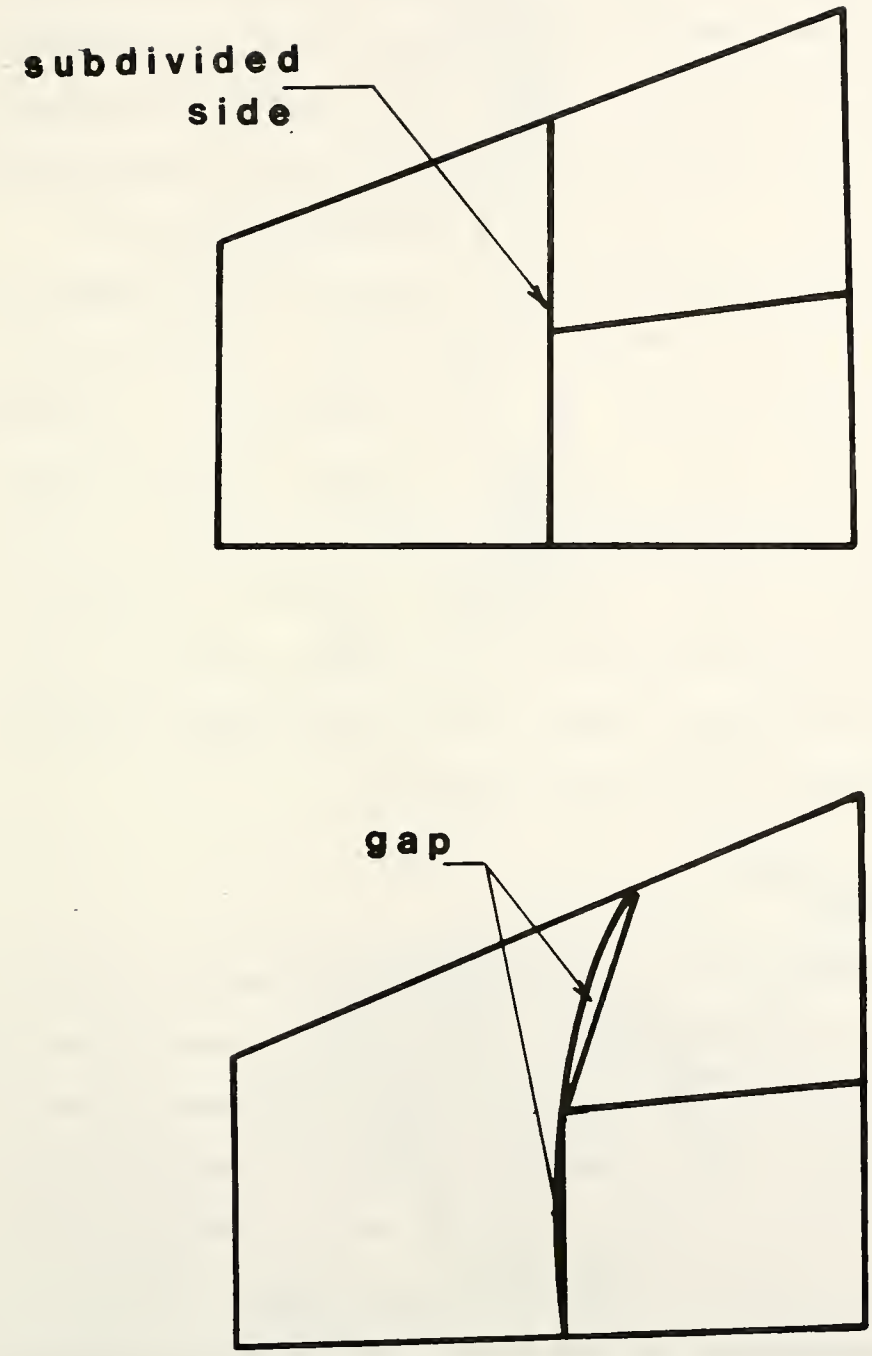

Figure 4.11: Mesh Nonconformity

midside node will have linear strain properties. This element, because of its midside node, will have quadratic displacement properties. Thus, this technique introduces noncompatibility between elements and strain discontinuity (figure 4.11b). To keep these discontinuities to a minimum it is recommended that the subdivided elements be placed near the bottom of the mesh where the strains are smallest (figure 4.11). Using the combination of elements shown in figure 4.11, parametric studies were performed for typical loading conditions which would exist in the foundation of a slope. Differences between the "exact" (i.e. with discontinuities) and the "approximate" (i.e. with discontinuities) Gauss point stresses and nodal displacements were less than 0.5 percent.

Pier Elements

The piers are represented by spar elements with four degrees of freedom, consisting of lateral translations and rotations at each end (figure 4.12a). The three dimensional behavior of the piers is insured by assigning the same node number to every point of contact between pier and soil at a given elevation (figure 4.12b). This prevents compression of the pile. The downslope side of the pier is not attached to the soil to allow a gap to form as the soil separates from the pier. Bachus and Barksdale (1984) noted such a gap when testing the lateral

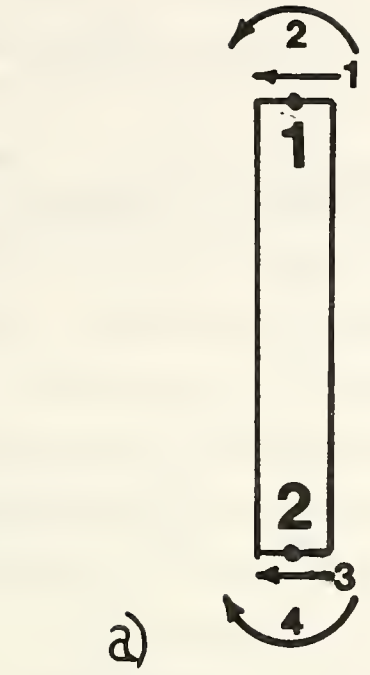

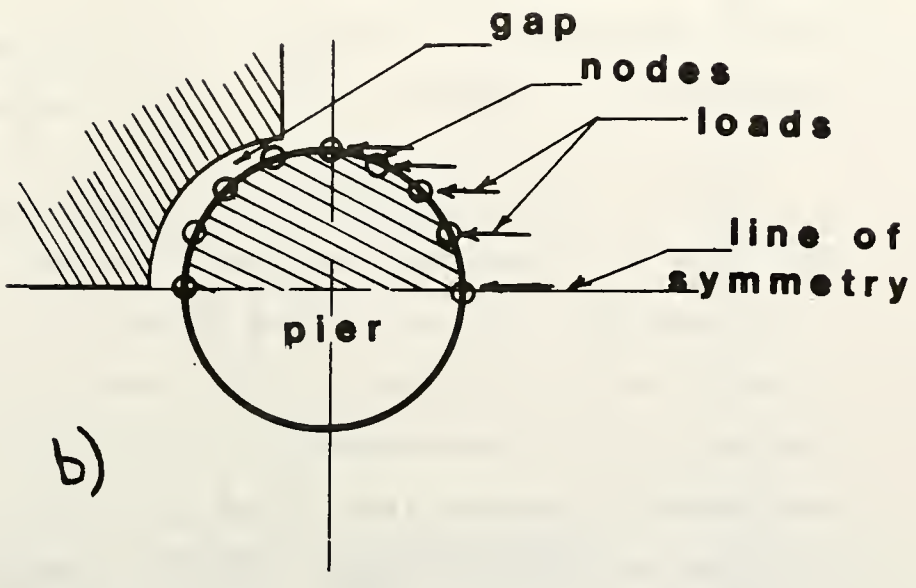

Figure 4.12: Pier Elements
a) Spar Elements
b) Nodal Relation to Soil

loading resistance of stone columns. The structural stiffness equations for the pier elements are shown in figure 4.13.

Spar elements were chosen to represent the piers because block elements may not be flexible enough in bending for long slender piers. Furthermore, many elements would be required to maintain a good aspect ratio, otherwise each element would have to be very long with respect to the width, and this would further reduce the flexibility of the elements (Clough, 1969). An added advantage of using the spar elements is a reduction in the number of degrees of freedom. As will be shown later, the pile is assumed fixed during the finite element solution of the soil displacement and, thus, there are no degrees of freedom at the pile-soil interface. This reduces substantially the total number of degrees of freedom.

There is one disadvantage to using the spar elements. The cubic interpolation function of the pier displacement is incompatible with either the quadratic or linear functions of the soil elements. This incompatibility is very similar to the incompatibility formed between the linear and quadratic element sides which was shown to be negligible (see above discussion). Typically, the displacements of the piers are much smaller than that of the soil. For these two reasons the errors involved can be neglected.

$$\begin{bmatrix} r_1 \\ r_2 \\ r_3 \\ r_4 \end{bmatrix} = \frac{2EI}{L} \begin{bmatrix} 6/L^2 & 3/L & -6/L^2 & 3/L \\ 3/L & 2 & -3/L & 1 \\ -6/L^2 & -3/L & 6/L^2 & -3/L \\ 3/L & 1 & -3/L & 2 \end{bmatrix} \begin{bmatrix} d_1 \\ d_2 \\ d_3 \\ d_4 \end{bmatrix}$$

Figure 4.13: Pier Element Structural Stiffness Equations

Slip Elements

Soil-pier interfaces and/or weak seams in the soil can be modelled by slip elements. The thin layer elements used by Desai and his co-workers (Desai, Eitani and Haycocks, 1985, Desai and Sargard, 1984, Desai and Lightner, 1985) are incorporated in the mesh. The thin element (figure 4.14) is similar to the soil element except they recommend that it should be proportioned so that the ratio of the shortest to the longest side, satisfies the following:

$$0.01 < t/B < 0.1 \qquad 4.1$$

where: t = thickness, and

B = width,

The thin elements are assigned a smaller shearing modulus, while the modulus against normal displacement remains the same as that of the soil elements. These elements have several advantages over the traditional infinitely thin slip elements:

1) Since they are essentially the same as the soil elements they are easily incorporated into the finite element solution routine.
2) They avoid the numerical difficulties which are sometimes associated with traditional slip elements.

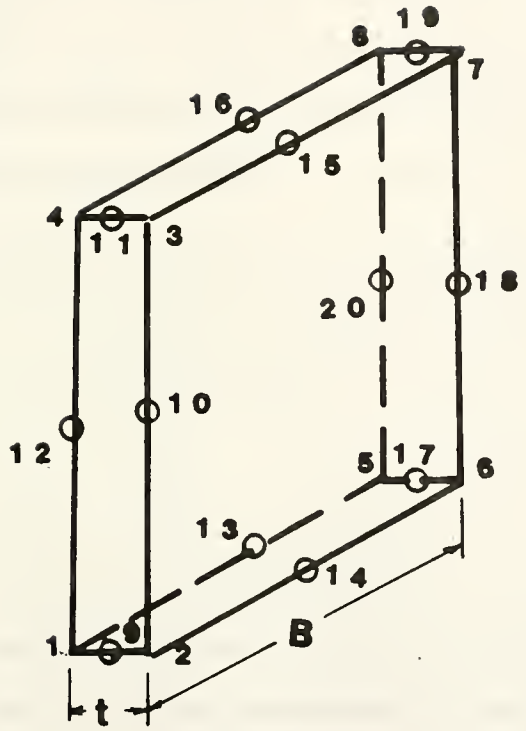

Figure 4.14: Slip Element

3) They not only provide for slippage around the pier, but also provide a means of representing a thin layer of "disturbed" soil due to drilling.

With regard to the third advantage, these slip elements can be incorporated in the analysis in two ways depending on the model and parameters used. They can be given very brittle parameters to act as true slip elements, that is to be relatively stiff and displace little until breaking when failure is reached. They may also be used as soft elements representing the remolded material around the pier. Here the modulus would be small, allowing large displacements.

Soil Modelling

The ultimate goal of this research program is to provide a reliable computer technique which can be used in practice; thus, several criteria must be met by the soil models. The models should provide realistic stress-strain paths under the loading conditions of the problem. The characteristics should be simple and amenable to use in practice (i.e., consistent with geotechnical data usually available for slope stability projects). This latter criterion implies that a large enough data base has to be available to help in the selection of model parameters.

Three models were selected and implemented in the program:

1) linear elastic,

2) Duncan-Chang (1970) with variable modulus only, and

3) Duncan-Chang with both variable modulus and Poisson's ratio.

The linear elastic model is provided because of its simplicity and economy in making predictions. The added effort of non-linear analysis can not be justified until the results of a linear elastic solution have been reviewed (Smith, 1982). Linear elastic embankment analyses have been conducted by Brown and King (1966), Penman et al. (1971), and Lefebvre et al. (1972). Linear elastic modelling is often appropriate for evaluating some aspects of stable slopes (which should be the case of a pier reinforced slope) and as a useful basis for initial investigations (Duncan and Dunlop, 1970).

Details of the Duncan-Chang hyperbolic model were given in Chapter 3. This model works well under conditions of monotonic loading, as this is how its stress-strain function is defined (Finn, 1980). The model parameters are simply obtained from triaxial testing and a wide data base currently exists in the literature. Early

applications of the Duncan-Chang (1970) soil model for slope stability studies were performed by Duncan (1972), Kulhawy and Duncan (1972), and Eisenstein, et al. (1972). Related studies performed for retaining structures by Duncan and Clough (1971), Clough (1972), and Smith and Boorman (1973), contributed greatly to the popularity of this model. More recently, this model was used by Chen and Saleeb (1982) to determine three dimensional embankment stresses and by Leonards, et al. (1982) to predict the performance of buried conduits.

The initial modulus incremental procedure (Naylor, et al., 1981) is used to implement the non-linear soil models in the computer program "SPILES". This procedure divides the total load into several increments. The existing stresses are calculated in each element and the corresponding modulus and Poisson's ratio are determined. The increment of load is then applied and the resulting increases in displacements and stresses are added to the existing displacements and stresses from previous increments.

The incremental technique avoids any problem of non-convergence since the modulus is determined at a point and does not depend on the results of previous increments. In addition, the degree of accuracy can be calculated from the number of increments used and the estimated stress

changes in the elements. For linear elasticity calculations the modulus does not change and only one increment is used.

Initial Stresses

The initial states of stress of all the elements are required to calculate moduli if a nonlinear soil model is used. Furthermore, it is also necessary to evaluate the final states of stress rather than just stress differences. The initial stresses depend on the K_o condition of the soil which is a function of the Poisson's ratio. Other important factors include the modulus of elasticity, slope angle, and formation processes. For example, the horizontal stresses are expected to be higher for a slope which was created due to erosion, than for a slope built up as a highway embankment.

While it is preferable to model the entire formation process of a slope from a horizontal halfspace, it does require significant effort and amount of data. Although it is possible to use this program in a sequential capacity, some simplified techniques are also provided. As a generic case, it is commonly assumed that the initial stresses are created by building a weightless slope and then instantly turning on gravity. This technique is able to allow for K_o conditions, the soil modulus of elasticity, and slope geometry and boundary conditions.

It is also possible to directly input the initial stresses in the program. There are generally three approaches to determine initial stresses:

1) Simplified approximate equations
2) Conformal mapping techniques
3) Finite elements

The simplified equations are based on the overburden weight. Ozawa and Duncan (1973) have developed the following relationships:

$$\sigma_y = \gamma h \qquad 4.2$$

$$\sigma_x = \sigma_z = K_o \gamma h \qquad 4.3$$

$$\tau_{xy} = \tau_{yz} = 0.5 \gamma h \sin \alpha \qquad 4.4$$

where: $K_o = \frac{\nu}{1 - \nu}$,

ν = Poisson's ratio,

γ = soil unit weight,

h = depth below surface, and

α = angle of the slope above the element.

While these equations will give good results for the vertical and horizontal stresses, the shearing stresses do not compare well with more rigorous solutions.

Conformal mapping solutions use transformed coordinate systems to formulate a problem which is solvable in

closed form and then transform the stresses back to the original coordinate system. Perloff, et al. (1967) derived a closed form solution to determine the stresses under a long elastic embankment. The method utilizes Cauchy integrals and a method proposed by Muskhelishvili (1963) which gives the boundary conditions in the half-space. This solution is complex and is not practical for engineering problems (Silvestri and Tabib, 1983[1]). A simplification of the Muskhelishvili method is used by Silvestri and Tabib (1983[1]) to develop solutions to specific problems. They mapped each problem as a linear half space which is readily solvable, then the inverse of the mapping is used to obtain the exact stresses for the original problem. An example of the resulting stresses given by Silvestri and Tabib (1983[2]) is shown in figure 4.15.

Even with the simplifications made by Silvestri and Tabib (1983[1]), conformal mapping solutions are limited to cases of simple homogeneous, elastic, trapezoidal embankments built on elastic half-spaces. More complex situations can only be analyzed using the finite element method. It allows for more realistic soil models as well as a greater variety of geometric shapes and boundary conditions. The finite element procedure also simplifies the modelling of formation or construction sequences. For linear elastic cases, simply utilizing self-weight in a

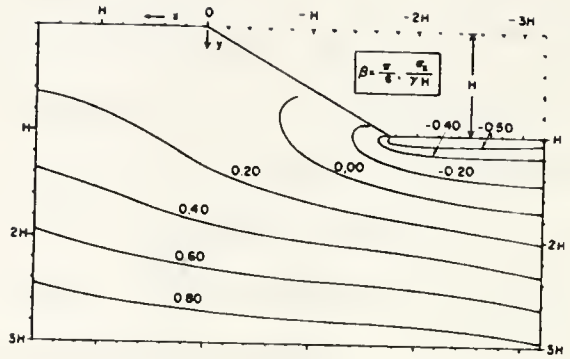

Contours of $\sigma_x/\gamma H$ for $K_0 = 0.5$ and $\beta = \pi/6$.

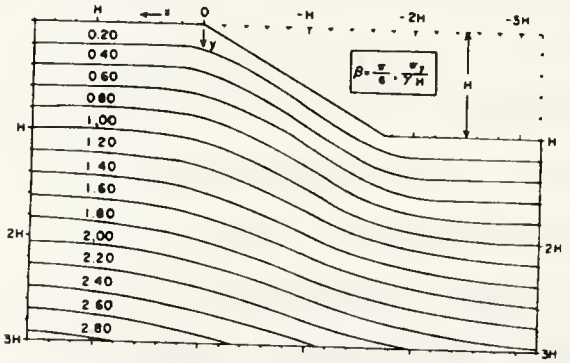

Contours of $\sigma_y/\gamma H$ for $K_0 = 0.5$ and $\beta = \pi/6$.

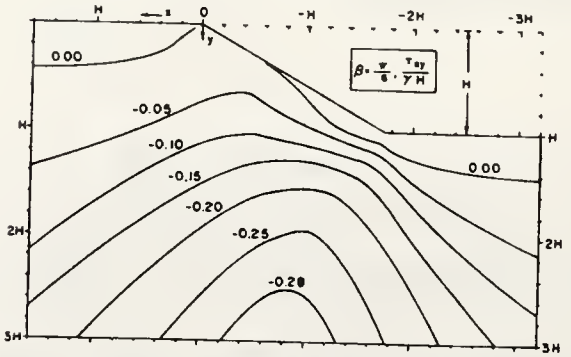

Contours of $\tau_{xy}/\gamma H$ for $K_0 = 0.5$ and $\beta = \pi/6$.

Figure 4.15: Initial Stresses by Conformal Mapping (From Silvestri and Tabib, 1983[2])

gravity turn-on condition will yield results very similar to those of conformal mapping. For example, the slope given in figure 4.15 was also analyzed using the program "SPILES". Figure 4.16 gives similar results using the gravity turn-on finite element method.

To examine the errors in initial stresses involved in an excavated slope, Wilson (1963) compared the results of the gravity turn-on method to those of an elastic analysis using construction sequences. The results are given in figure 4.17. The average difference is only 16 psf, while the average stress is over 1000 psf. This yields an error of less than 2 percent. The accuracy would be even higher if triangular elements had not been used along the slope surface, as they produced the highest differences. While the errors may be greater if both of these analyses had been performed as nonlinear processes, gravity turn-on must still be considered as an accurate method of determining the initial stresses.

Naylor, et al. (1981) recommended the use of self equilibrating initial stresses rather than the simple scheme of nodal loading used above. For a sloping ground surface, this technique requires that the stresses be first calculated for a horizontal ground surface above the existing level. Then an incremental excavation technique is used to determine a set of self equilibrated initial

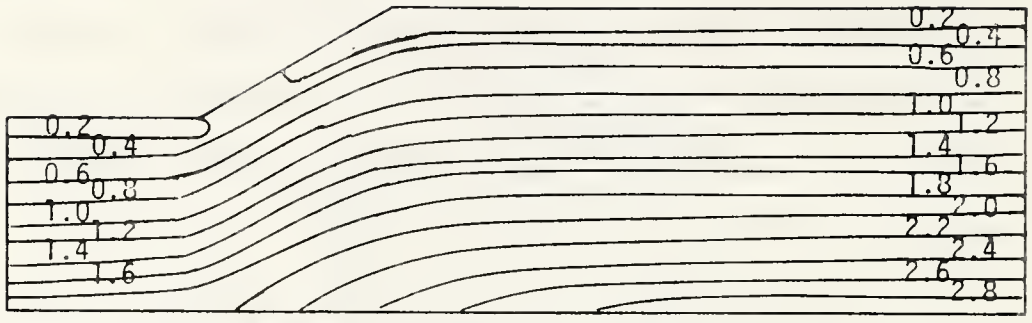

vert. stress/unit wt./height

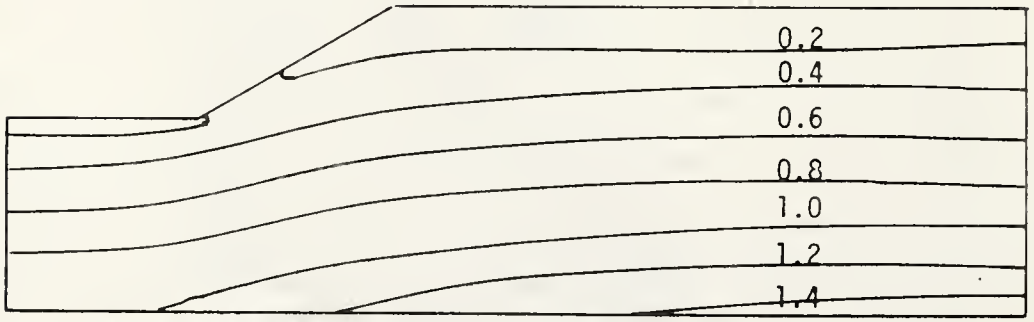

horz. stress/unit wt./height

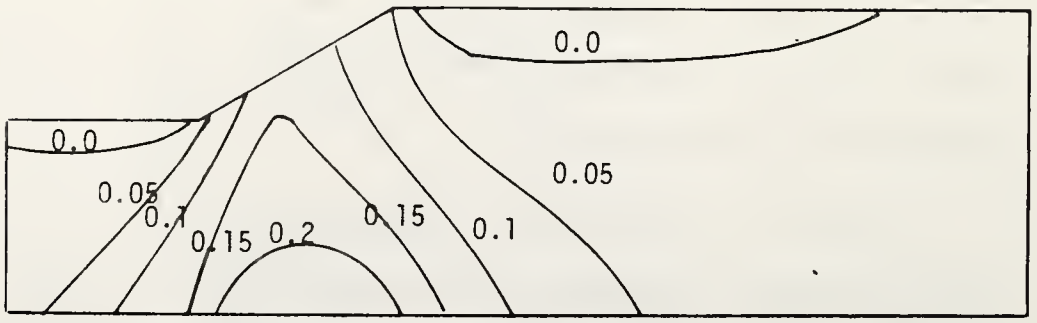

shear stress/unit wt./height

Figure 4.16: Initial Stresses by Gravity Turn-On

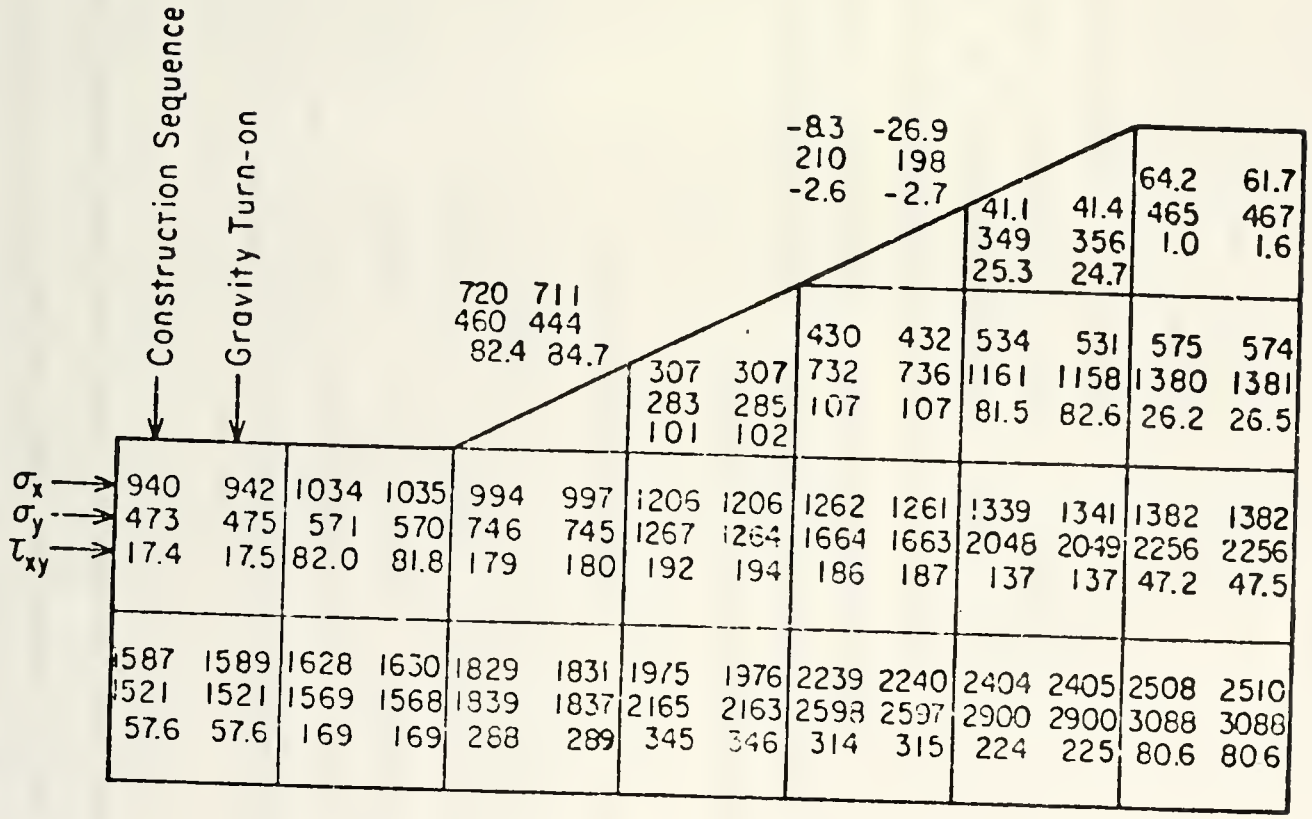

Figure 4.17: Comparison of Initial Stresses between Gravity Turn-On and Sequential Excavation (From Duncan and Dunlop, 1970)

stresses which are also in equilibrium with gravity forces. Provisions have been implemented in the program "SPILES" compute stresses in this manner.

In comparing the three solutions, the simplified equations seems reasonable for cases where embankments are being constructed, however, they may not be applicable to cases of existing slopes. In the case of the mapping solution, the horizontal stresses are not a K_o function of the vertical stresses even at some depth below the foundation. The finite element procedure produces stresses which appear correct for general cases. In addition, only the finite element procedure can easily give the complete three dimensional state of stress.

Solution Processes

The program "SPILES" is composed of two major finite element sub-programs. The first sub-program solves for the displacements in the soil while assuming that the piers are rigid. The second sub-program solves for the pile displacements using the forces obtained at the soil nodes.

The solution process follows the displacement based finite element technique using constrained and unconstrained degrees of freedom. A constrained degree of freedom can be temporarily fixed, maintaining a specified

displacement. Any soil degree of freedom in contact with a pier will be constrained (figure 4.18). The solution process can the be broken into two sets of equations:

$$r_u = sk_{uu} d_u + sk_{uc} d_c \qquad 4.5$$

$$r_c = sk_{cu} d_u + sk_{cc} d_c \qquad 4.6$$

where: r_u = forces at unconstrained degrees of freedom,

r_c = forces at constrained degrees of freedom,

d_u = displacements at unconstrained degrees of freedom,

d_c = displacements at constrained degrees of freedom,

sk_{uu} = totally unconstrained stiffness matrix,

$sk_{uc} = sk_{cu}^{-1}$ = partially constrained stiffness matrix, and

sk_{cc} = totally constrained stiffness matrix.

Since the initial pier displacements are known (the constrained displacements), the first equation can be solved for the unconstrained displacements. These are the displacements throughout the soil mass. The solution process uses a revolving block by block Gauss elimination developed for this study. Core space requirements are reduced in the computer since each block is only one bandwidth long. By revolving the lines in each block, only one block needs to be in core at any one time, instead of the usual two blocks. The other blocks can be kept in secondary storage. Once the unconstrained displacements are known, the constrained forces can be calculated

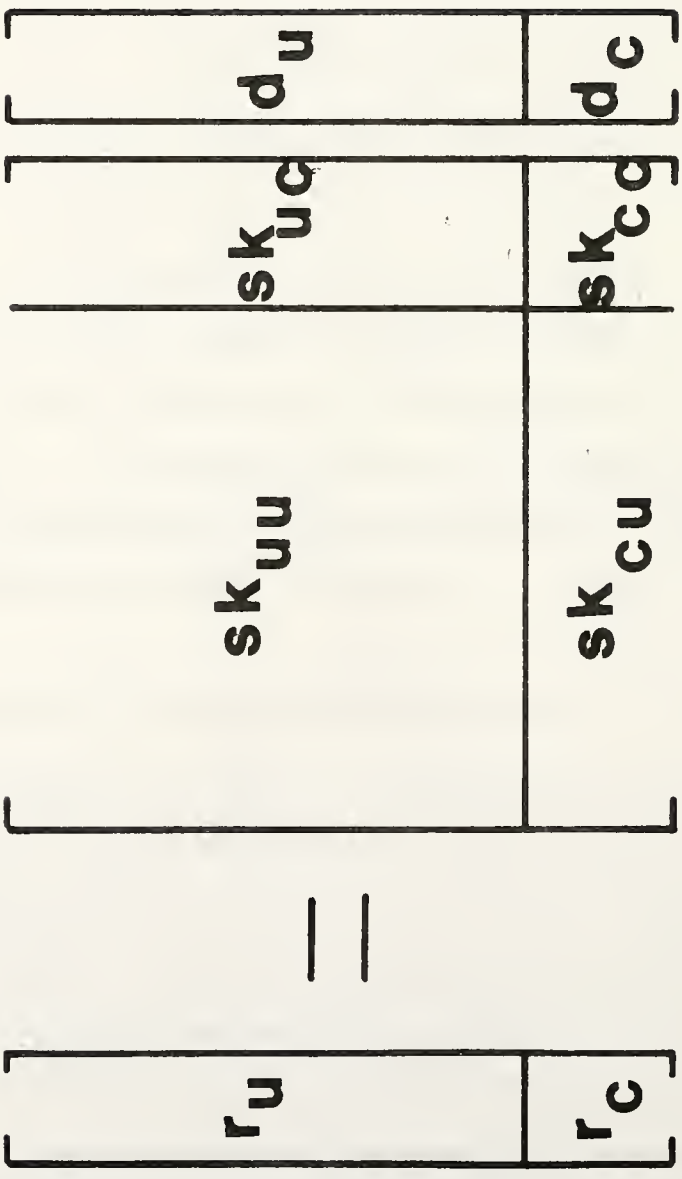

Figure 4.18: Solution Process

through the second equation. These would be the forces against a rigid pier.

The solution technique for the pile displacements is one of matrix structural analysis using beam elements (Meyers, 1981). Here, another advantage is gained by using the spar elements over the parallelepipeds. Their solution requires much less computer time since the element stiffness matrix can be formed directly based on the length of each element.

The forces against the piers are absorbed in two ways. First, there is a transfer of energy to the bedrock through cantilever resistance; this results in stresses which are subtracted from the soil. Second, there is the passive resistance of the soil as the pier pushes against it; this is a simple transfer of stresses from the soil on one side of the pier to the soil on the other side. Both of these resistances are a function of the pier displacements, and both increase as the pier bends. The equation to be solved is:

$$r_c = a * d_c + sk_{cc} * d_c \qquad 4.7$$

or

$$r_c = (a + sk_{cc}) d_c \qquad 4.8$$

where r, d, sk have been defined above, and a = pier stiffness matrix. The pier displacements can be

calculated and then used in the calculation of the new element stresses.

In the case of an excavation, a similar process is followed. An additional finite element mesh is generated for the excavated area. Constrained degrees of freedom are used along the boundary between the wedge which is to be excavated and the final surface of the slope. Automatic excavation increments are performed by the program, removing one layer of elements at a time. During each increment the forces at the unconstrained degrees of freedom due to the excavation are transmitted across the boundary and serve as the forces on the final slope. The resulting displacements along the slope surface are then used to recompute the existing state of stresses in the rest of the wedge to be excavated.

Part III: Stability Analysis

The program "SPILES" generates stress, strain, and displacement fields within the slope being analyzed. While this information is extremely useful in understanding the general influence of the piers, it may often be desirable to condense it to a specific value which is an index of the stability. The index typically used by geotechnical engineers is the factor of safety. In this

section, the approach taken to estimate a factor of safety from the finite element results is discussed. This discussion concentrates on the definition of the "point of collapse" and on the stability calculations.

Point of Collapse

"The power of the FE method lies in its capability to model details of the configuration. Ironically, its application to some geotechnical problems such as the stability of soil slopes is also hindered by this versatility" (Wong, 1984). Between the states of initial yielding and final failure there can exist a wide range of loading. The critical load depends on the definition of failure. Several of the most common definitions are given below.

Nonconvergence

When an iterative procedure within the finite element method is used to establish force equilibrium, Zienkiewicz (1977) suggests that a lack of convergence indicates collapse of the structure. This method, however, requires that a nonlinear analysis be conducted under an iterative technique which is sensitive to nonconvergence. Wong (1984) states that the nonconvergence condition is an upper bound, that is failure will always occur before this condition is reached. Safety based on this analysis will be unconservative.

Continuous Surface of Yielded Elements

It is possible to calculate the point of failure of individual elements based on failure criteria like the Mohr-Coulomb criterion. As incremental loading is applied, a plot of these failed elements may show a trend towards a continuous failed surface which indicates collapse. Wong (1984) states that when a full slip condition has formed, the stability is always a lower bound and is a conservative estimate of safety. A major drawback of this technique is that a wide band of elements may fail before a path to the surface is reached. This hides the location of the most critical surface.

Critical Displacement

During a nonlinear analysis, failure may be defined as a state of rapidly accelerating strains under constantly increasing stresses. The most noticeable condition of failure may be excessively large displacements. Snitbahn and Chen (1976) suggested that the horizontal displacement of a node, just above the toe in a vertical slope, will displace excessively at failure. Similar points may be defined for other slopes. While the simplest of the techniques, it requires experience and judgement to define the point to be monitored and to establish a limit which defines failure.

Limiting Equilibrium

Failure surfaces can be superimposed over the finite element stress field and the ratio of resisting stress to shearing stress calculated (Duncan and Dunlop, 1969; and Wright, 1974). This will yield a factor of safety similar to that which is currently computed by typical limiting equilibrium analysis (Siegel, 1975; Chen and Saleeb, 1982; Hassiotis, 1982)

The advantages of using finite elements to compute the stress field are based on the versatility of the method. Using the finite element procedure, it is possible to account for the formation and construction processes of the slope. In addition, the constitutive relations of the soil are taken into account. Finally, complex boundary conditions, such as the piers in this case, are implemented.

Security Factor

In geotechnical engineering, the physical meaning of the factor of safety is often obscured by its method of calculation. In structural engineering, when calculating the security of a truss member, the factor of safety is simply the load which the member can carry divided by the applied load. If the applied load is doubled, the "security" is halved. When considering the factor of safety of

a slope, however, it is not generally in terms of loads. The factor of safety for slope stability depends on the stresses along a potential failure surface. Although these stresses are produced by various loads in the slope (soil weight, hydrostatic pressure, seepage forces, surface loads, seismic forces, etc.), the factor of safety is not directly proportional to any one of these loads.

The global factor of safety, as commonly defined by the method of slices, is satisfactory in comparing similar slopes under similar loadings. However, this factor of safety does not relate well to how the individual forces within the slope affect its stability. To fully appreciate the significance of the factor of safety, it must be reduced to more specific terms. It is not only necessary to compute the factor of safety using the stresses along a specified potential failure surface, but also to compute the "security" with respect to individual loads. The "security" with respect to a load is defined as the ratio of load to cause failure divided by the working value of that load. This can be done by computing a factor of safety along the most probable failure surface, at incrementally increasing values of load, until unity is reached. This is the point of collapse and will be the load at failure. This value of stability has the advantage of scaling linearly with load. Furthermore, the securities for the major variables, and the probabilistic

characteristics of the loads on which they are based, can be used to define a more meaningful "global" factor of safety. The actual application of this technique will be discussed more fully in Chapter 6.

The Program "LOGFIND"

A complementary two-dimensional limiting equilibrium program was developed to analyze the factor of safety using the stress field provided by the finite element program "SPILES". Incremental stresses at increasing load levels can be used to determine the stability of the slope with respect to a selected load variable.

The program "LOGFIND" establishes the same element boundaries used in the finite element program. The stresses in these elements are defined as the average stresses from the eight Gauss points in each element. The program will analyze the two dimensional factor of safety for the center plane of each row of elements. A two dimensional grid is built as a searching pattern to locate the center for the most critical failure surfaces (figure 4.19). Potential failure surfaces enter the slope at a defined point at or near the toe of the slope and extend as circles or log spirals until they exit the soil profile. The shearing stresses and resisting stresses are calculated at specified intervals along the arc. The

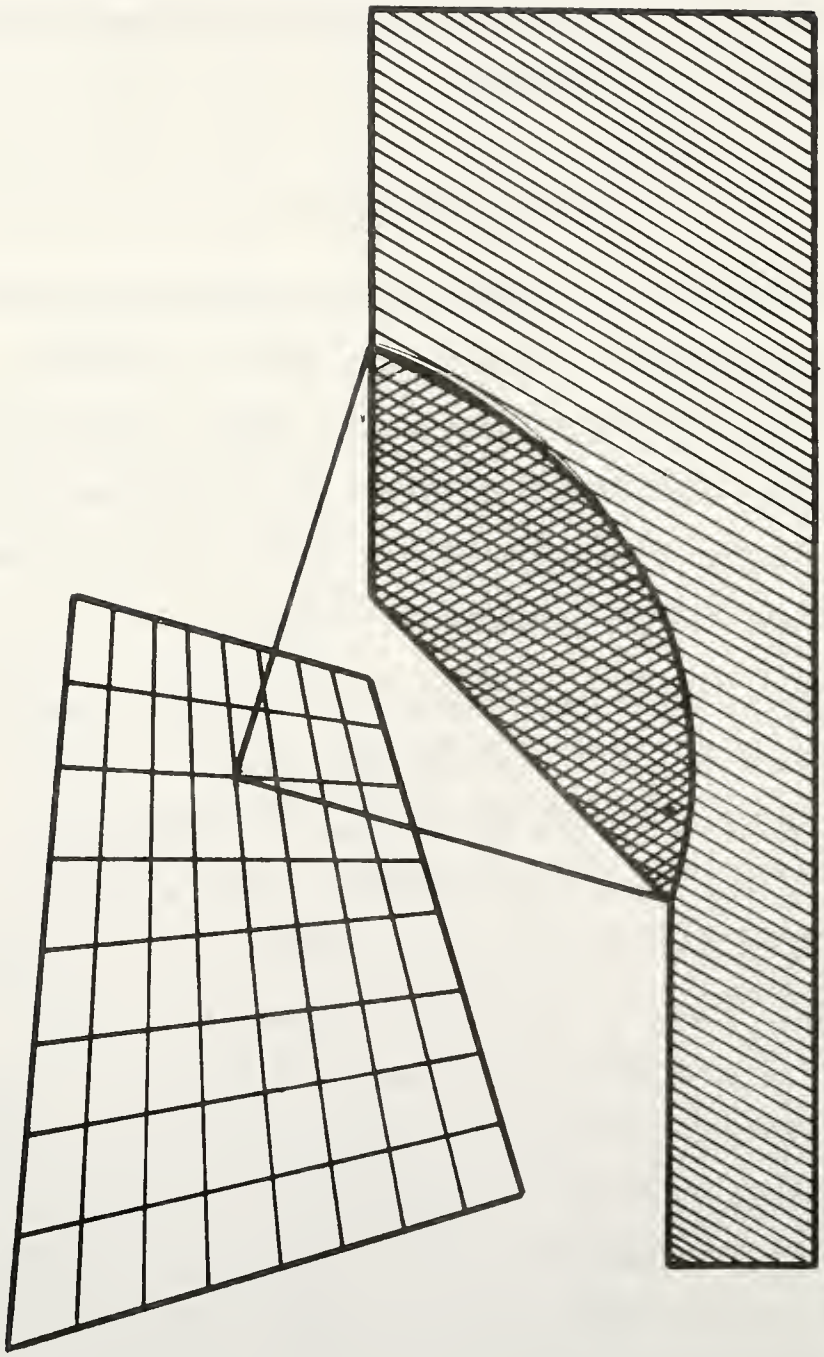

Figure 4.19: Searching Grid

factor of safety is defined as the sum of the resisting stresses over the sum of the shearing stresses.

The resisting stresses are calculated using the Mohr-Coulomb failure criterion:

$$\tau = c + \sigma\phi \qquad 4.9$$

where: τ = shear strength,

c = cohesion,

σ = normal stress, and

ϕ = friction angle.

Several options are included in the program to place limitations on the potential failure surfaces. The first of these options is to specify that the same surface be used for all load increments once it has been established under the first increment. This eliminates unnecessary searching under linear elastic cases with no pier present. It also enables direct comparison of specific surfaces under increasing load conditions. Second, it can be specified that all surfaces exit beyond the crest. This enables a search of deep seated slides or elimination of potential surfaces which are too shallow to be a factor. A third option specifies that if a surface encounters bedrock or a weak seam, it extends linearly along it as a block failure (figure 4.20). If this option is not evoked, any surface intersecting the bedrock will be ignored.

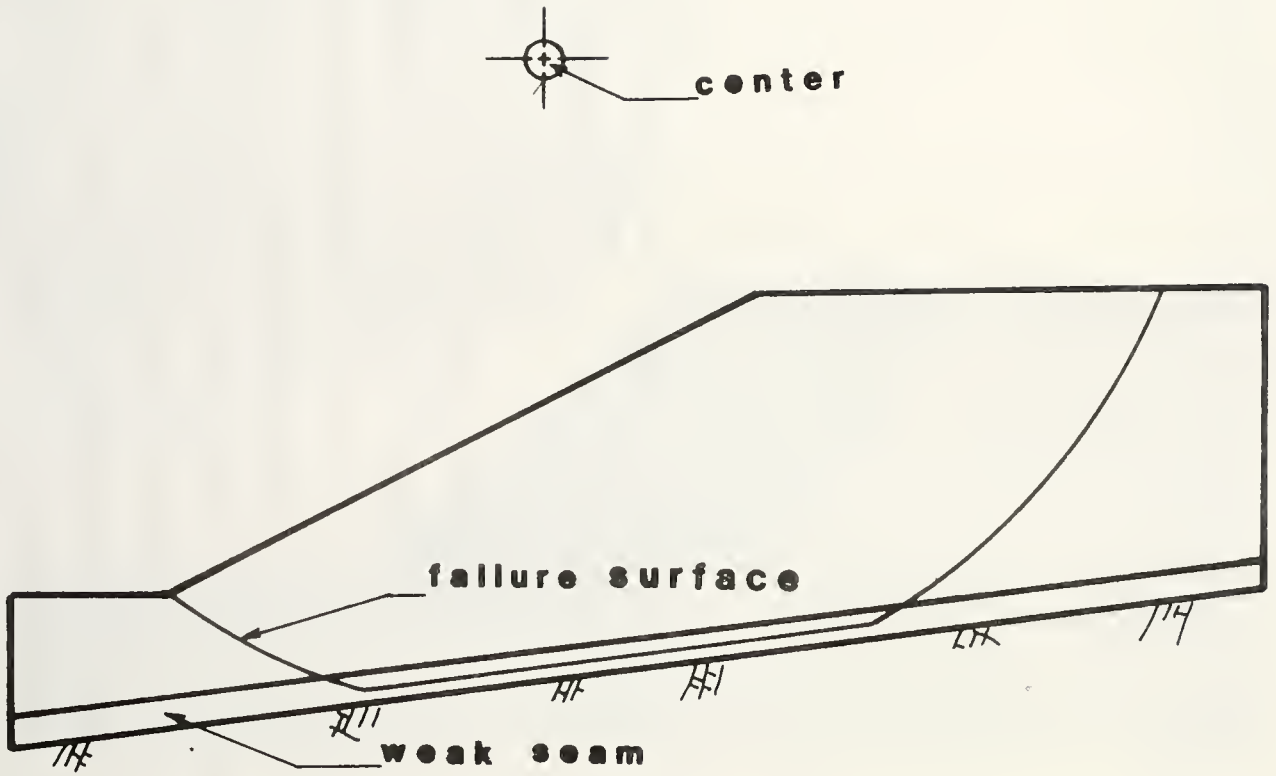

Figure 4.20: Block Slip Surface

CHAPTER 5: EXCAVATION AND CUT SLOPE REINFORCEMENT EXAMPLES

Introduction

Cut slope stability was one of the three loading conditions discussed in the previous chapter. In order to explore the capability of drilled piers to provide a permanent method of increasing the stability under this loading condition, the specific example of an excavation will be studied. This example problem will yield insight into the use of drilled piers as retaining structures during and at the end of an excavation. It will also be used to illustrate the capabilities of the computing technique provided by the programs written for this study.

There are two reasons for using an excavation as a specific example problem. First, the case of an excavation helps illustrate a potential application of the piers which has not been reviewed in any other part of this study. Surcharge load has been studied in a previous phase of this research and presented by Oakland and Chameau (1984). Self weight loading of the embankment material will be discussed in parametric studies in the

next chapter. Second, an excavation eliminates one variable, the loading. The loading, or unloading in this case, is defined by the final geometry of the slope and the unit weight of the soil.

As described in the previous chapter the computing process consists of three parts: mesh generation, finite element analysis and a limiting equilibrium evaluation of stability. In general, the output from one process is used as the input for the next one. Between processes, however, some user intervention is required. The output of each process is also complemented by a graphical representation of the data to be used in the next process. This allows for a rapid evaluation of the correctness of the input for the next process.

Example Problem

The problem to be solved is similar to the one explored by Duncan and Dunlop (1968): A 40 foot excavation in 60 feet of soft clay using 1:1.5 side slopes. The problem will be analyzed with and without drilled piers installed at the future crest of the excavation. The bedrock is very hard and stiff with respect to the soil and acts as a rigid boundary in which the piers can be socketed. It is located 20 feet below the final excavation depth, one half of the slope height.

The soil is a frictionless material with a cohesion (c = 800 psf) and unit weight (γ = 130 pcf) constant with depth. The soil strength was chosen such that the unreinforced slope has a non-acceptable factor of safety when the final increment of excavation is completed. With a cohesion of 800 psf, the Bishop factor of safety is 0.95 at the end of the excavation.

Four foot diameter piers with 8 foot center to center spacings will be used to support the excavation.

Soil Model

Duncan and Dunlop (1968) used three different soil models in their study: linear elastic, bilinear elastic, and nonlinear. Their conclusions were that the linear elastic analysis may be suitable for analysis of some aspects of stable slopes. Bilinear analysis is useful in determining where local failure begins and how it progresses with further excavation. Detailed stress and displacement analysis must be determined using a nonlinear model.

For this example, a nonlinear hyperbolic model will be used to determine the modulus of elasticity in each soil element during each increment. The initial tangent modulus is 100,000 psf. The equivalent parameters in the

Duncan-Chang soil model are: K = 47.2, n = 0.5, c = 800.0, ϕ = 0.0, and R_f = 1.0. This value of "K" corresponds to the initial modulus of 100,000 psf, the "n" is an average value for clay (see table 3.2), and R_f of 1.0 represents a normally consolidated clay where the ultimate strength is the same as the strength at failure, i.e. it represents a normally consolidated clay with no peak strength. Weak plastic clays tend to have high Poisson's ratios of the order of 0.4 to 0.5 (Leonards, 1962, pg 789). The range of variation is small and thus a constant value of 0.45 is assumed in the analysis.

Initial Stresses

When starting an excavation from a horizontal ground surface it is possible to calculate the initial stresses as a function of depth below ground surface as:

$$\sigma_y = \gamma h$$

$$\sigma_x = \sigma_z = K_o \gamma h$$

The program assigns these values to each node or gauss point located at depth h.

Two techniques of installing the piers at positions within the slope are possible. The first would be to partially excavate the slope to the desired level of the

piers, install the piers, then continue the excavation. In this case, the stresses which are present at the final increment before the piers are installed are used as the initial stresses for the second part of the excavation with the piers. Two problems are associated with this procedure. The piers do nothing to alleviate the stresses induced during the first part of the excavation, thus losing much of the efficiency of the piers. Also, a break in the excavation procedure is needed to install the piers and allow them to cure. This may add to the cost of the construction.

A second procedure would be to drill the piers at the desired locations, but only fill the shafts up the the future excavated level. The remainder of the shaft can be backfilled with soil. This can be done well in advance of the excavation to allow adequate curing time for the concrete and not interfere with construction. This procedure has the advantage of maximum efficiency in absorbing the induced stresses. Also, this problem can be modelled in one stage.

Simulation of Excavation

Numerical simulation of the excavation can be made by removing either layers of elements or layers of nodes. In

the elemental approach, the average stress in an element is extrapolated to the next excavation boundary. This boundary is between the element to be removed and the next lower element. The forces on this boundary are computed and applied as upward forces on the new surface boundary. An assumption, however, must be made concerning the distribution of stress with depth. In this study, it is assumed to be linear across the element.

The nodal method of simulating the excavation has the advantage that no assumption of this kind is needed. The forces at the nodes to be excavated are calculated based on the average stresses in the element. This is correct since the border of the layer goes through the middle of the element below that layer of nodes. The layer of nodes actually represents the middle of the excavated material. Since the elements above the layer of nodes are not added into the total stiffness array while the elements below are, the stiffness array represents an average stiffness during the excavation of each layer. This is an advantage over the elemental method where the stiffness is simply the final stiffness after the layer has been excavated. While the nodal method may be numerically superior, it has several disadvantages. First, the first and last increments must be treated as half layers, this is computationally difficult and adds an extra increment to the process. Second, since the stressea are calculated based on the

excavation levels between the boundaries, it is difficult to stop and restart the process between increments. This leads to difficulties when a pier is to be added after the excavation is partially completed. For these reasons, the elemental method will be used in this example.

Mesh Generation

The first step towards the solution of the problem is to form a digital representation using a mesh generator. A variety of mesh generators which discretize the final slope have been developed for this study. The basic input for each slope generator has been reduced to the boundary dimensions of the soil profile, the pier diameter and spacing, default values for the modulus of elasticity and the Poisson's ratio, and a few parameters to control the mesh fineness.

The wedge shaped soil mass which is to be excavated to form the final slope geometry from a horizontal ground surface is created by a special generator. In order for the nodes along the boundary of this mass to be compatible with the nodes on the surface of the final slope, they must be input directly by the user. The locations of these boundary nodes are used to generate the mesh.

The mesh generator creates a file made of a nodal code and an elemental code which can be input directly into the finite element program. An isometric graphics routine can plot the mesh from any vantage point. This allows for a rapid check against errors in the coding. The final slope geometries for the cases with and without piers are shown in isometric and plan views in figures 5.1 and 5.2. The compatible wedge to be excavated is shown in these isometric and plan views slightly offset from the final slopes.

The gradation of the mesh is an important factor in the accuracy of the results. Snitbhan and Chen (1978) found that in the case of vertical slopes a great number of elements are required around the toe to reduce problems of singularities. Preliminary trials of the problem to be solved indicate that there is a singularity problem involving the load transition from the wedge to the final slope. The effect of this singularity can be reduced by additional elements in the wedge and corresponding elements in the toe of the slope. Figure 5.3 shows the relation between the angle of the displacement at the toe after the final increment of excavation and the number of elements used in each layer of the excavation. The computed angle for a small number of elements (4) is far from the asymptotic value reached for larger numbers of elements, but dramatic improvements are obtained by increasing the number of elements to 6 or 8.

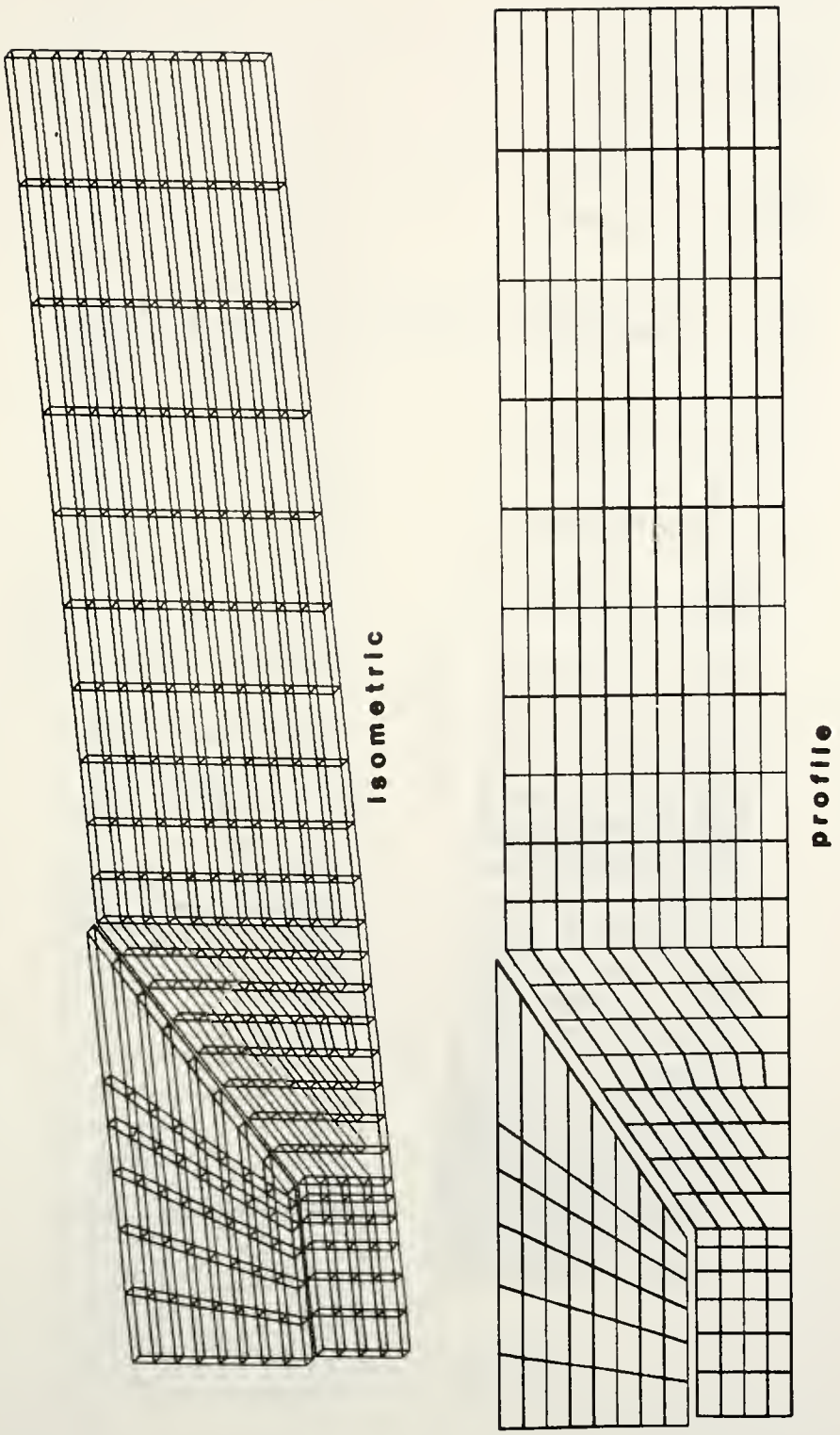

Figure 5.1: Isometric and Profile Views of the Slope Mesh with No Pier

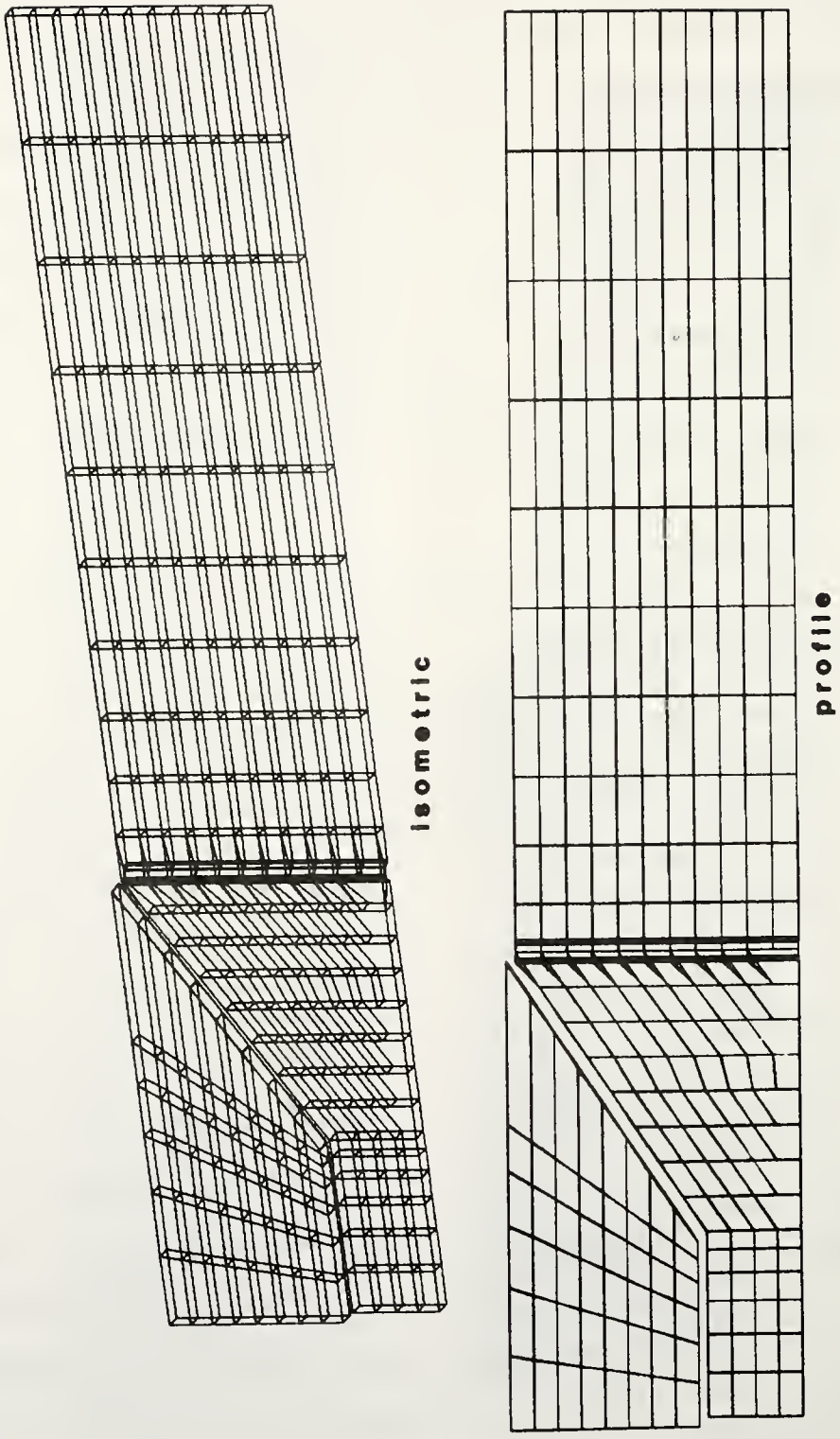

Figure 5.2: Isometric and Profile Views of the Slope Mesh with a Pier

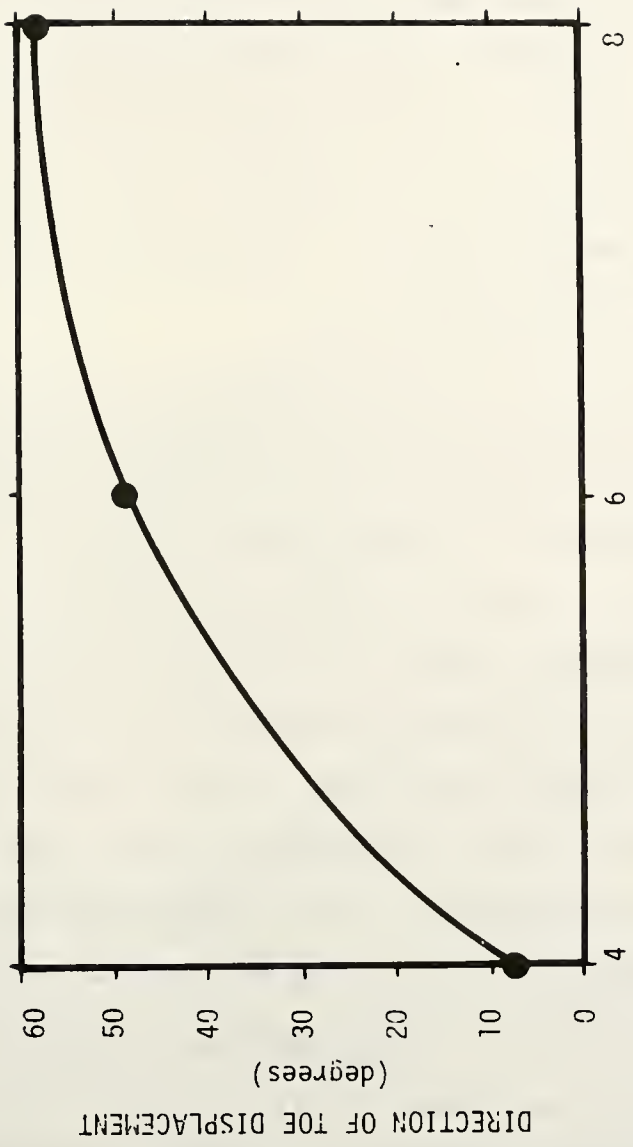

Figure 5.3: Effect of Mesh Size on Singularity at Toe

Analysis Using the Finite Element Code

Once the mesh has been created and checked for mistakes, the actual simulation of the construction process can be modelled using the finite element program. The bulk of the input to the program comes directly from the mesh generator. However, some additional information concerning the general nature of the problem and secondary elemental information must be added to the existing data file. The secondary elemental information consists of the properties of the elements.

Finite element programs can produce a large amount of numerical output. Most of this information consists of stresses and strains for each element or each Gauss point, and displacements and equivalent nodal forces for each node. For the three dimensional problem solved in this study, there are six stress components at each Gauss point and three displacement and load values at each node. Also calculated are principal stresses and rotations, and total accumulated displacements. This information is recomputed for each increment, however, can be reduced to a comprehendable format using a post processing computer graphics package developed for this study. Figures 5.4 to 5.21 summarizes the output for the eight excavation

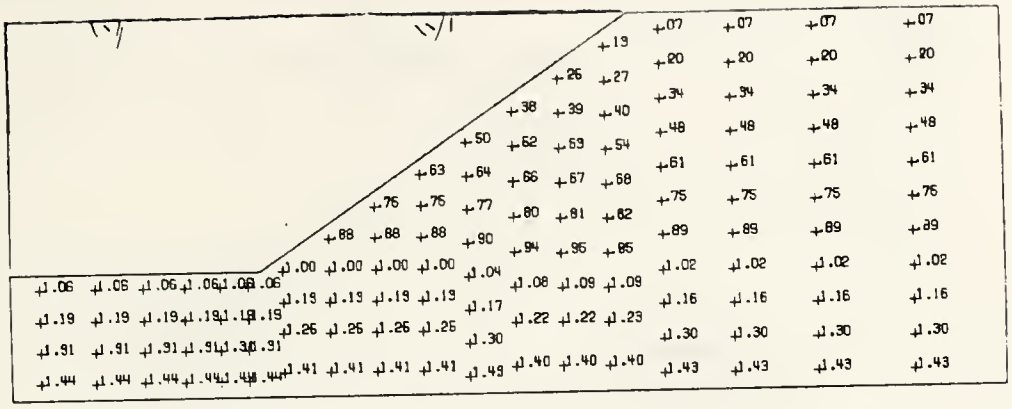

VERT STR/UNIT WT/HEIGHT

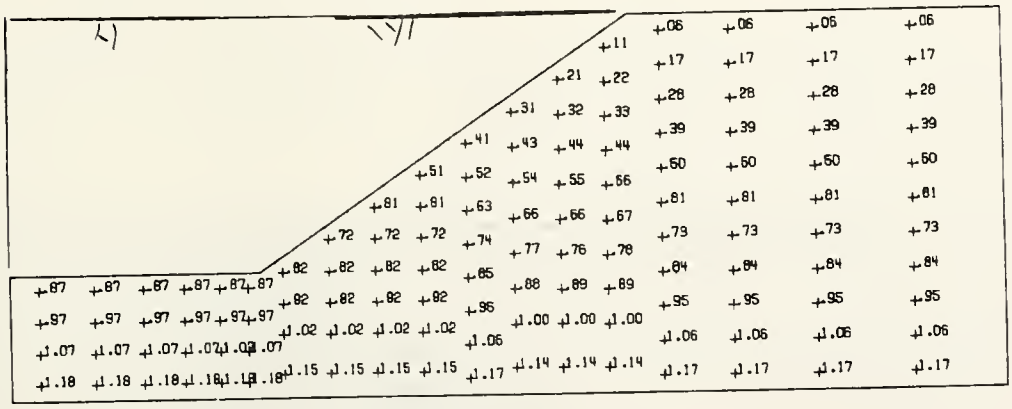

HORZ STR/UNIT WT/HEIGHT

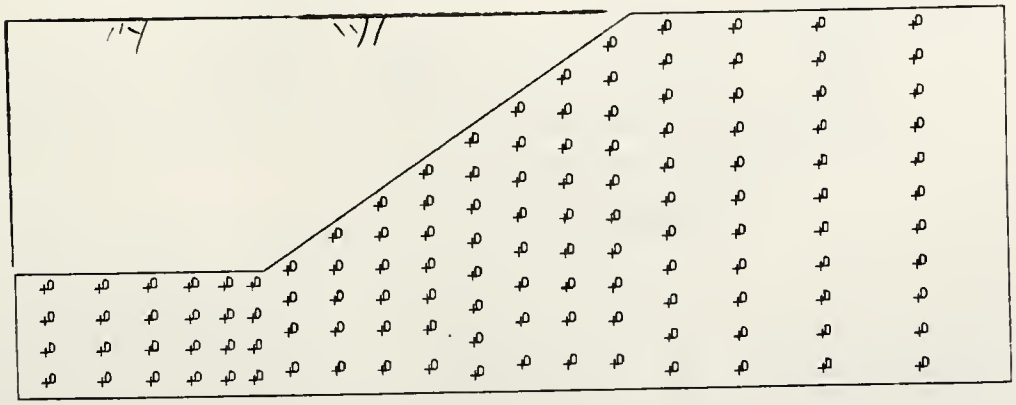

SHEAR STR/UNIT WT/HEIGHT

Figure 5.4: Vertical, Horizontal, and Shearing Stresses, Displacements and Stress Direction for Increment 0 for the Case of a Slope with No Pier

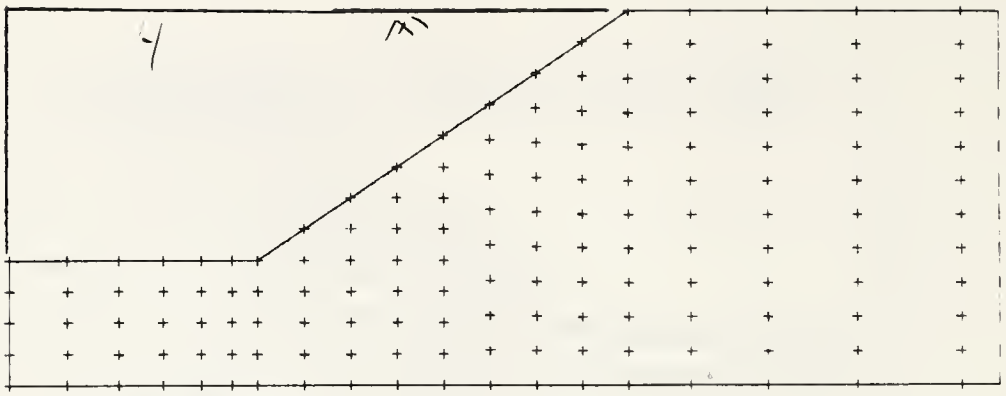

DISPLACEMENTS

VECTOR SCALE = 5.0

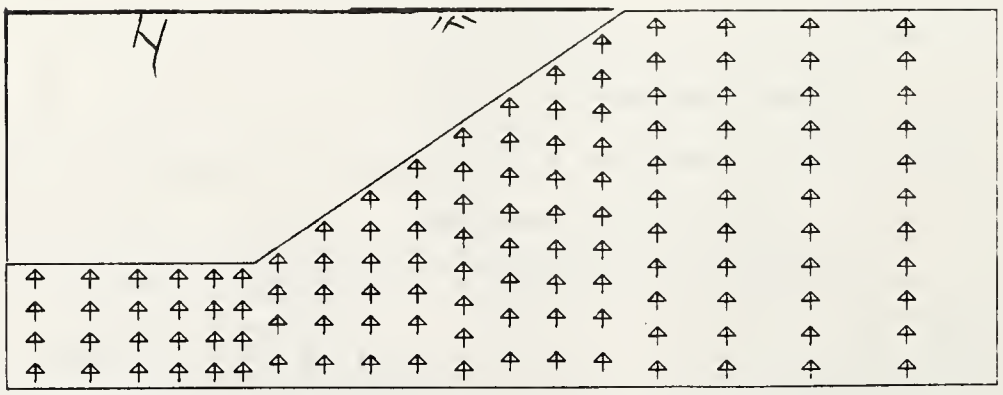

STRESS DIRECTION

- = FAILED ELEM.

Figure 5.4: Continued

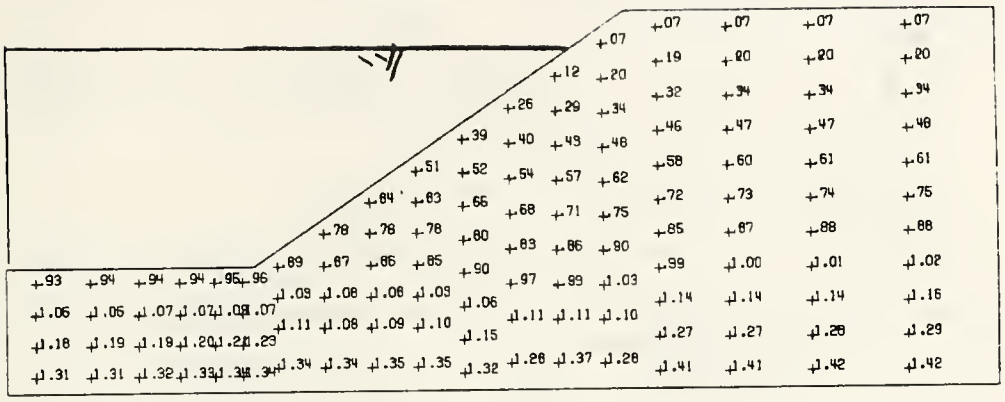

VERT STR/UNIT WT/HEIGHT

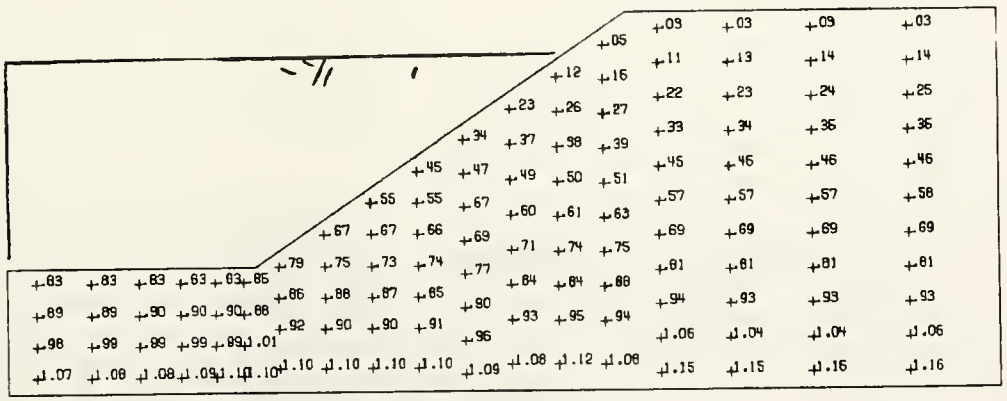

HORZ STR/UNIT WT/HEIGHT

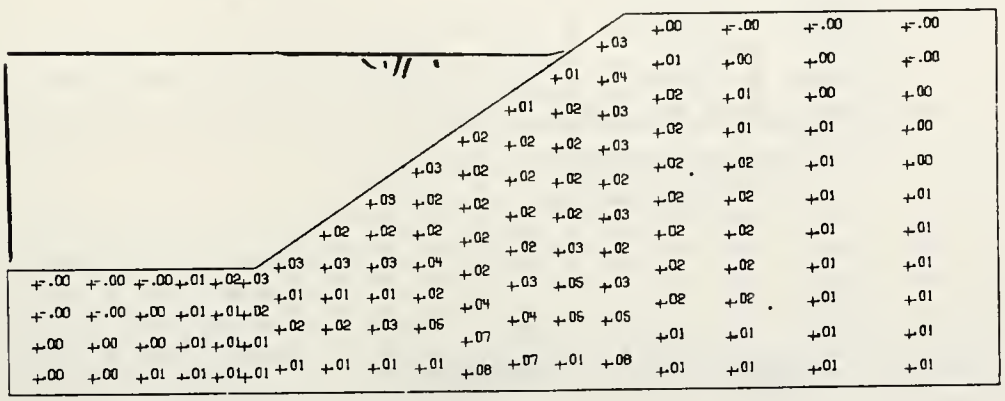

SHEAR STR/UNIT WT/HEIGHT

Figure 5.5: Vertical, Horizontal, and Shearing Stresses, Displacements and Stress Direction for Increment 1 for the Case of a Slope with No Pier

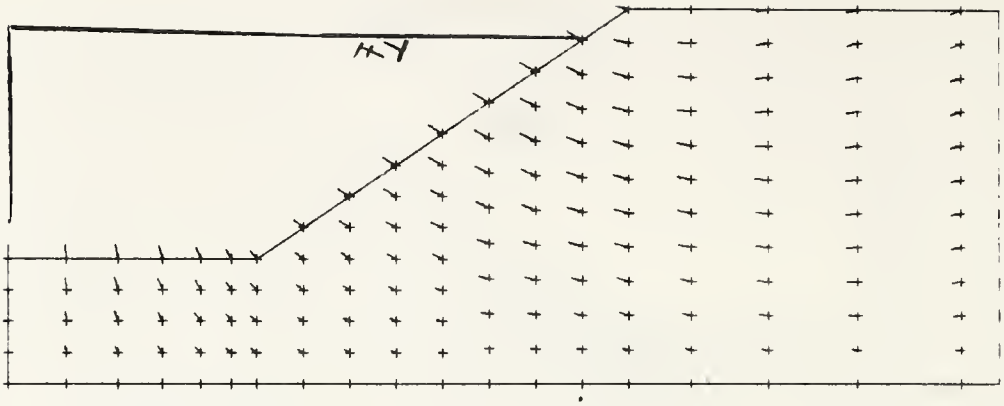

DISPLACEMENTS

VECTOR SCALE = 5.0

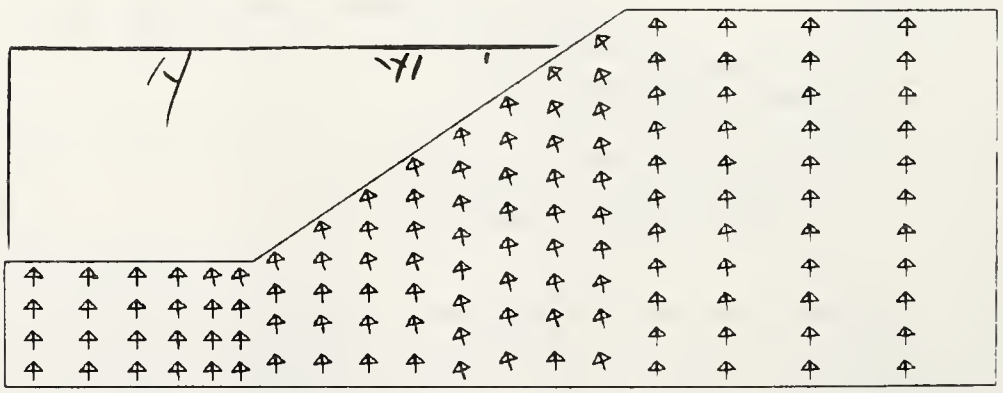

STRESS DIRECTION

- = FAILED ELEM.

Figure 5.5: Continued

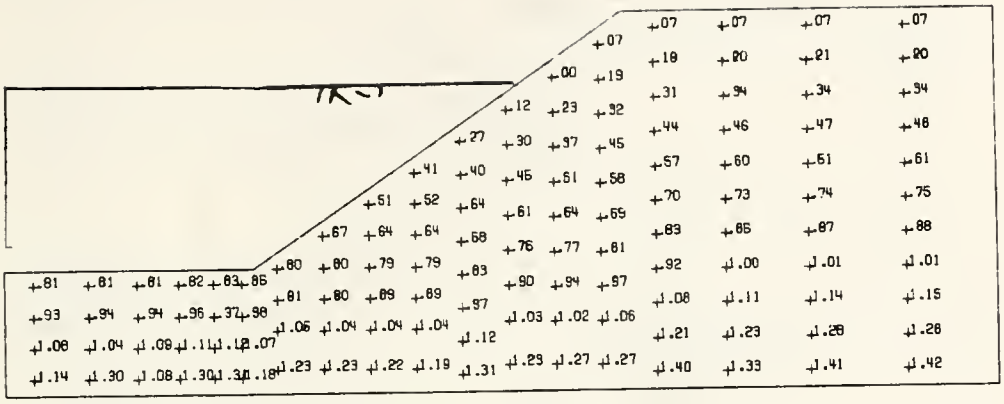

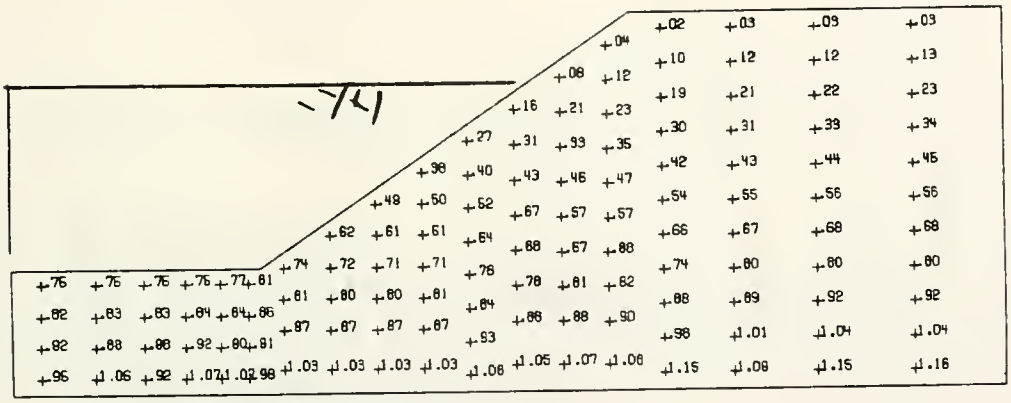

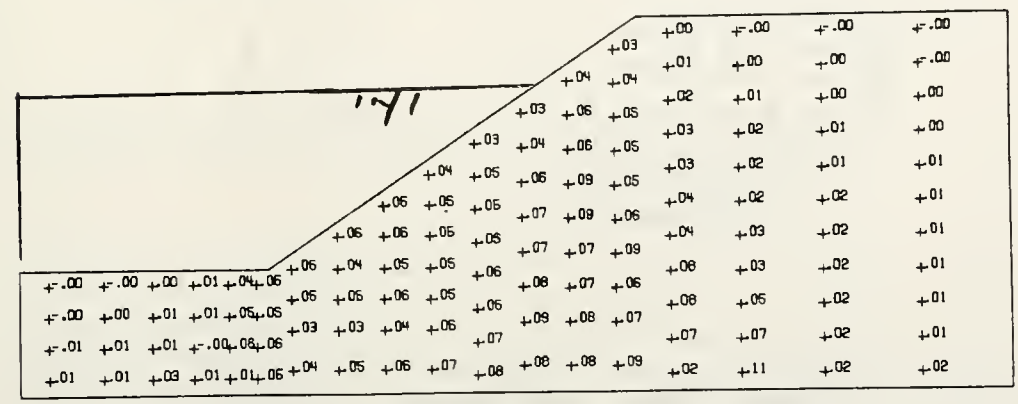

Figure 5.6: Vertical, Horizontal, and Shearing Stresses, Displacements and Stress Direction for Increment 2 for the Case of a Slope with No Pier

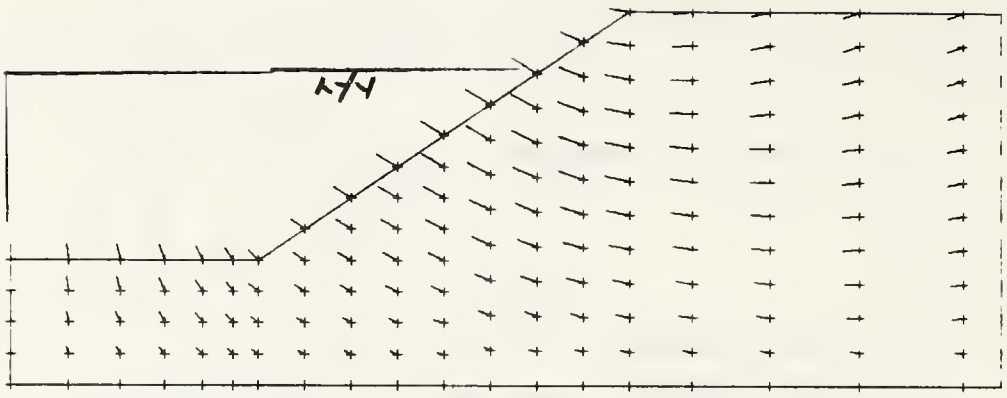

DISPLACEMENTS

VECTOR SCALE = 5.0

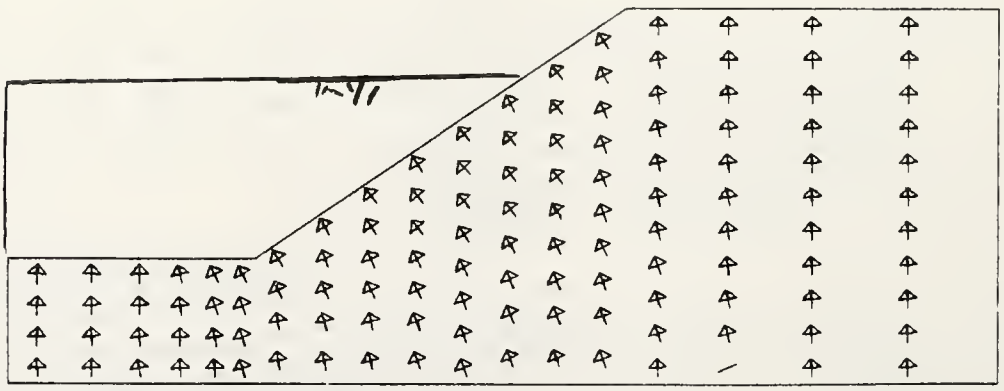

STRESS DIRECTION

- = FAILED ELEM. .

Figure 5.6: Continued

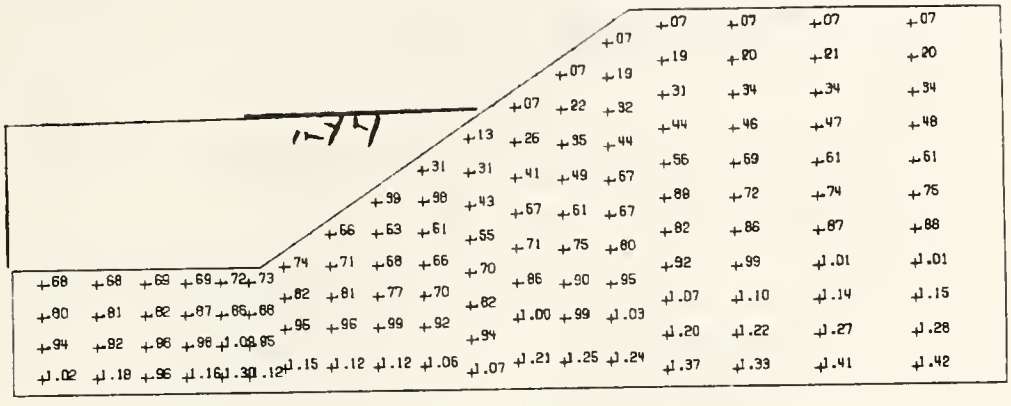

VERT STR/UNIT WT/HEIGHT

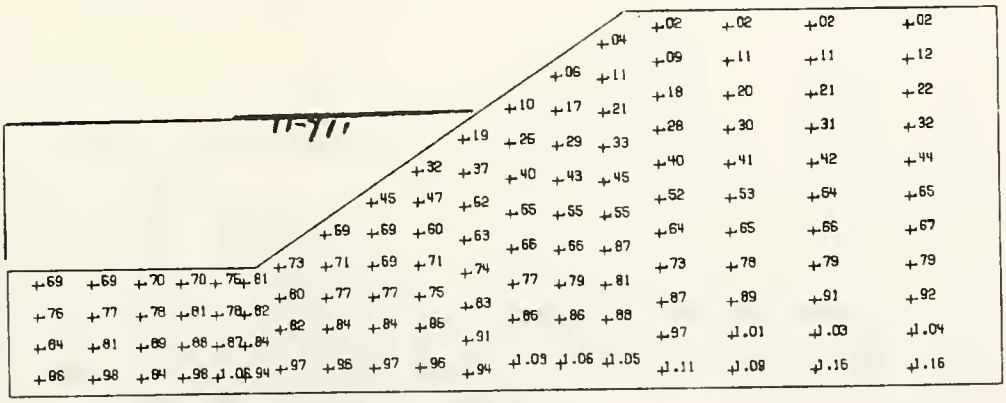

HORZ STR/UNIT WT/HEIGHT

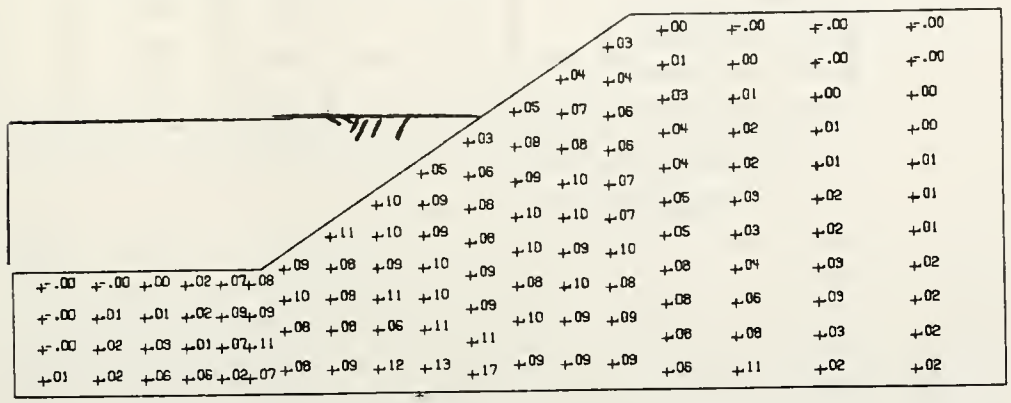

SHEAR STR/UNIT WT/HEIGHT

Figure 5.7: Vertical, Horizontal, and Shearing Stresses, Displacements and Stress Direction for Increment 3 for the Case of a Slope with No Pier

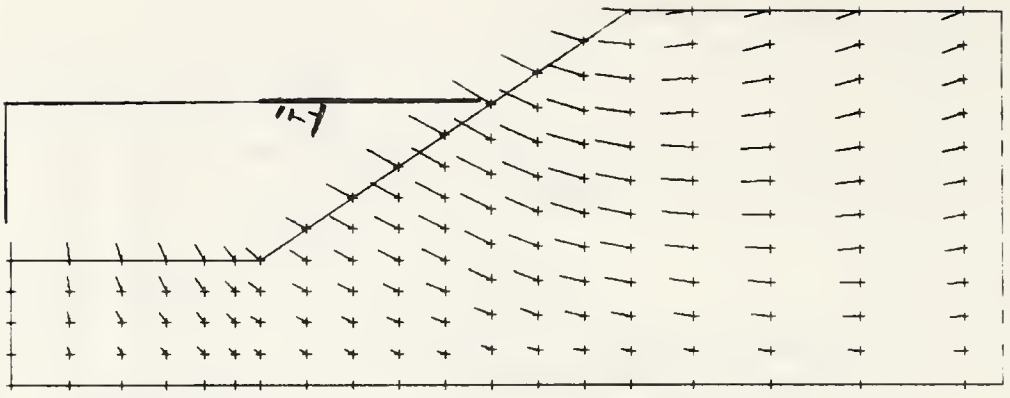

DISPLACEMENTS

VECTOR SCALE = 5.0

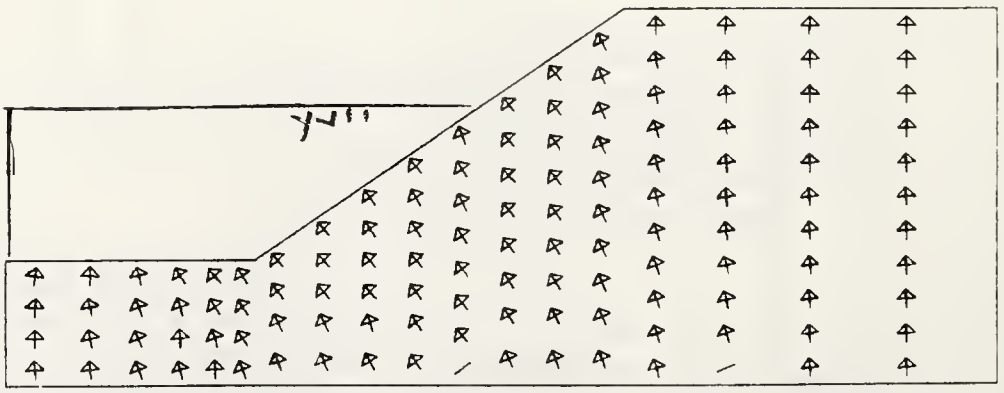

STRESS DIRECTION

.- = FAILED ELEM.

Figure 5.7: Continued

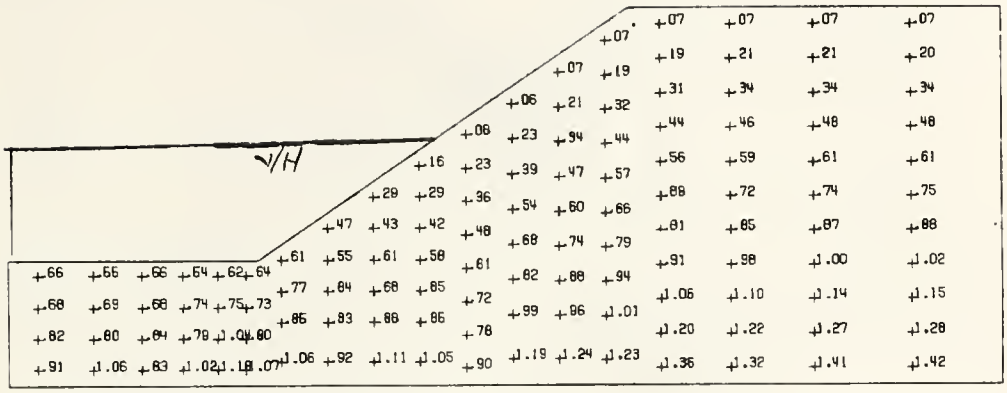

VERT STR/UNIT WT/HEIGHT

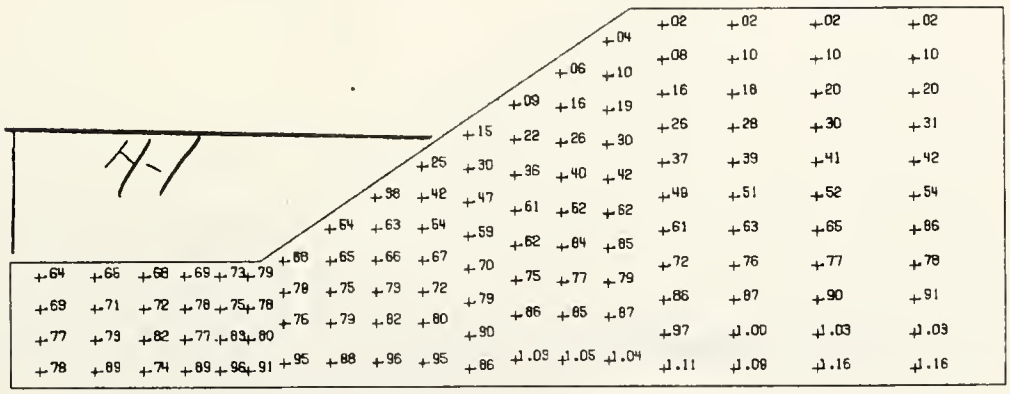

HORZ STR/UNIT WT/HEIGHT

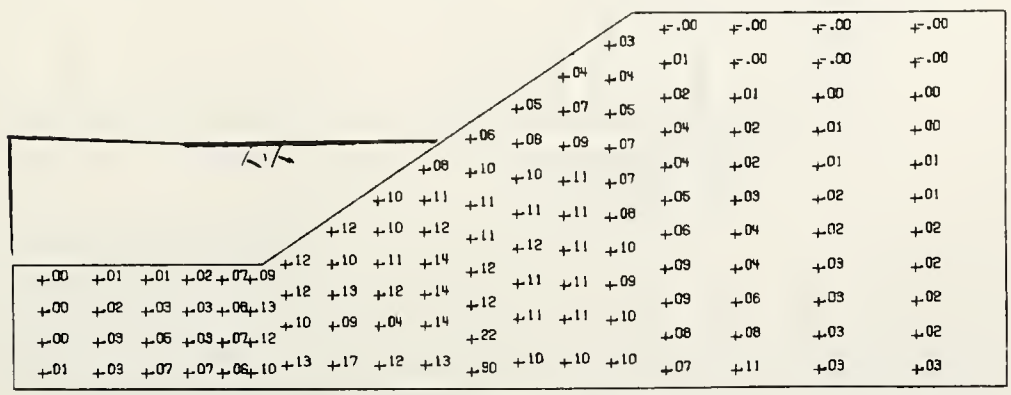

SHEAR STR/UNIT WT/HEIGHT

Figure 5.8: Vertical, Horizontal, and Shearing Stresses, Displacements and Stress Direction for Increment 4 for the Case of a Slope with No Pier

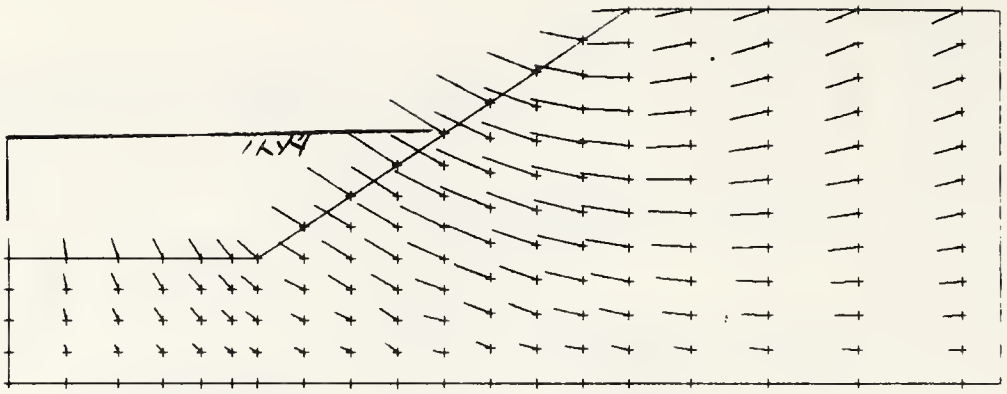

DISPLACEMENTS

VECTOR SCALE = 5.0

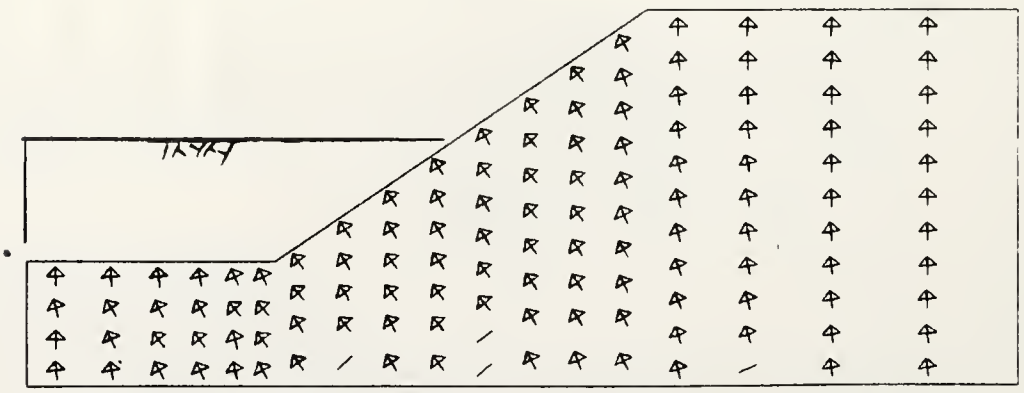

STRESS DIRECTION

- = FAILED ELEM.

Figure 5.8: Continued

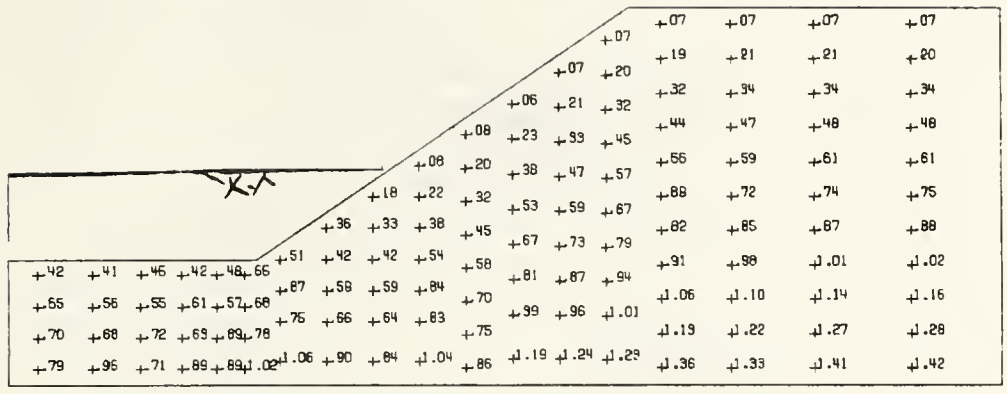

VERT STR/UNIT WT/HEIGHT

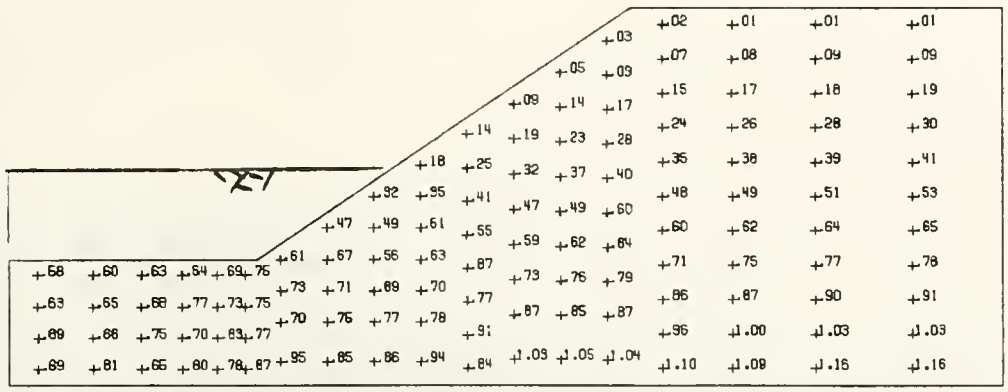

HORZ STR/UNIT WT/HEIGHT

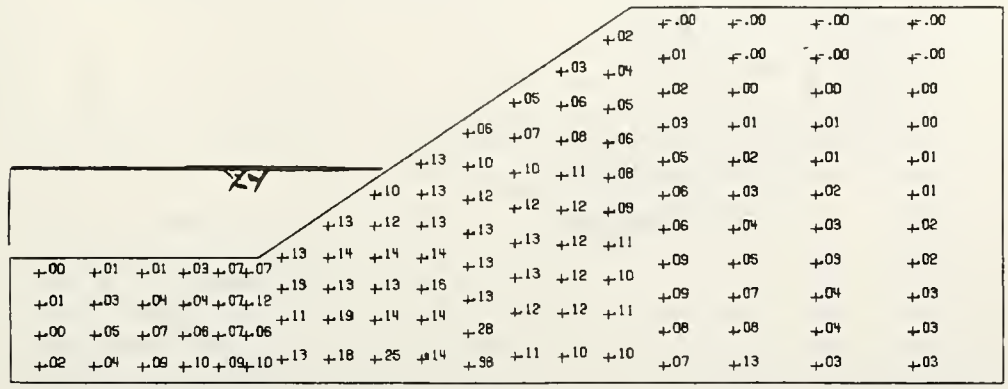

SHEAR STR/UNIT WT/HEIGHT

Figure 5.9: Vertical, Horizontal, and Shearing Stresses, Displacements and Stress Direction for Increment 5 for the Case of a Slope with No Pier

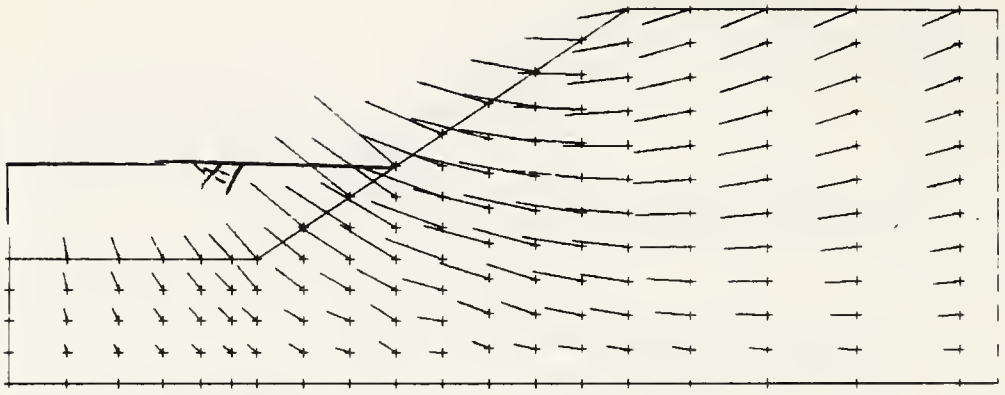

DISPLACEMENTS

VECTOR SCALE = 5.0

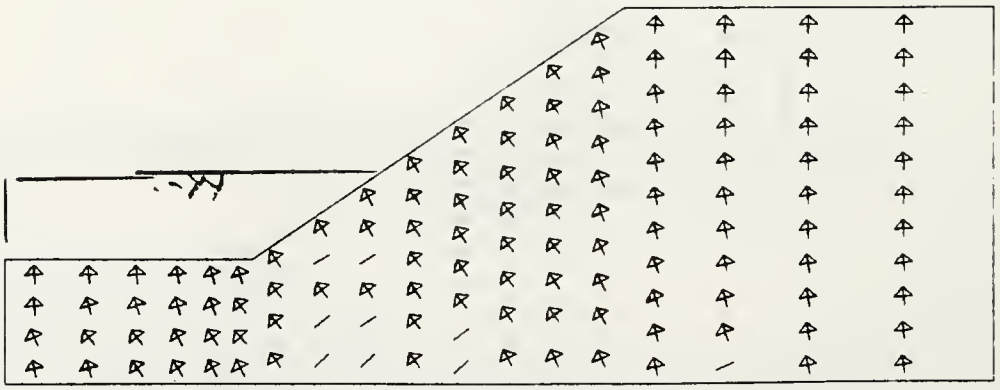

STRESS DIRECTION

- = FAILED ELEM.

Figure 5.9: Continued

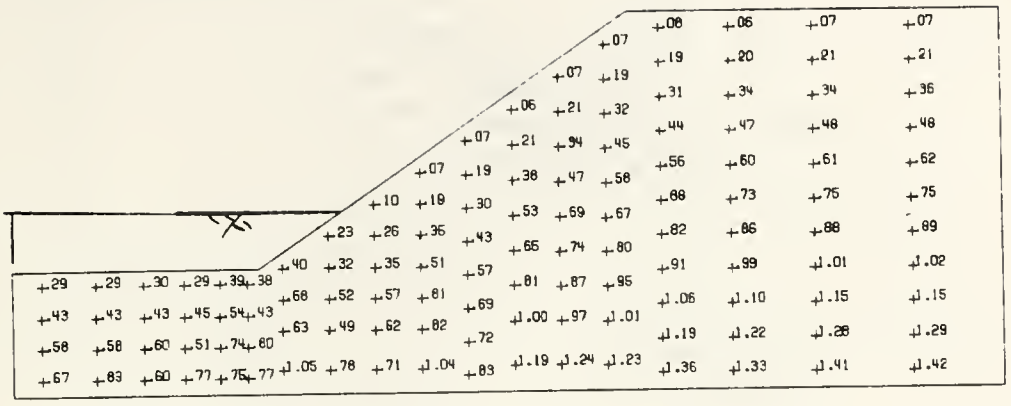

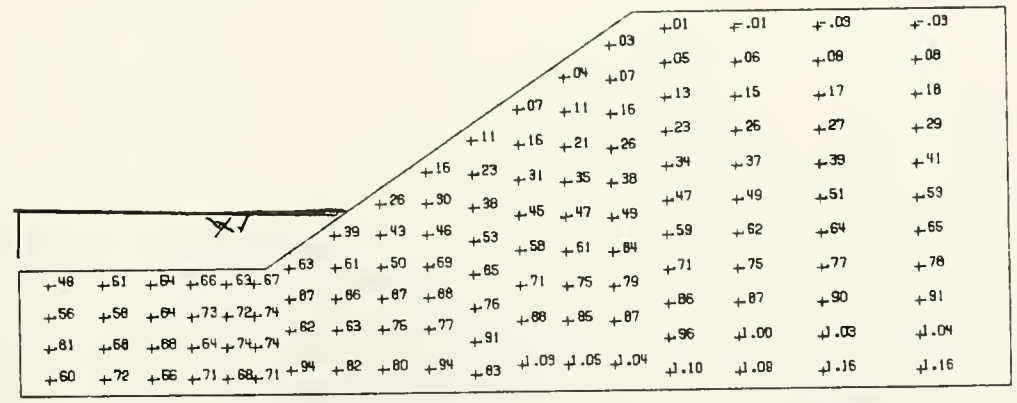

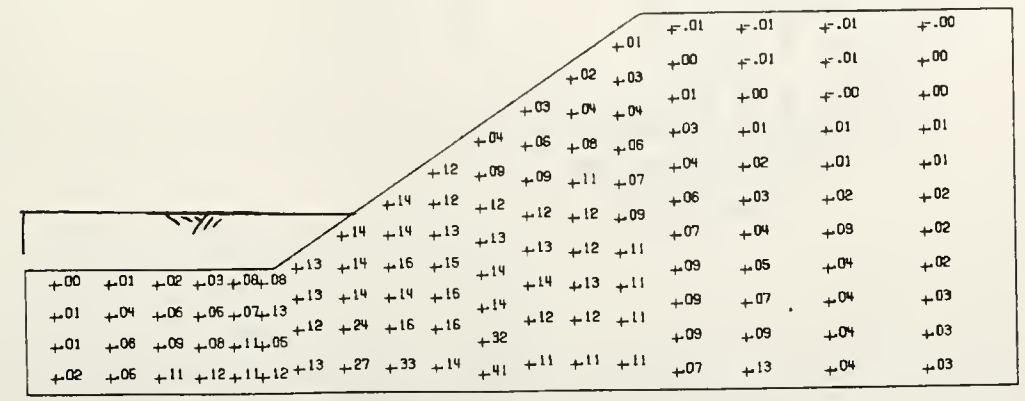

Figure 5.10: Vertical, Horizontal, and Shearing Stresses, Displacements and Stress Direction for Increment 6 for the Case of a Slope with No Pier

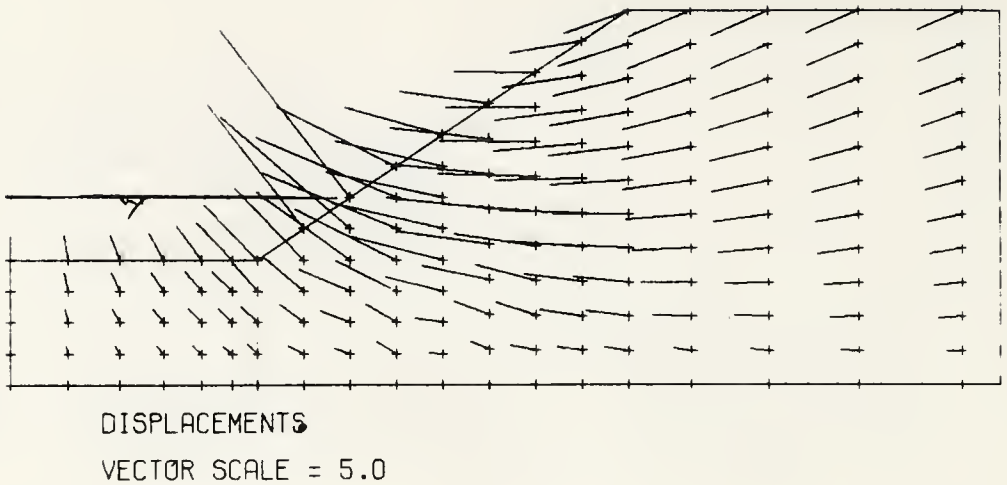

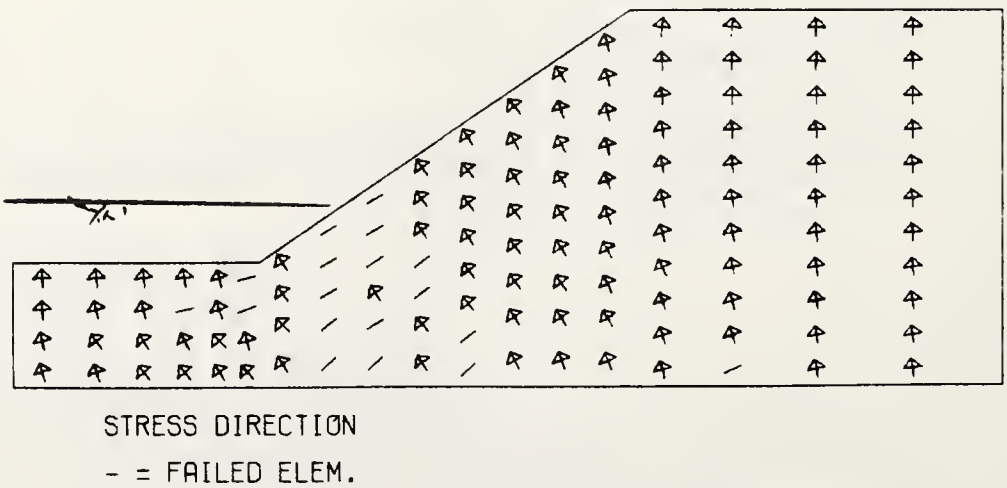

Figure 5.10: Continued

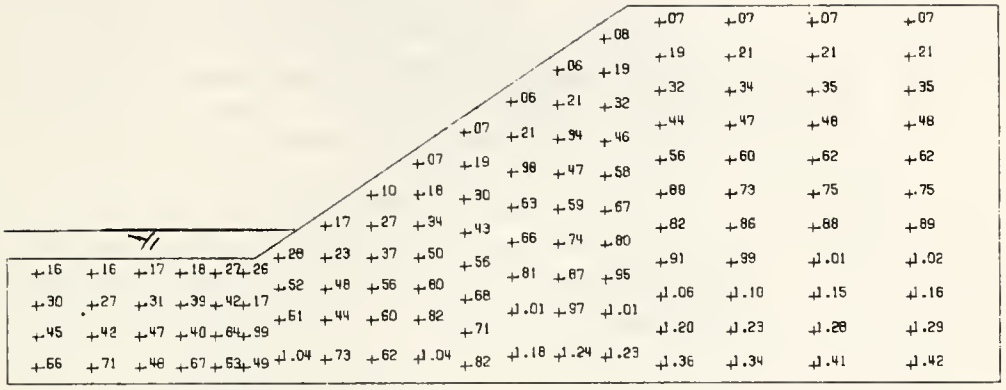

VERT STR/UNIT WT/HEIGHT

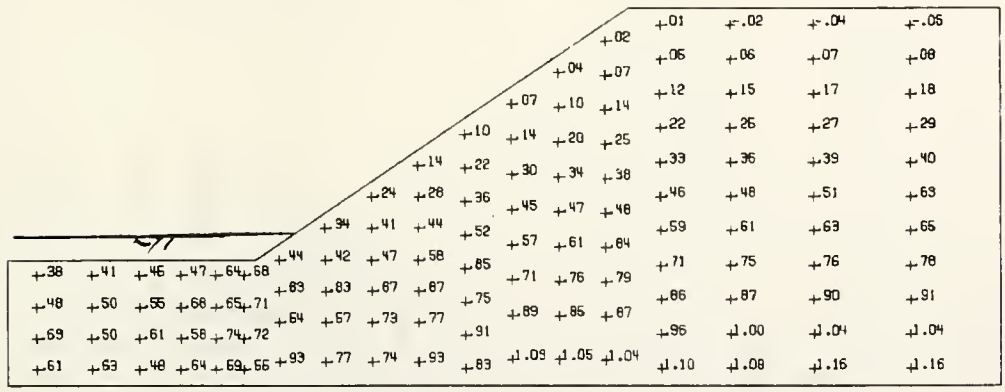

HORZ STR/UNIT WT/HEIGHT

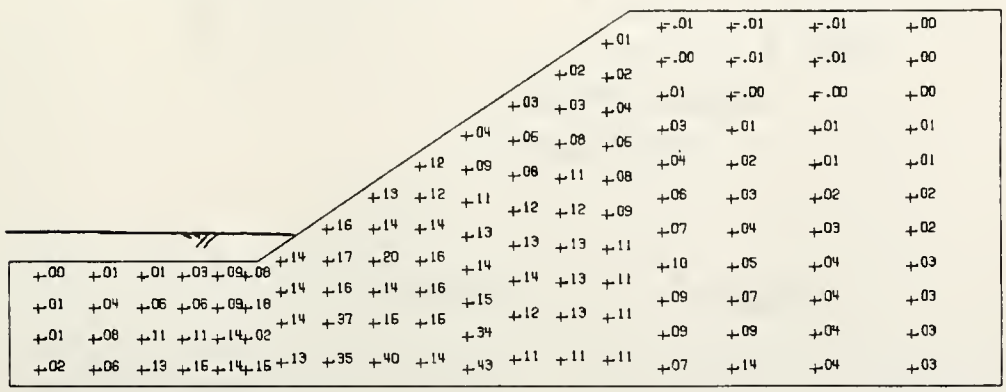

SHEAR STR/UNIT WT/HEIGHT

Figure 5.11: Vertical, Horizontal, and Shearing Stresses, Displacements and Stress Direction for Increment 7 for the Case of a Slope with No Pier

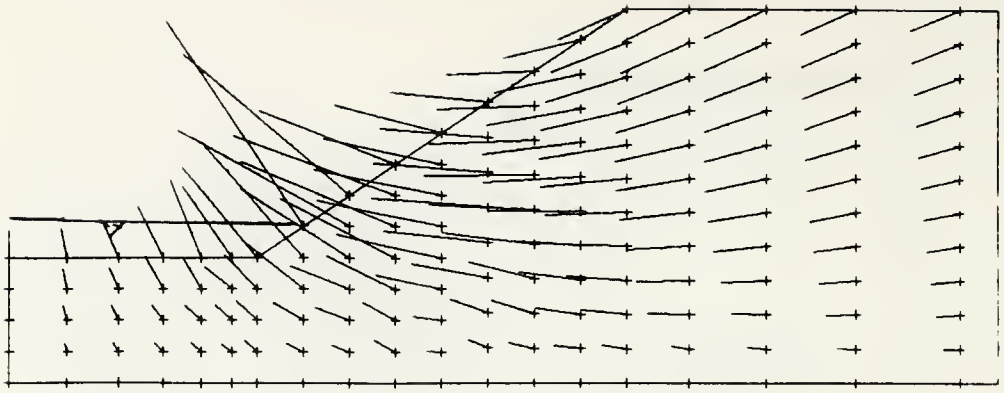

DISPLACEMENTS

VECTOR SCALE = 5.0

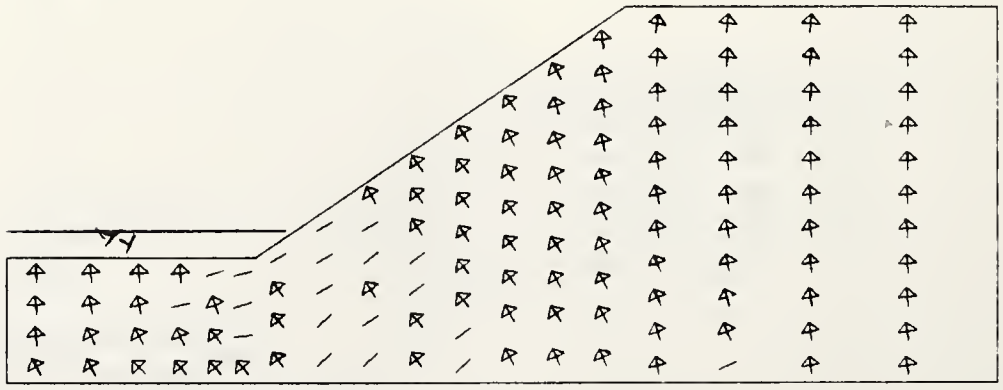

STRESS DIRECTION

- = FAILED ELEM.

Figure 5.11: Continued

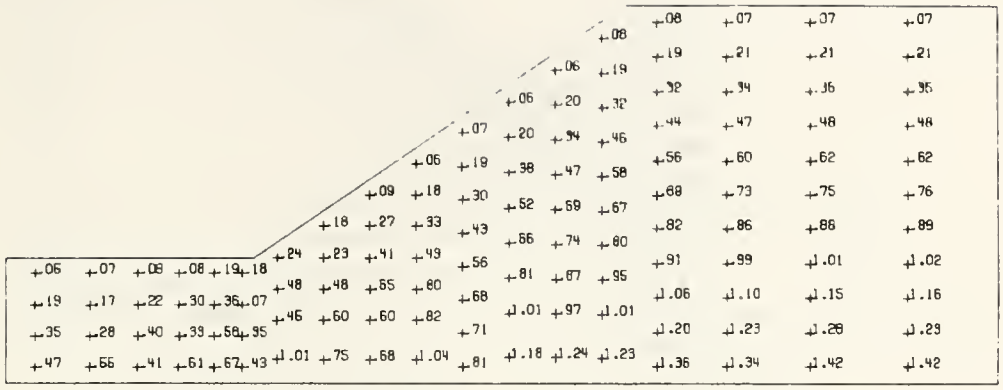

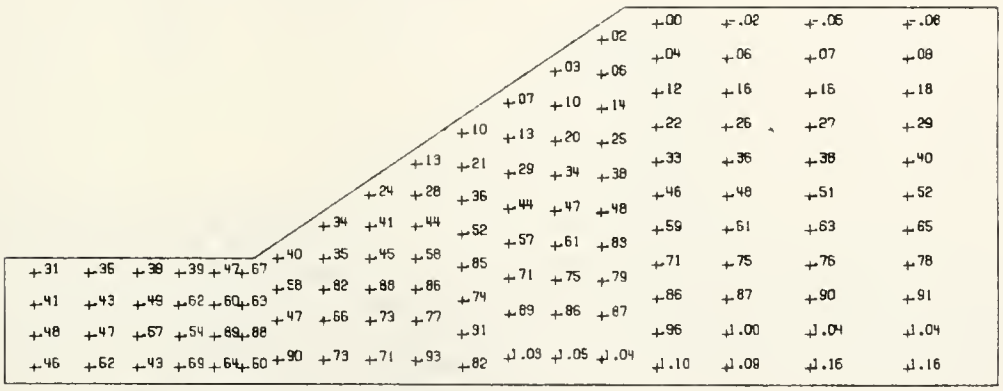

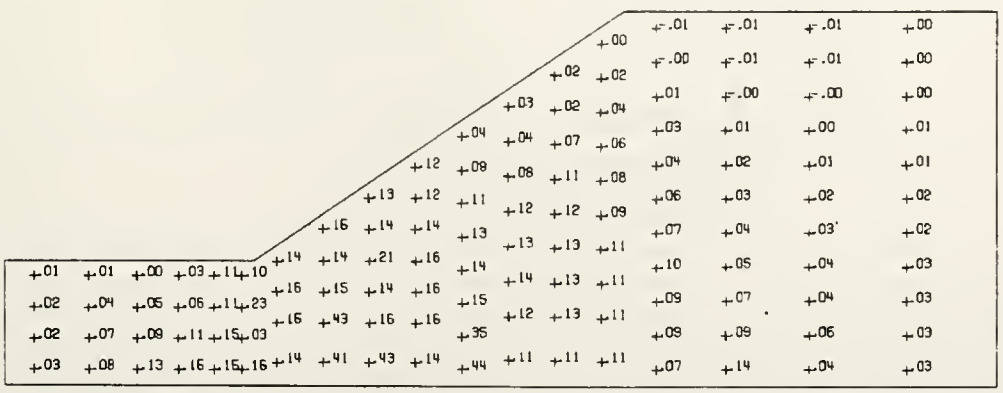

Figure 5.12: Vertical, Horizontal, and Shearing Stresses, Displacements and Stress Direction for Increment 8 for the Case of a Slope with No Pier

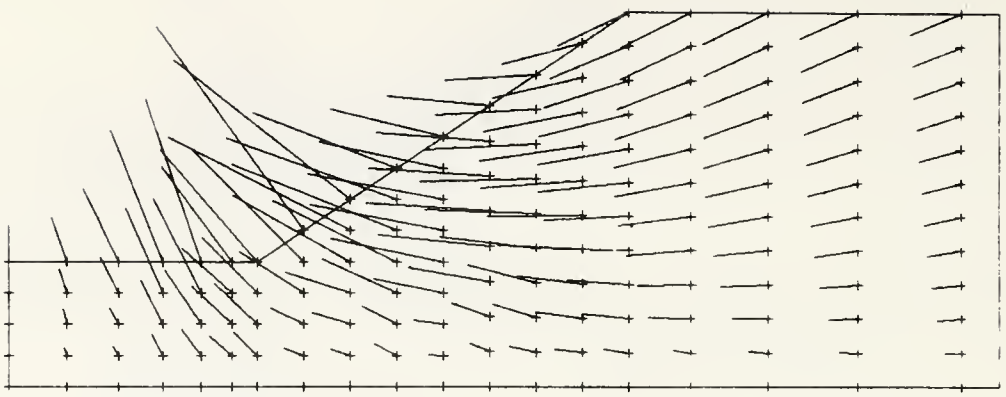

DISPLACEMENTS

VECTOR SCALE = 5.0

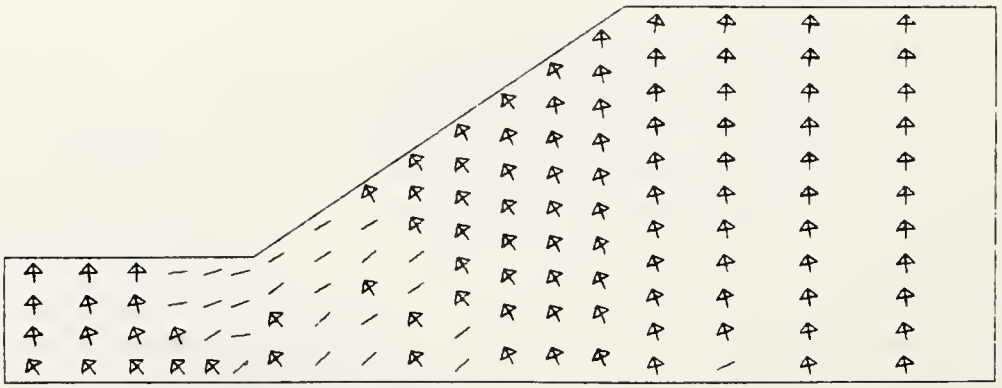

STRESS DIRECTION

- = FAILED ELEM.

Figure 5.12: Continued

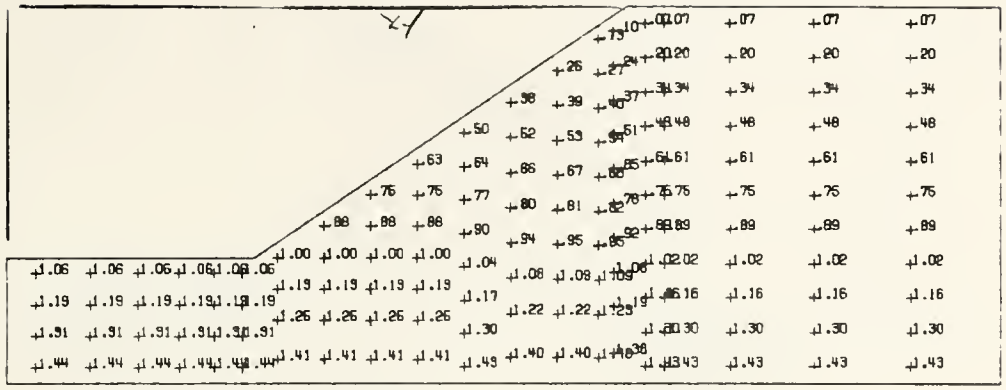

VERT STR/UNIT WT/HEIGHT

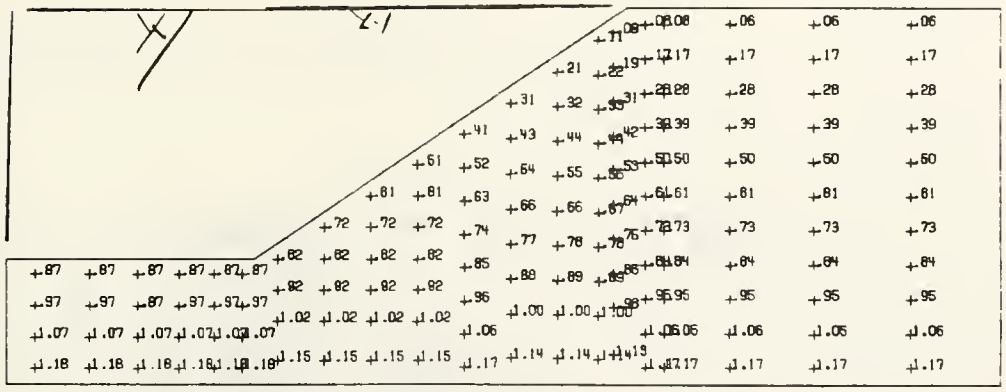

HORZ STR/UNIT WT/HEIGHT

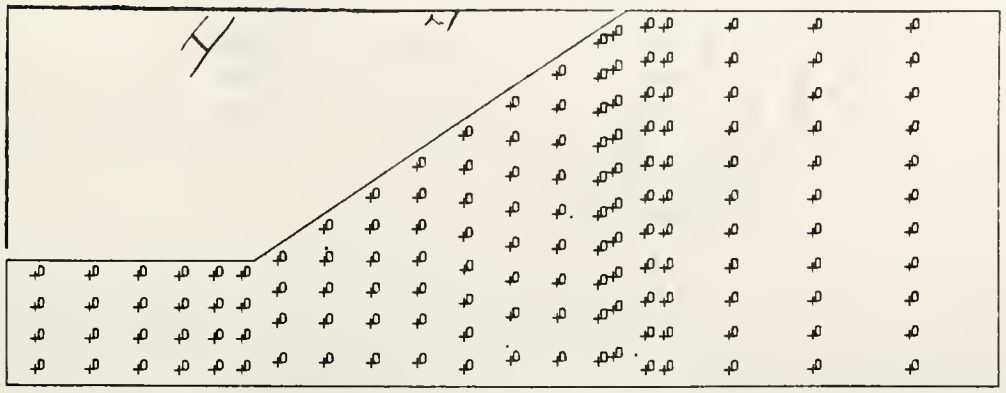

SHEAR STR/UNIT WT/HEIGHT

Figure 5.13: Vertical, Horizontal, and Shearing Stresses, Displacements and Stress Direction for Increment 0 for the Case of a Slope with a Pier

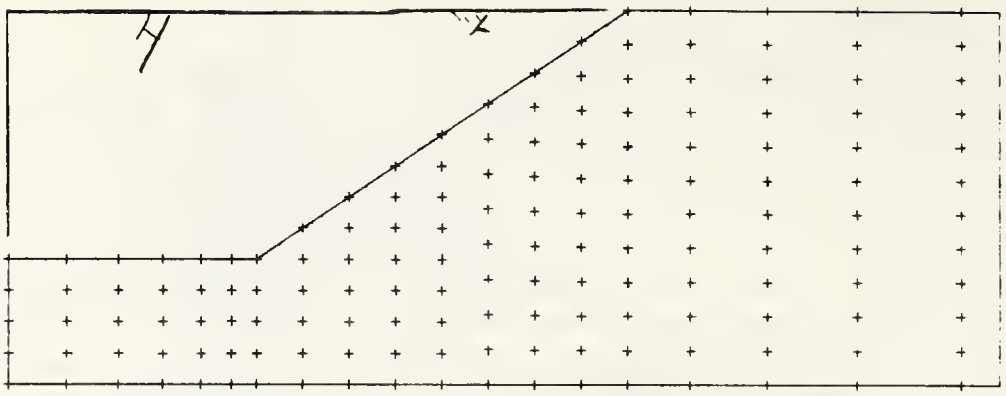

DISPLACEMENTS

VECTOR SCALE = 5.0

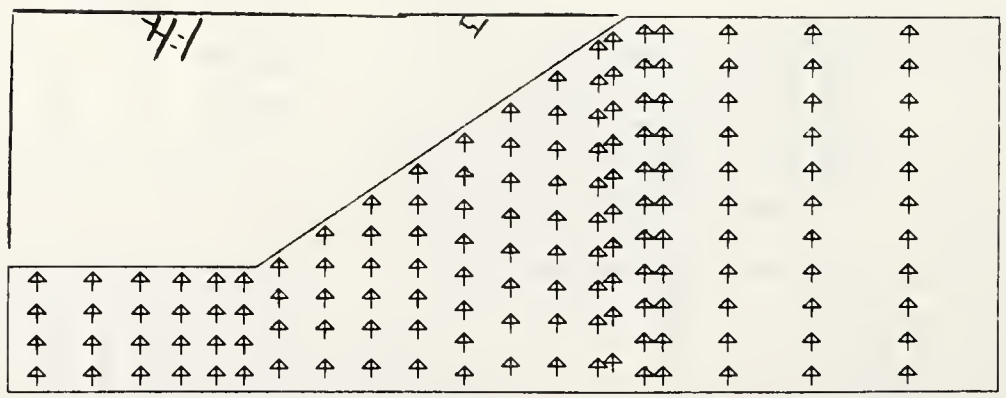

STRESS DIRECTION

- = FAILED ELEM.

Figure 5.13: Continued

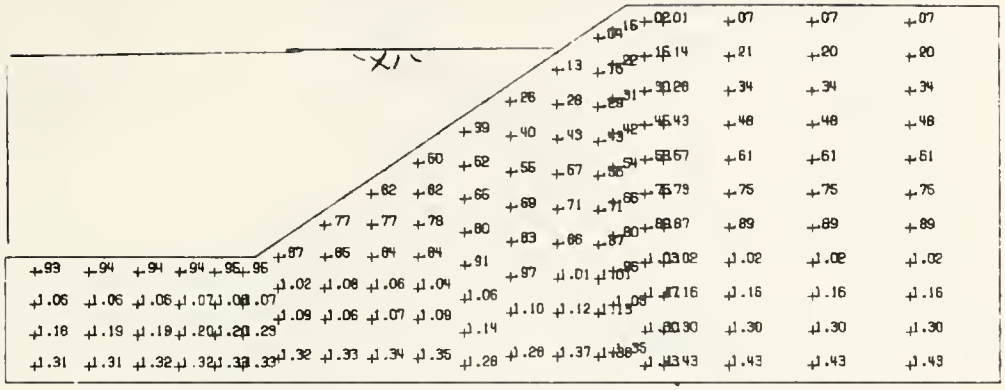

VERT STR/UNIT WT/HEIGHT

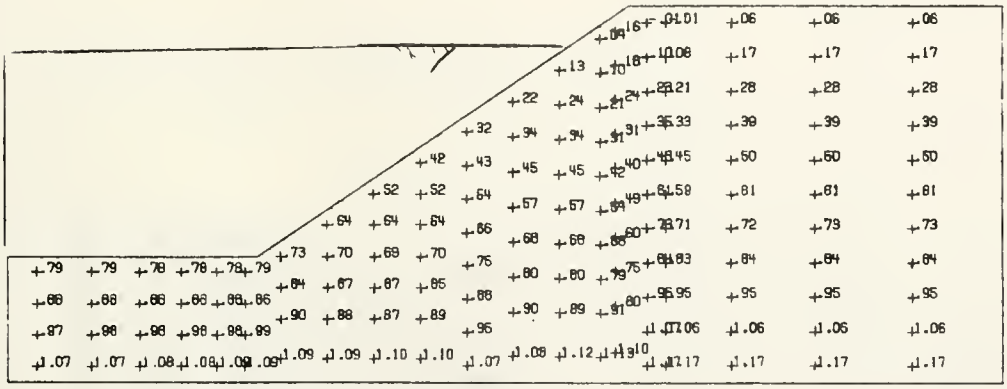

HORZ STR/UNIT WT/HEIGHT

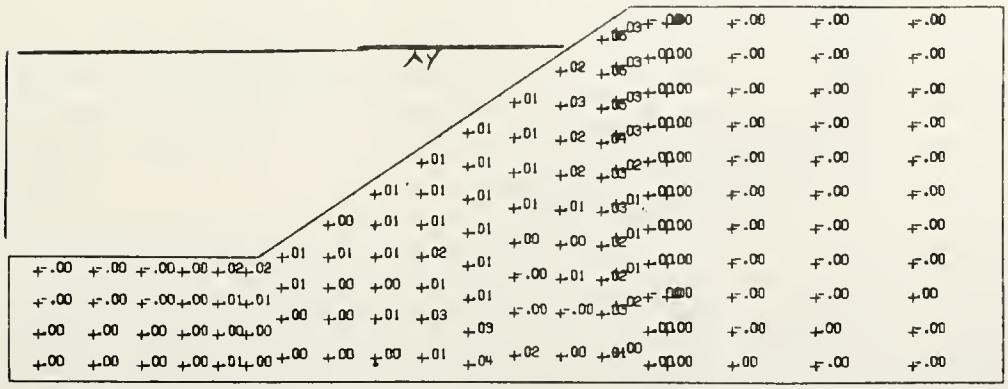

SHEAR STR/UNIT WT/HEIGHT

Figure 5.14: Vertical, Horizontal, and Shearing Stresses, Displacements and Stress Direction for Increment 1 for the Case of a Slope with a Pier

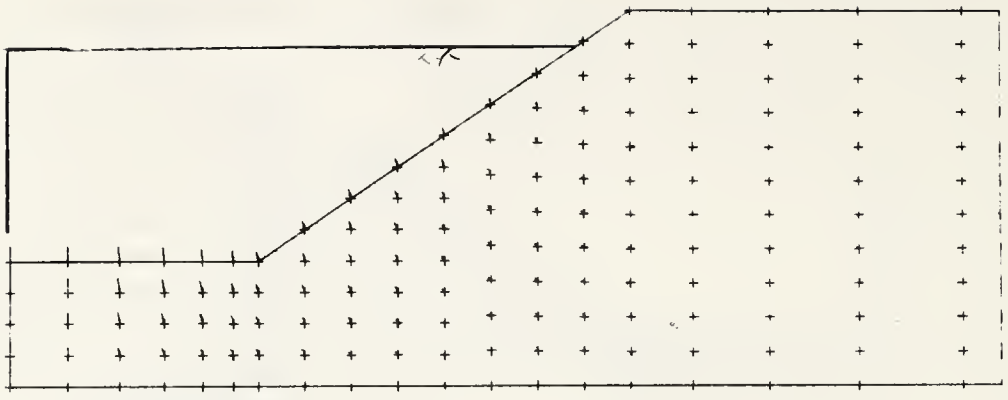

DISPLACEMENTS

VECTOR SCALE = 5.0

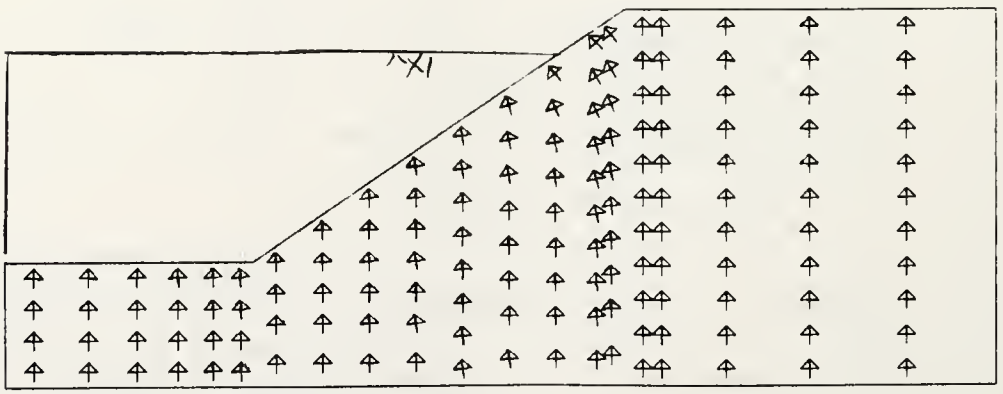

STRESS DIRECTION

- = FAILED ELEM.

Figure 5.14: Continued

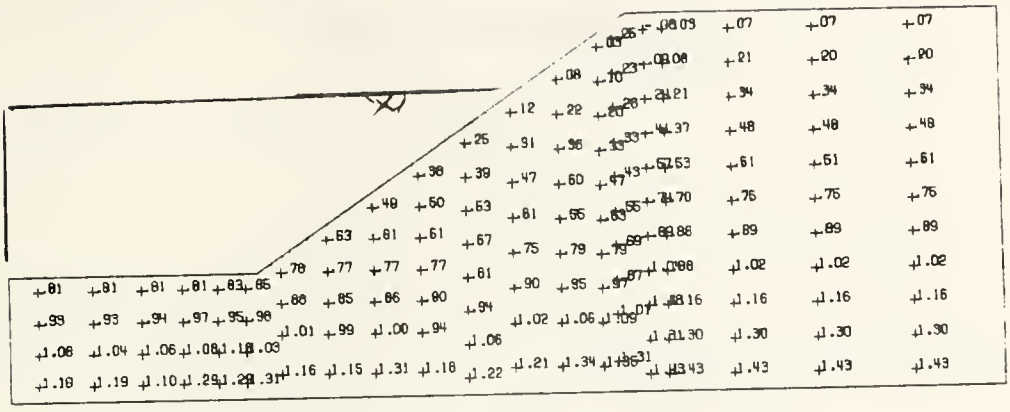

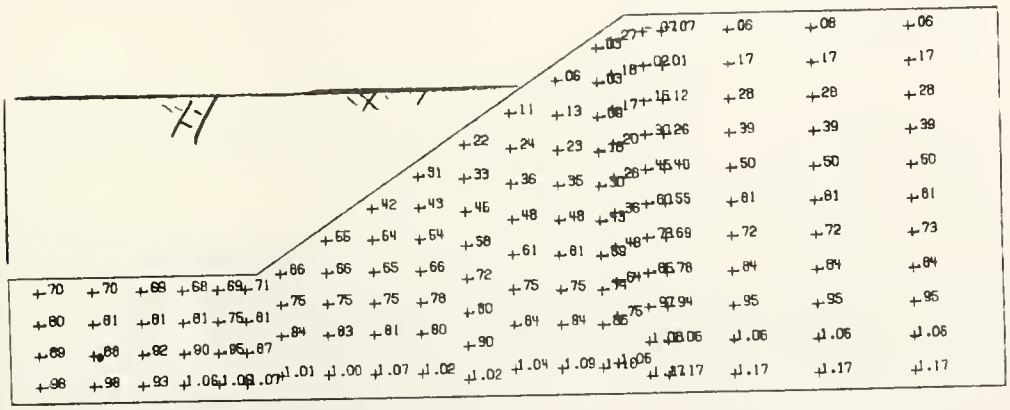

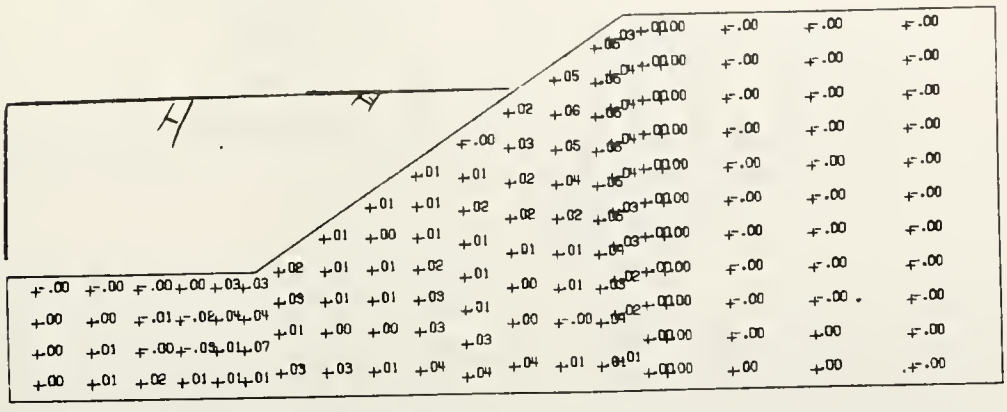

Figure 5.15: Vertical, Horizontal, and Shearing Stresses, Displacements and Stress Direction for Increment 2 for the Case of a Slope with a Pier

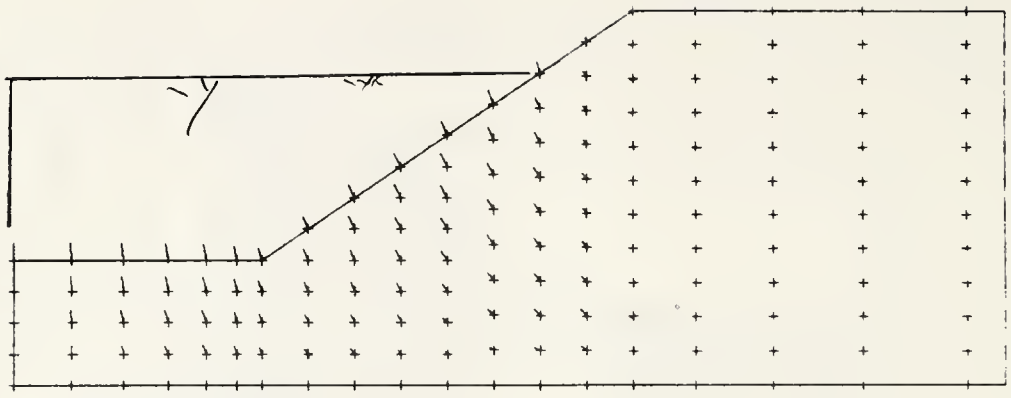

DISPLACEMENTS

VECTOR SCALE = 5.0

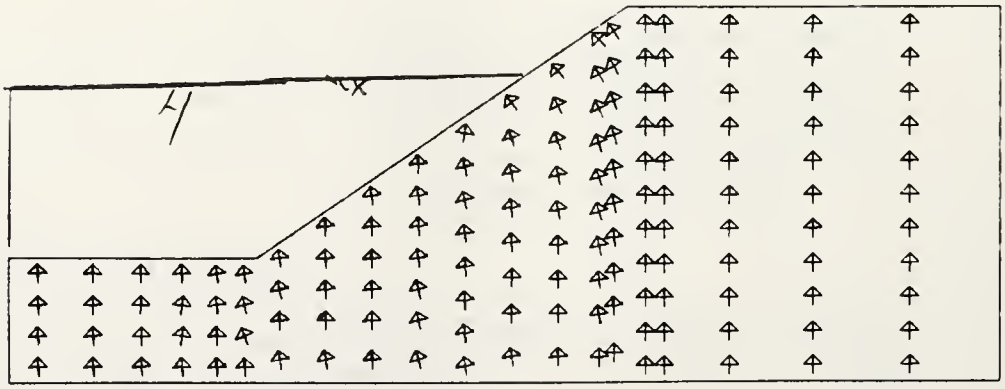

STRESS DIRECTION

- = FAILED ELEM.

Figure 5.15: Continued

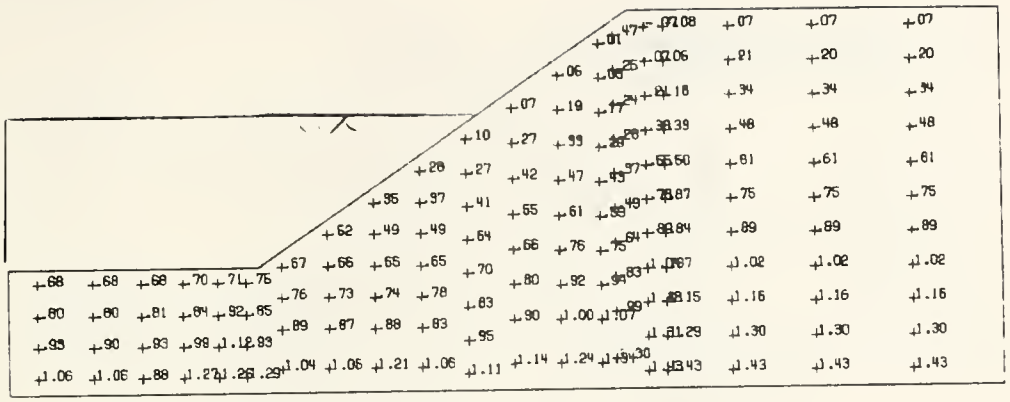

VERT STR/UNIT WT/HEIGHT

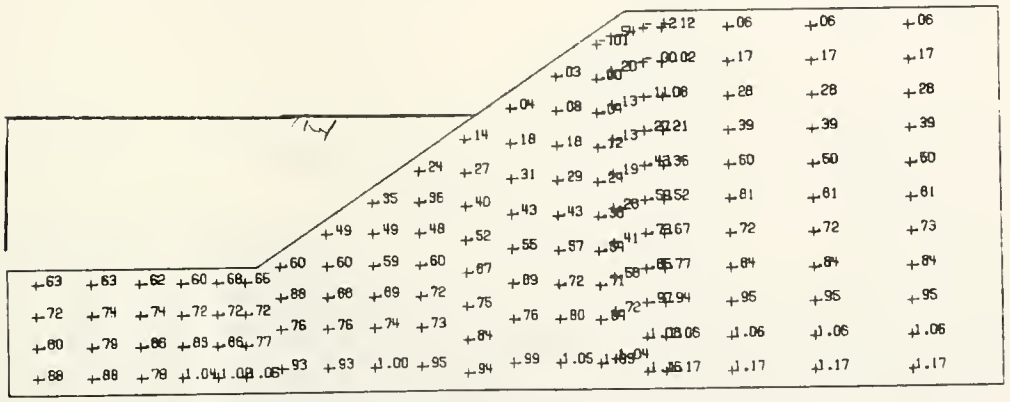

HORZ STR/UNIT WT/HEIGHT

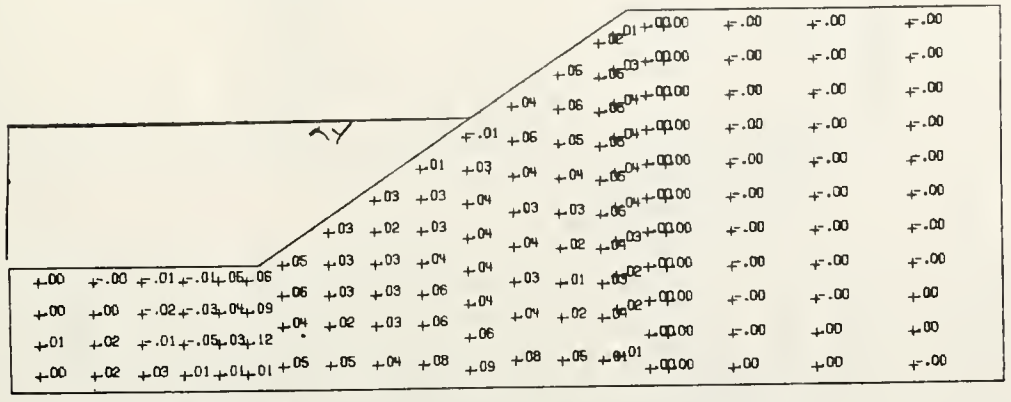

SHEAR STR/UNIT WT/HEIGHT

Figure 5.16: Vertical, Horizontal, and Shearing Stresses, Displacements and Stress Direction for Increment 3 for the Case of a Slope with a Pier

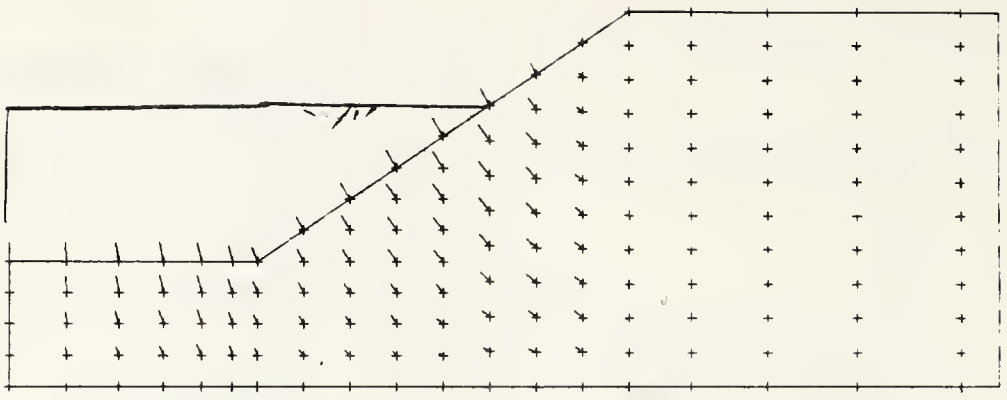

DISPLACEMENTS

VECTOR SCALE = 5.0

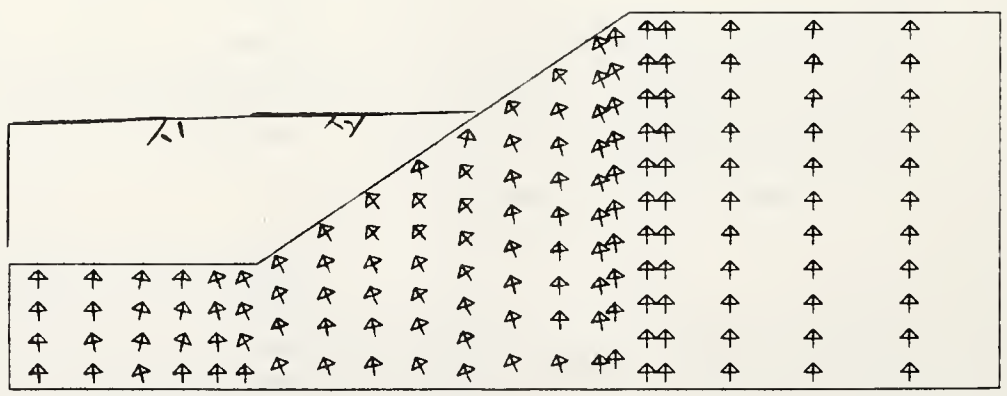

STRESS DIRECTION

- = FAILED ELEM.

Figure 5.16: Continued

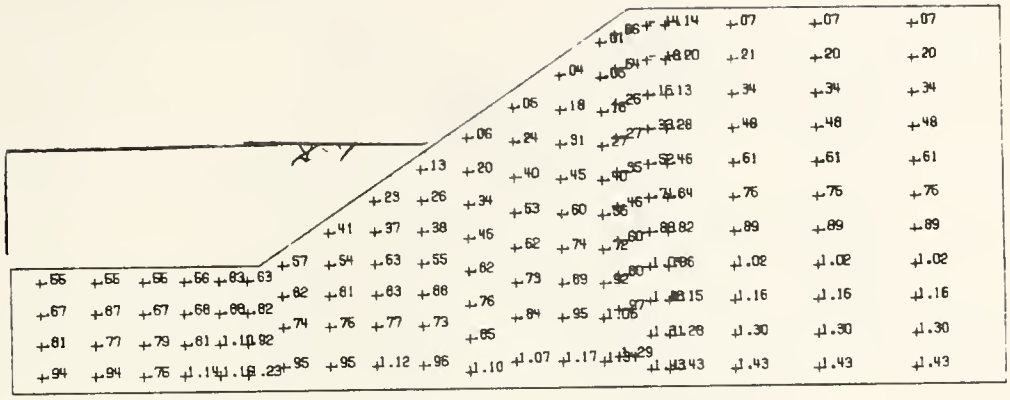

VERT STR/UNIT WT/HEIGHT

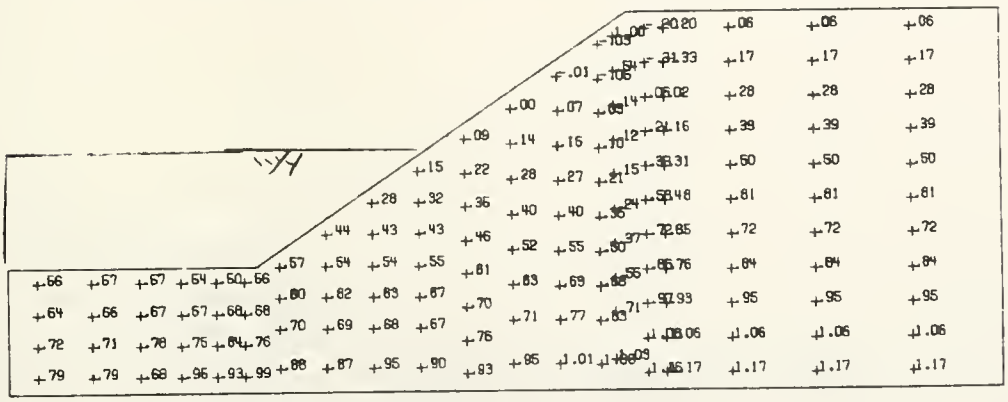

HORZ STR/UNIT WT/HEIGHT

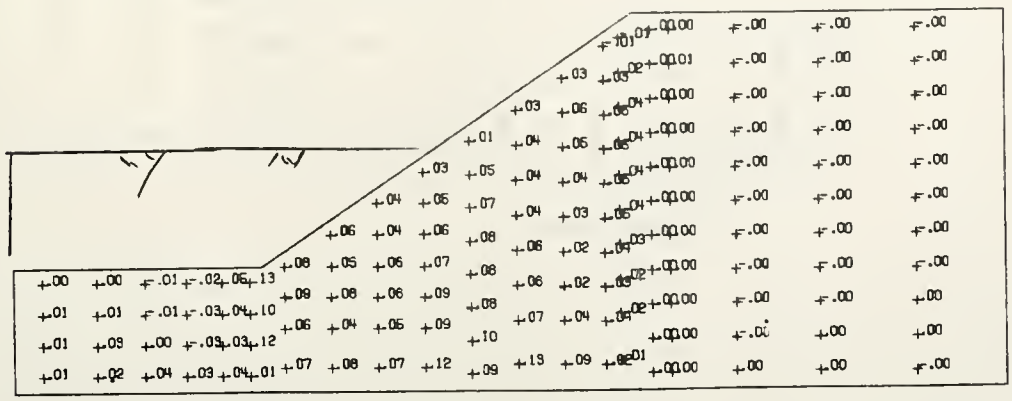

SHEAR STR/UNIT WT/HEIGHT

Figure 5.17: Vertical, Horizontal, and Shearing Stresses, Displacements and Stress Direction for Increment 4 for the Case of a Slope with a Pier

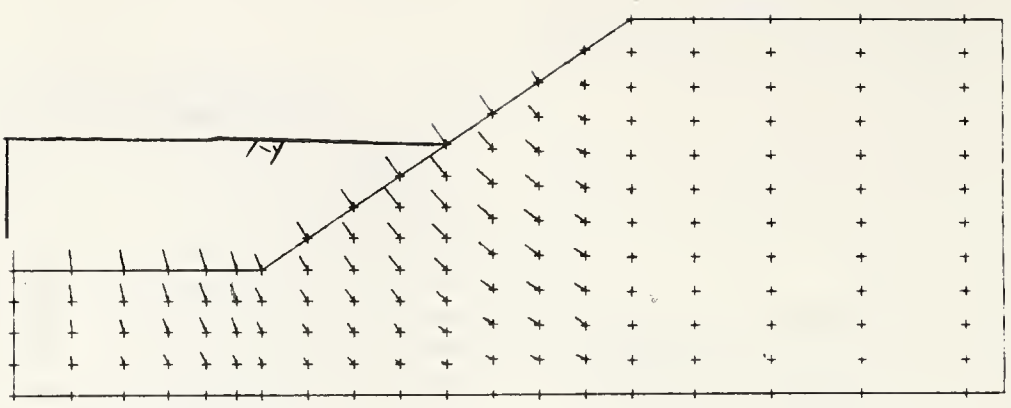

DISPLACEMENTS

VECTOR SCALE = 5.0

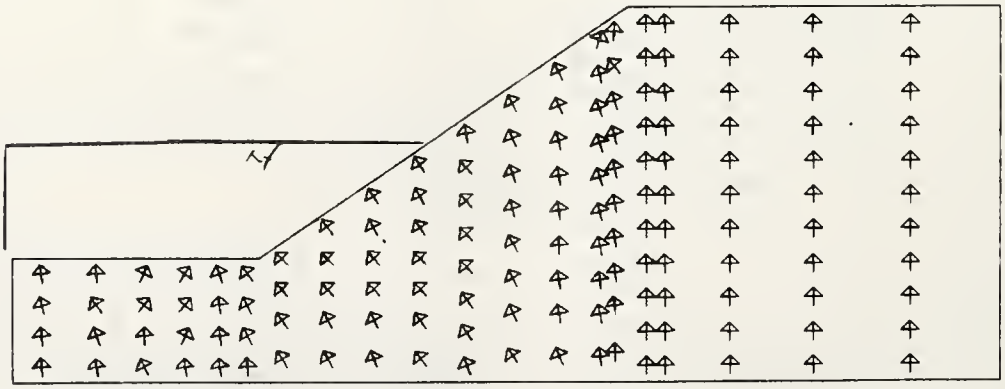

STRESS DIRECTION

- = FAILED ELEM.

Figure 5.17: Continued

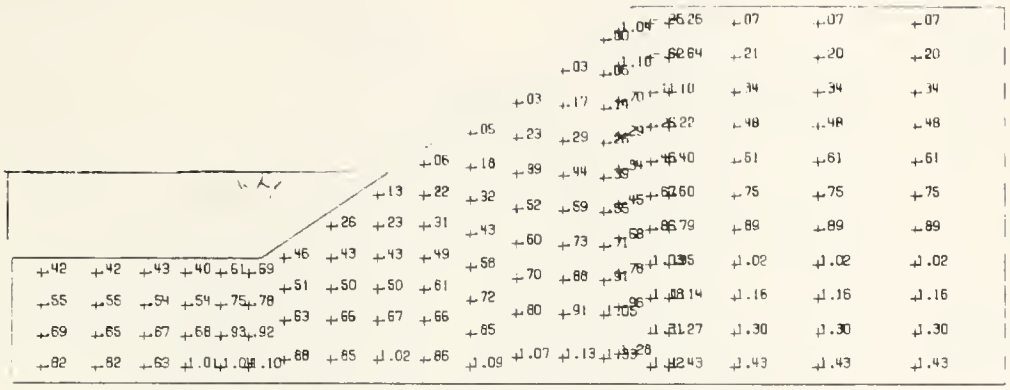

VERT STR/UNIT WT/HEIGHT

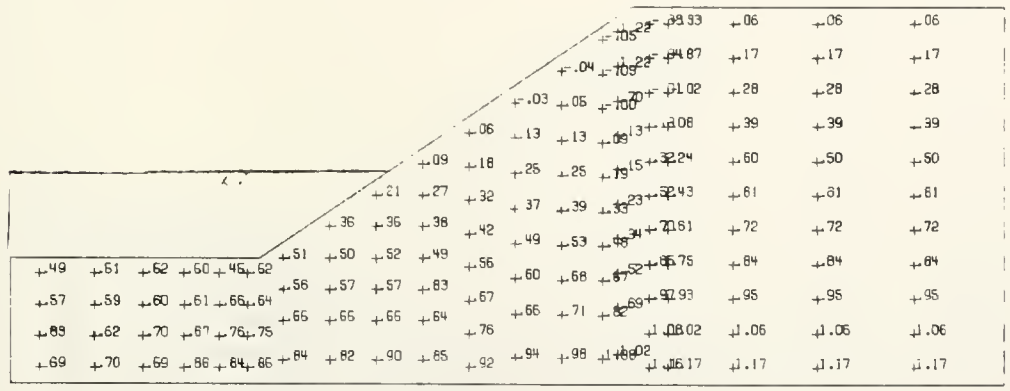

HORZ STR/UNIT WT/HEIGHT

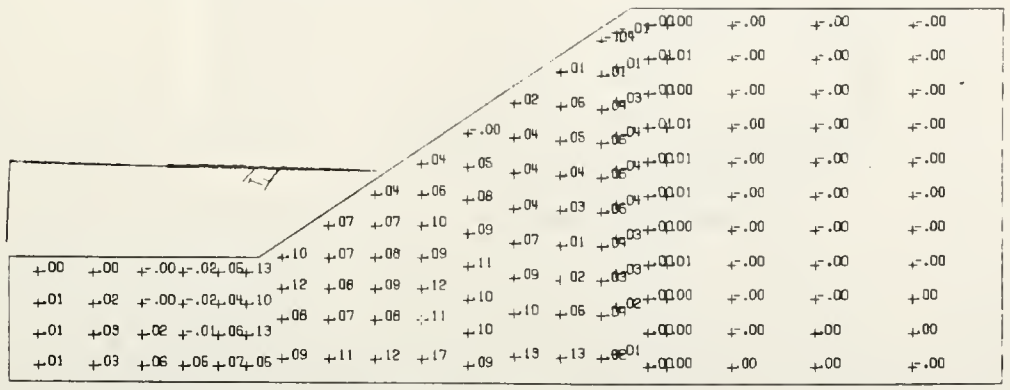

SHEAR STR/UNIT WT/HEIGHT

Figure 5.18: Vertical, Horizontal, and Shearing Stresses, Displacements and Stress Direction for Increment 5 for the Case of a Slope with a Pier

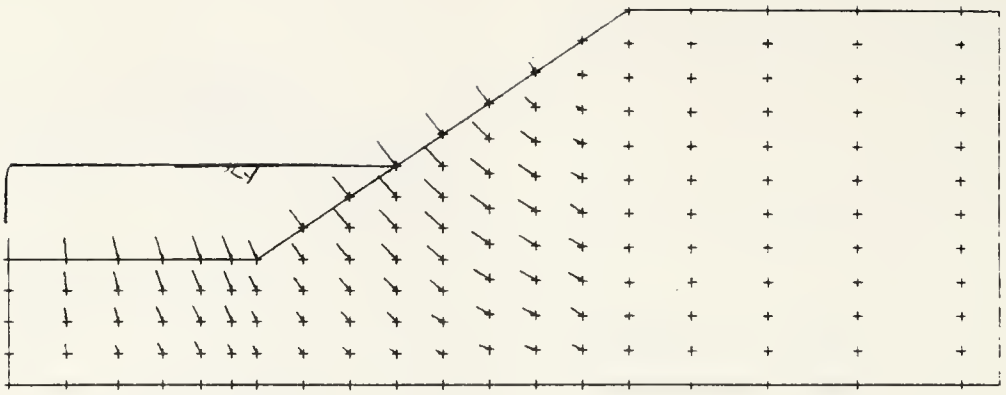

DISPLACEMENTS

VECTOR SCALE = 5.0

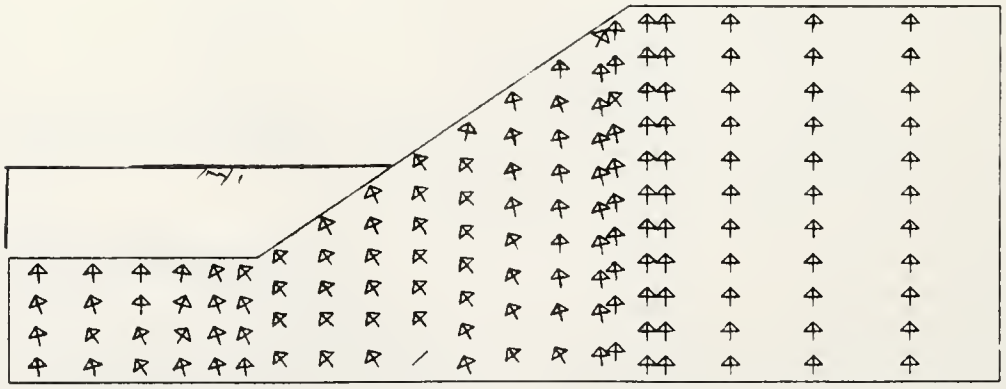

STRESS DIRECTION

- = FAILED ELEM.

Figure 5.18: Continued

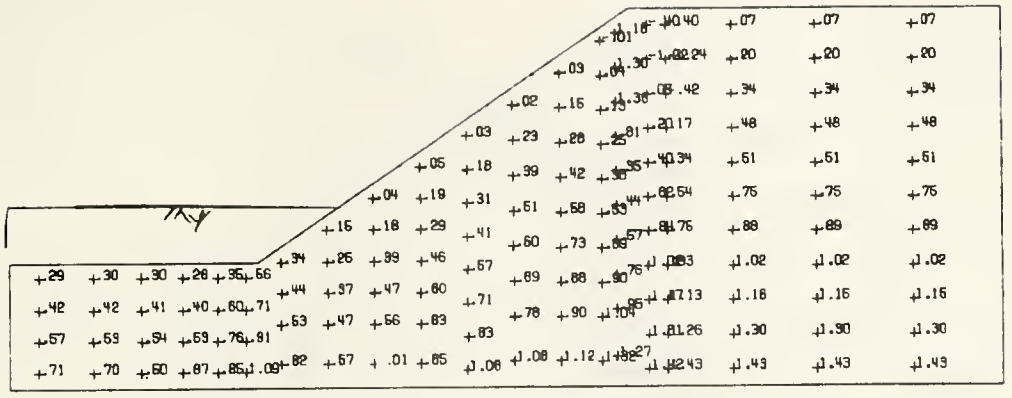

VERT STR/UNIT WT/HEIGHT

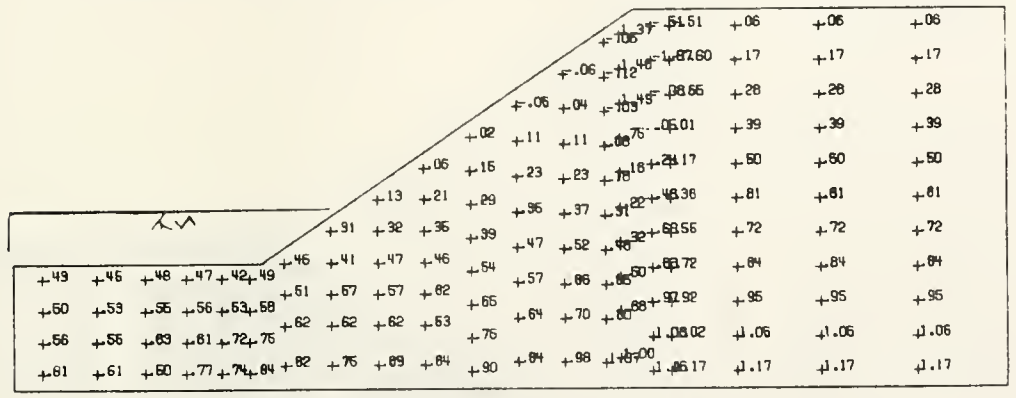

HORZ STR/UNIT WT/HEIGHT

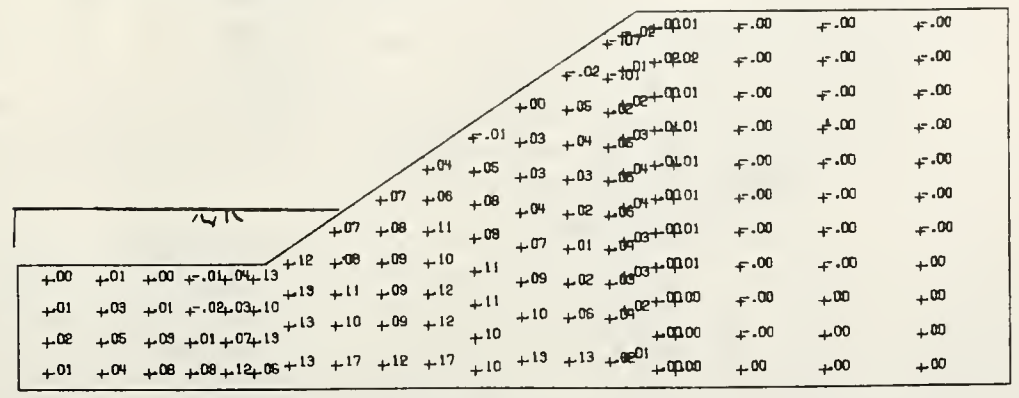

SHEAR STR/UNIT WT/HEIGHT

Figure 5.19: Vertical, Horizontal, and Shearing Stresses, Displacements and Stress Direction for Increment 6 for the Case of a Slope with a Pier

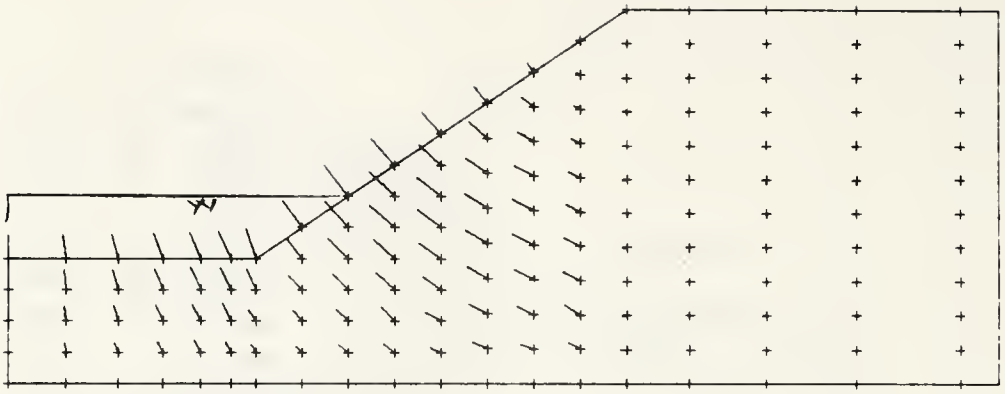

DISPLACEMENTS

VECTOR SCALE = 5.0

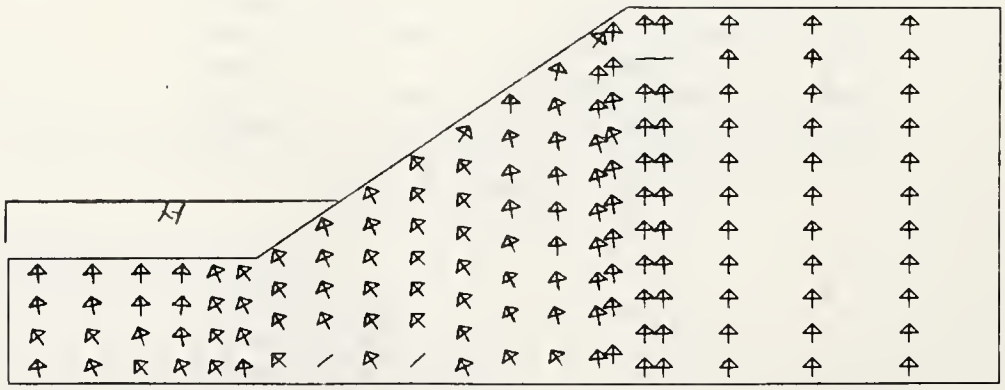

STRESS DIRECTION

- = FAILED ELEM.

Figure 5.19: Continued

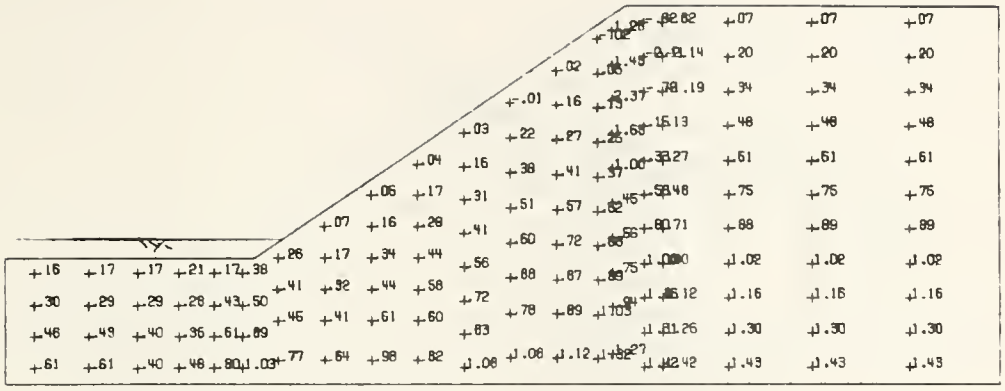

VERT STR/UNIT WT/HEIGHT

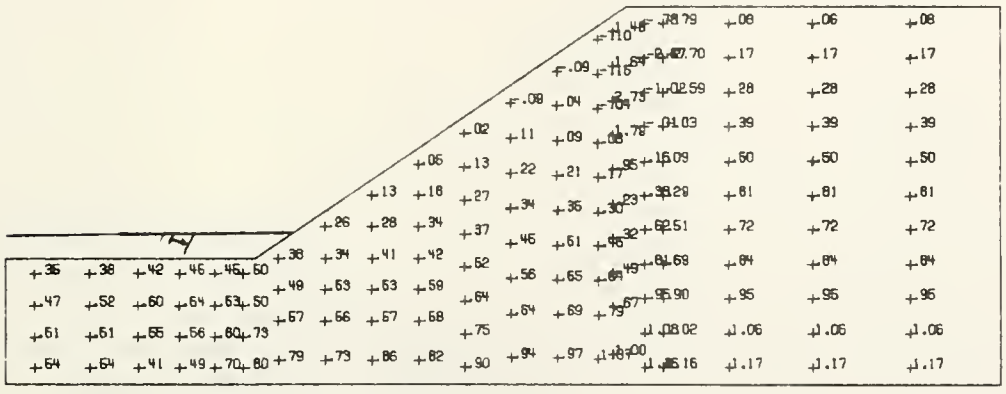

HORZ STR/UNIT WT/HEIGHT

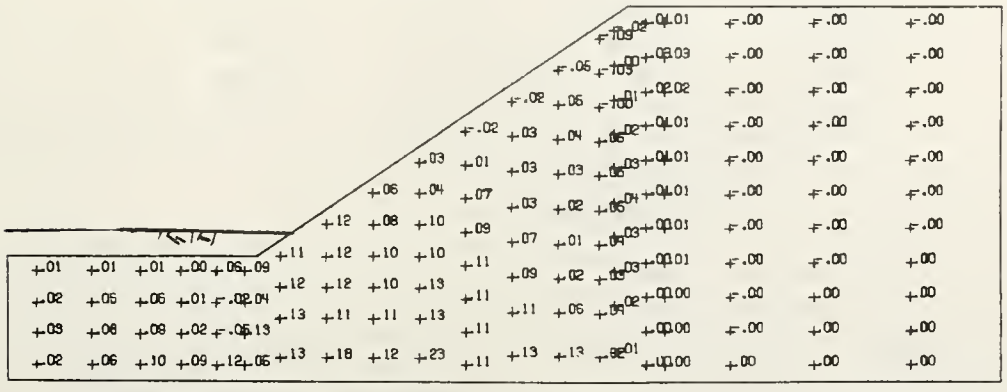

SHEAR STR/UNIT WT/HEIGHT

Figure 5.20: Vertical, Horizontal, and Shearing Stresses, Displacements and Stress Direction for Increment 7 for the Case of a Slope with a Pier

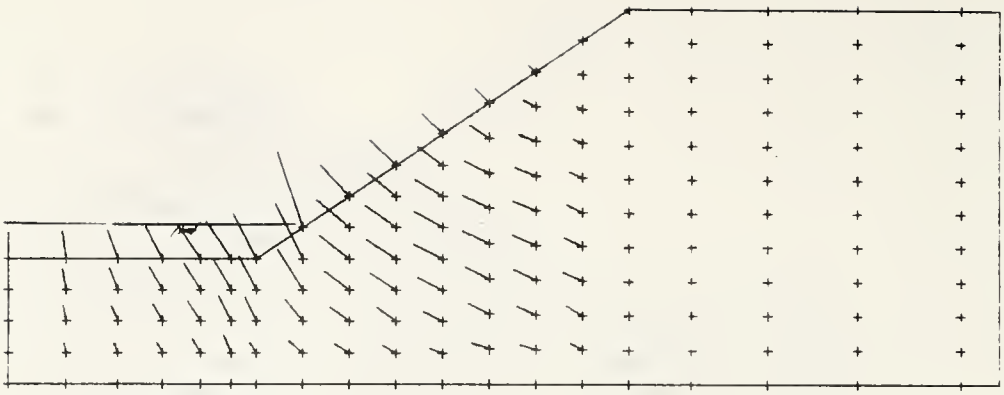

DISPLACEMENTS

VECTOR SCALE = 5.0

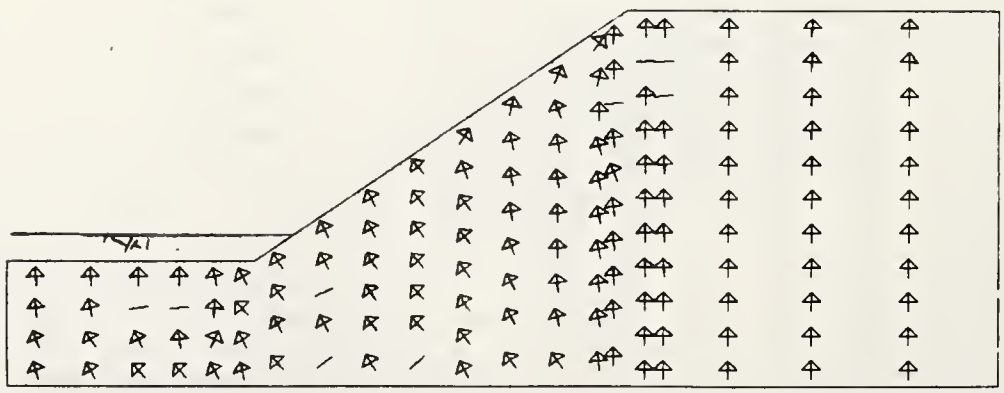

STRESS DIRECTION

- = FAILED ELEM.

Figure 5.20: Continued

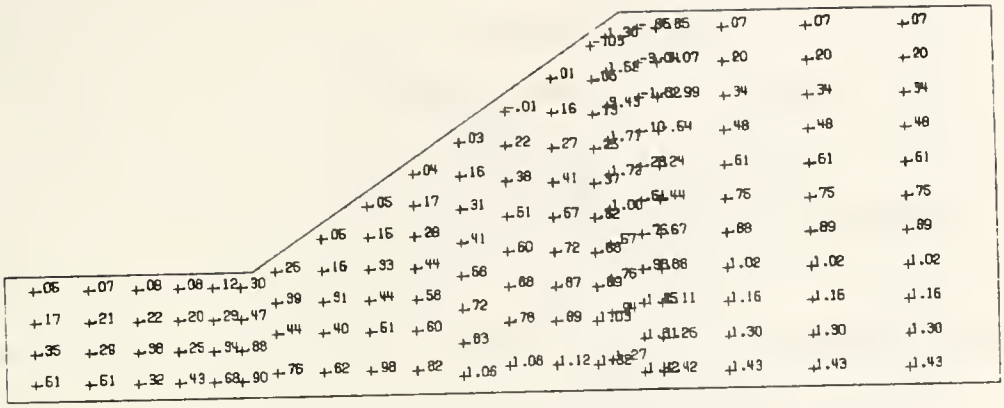

VERT STR/UNIT WT/HEIGHT

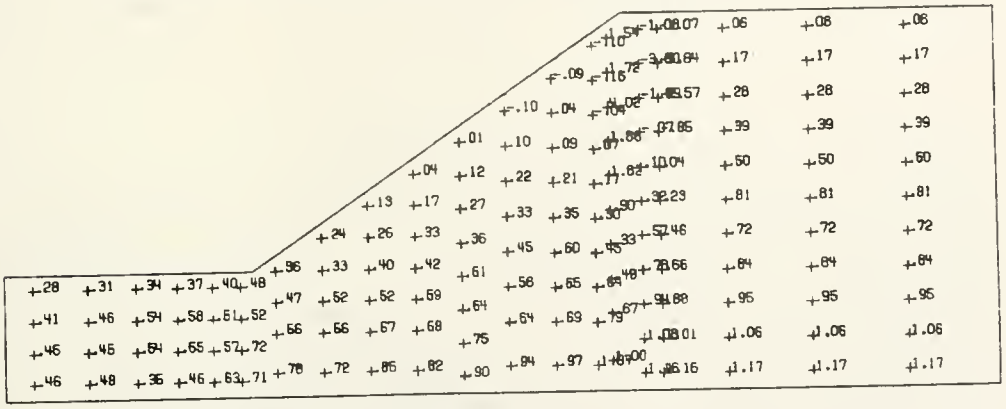

HORZ STR/UNIT WT/HEIGHT

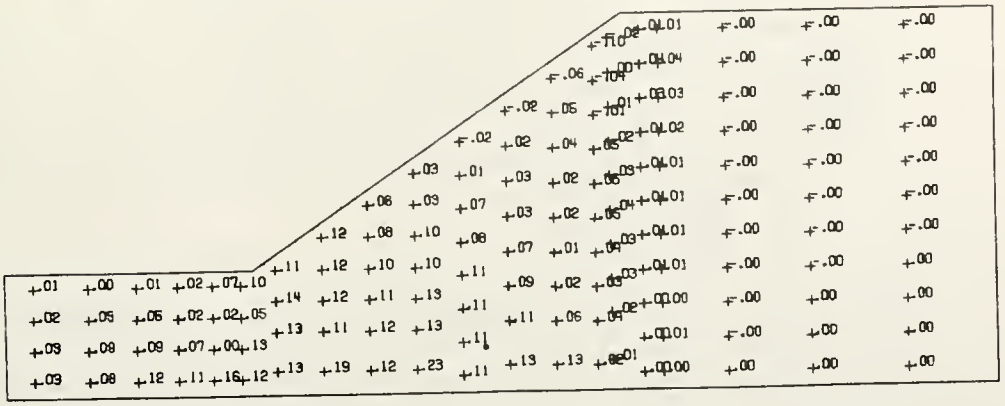

SHEAR STR/UNIT WT/HEIGHT

Figure 5.21: Vertical, Horizontal, and Shearing Stresses, Displacements and Stress Direction for Increment 8 for the Case of a Slope with a Pier

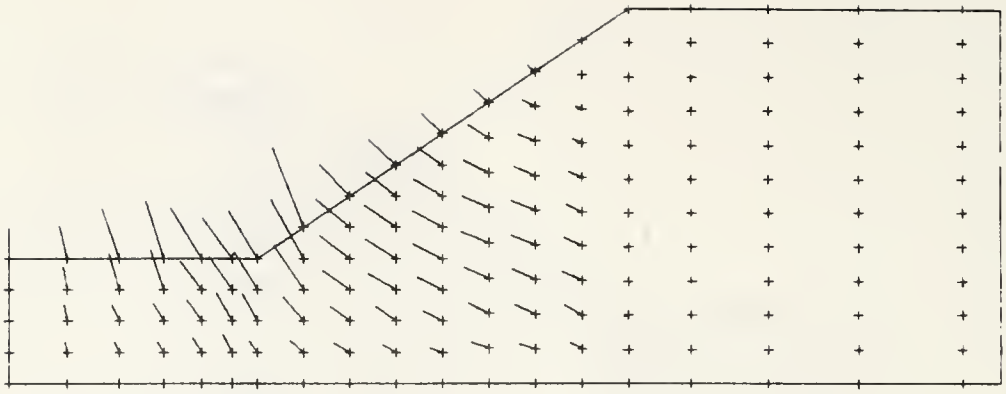

DISPLACEMENTS

VECTOR SCALE = 5.0

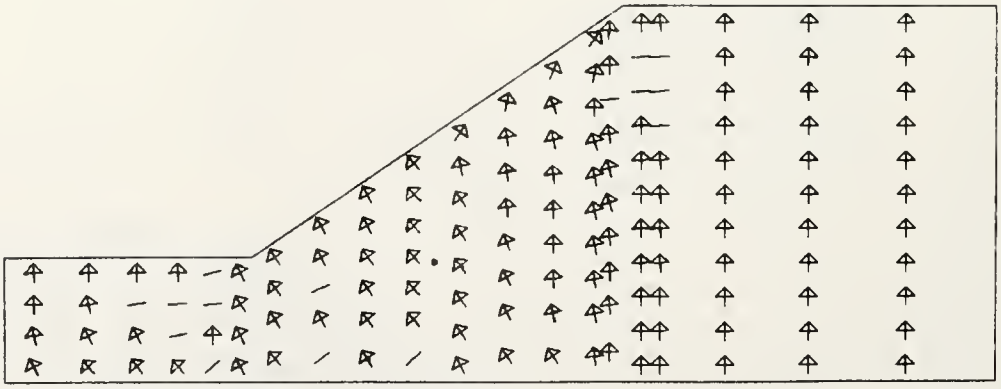

STRESS DIRECTION

- = FAILED ELEM.

Figure 5.21: Continued

increments of each of the two cases examined: case with no pier (figures 5.4 to 5.12), and case with piers at the crest of the slope (figures 5.13 to 5.21). These figures include the vertical, horizontal, and shearing stresses normalized by the unit weight of the soil and the slope height. Also shown are the displacement vectors and principal stress directions as well as a representation of yielded elements. A discussion of those results follows.

Displacements

The nodal displacements for each increment are the primary output of this finite element program. These are achieved in a global calculation directly from the nodal loads. While the displacements are not directly applicable to the stability analysis, they are useful if the deformation of nearby existing structures is critical. Plots of the displacement fields may also give some insight into the failure mechanism.

The difference in the nature of the two problems can be seen when comparing the displacement fields of both cases at each excavation stage and in particular during the last stage (figure 5.12 and 5.21 for the cases without and with pier, respectively). The most striking feature of the displacement plots is how effective the piers are as a barrier, as shown by the almost nonexistent displacements above the crest (figure 5.21), which is the pier

location, compared to the large displacements which occur throughout the profile for the case with no pier (figure 5.12). This barrier action eliminates a significant portion of the horizontal component of the nodal displacement vectors. This significantly reduces the overall slope movement and yields a more vertical direction of the displacement vectors. The displacements for the case of the reinforced slope represent the elastic rebounding of the unloaded soil.

For the case of a slope with no pier (figure 5.12), typical "circular" displacement patterns form. In addition to elastic rebound which occurs at the base of the excavation, heaving also occurs to compensate for the sloughing at the crest of the slope.

In addition to studying the final displacement field, it is also useful to monitor the progression of displacements during the excavation. For the case of the unreinforced slope these are given in figures 5.4 to 5.12. The point of maximum displacement on the slope surface moves downward as the excavation progresses and is approximately at the level of the excavation. The magnitude of these maximum displacements does not grow proportionally with the excavation, but rather increases very rapidly during the last increments. This is because of the combination of increased shearing stresses and reduced confinement,

causing the soil modulus to become small. It is also possible to see the deepening of the failure surface as the displacement vectors at each point continually bend downward with each increment. The most dramatic change in the displacement pattern occurs during the 6th increment (figure 5.10) where the surface displacement vector at the level of the excavation bottom almost doubles in length, primarily in an upward direction (heave and rebound) while the node just above the bottom turns sharply downward (sloughing). This corresponds to the increment where most of the elements with reduced modulus ("failed elements") are located at the base of the excavation, near the toe.

The progression of displacements for the case of an excavation reinforced by piers is given in figures 5.13 to 5.21. For this case, the relative magnitudes of the displacement fields do not change significantly during excavation. Also, the magnitudes increase almost proportionally with the number of excavation increments. The modulus of most soil elements is not changing, thus the deviator stress in each element must be decreasing to account for the reduced soil modulus which would occur if only the confining stress were being relieved.

Strains and Streases

Element strains and stresses are back calculated from the nodal displacements. They are calculated on an

elemental basis instead of the global approach used to compute the displacements. The strain and stress values are calculated at each of the eight Gauss points then averaged over the element. The gauss point values and/or the average values can be included in the output. The average values of stress are used in the stability analysis.

The final stress states for the two cases are given in figures 5.12 and 5.21. Unlike the cases of surcharge loading or self weight, the case of an excavation does not take full advantage of the vertical support which the piers have to offer. For this reason, the vertical stress fields between the two cases is not dramatically different. The vertical stresses are primarily influenced by the position of the yielded elements. For example, consider the stress in the element located along the foundation under the toe in figure 5.12. The vertical stress ratio of 1.01 is high when compared to its neighbors, however, it must be noted that the elements on both sides of this element have previously yielded (reduced modulus). This element must carry part of the load of its "soft" neighbors. The vertical stresses above the crest are very well preaerved through the excavation, especially for the case reinforced by a pier.

The horizontal stresses for the case of no pier (figure 5.12) show trends which are well established for typical excavations. The most noticeable trend is the development of a tension zone along the surface above the crest. Also, near the boundary of the excavation, the horizontal stresses exceed the vertical stress as a result of overburden removal. For the case with a pier (figure 5.21), the horizontal stresses are preserved above the piers and no tension zone forms. A tension bulb does, however, form in front of the piers. This tension is a result of negative "drawdown" against the piers as the excavation progresses and explains that there is no sign of sloughing at the crest.

The development of the shearing stresses given in figures 5.12 and 5.21 is the most important comparison to be made (in frictionless material) with regard to slope stability. Again, the initial shearing stresses (null) are preserved above the pier in figure 5.21. Under the slope itself, within the region where a shallow failure surface is likely to develop, the shearing stresses are reduced only marginally. However, there is a substantial reduction in the shearing stresses along the foundation of the problem. If a weak seam had existed in this problem along the foundation, the piers may have had a more profound impact.

A final comparison can be made using the plots of stress directions and "failed" elements. In comparing the final states for each case (figures 5.12 and 5.21) the more random distribution of these elements for the case with piers is a contributing factor in the stabilizing effect of the piers. In the case with no pier, the distribution of the yielded elements shows that a failure surface is forming at the toe of the slope (figure 5.12), while in the case of the slope supported by piers, the yielded elements largely occur outside the range of a potential failure surface.

Nodal Loads

Through the equations of equilibrium, the elemental nodal loads can be calculated from the elemental stresses. These are the loads which would be necessary to achieve the given stress state. A summation of all of the element nodal loads will yield the global nodal load field. These nodal loads are used to calculate the boundary forces from the excavated material on the slope and the forces against the piers.

The nodal loads against the piers are shown in figure 5.22. These loads are highly variable during the first three increments for two reasons. First, these increments involve the layers closest to the piers and so most affect the loads against them. As the excavation moves deeper,

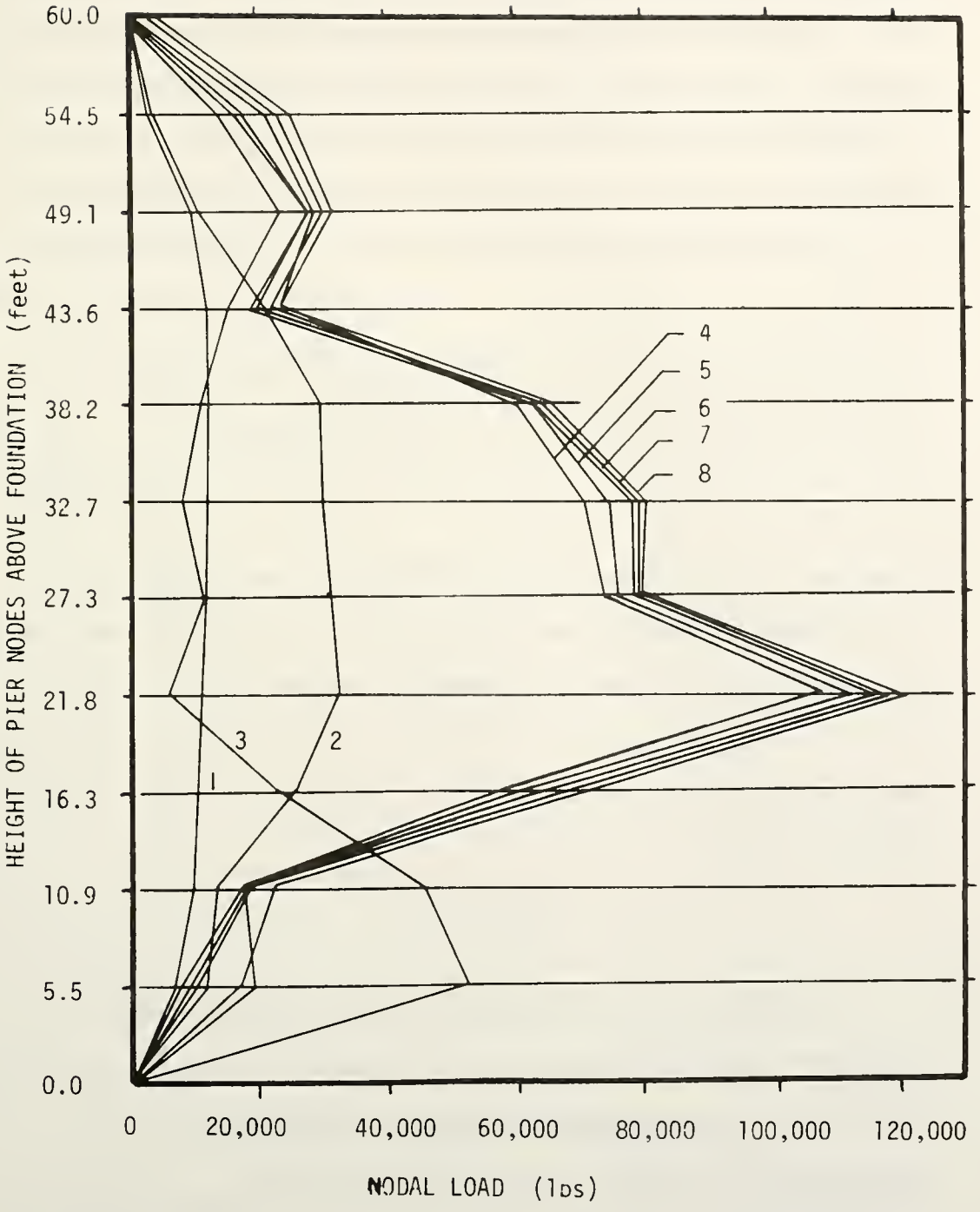

Figure 5.22: Nodal Loads Against the Piers for Each Increment

it also moves away from the piers affecting them less. Second, because of the high variations in load against the pier, the iterative process, which balances the forces against the pier and the pier displacements, is lagging a little. This is apparent in the third increment which is responding to an excessive displacement during the second increment by inverting the load pattern. This is caused by the loads on the back (upslope) of the pier building up as the pier is held rigid during that increment. The pier displacements are then exaggerated and in the next increment the passive pressures on the front (downslope) of the pier exceed the additional loads from the previous increment on the back of the pier. In some case, this condition becomes nonconvergent. In this case, however, the excavation is moving away from the piers and its influence is reduced, allowing the piers to regain equilibrium. Once an equilibrium is established and the excavation has moved away from the pier, there is little further change in the loads.

Output Files

In addition to the general output given above, several files are created which contain information to be used in post-processing analysis. A list and short description of these files is given below.

1) STO. This file contains all of the information needed to build the individual element stiffness arrays and to assemble them into the total stiffness array. This file is created so that the elemental information does not have to be stored in core. Also, creating this file prevents reintegration of the elemental stiffness matrices for each increment. This is a temporary file which is only created for the duration of the computations.

2) STFS. This file contains the total stiffness array. It is updated for each increment. It is also a temporary file.

3) SOLVE. Nodal, elemental and incremental stress information is stored in this permanent file. This file is used as input to the limiting equilibrium analysis program "LOGFIND".

4) PLO. All plotting information for the displacements, stress magnitudes and stress directions are stored in this permanent file. The post-processing program "XPLOTTER" produced the plots shown in this chapter.

Limiting Equilibrium Analysis

An assessment of the overall stability of the slope is made using a two dimensional limiting equilibrium analysis. The program "LOGFIND" was developed to utilize

the stress output from the finite element analysis unlike existing slope stability programs which generate the forces along the failure surface using a method of slices. The limiting equilibrium calculations are made as a summation of the strength of the soil and existing stresses at a discrete number of points along a circular or log spiral failure surface. A grid pattern searching technique is used to locate the most likely failure surface.

The information needed to conduct the limiting equilibrium analysis is contained in the file "SOLVE" which is created during the finite element analysis. This file contains the nodal and primary elemental information necessary to establish the two dimensional mesh. The stresses for each element at the end of each increment are also stored. The only additional input needed is a set of coordinates to establish the searching routine. A limiting equilibrium factor of safety is calculated for each row of elements in the problem.

The result of this program is a listing of the five most probable failure surfaces for each increment. A graphical representation of the three most likely failure surfaces is also printed. The most likely circular failure surfaces for each increment are shown in figures 5.23 and 5.24 for the cases without and with a pier, respectively. The piers tend to reduce the volume of

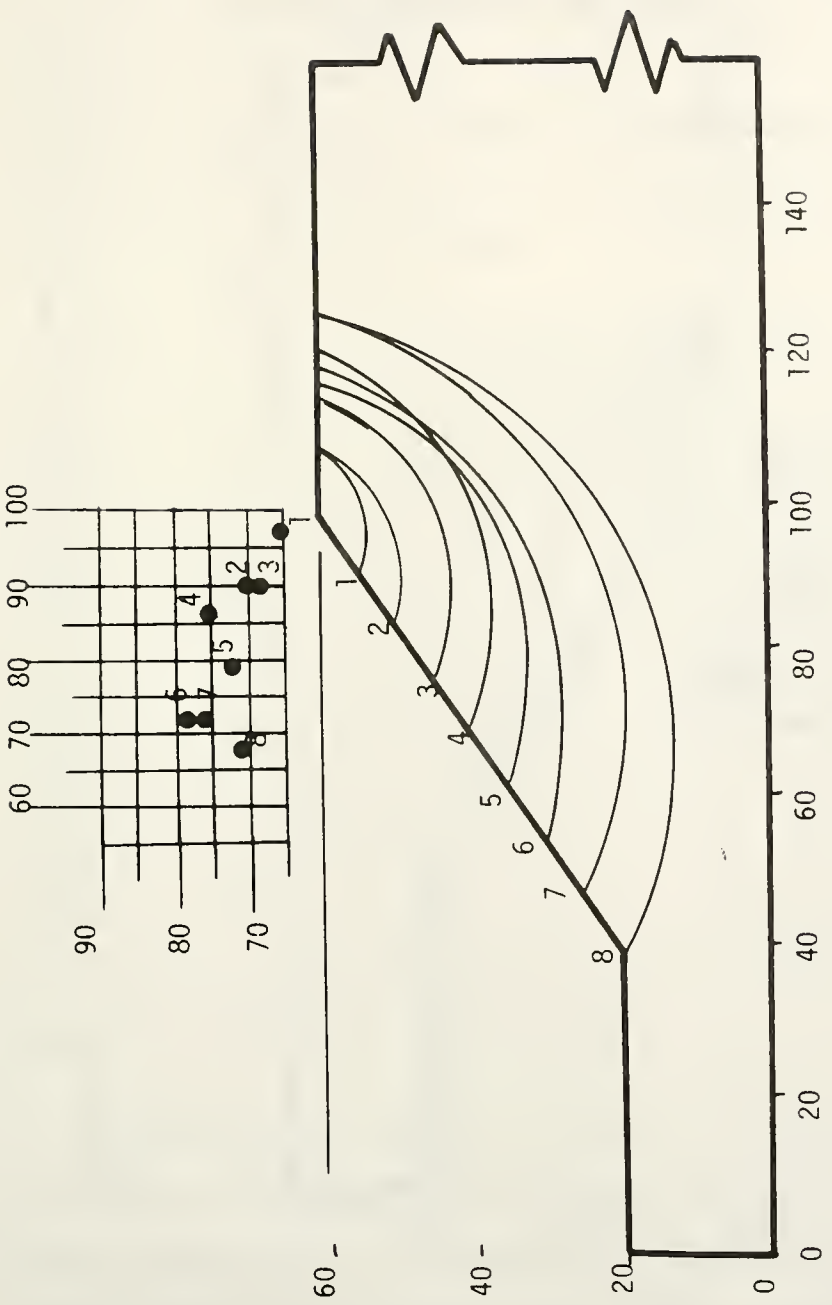

Figure 5.23: Most Probable Failure Surface for Each Increment for the Case of a Slope with No Pier

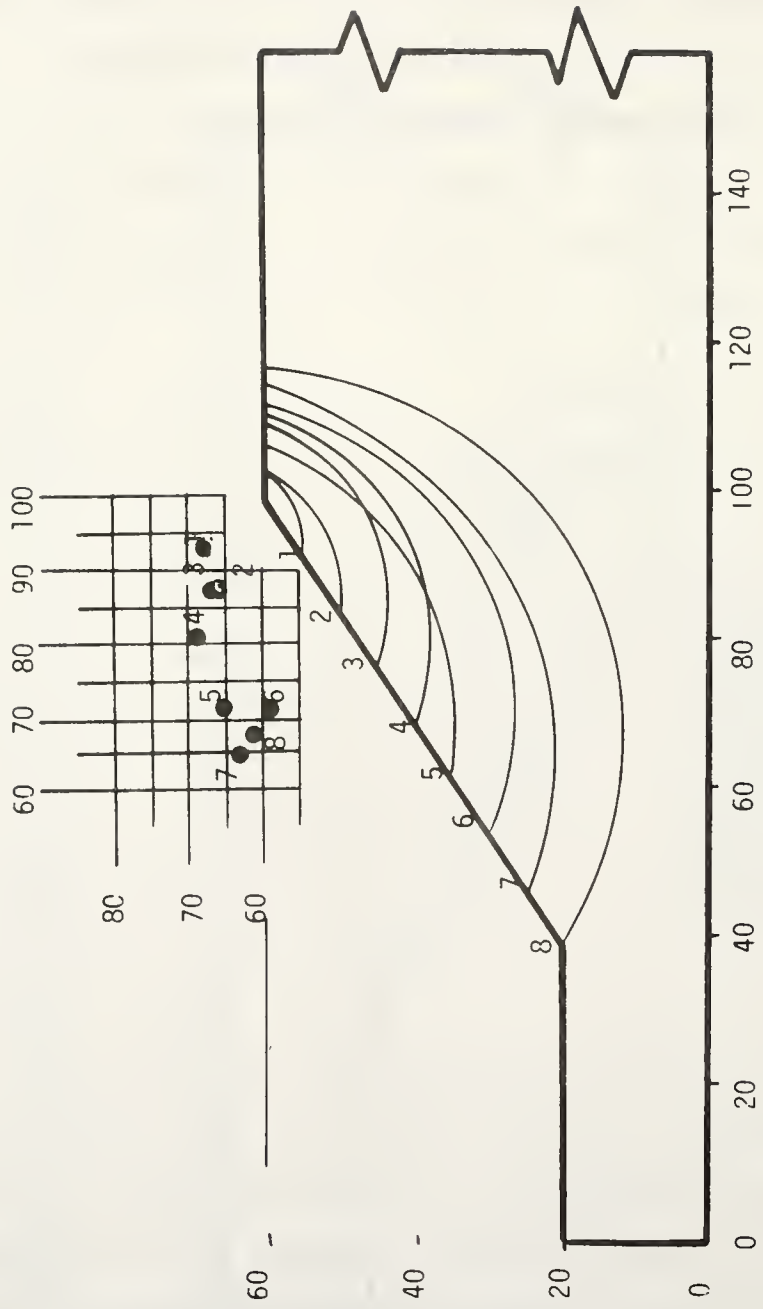

Figure 5.24: Most Probable Failure Surface for Each Increment for the Case of a Slope with a Pier

material involved in the slide. This reduction increases with excavation depth as the trend for the centers in the case of a slope without a pier is to move up, it is to move down in the case of a slope with piers - thus shortening the arc radius. A plot of the factor of safety with respect to the elevation of the bottom of the excavation is given in figure 5.25.

While there is a significant improvement in the stability of the reinforced slope, it is not as much as might be expected or as will be displayed by the case of piers used to support slopes under self weight in the next chapter. Because the direction of soil movement at the level of the pier is primarily in the horizontal direction (or vertically upwards), the vertical support of the soil by the piers, a major benefit of the piers for other conditions, is not utilized. Under conditions of downward forces acting on the slope, such as in the other two loading cases of surcharge loading or self weight, this component can be used to great benefit.

In conclusion, while the piers do increase the factor of safety of a slope during excavation, their greatest benefit under this loading condition may be to control displacements and prevent bottom heave. Better reinforcement of the slope may have been achieved by positioning the piers lower in the slope. At lower positions the

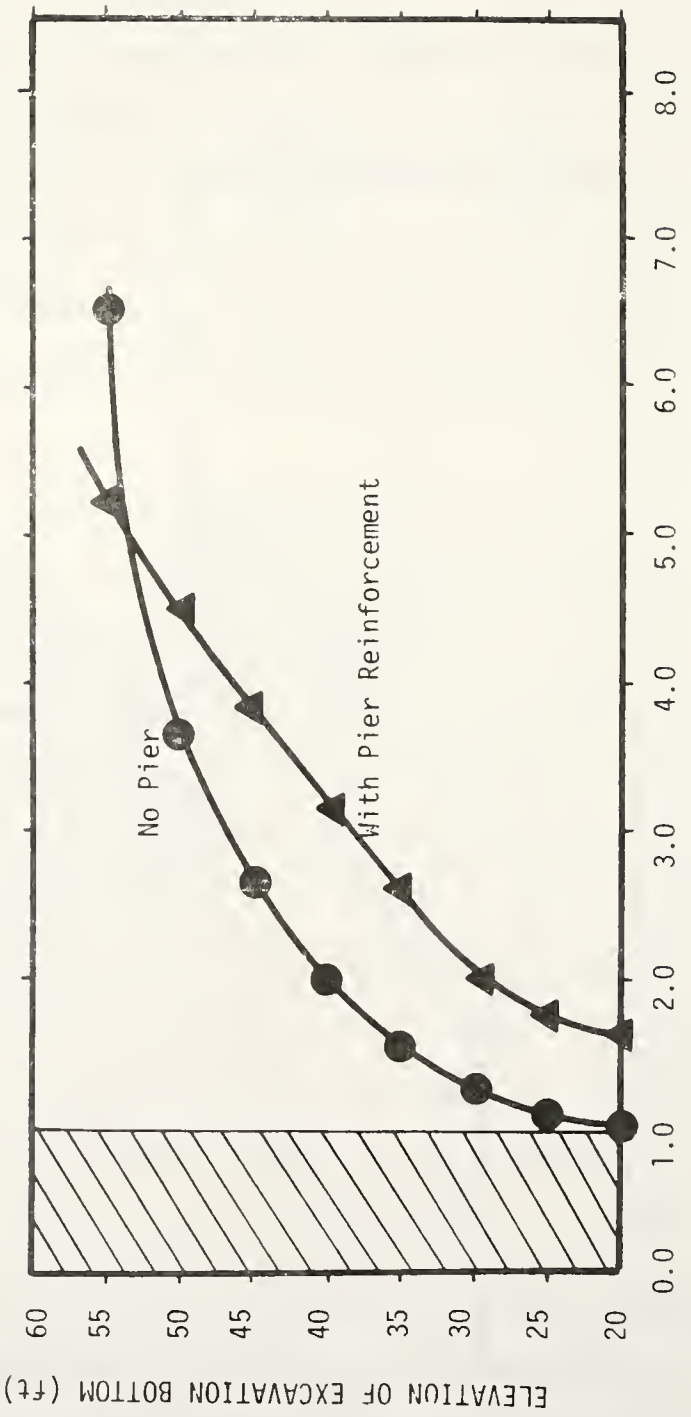

Figure 5.25: Factors of Safety for Each Increment for Both Cases

piers could have absorbed additional stresses from the larger movements. However, the loads on the piers would have been primarily horizontal and it is unlikely that the piers could be constructed to withstand such loads. The piers would probably be more beneficial in cases of smaller excavations and steeper slopes with more vertical movement.

Analysis of the Case of Cut Slope Stability

To further demonstrate the potential of the finite element program "SPILES", the example of piers used to reinforce a cut slope in a sandy clay is analyzed. Three additional features of the finite element model will be illustrated through this example. First, equivalent surface loads will be calculated based on the initial stress state to simulate the excavation rather than the automatic removal of elements used in the previous example. Second, the sandy soil allows the use of a variable Poisson's ratio (i.e. extended Duncan-Chang Model). Third, in this example the piers will be constrained laterally at the top to simulate the use of tiebacks.

The problem to be considered is a 1:2 slope with a height of 30 ft. and a depth to bedrock under the toe of 12 ft. The soil properties are nonlinear with regard to both the modulus of elasticity and the Poisson's ratio.

For the basic example, the soil has a cohesion of 200.0 psf and a friction angle of 36 degrees. The following Duncan-Chang parameters are used to model the nonlinear stress-strain behavior: K = 47.2, n = 0.5, R_f = 0.8. The additional parameters needed to model the nonlinear Poisson's ratio are: G = 0.33, F = 0.06, and d = 4.0. A modulus of 50,000 psf and Poisson's ratio of 0.45 (K_o = 0.83) will be used to establish the initial stresses. The slope will be cut to a 1:1 slope and reinforced by 4 ft. diameter piers with 8 ft. spacings.

Four cases will be examined: no pier, a pier at the crest, a pier 12 feet from the toe, and a pier at the toe. Because of the their length, the piers at the crest will be restrained by tiebacks to ease the structural demands applied to them and to reduce their movements. The piers in the last two cases must be installed below the existing ground surface. This is accomplished by drilling the shaft as normally would be done, however, the pier is constructed only up to the future ground surface. The remainder of the shaft is backfilled with soil. Once the pier has cured, excavation of the slope can proceed unhindered down to the level of the top of the pier. Tiebacks will not be used in these last two cases because of the reduced length of the pier and of the impracticality of the procedure below the ground level.

Initial Stresses and Surface Loads

The initial stresses are established for the original 1:2 slope through the gravity turn-on procedure discussed in Chapter 4. These stresses, once established (figure 5.26), are used to estimate the initial stresses for the elements present in the final cut slope (figure 5.27). This transformation must be performed by the user. Care should be taken in establishing the meshes for the original and final slopes to insure that they are as similar as possible so that the amount of user intervention is limited.

Because the gravity turn-on method used in this program establishes the nodal loads for the initial stresses by dividing the total weight of each element equally among its eight primary nodes, some error is introduced for element shapes other than rectangles. Consider the simple one element examples in figure 5.28. Both elements have the same average dimensions and volume. The situation illustrated by these two elements occurs in the original 1:2 slope. If a unit weight of 130 pcf where used, a vertical stress of 292 psf should be calculated at an average depth of 2.25 ft. The gravity turn-on procedure in this program yields a vertical stress of 281 psf for case A and 329 psf for case B. Alternating low and high values of vertical stress along the slope face represent

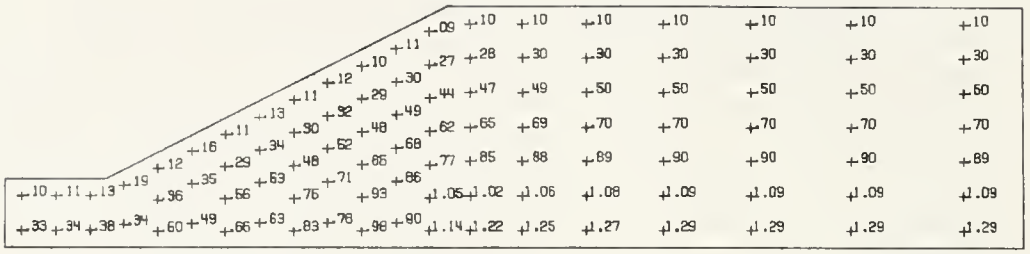

VERT STR/UNIT WT/HEIGHT

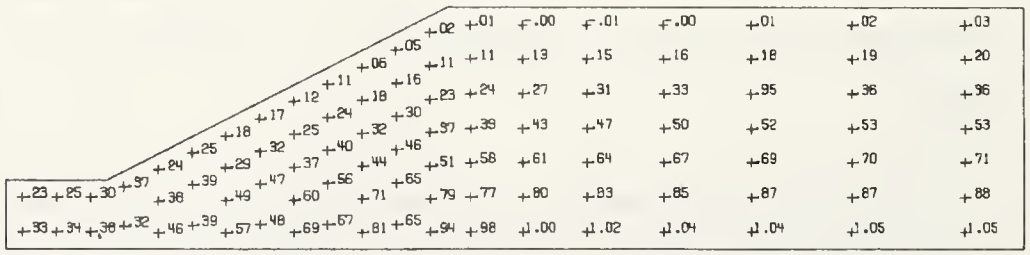

HORZ STR/UNIT WT/HEIGHT

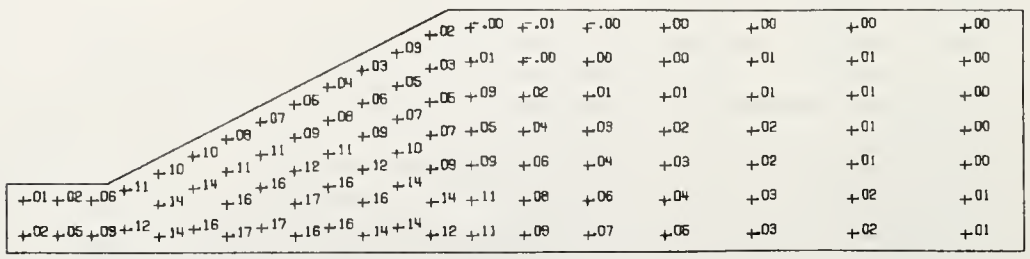

SHEAR STR/UNIT WT/HEIGHT

Figure 5.26: Initial Stresses for 1:2 Slope

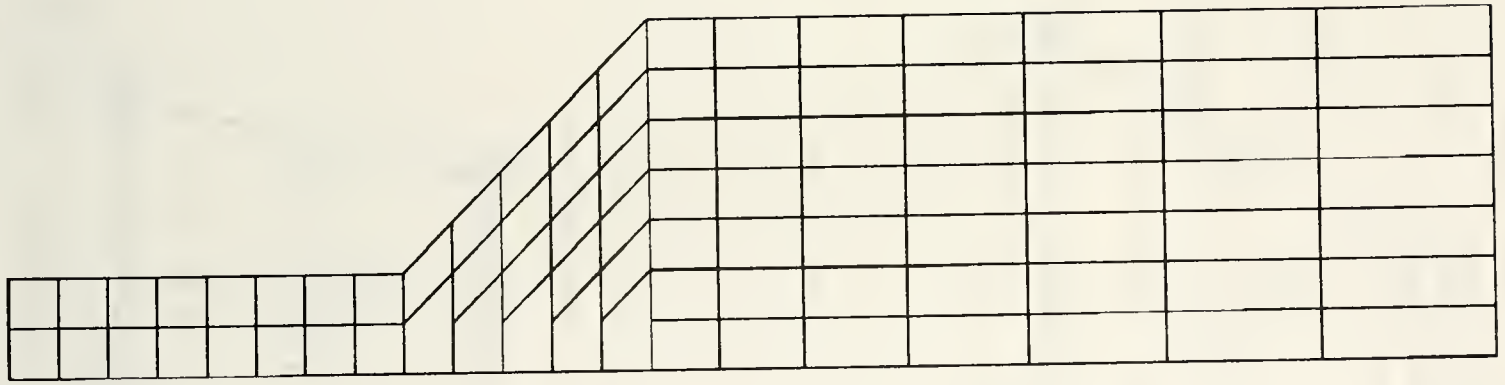

Figure 5.27: Mesh for Excavated 1:1 Slope

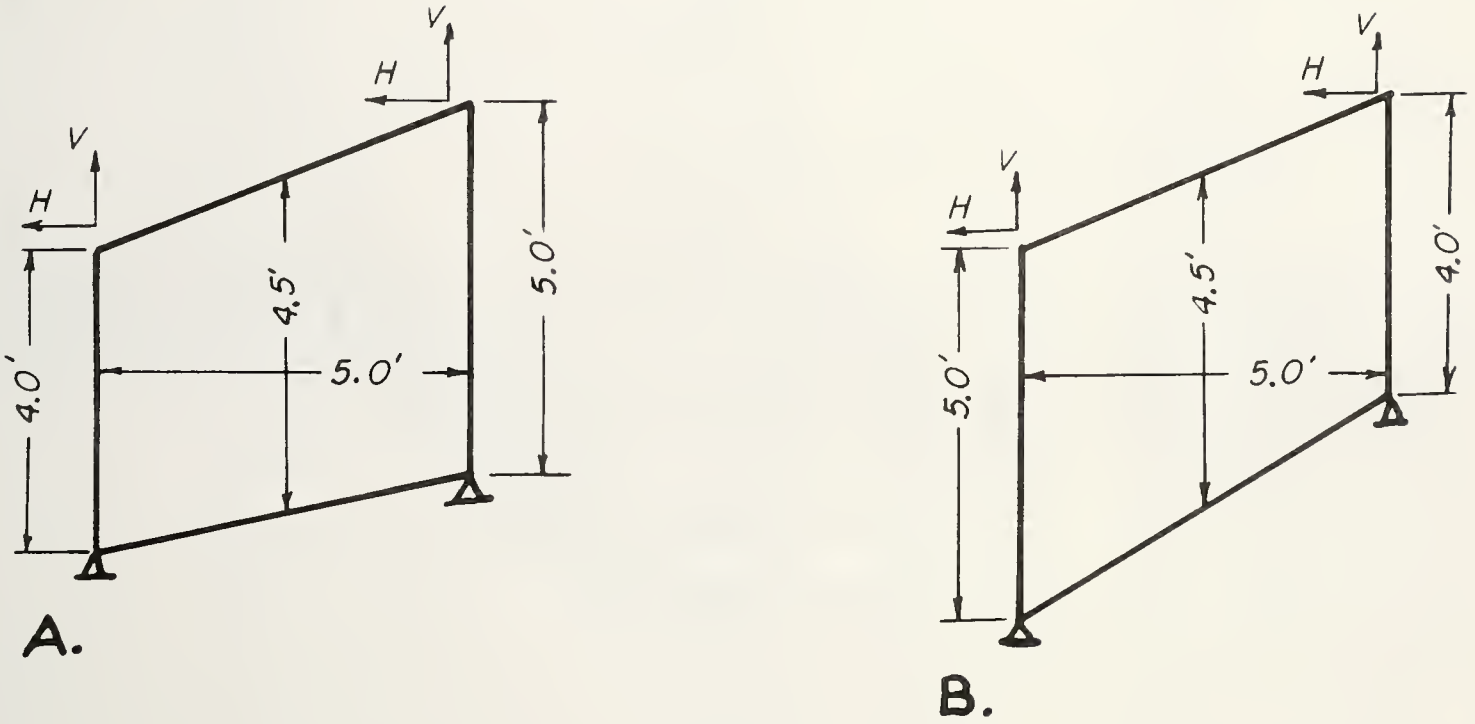

Figure 5.28: Elements used to Illustrate Errors in the Gravity Turn-On Procedure

elements similar to the elements A and B. Better approximations of the stresses in these elements are possible by using a consistent mass approach to determine the nodal loads used to establish the initial stresses. In this method the average stress difference across the elements is integrated over the element using the shape functions. More elements can also be used to reduce the effect (figure 5.29). However, while the effect of these approximations may be quite dramatic for an individual element, they have a minimal effect on the entire stress field. Figure 5.30 plots the average vertical, horizontal and shearing stresses for each element along the final cut slope surface. Allowing for discrete nature of the elements, the differences in the stress distributions are negligible, and do not alter the evaluation of the surface loads applied to the cut slope.

These surface loads which simulate the excavation process are established from the average elemental initial stresses. The following equations are used to calculate the horizontal and vertical equivalent forces:

$$F_h = (-V_n \sigma_x + H_n \sigma_{xy})\ w/4 \qquad 5.1$$

$$F_v = (H_n \sigma_y - V_n \sigma_{xy})\ w/4 \qquad 5.2$$

where: F_h = horizontal load at each node,

F_v = vertical load at each node,

H_n = horizontal span across each element,

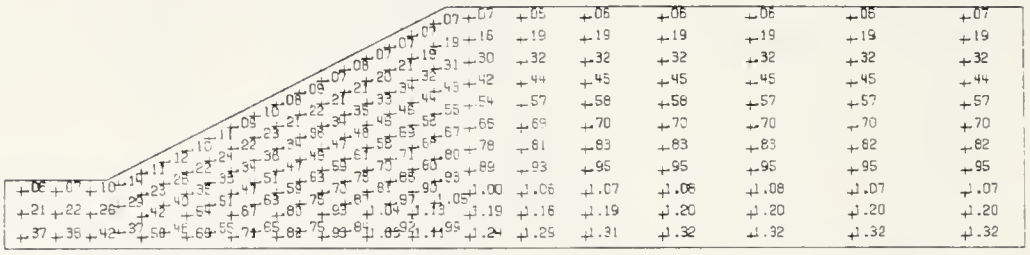

VERT STR/UNIT WT/HEIGHT

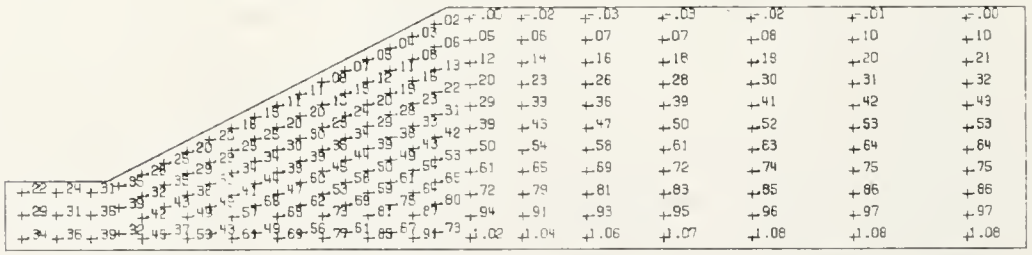

HORZ STR/UNIT WT/HEIGHT

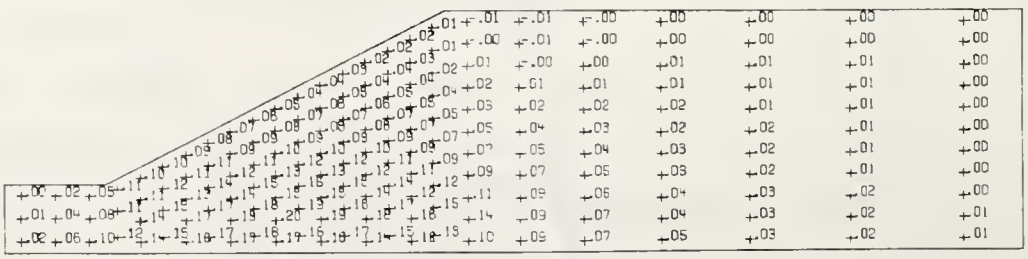

SHEAR STR/UNIT WT/HEIGHT

Figure 5.29: Initial Stresses Using a Finer Mesh

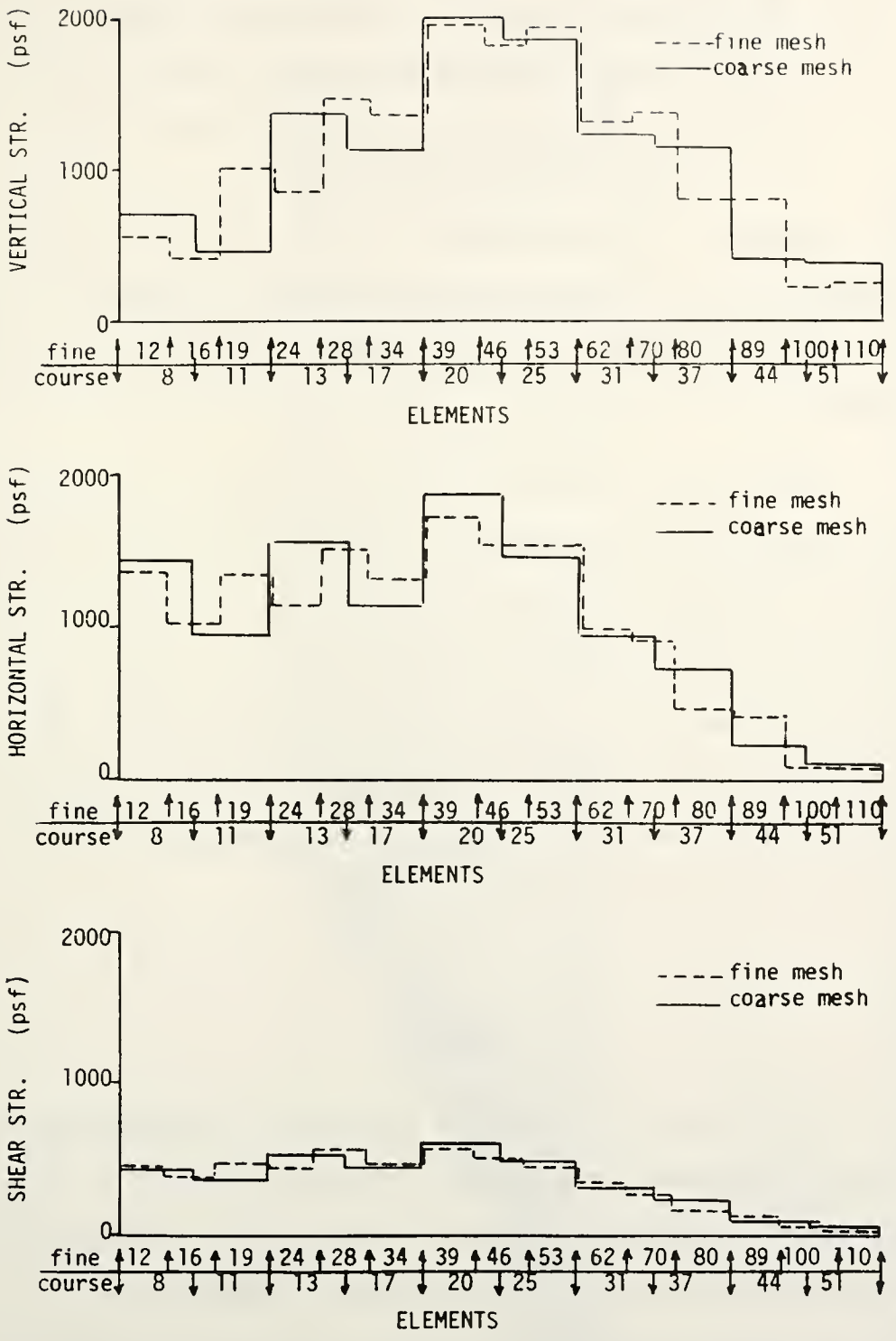

Figure 5.30: Average Stresses Used to Determine Surface Loads

V_n = vertical span across each element,

σ_x = average elemental horizontal stress,

σ_y = average elemental vertical stress,

$_{xy}$ = average elemental shearing stress, and

w = element width.

Nodal loads are calculated for all the elements intersected by the new surface (figure 5.31). A summary of the corresponding loads for each element involved is given in table 5.1.

Incremental solution of this problem can be conducted in two ways. First, if the excavation procedure is known, several different meshes can be created to represent the different stages of construction. Second, within each stage of construction, the surface loads for that particular stage can be applied in several increments. For this example only the final stage will be considered and the loads will be applied in four increments.

Results

The results, in terms of stresses, displacements and stress directions, are given in figures 5.32 to 5.35 for the cases of no pier, a pier at the crest, a pier 12 feet from the toe, and a pier at the toe, respectively.

To understand how the piers can be best utilized in

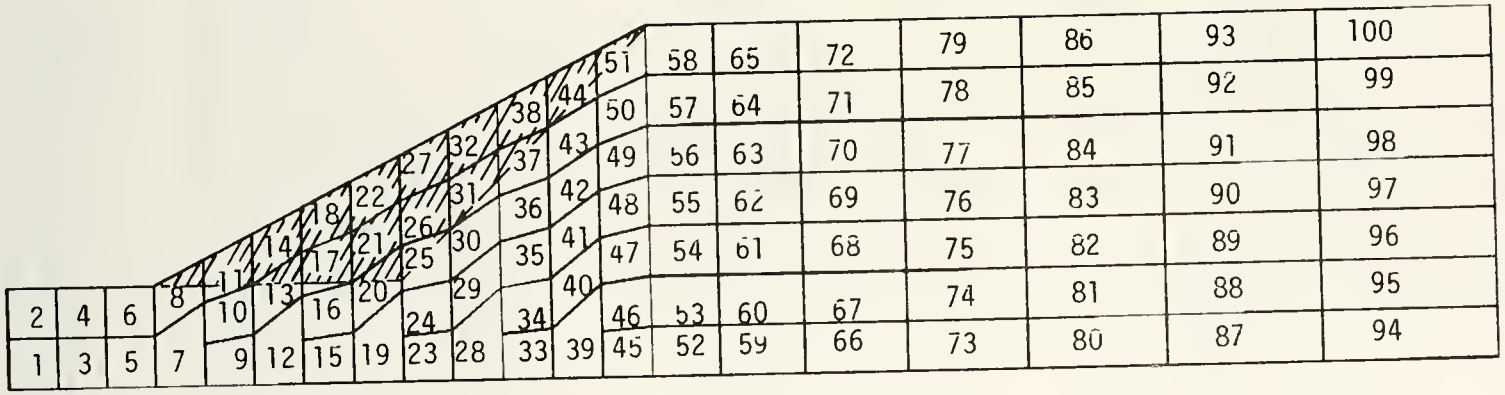

Figure 5.31: Excavated Mass and Transversed Elements to Determine Forces

Table 5.1: Determination of Cut Slope Forces

Element n	Horizontal Span H_n (ft)	Vertical Span V_n (ft)	Horizontal Stress σ_x (psf)	Vertical Stress σ_y (psf)	Shear Stress τ_{xy} (psf)	Horizontal Force F_x (lb)	Vertical Force F_y (lb)
8	6.0	0.0	1448.0	739.0	419.0	2514.0	4434.0
11	6.0	0.0	936.0	471.0	376.0	2256.0	2826.0
13	6.0	0.0	1541.0	1384.0	540.0	3240.0	9246.0
17	6.0	0.0	1151.0	1157.0	436.0	2616.0	6942.0
20	6.0	0.0	1863.0	2084.0	605.0	3630.0	12504.0
25	6.0	6.0	1454.0	1876.0	471.0	-5898.0	8430.0
31	6.0	6.0	959.0	1257.0	299.0	-5455.0	5748.0
37	6.0	6.0	711.0	1149.0	239.0	-2832.0	5460.0
44	6.0	6.0	219.0	416.0	105.0	-684.0	1866.0
51	6.0	6.0	101.0	373.0	64.0	-222.0	1854.0

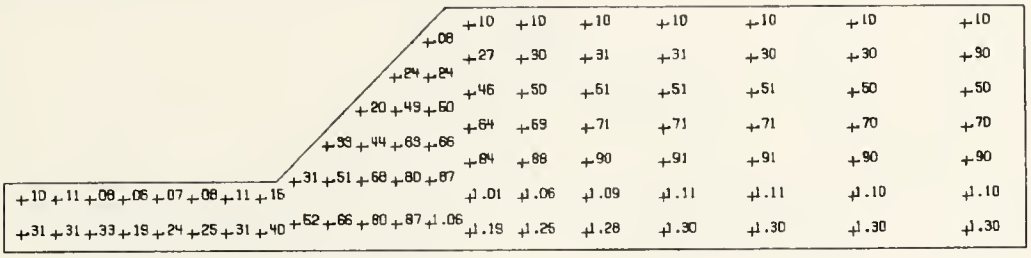

VERT STR/UNIT WT/HEIGHT

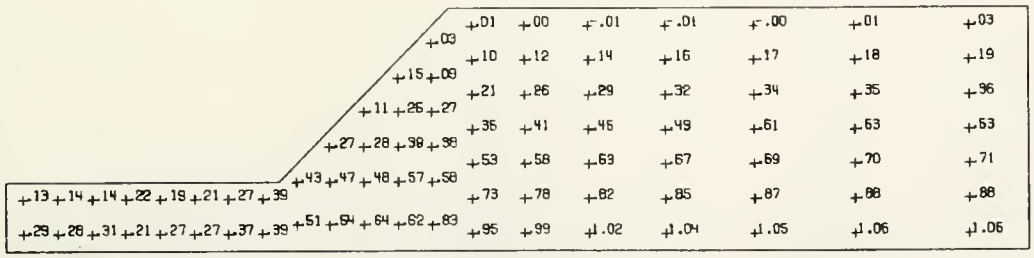

HORZ STR/UNIT WT/HEIGHT

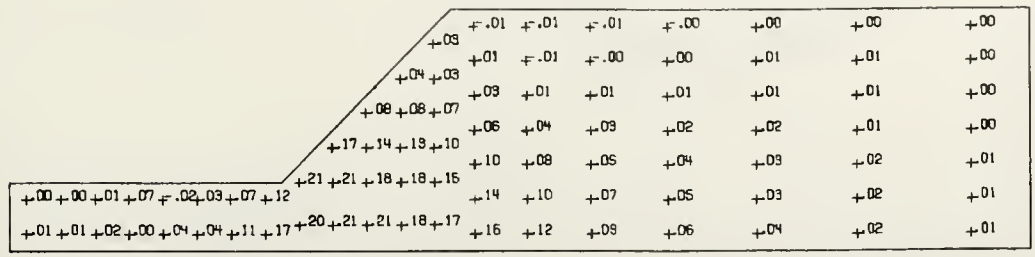

SHEAR STR/UNIT WT/HEIGHT

Figure 5.32: Vertical, Horizontal, and Shearing Stresses, Displacements and Stress Direction for the Final Increment for the Case of No Pier

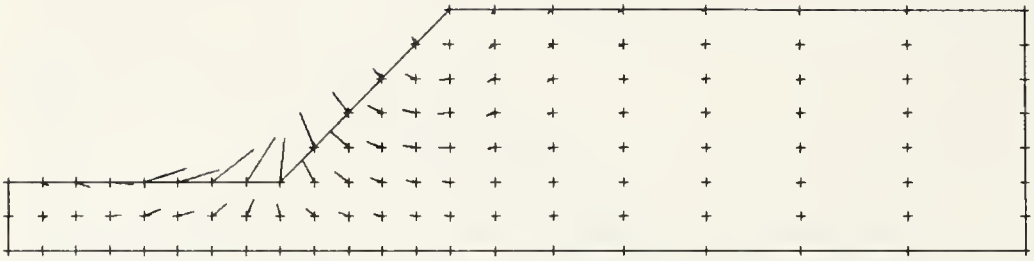

DISPLACEMENTS

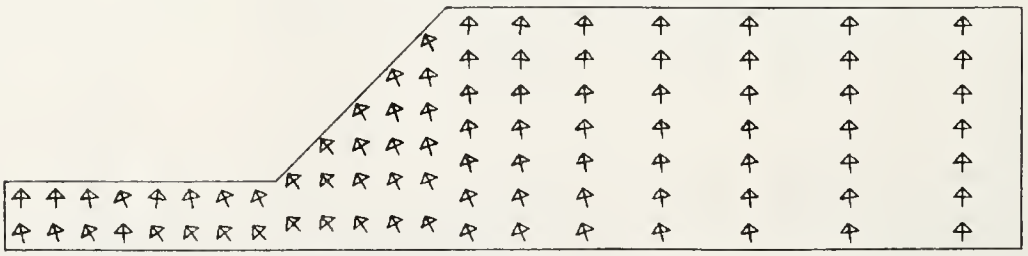

STRESS DIRECTION

- = FAILED ELEM.

Figure 5.32: Continued

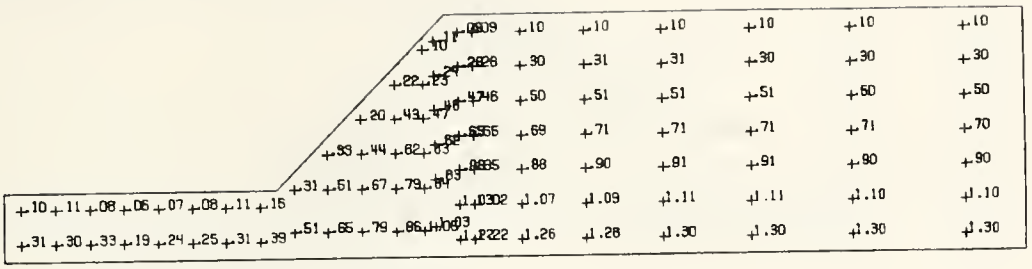

VERT STR/UNIT WT/HEIGHT

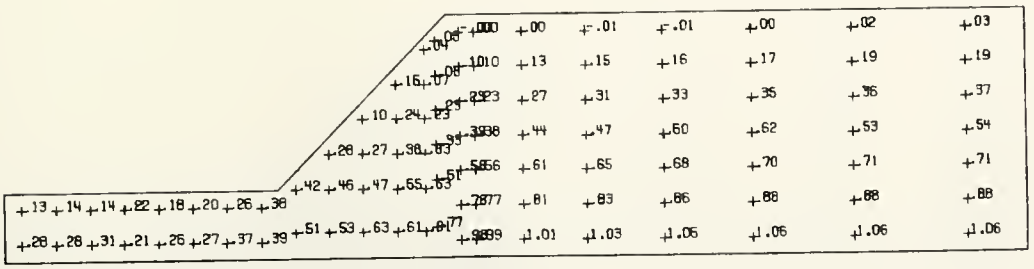

HORZ STR/UNIT WT/HEIGHT

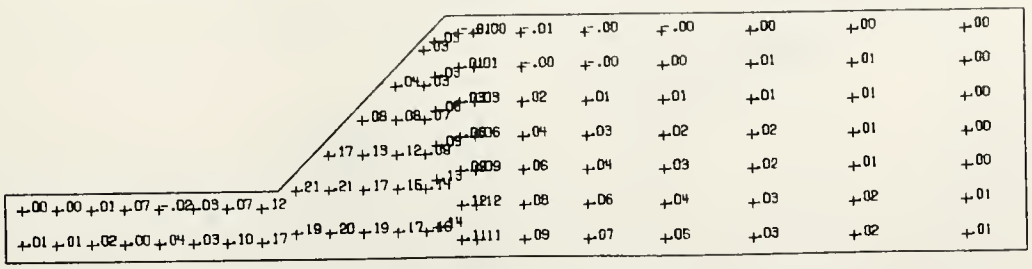

SHEAR STR/UNIT WT/HEIGHT

Figure 5.33: Vertical, Horizontal, and Shearing Stresses, Displacements and Stress Direction for the Final Increment for the Case of a Pier at the Crest

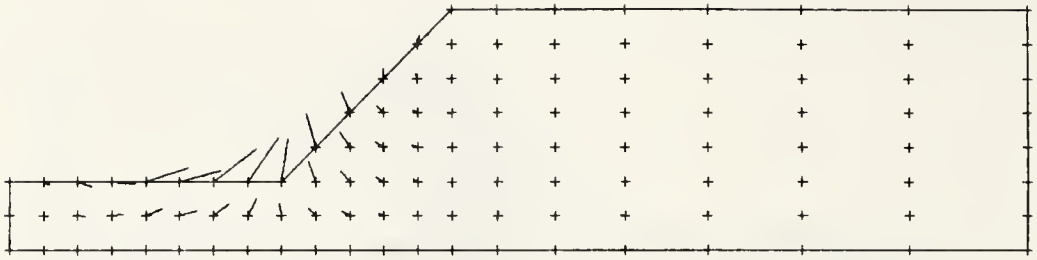

DISPLACEMENTS

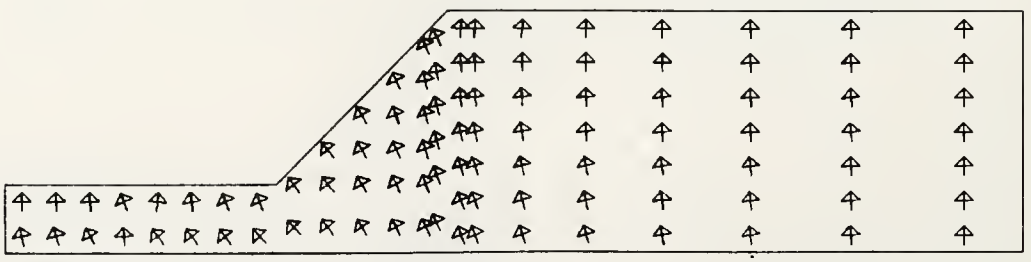

STRESS DIRECTION

- = FAILED ELEM.

Figure 5.33: Continued

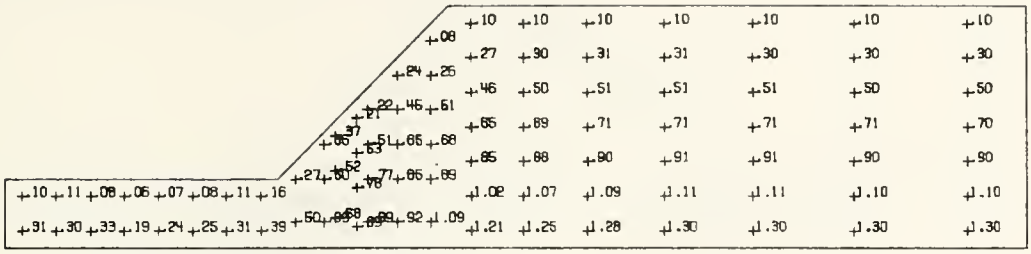

VERT STR/UNIT WT/HEIGHT

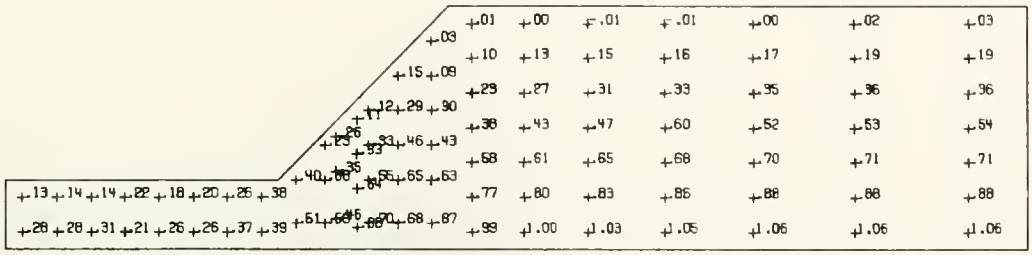

HORZ STR/UNIT WT/HEIGHT

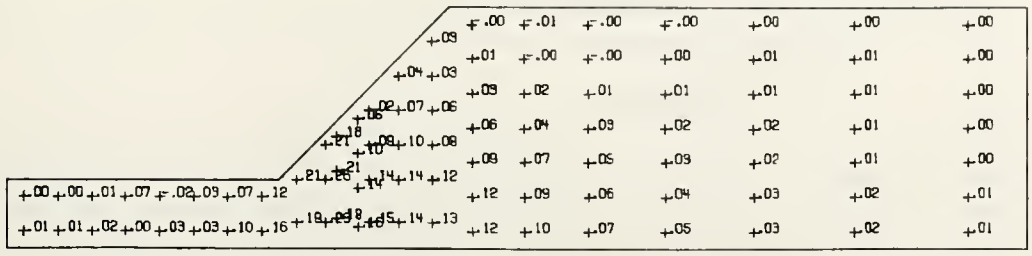

SHEAR STR/UNIT WT/HEIGHT

Figure 5.34: Vertical, Horizontal, and Shearing Stresses, Displacements and Stress Direction for the Final Increment for the Case of a Pier at 12′ from the Toe

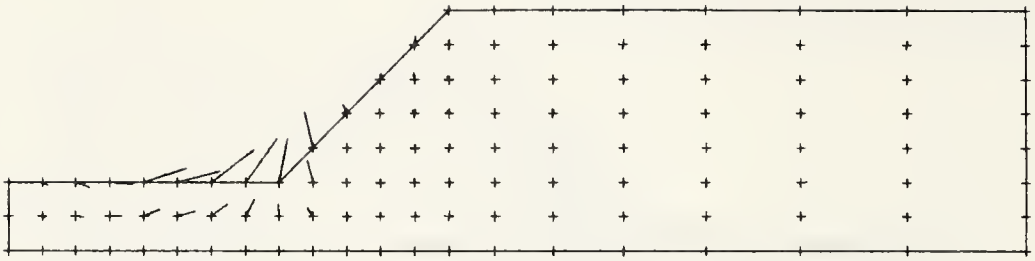

DISPLACEMENTS

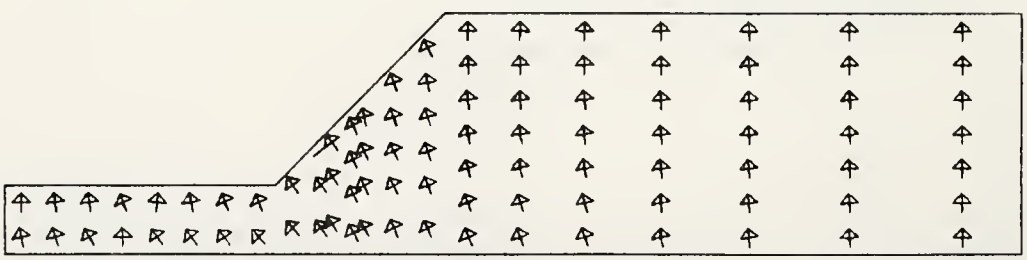

STRESS DIRECTION

- = FAILED ELEM.

Figure 5.34: Continued

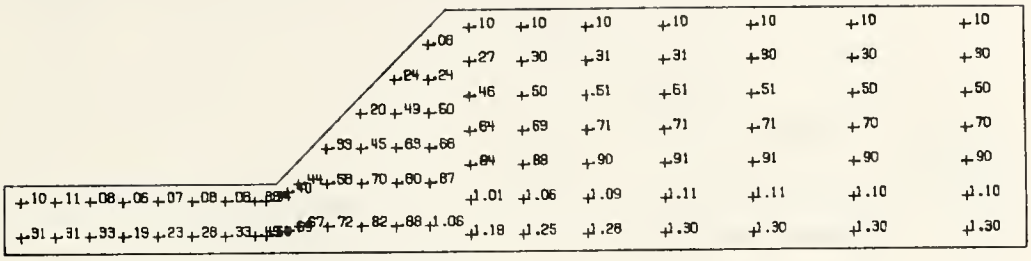

VERT STR/UNIT WT/HEIGHT

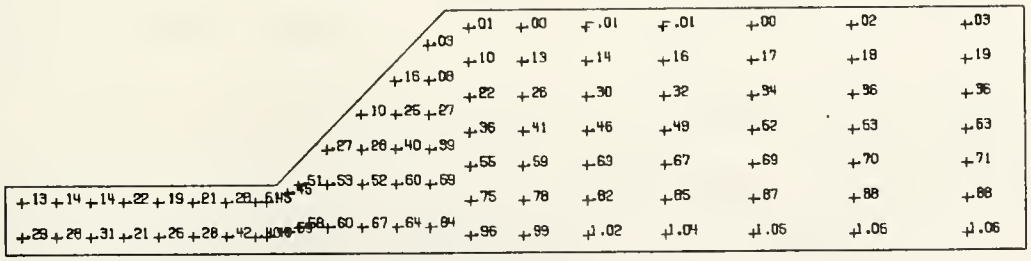

HORZ STR/UNIT WT/HEIGHT

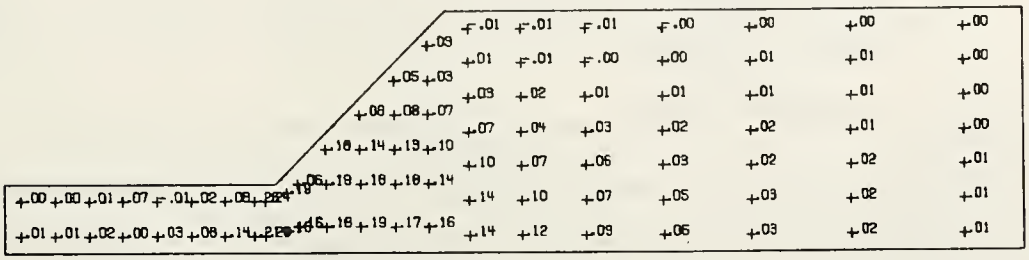

SHEAR STR/UNIT WT/HEIGHT

Figure 5.35: Vertical, Horizontal, and Shearing Stresses, Displacements and Stress Direction for the Final Increment for the Case of a Pier at the Toe

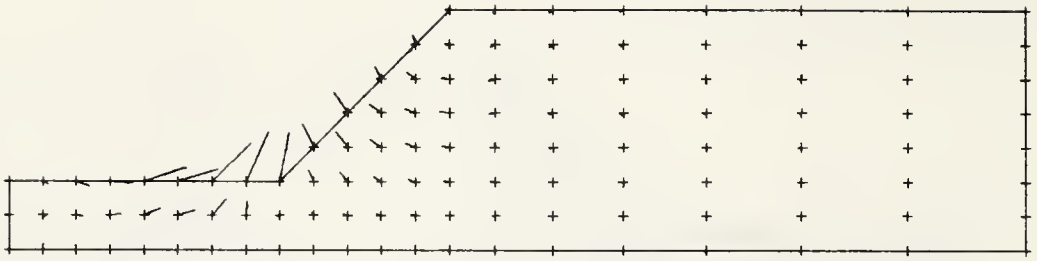

DISPLACEMENTS

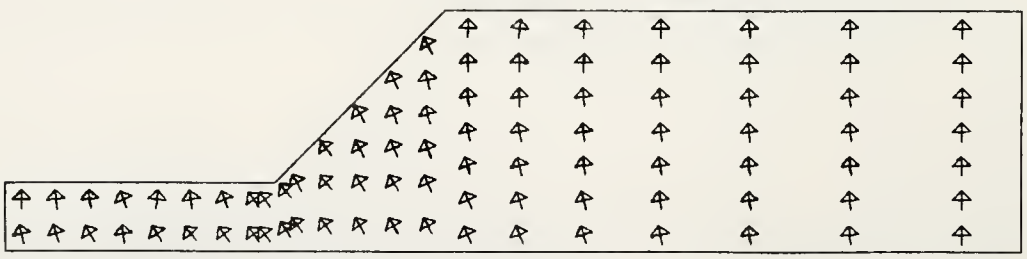

STRESS DIRECTION

- = FAILED ELEM.

Figure 5.35: Continued

this case, it must be recognized that the changes in shearing stresses are small. When comparing the final stresses for the case with no pier (figure 5.32) to the initial stresses (figure 5.26 or 5.29), only minimal differences can be noticed, and these are limited to a short distance from the future toe of the slope. A limiting equilibrium analysis gives a factor of safety of 2.35 for the original condition and 1.88 for the case of the unreinforced cut slope. Likewise, the displacements in these cases are relatively small (exaggerated by a factor of 30 in these plots).

A pier at the crest (figure 5.33), installed before excavation, does little to affect the stress state or the displacements. This is reflected by a decrease in the factor of safety to 1.81. This decrease is due to the piers absorbing the small vertical loads present in that portion of the slope and preventing an increase in the normal stresses along the potential failure surfaces.

Because of the existing slope face, relatively small lateral stresses exist in the original slope as compared to the previous study of an excavation in clay. The stress relief is largely vertical. For this reason, and also because of the close proximity of the foundation level, lateral movements and increased shear stresses are small near the piers. Thus, piers at the crest did not

absorb much stress from the slope. Because of the lack of soil movement near the crest of the slope even in the unreinforced case, very little pressure could develop against the piers. The effect of the tiebacks in this case was small. To achieve maximum utilization of the piers they should be placed closer to the point of maximum displacement in the unreinforced case. This supports the conclusions of Oakland and Chameau (1984).

Piers placed at 12 feet above the toe were found to be the most effective in controlling the overall movements (figure 5.34), especially above the piers. The soil near the piers is prevented from rebounding fully upon unloading due to the negative skin friction effect of the piers. This retains part of the initial confinement, adding to the strength of the soil. Because the support offered by the pier is dependent on the retention of confinement rather than reduction of the shearing stresses, their effectiveness is dependent on the friction angle of the soil. This mechanism can be demonstrated by monitoring the elements with reduced modulus ("yielded") for a variety of cohesion and friction values. For the original soil model no elements yield under the final loading conditions. If, however, the same stress state is assumed for weaker soils a bulb of yielded elements would form. Figure 5.36 shows the effect of a decreasing friction angle. Failure is initiated from the foundation level

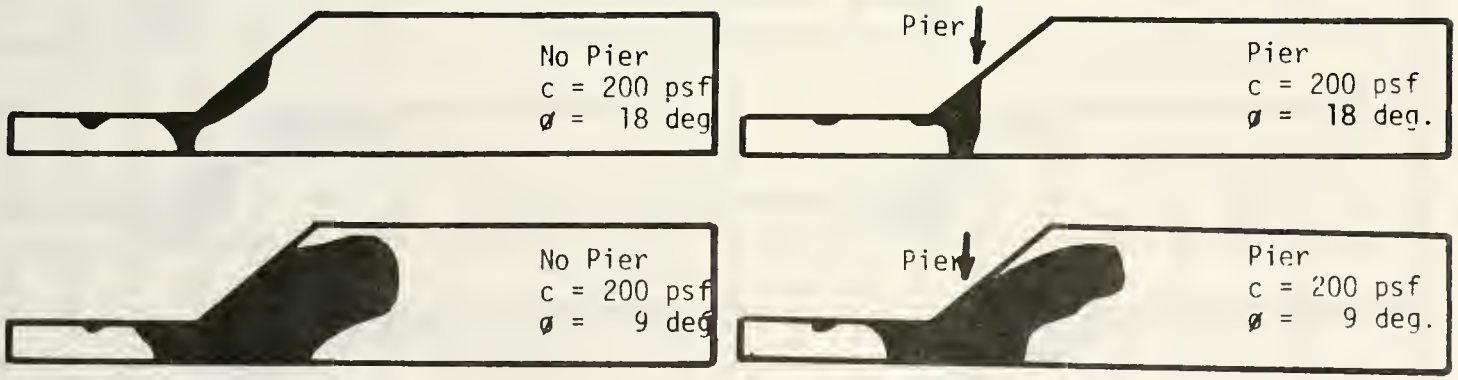

Figure 5.36: Yielded Elements with Decreasing Friction Angle

where the deviator stresses are highest. Because of the reduced friction angle, the retention of confining stress is of decreasing importance and the bulb grows rapidly and about equally for the cases of no pier and with a pier 12 feet from the toe. The piers have less of an effect as the soil strength becomes more dominated by its cohesive component for these loading conditions. The effect of a decreasing cohesion is shown in figure 5.37. As the effect of the frictional strength becomes more dominant, the failure bulb grows from the surface where the confining pressures are smallest. The retention of the confining stresses in the case of a slope with a pier tends to prevent the growth of the failure bulb. The case of a pier 12 ft. from the toe, while showing the greatest reduction in displacements and effect on the stress patterns, resulted in only a modest increase in the factor of safety to 1.93 compared to the 1.88 for the case with no pier.

The most effective position of the piers, with regard to stability, was at the toe (figure 5.35). The factor of safety was 2.25 for this case indicating that a large percentage of the original confinement was maintained from the original stresses at critical portions of the slope. This position of the piers, however, did little in reducing displacements or the stresses leading to failed elements.

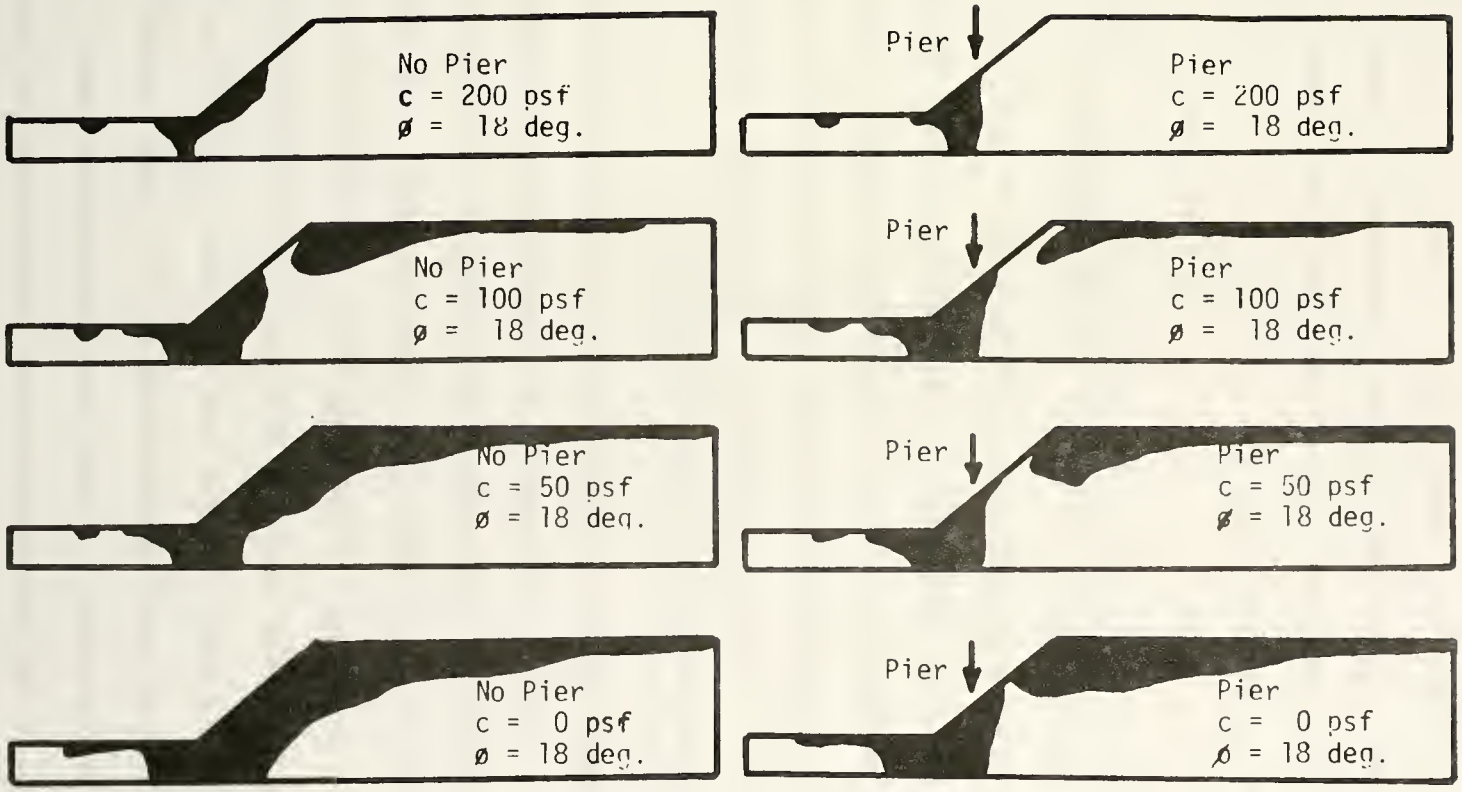

Figure 5.37: Yielded Elements with Decreasing Cohesion

Decause of time dependent movement which may occur in sandy soils, it may be unsafe to depend on the piers to permanently retain the confinement. The piers in this case may best be used as a temporary measure, later to serve as the foundation for a building or retaining wall which is to be backfilled.

The Use of Drilled Piers for Slope Stabilization

So far three practical applications of the use of drilled piers for slope stabilization have been investigated: surcharge loading (Oakland and Chameau, 1984), excavation from a horizontal ground surface and cut slope stabilization. Several important conclusions regarding the slope/pier interaction can be drawn.

Of prime importance is that the piers must be positioned at a point where relatively large displacement will occur, the magnitude of these displacements determines how much stress will be mobilized against the pier (i.e., how much stress the piers will absorb). For the case of the surcharge load, the maximum displacements were near the crest, while in the case of the cut slope they were near the toe. The case of the excavation is complicated by the fact that the maximum vertical displacements upward were near the toe, the maximum vertical displacements downward were near the crest, and the maximum horizontal

displacements were more widely distributed throughout the slope.

The direction of the displacement and, thus, the direction of the stresses on the pier are also to be considered. It is better to load the piers in axial compression, taking advantage of their greatest structural strength. For this reason, the case of surcharge loading lends itself well to this solution, the maximum displacements at the crest are primarily vertical. The vertical loads of the surcharge may be directly absorbed by the vertical support of the piers. This provides the least opportunity for stresses being transferred to the slope.

The movements are primarily lateral, not downward, for the case of the excavation from a horizontal ground surface. Again, the piers can be very effective in absorbing the stresses and transmitting them to the foundation layers, however, laterally loaded piers are structurally weak and the load must be limited. The strength of the piers can be improved using tiebacks. The piers in this case were placed at the crest to take full advantage of any vertical load, however, the limited mobilization of horizontal load at this point made them somewhat ineffective in improving the stability. Better stability could be achieved by placing the piers lower in the slope, but analysis (not presented) shows that this results in the

lateral shearing strength of the concrete piers to be exceeded.

The lack of a significant downward vertical or horizontal component of the displacements in the example case of cut slope stability results in very little reduction of the stresses for any pier position. The support offered by the piers becomes very indirect. In this case they were simply used to increase the frictional component of the soil strength.

The third important factor to consider in evaluating the applicability of the piers are the soil properties. In a purely cohesive material, it is only the reduction of the driving forces (i.e. stress absorption by the piers) which has a significant effect on the stability. The effectiveness of the piers depends directly on the amount of load transfer to the piers.

The effectiveness of the piers in a soil with a frictional component is more complicated. Reduction of the vertical stresses of the slope may have a negative effect in these cases because confining (normal) stress is also being relieved from the potential failure surface. Thus, a major component of the piers supporting action is of no benefit. The piers can improve the stability by retaining the vertical component of stress in areas of uplift, as shown in the example of cut slope stabilization. In

general, however, unless the lateral reinforcement properties of the piers can be used, drilled piers may not be on optimal solution to stability problems in frictional soils.

In summary, the best applications of the piers seems to be in purely cohesive materials under loading conditions which can be absorbed by the vertical resistance of the piers. The second application of the piers would be to support the slope laterally, however, the structural requirements of the piers may increase more rapidly than the benefit which they provide.

The next chapter will study the problem of supporting a slope under increasing self weight. While this application has no direct physical parallel, it is believed to assess the general stability of a slope and yield insight into the stabilizing effects of the drilled piers.

CHAPTER 6: PARAMETRIC STUDIES USING SELF-WEIGHT

Introduction

Drilled piers increase slope stability by two general modes. First, dowel resistance is added to the failure plane. The piers absorb stress and transfer it to the more stable rock layers below. Second, the presence of the piers changes the stress patterns in the soil. The effect of this may range from adding confinement and increasing the soil strength to inducing a change in the failure surface which requires a higher driving force to rupture.

Piers absorb stresses in two ways. The piers resist the lateral forces in the soil, reducing the driving forces along the failure plane directly. This case has been reviewed by Hassiotis (1984) and incorporated in the stability analysis by adding a term equal to the force against the pier to the resisting forces in the numerator of the factor of safety equation. The piers also transfer some of the weight of the soil mass above the failure surface to the layers below (Broms, 1981). This action is

equivalent to negative skin friction against the piers, and indirectly reduces the driving forces along the failure plane.

The shearing resistance through the soil along the failure surface can be improved by changing the stress patterns. The piers disrupt the natural circular displacement and strain patterns which develop in an unreinforced slope. The direction of the principal stresses becomes more random and noncircular, no longer complementing the potential failure surfaces. These potential failure surfaces are now forced to shear the soil along planes other than that of the maximum shearing stress.

The shape of the failure surface is important in another respect. An unreinforced slope may allow a deep seated slide involving a large volume of material. A slope reinforced by a pier tends to force the failure surface to exit before the pier row. This reduces the volume of the slide and may save a structure built above the pier row.

Factor of Safety

Traditionally, in geotechnical engineering, the factor of safety is defined as the ratio of strength available to strength utilized (resisting forces over driving

forces). In some cases, this is a difficult value to evaluate. For example in the case of a pier used to stabilize a slope, it would involve establishing a potential failure surface. Between the piers this could be done by using circular or log spiral surfaces. At the piers, however, the surface is complicated by soil movements around the piers. It would be difficult to evaluate the factor of safety over this entire surface. It may be acceptable to introduce a corrective term into the factor of safety equation for some surface between the piers to account for the added resistance of the soil moving around the piers (Hassiotis, 1984). However, this will not account for the effect that the piers have on the surrounding stress fields and may not be a very good approximation for complex cases involving vertical support.

A simpler evaluation of stability may be accomplished by using loads. Defining the stability as the ratio of ultimate load to working (service) load is more easily evaluated and is more physically meaningful. To evaluate the stability in this manner, a factor of safety along a potential failure surface is computed. This is the traditional factor of safety evaluated using working loads to define the initial stress state. The loads are proportionally increased until a factor of safety of unity is reached. The stability is evaluated as the ratio of the load which causes failure (i.e. factor of safety of unity)

over the working load. Throughout this chapter, stability defined in this manner will be referred to a the "security". This definition of stability depends on the energy which is absorbed by the piers. The ratio of the security of a slope with a pier to that of a slope without a pier is related to this energy and will be referred to as the "efficiency" of the system.

Consider the simple example of a slope made of a frictionless and weightless material. In a first step, gravity turn-on is used to bring the stresses to their initial condition. The initial shearing stress, and so the factor of safety, are functions of the unit weight of the soil. For the case of no pier the factor of safety is simply inversely proportional to the unit weight of the soil. Since there are no other factor involved, the security is equal to the initial factor of safety. This is shown in figure 6.1. If it were possible to place the piers in the slope while the soil is still weightless, and then turn the gravity on, a similar line, with a higher factor of safety and security could be drawn. The failure surface of this second case would be different from that of the first. When a pier is added to a slope, it changes the geometry and boundary conditions of the problem creating a new stress pattern which is overlain onto the initial stress pattern. Initially, before any soil movement, there will be no load against the pier and any shearing

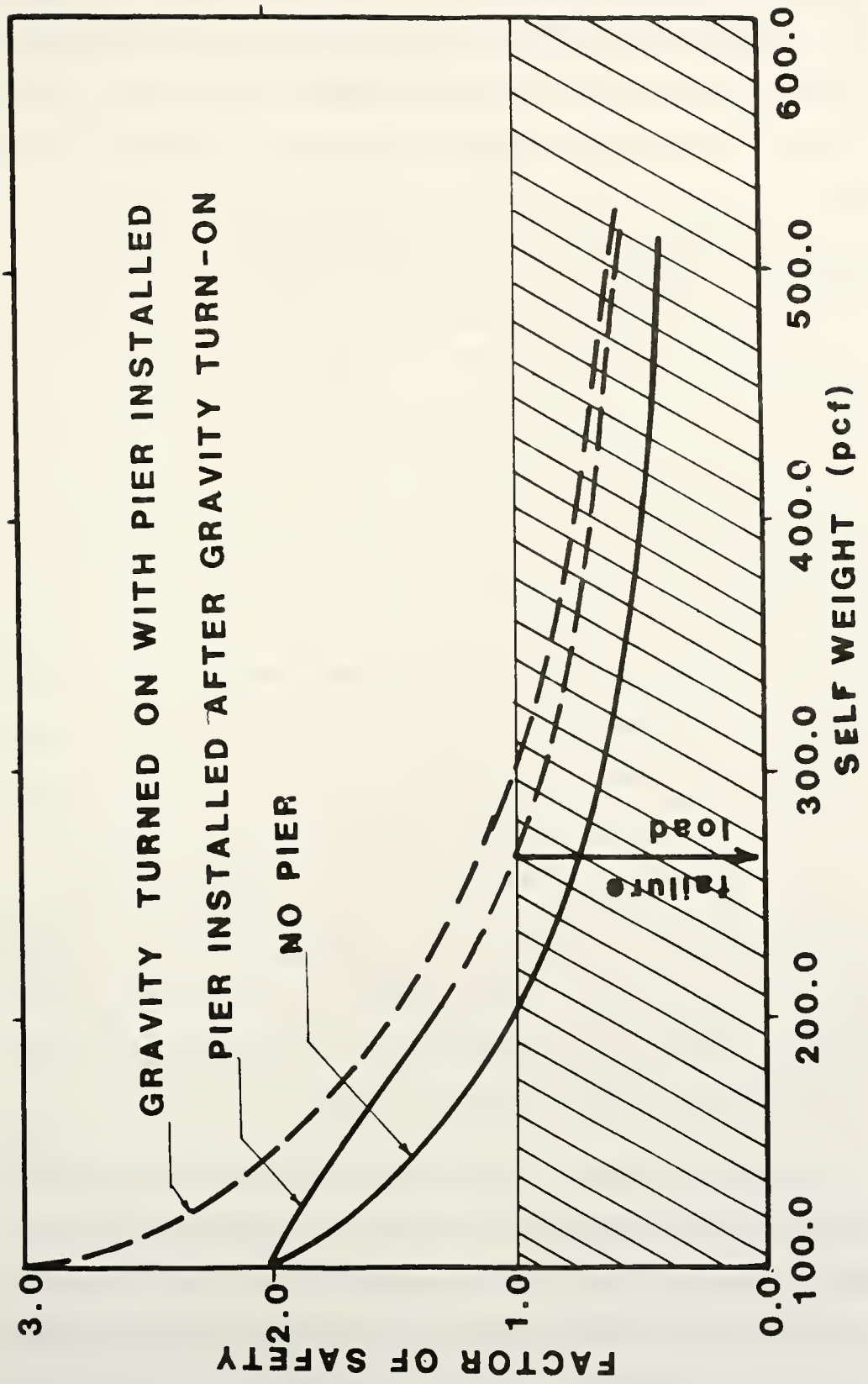

Figure 6.1: Definition of Security

stresses which existed along a potential failure surface will still exist. Therefore, for the case of a pier reinforcing a slope with initial stresses, the initial factor of safety will be the same as the factor of safety for the case of no pier (figure 6.1). Until the pier begins to absorb some stress, either by creep movement or further loading, the piers will not absorb any loads. The most probable failure surface, in the plane between the piers, and factor of safety along that surface will also be the same as that of the case with no pier. As the loading progresses, the new stress pattern may not significantly increase the stresses along the original most probable surface due to the presence of the piers. As the overlain pattern becomes increasingly dominant, new surfaces become critical. The cases of no pier and a pier installed under conditions of zero gravity represent single stress relationships. These lines form boundaries which the real case can not exceed. The real case is shown by a line spanning these two limits. The solid portion of the curve represents a failure surface similar to that with no pier and the dashed portion represents a surface close to that of the fictional upper boundary case.

An added feature of defining the stability of the slope in terms of security rather than the traditional factor of safety is that the security is directly proportional to the loading. Often the decrease in the stress

factor of safety is not proportional to the increase in load. However, by computing the security directly in terms of loads, its value is easy to interpret.

In order to establish the security, a factor of safety is calculated as the ratio of strength available to strength utilized along some failure surface without correcting for the effect of the pier. The true factor of safety of the system reinforced by a pier, if it could be evaluated, would be greater than this value along the line of symmetry between the piers. If it is assumed that this plane represents the critical support of the slope, all that is required is the load at which the factor of safety falls below unity. It must be assumed that the soil will begin to flow around the pier before the soil along the failure surface shears. Therefore, near failure, the lateral resistance utilized by the pier is equal to the ultimate resistance which can be provided by the piers (similar to the limiting equilibrium approach of Hassiotis (1984)), however, the piers can continue to offer vertical support which reduce the rate of loading to the remainder of the slope. Being above or below unity is then only a function of the stresses along the failure surface which can easily be evaluated from the output of the finite element program. The stability defined in this manner will be conservative. Even if it is not the soil around the piers which fails first, this can be considered added

strength which would increase the real factor of safety and thus the security. Furthermore, it should be the intent that the piers help the slope stabilize itself, and not support it by dowel action alone. If the piers were the only remaining support, the piers might shear, resulting in a rapid, potentially more hazardous slide.

Variables

The parametric studies presented in this chapter investigate the influence of four groups of variables or characteristics of the pier-slope problem on the stability of the slope:

1) Pier variables (spacing, position, size, stiffness)
2) Slope geometry and soil parameters
3) Weak soil layers
4) Loading variables

The number of these parametric studies cover a wide range of the selected variables and can allow predictions to be made for other cases which may arise.

Pier Variables

The first category to be studied are the pier variables. These are the design parameters. Oakland and Chameau (1984) studied these variables for the case of a

surcharge loading with emphasis on the effect on slope surface displacements.

The basic problem to be solved is shown in figure 6.2. The capabilities of the computer program to solve large size problems was established in the previous chapter and, thus, the dimensions of this problem are relatively small to limit the computing time and keep the amount of output data to a manageable volume. The soil is first considered frictionless and linear elastic. The first of these assumptions allows for an easy evaluation of the factor of safety since the resisting forces will not change with the load. Although restrictive, the second assumption is sufficient to study the trends useful in design. More realistic soil models will be introduced later (see also Chapter 5 for general cases).

As indicated earlier, the loading pattern is generated by increasing the self weight uniformly. The factor of safety is first computed for the case of no pier as a function of self weight. This results in the "no pier" curve in figure 6.3, which will serve as a datum to evaluate the effect of the piers.

The technique of increasing self weight has been used in several previous studies of vertical slope stability (Snitbhan and Chen, 1978; Mizuno and Chen, 1982).

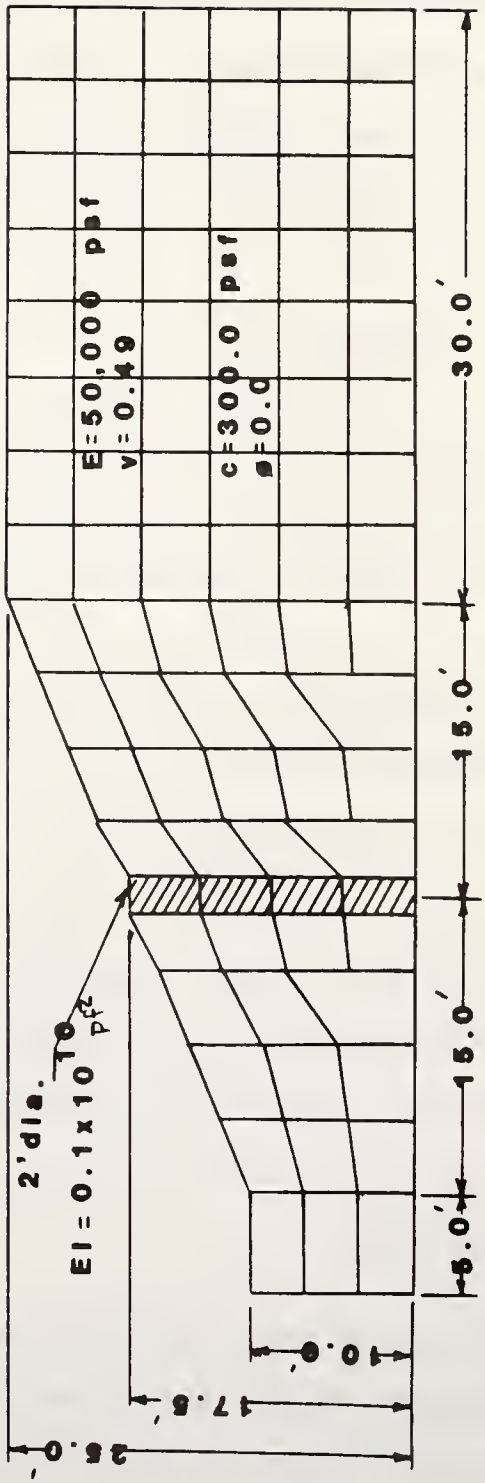

Figure 6.2: Mesh Used to Study Pier Variables

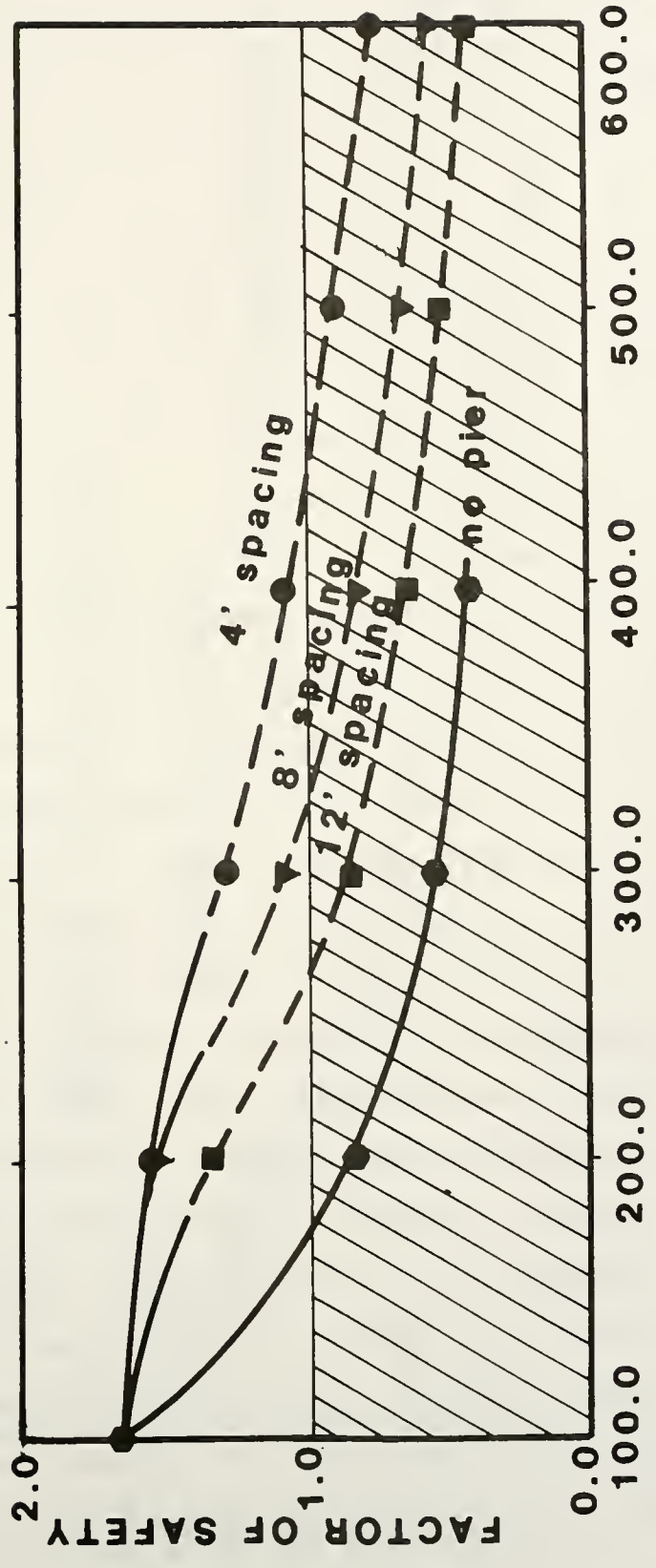

Figure 6.3: Factor of Safety as a Function of Pier Spacing and Self Weight

Effect of Pier Spacing

Figure 6.3 shows the factor of safety analysis for several pier spacings. The factors of safety were obtained from the output of the F.E. program (see Chapter 4) in the plane located at the centerline between the piers. The solid portion of the line indicates that the most probable failure surface extends beyond the piers and the dashed portion indicates that the failure surface was shallow and exited before the line of piers. The point of transition between these two curves is significant in several respects. It is the intersection between two curves, one forcing the failure surface in front of the line of piers and one forcing the failure surface to exit beyond the line of piers. This is idealized in figure 6.4. If this intersection falls above a factor of safety of unity, then the slide will be restricted to a shallow failure. If, on the other hand, this point falls below unity the slide will be deeper and larger, involving part of the surface above the crest. This point is also important with regard to stress patterns. A deep seated slide, for this example, represents a failure surface which is strongly dominated by the initial stress pattern. Additional loading with a pier in place overlays a new stress pattern. This new stress pattern tends to develop a most probable failure surface which exits before the line of piers. The load at which this transition occurs indicates

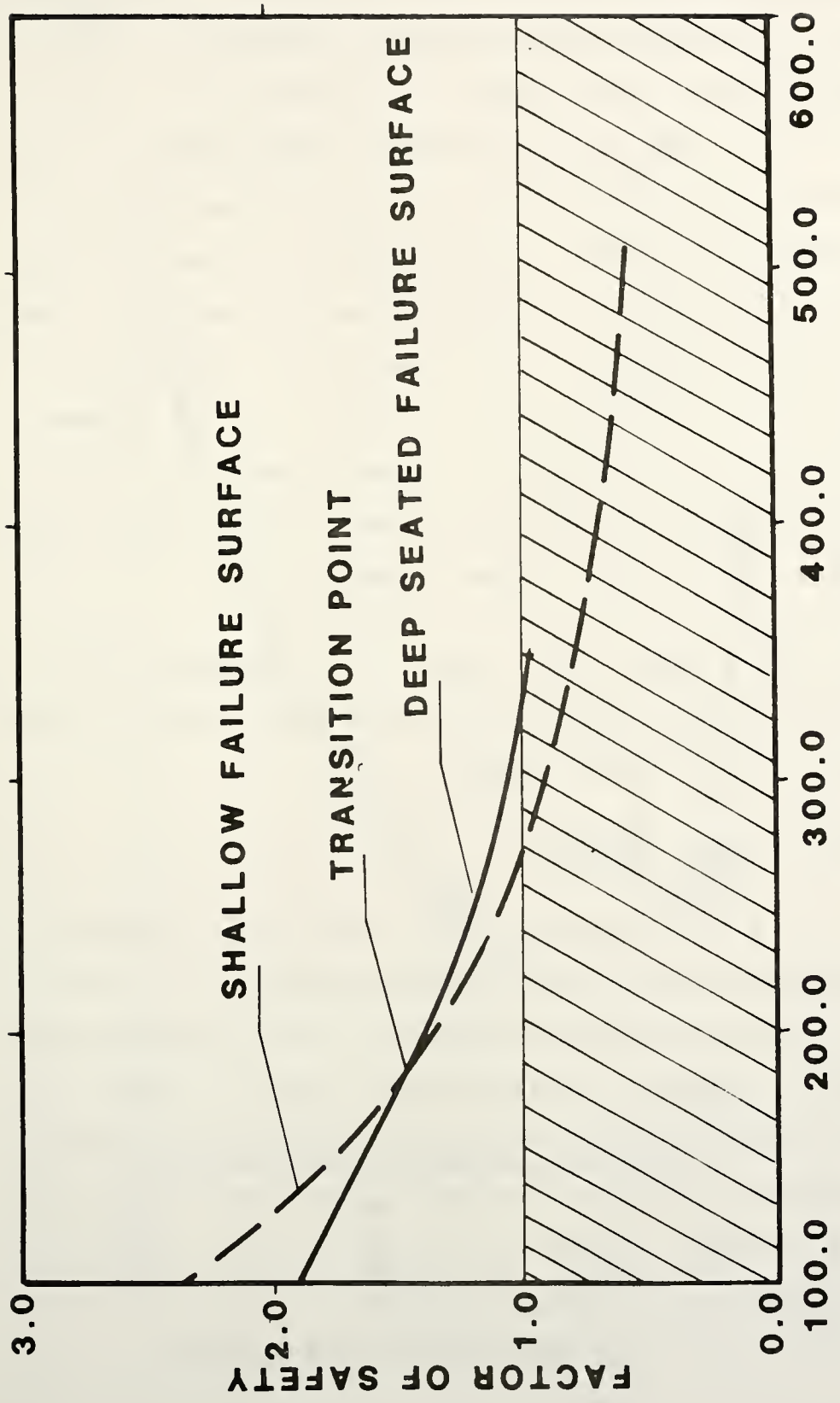

Figure 6.4: Factor of Safety as a Function of Failure Surface and Self Weight

when the new stress pattern becomes dominant. Figure 6.5 shows a plot of pier spacing versus transitional load. With the piers widely spaced the transition occurs at a relatively small increase in load. This indicates that a very small percentage of the additional load is being absorbed by the piers. When the piers are more closely spaced a significant increase in load is required to make the transition occur. This means that the piers are absorbing most of the additional load. It can be seen that the curve in figure 6.5 becomes steeper for the closer spacings indicating improved arching action of the soil for smaller clear spans between piers.

Finally, the overall stability as measured by the security against increase in self weight versus pier spacing is shown in figure 6.6.

Effect of Pier Position

The general stability of a slope can be increased by decreasing the possibility that any slide will occur (i.e. by increasing the overall security), or by limiting the amount of material involved in the event of a slide (i.e. by increasing the security against a deep-seated slide). The position of the row of piers within the slope has a large influence on both the overall security and the security against a deep-seated slide.

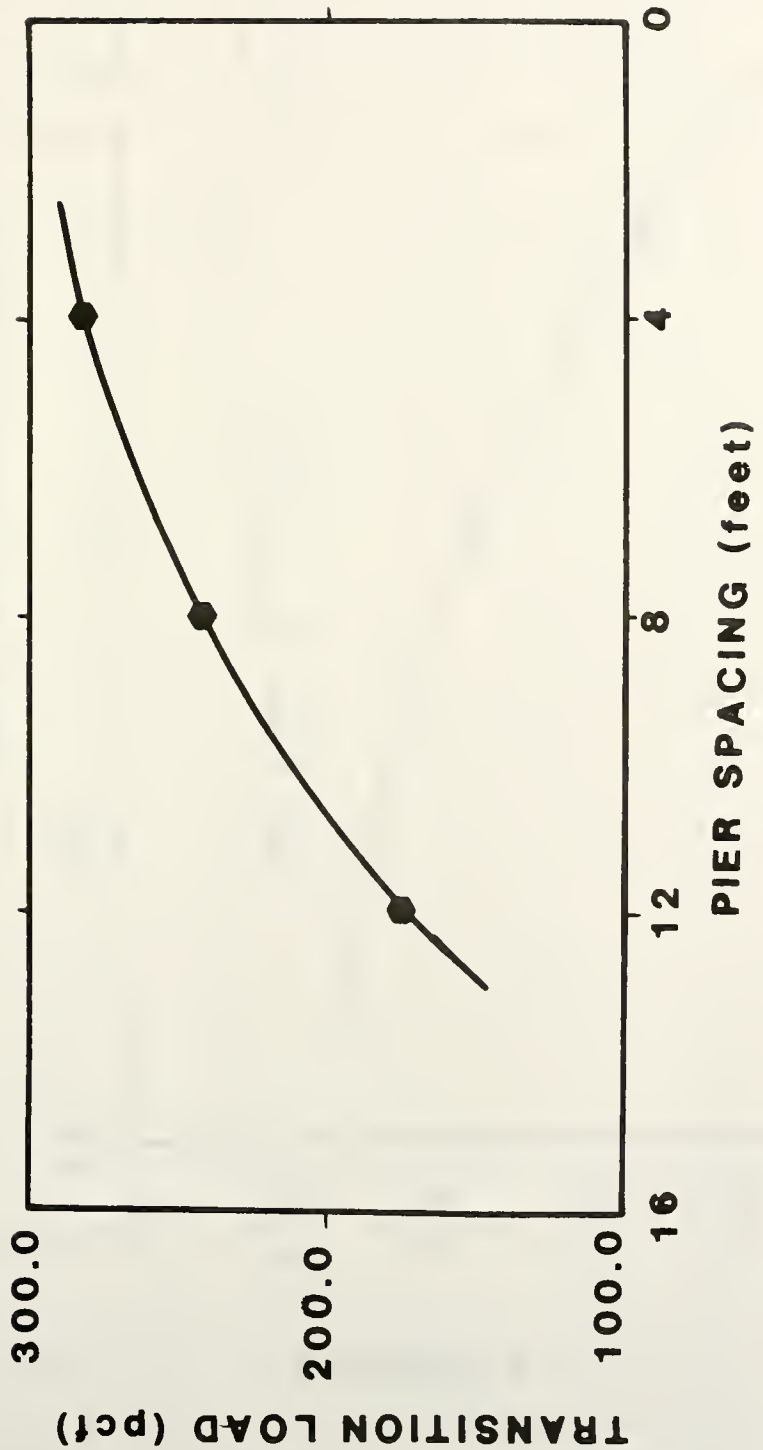

Figure 6.5: Transition Load vs. Pier Spacing

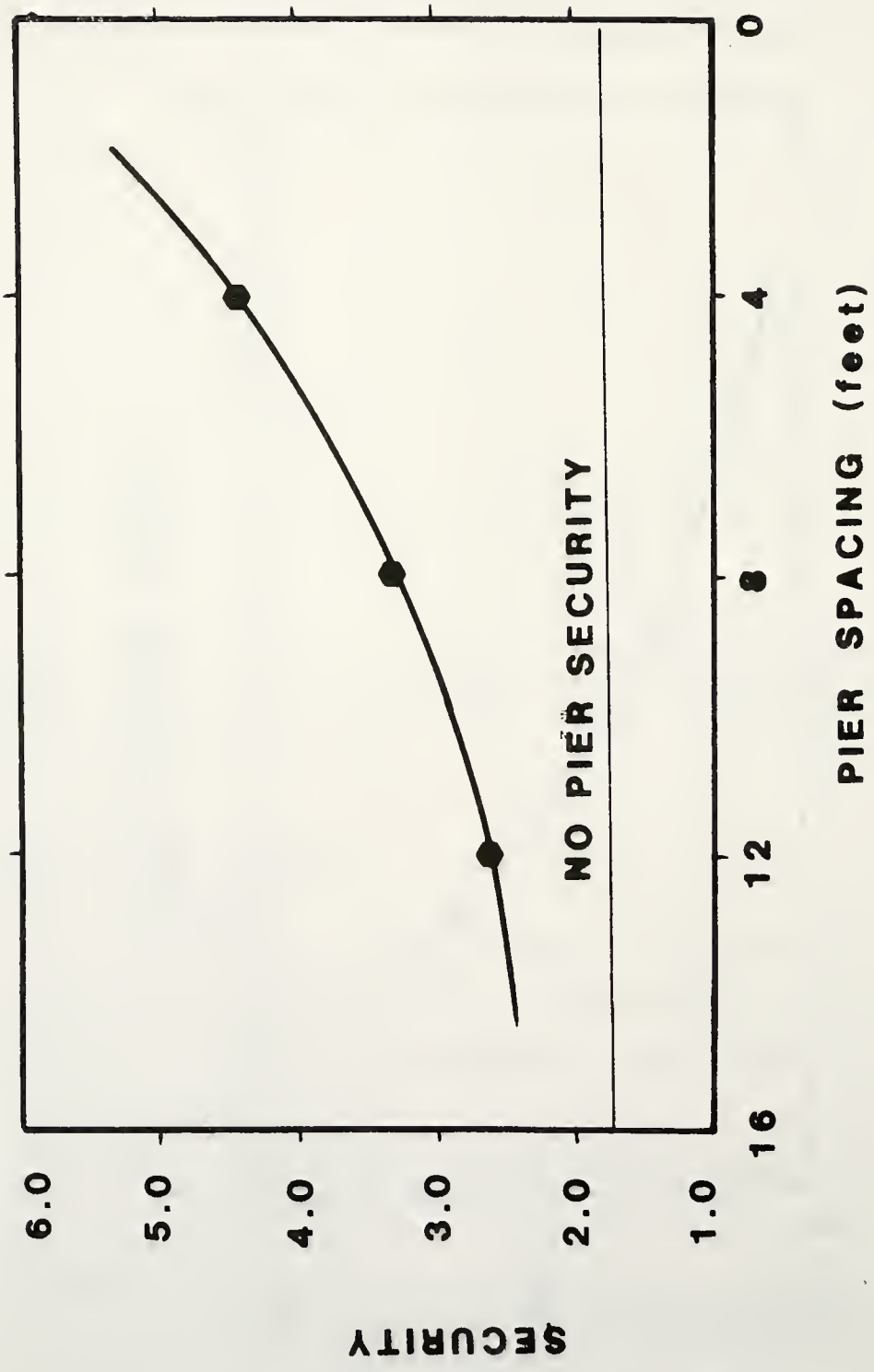

Figure 6.6: Security vs. Pier Spacing

The factor of safety is given in figure 6.7 for three pier positions, 10, 15 and 25 feet from the toe of the slope as a function of self weight. The factor of safety depends, in part, on when the failure surface changes from exiting beyond the pier to that of exiting before the pier. If it becomes kinematically more difficult for the latter surface to form, then the overall factor of safety would be increased. One method of accomplishing this would be to move the pier farther down the slope. This creates a greater difference between the original failure surface which exits beyond the crest of the slope and the critical failure surface at a factor of safety of unity. The greater this difference, the higher the stability for a particular slope. There is a point when the piers are so close to the toe of the slope that a failure in front of the pier row will never occur. A pier row 10 feet from the toe is close to this limiting case.

Although a pier at 10 feet from the toe provides the best overall security because it does not allow a failure in front of the pier row, it may not provide enough protection against a deep seated slide. Deep-seated slides are analyzed by "forcing" the failure surface to extend beyond the crest of the slope. A row of piers at 15 feet from the toe, although allowing a lower overall factor of safety for a minor failure in front of the piers, is more efficient against a larger failure extending beyond the

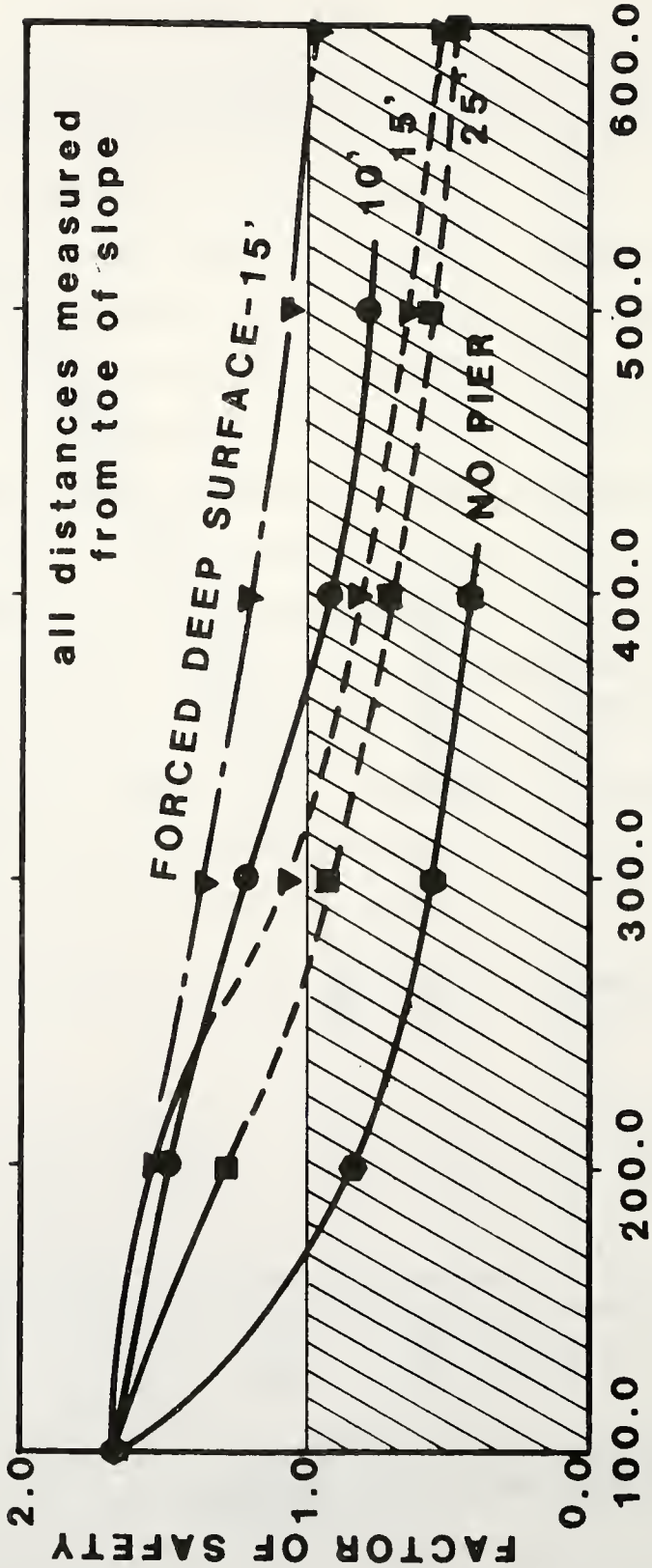

Figure 6.7: Factor of Safety as a Function of Pier Position and Self Weight

row of piers. There is a trade off between overall security and security against deep-seated slides (figure 6.8). As the distance of the piers from the toe of the slope increases, the security against deep seated failures increase, while the overall security decreases.

In summary, the piers' position has a complicated effect on the slope stability. There are three important factors to consider. First, as the piers move down the slope, the likelihood of a failure surfacing before the pier will diminish, but support against a deep seated slide may decrease. Second, as the piers move down the slope, their vertical support of additional overburden loads will decrease due to the primary direction of loading changing to a horizontal direction. Third, by the same token the improved effect on stability will result from the piers utilizing more of the horizontal load capacity. The relative effects of each of these factors must be considered in the design.

Effect of Pier Size

Similar to pier spacing, the pier size regulates the clear spacing between piers and influence the stability of the slope. In this respect it might be expected that the effects of the piers will be similar to those shown in figure 6.3. Figure 6.9 shows the results of varying the size of the piers with respect to the factor of safety and

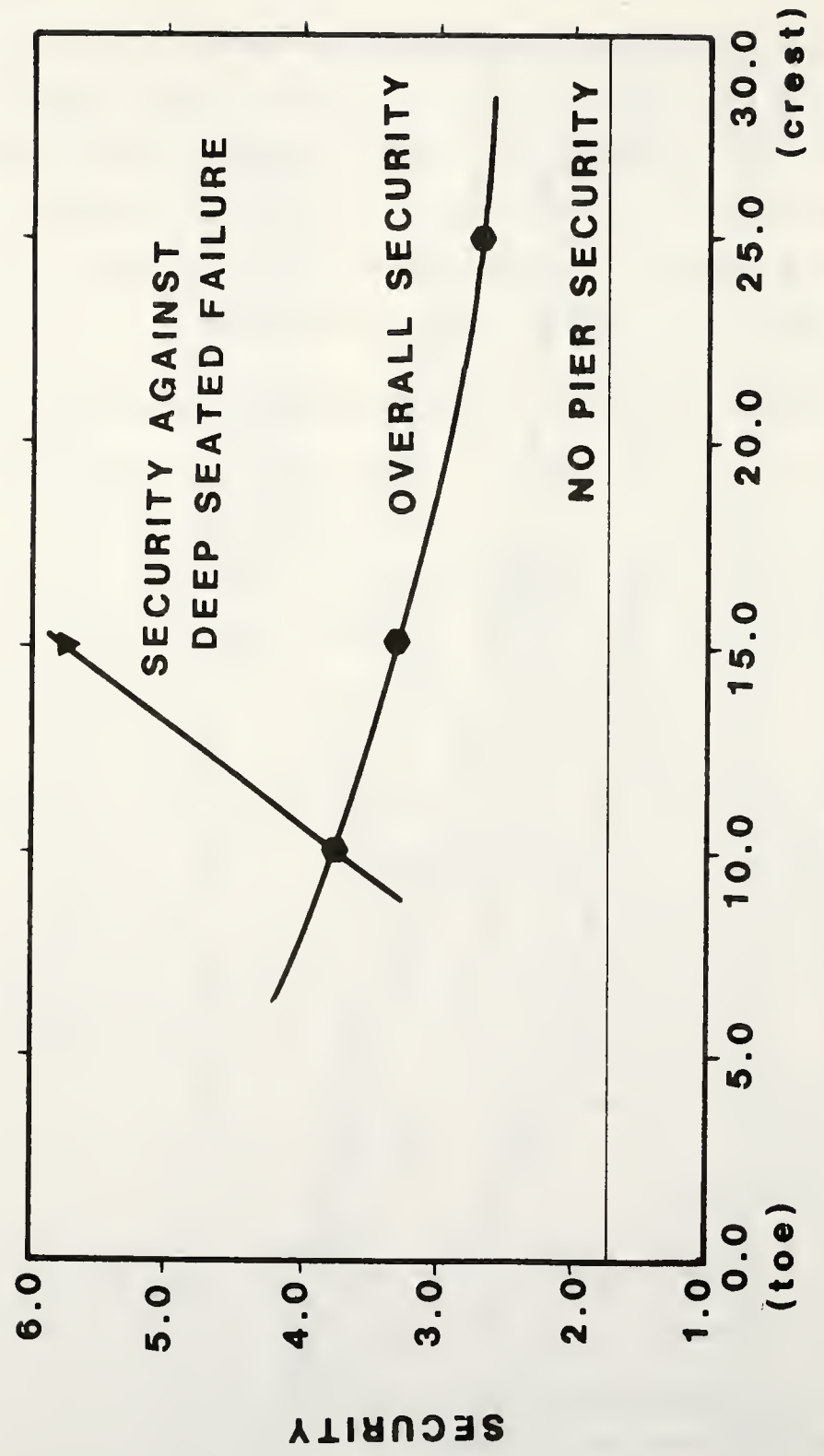

Figure 6.8: Security as a Function of Failure Type and Pier Position

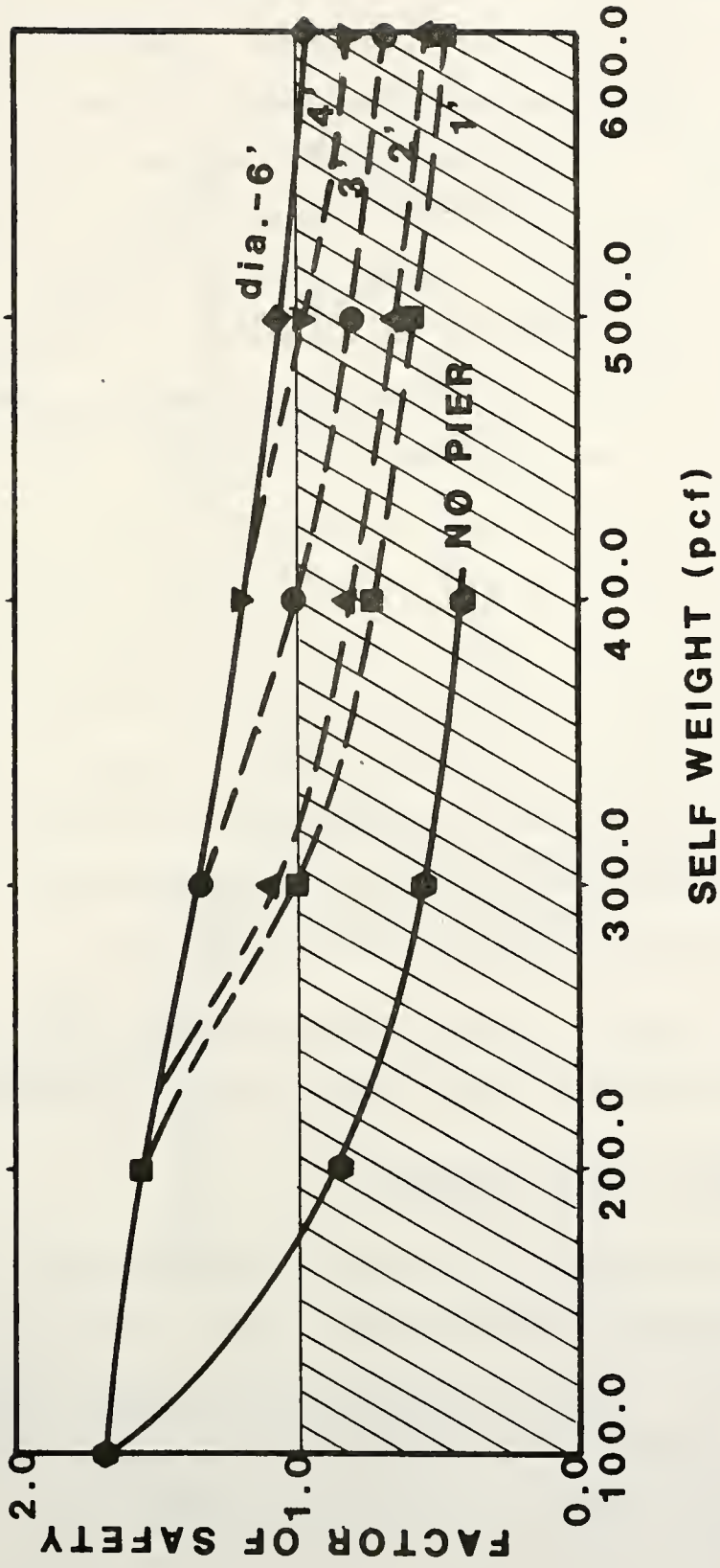

Figure 6.9: Factor of Safety as a Function of Pier Diameter and Self Weight

loading. There is a difference between the patterns of the curves for these two cases (comparing figures 6.3 and 6.9). This indicates that other factors in addition to the clear spacing control the mechanism of stress absorption to the piers. A "backbone" curve is obtained for factors of safety corresponding to failure surfaces extending beyond the row of piers. The individual curve for each of the different pier diameters branches downward when the transition point is reached. This "backbone" curve indicates that the pier size does not have a significant effect on the security against a deep seated slide in this case. Figure 6.10 shows how the primary direction of movement is generally horizontal for deep seated slides and vertical for shallow slides. Since it is the shallow slides which are controlled by the pier size, then it can be assumed that it is the increasing surface area which is absorbing the load in these cases.

Figure 6.11 shows the overall security against increased soil weight versus pier diameter.

Effect of Pier Stiffness

The range of possible stiffnesses which can be used in practice has a negligible effect on the factor of safety. There is a slight effect on displacements with the stiffer piers reducing movement more (Oakland and Chameau, 1984).

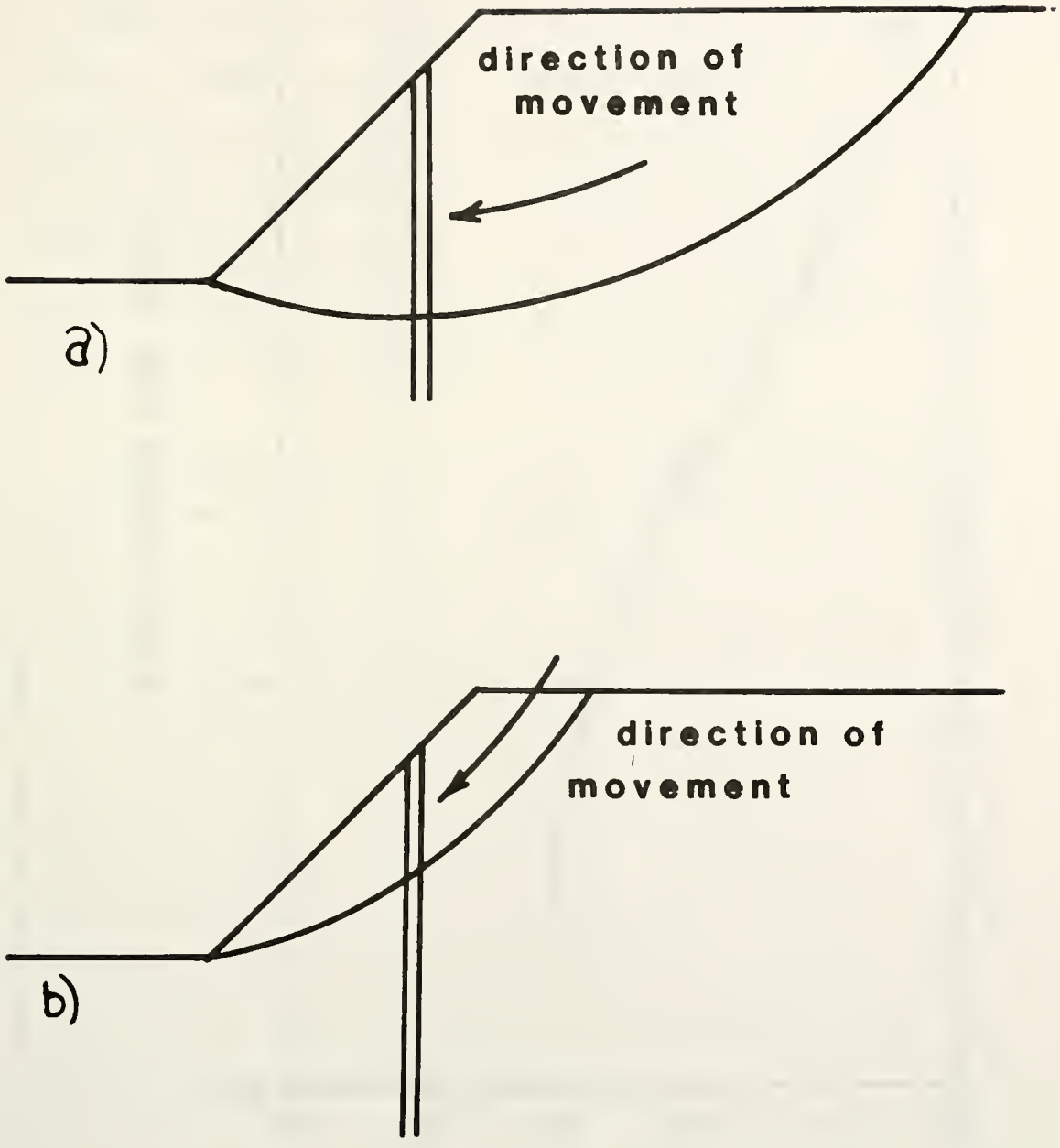

Figure 6.10: Direction of Movement for Deep and Shallow Slides

a) Deep Seated Failure
b) Shallow Failure

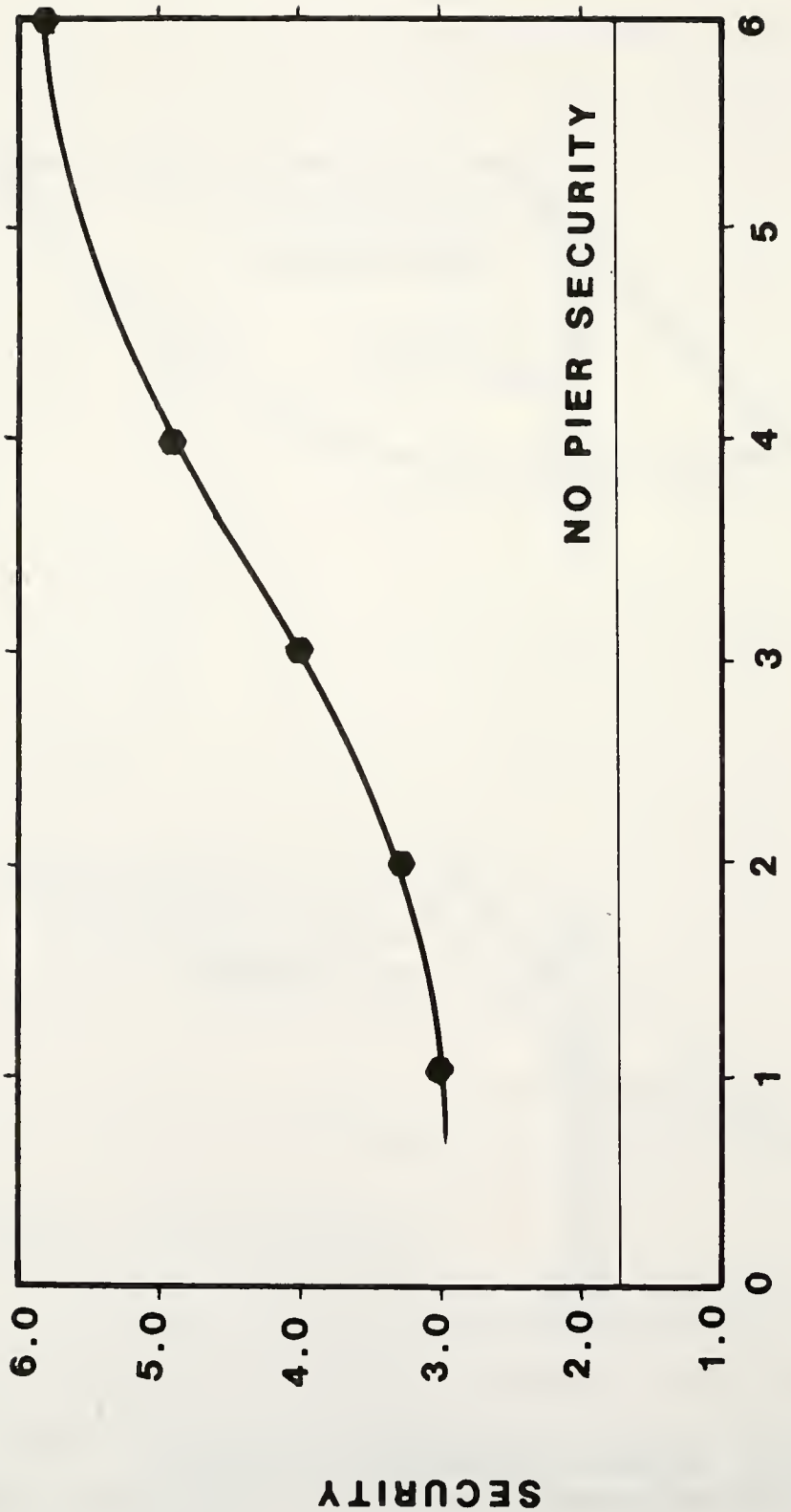

Figure 6.11: Security vs. Pier Diameter

Slope Geometry and Soil Parameters

The purpose of studying the effects of the slope geometry and soil parameters is to establish the circumstances for which drilled piers are most advantageous. The geometric parameters include slope height, foundation depth and slope angle as the major variables. The cohesion, friction angle, modulus of elasticity and Poisson's ratio are the most important soil parameters.

In the previous section, the basic slope-pier relationships were studied by changing the pier. In this section the opposite viewpoint will be used. The slope conditions will be varied while the pier characteristics will be kept constant. Comparisons between cases becomes a little more complex because of a lack of a single reference point, i.e. the stability of the case with no pier, as was used in the previous section. As the slope varies, the stability without a pier varies also. For this reason it becomes important to compare the results in terms of relative improvement of the stability using the "efficiency" as defined previously.

A larger variety of more complex problems will be used to study the effect of the geometric and soil variables. The basic slope configuration is given in figure 6.12, but variations will be specified for each variable as needed.

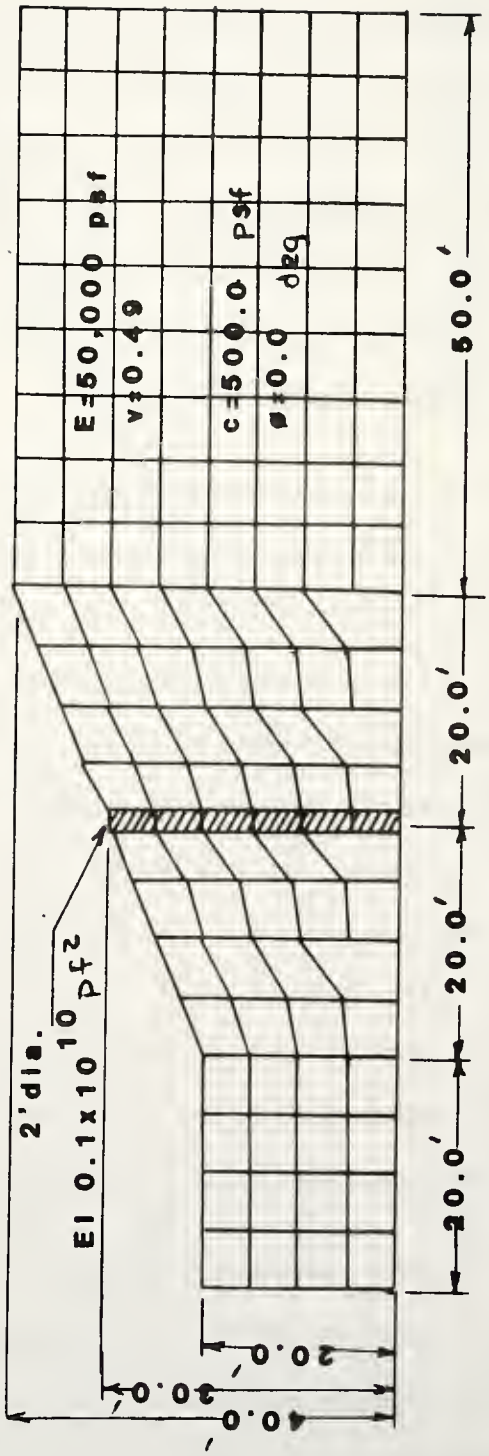

Figure 6.12: Mesh Used to Study Slope Geometry and Soil Variables

Geometric Variables

Effect of Slope Angle

Modelling different slopes using the same pier can give insight as to when the piers are most applicable as reinforcement. For the case given above, the slope inclination is varied from 1:1 to 1:4. This has a complex effect on the direction of the loads which are transferred to the piers. The calculation of the factor of safety is further complicated by the fact that the shape and length of the failure surfaces for each case are very different. Figure 6.13 shows the results obtained from the slope in figure 6.12 under conditions of self loading. The most striking feature of these curves is that while the cases of different slopes with no piers maintain the same shape, the cases with piers vary in shape. This is very noticeable in the steeper slopes. This variation is due to changing the stress field from one which has little resistance to failure before the pier to one which is less likely to fail before the pier. This variation is most likely due to the steepening direction of slope movement, however, the abruptness of the change with slope angle is difficult to explain.

Figure 6.14 shows the relationship for this case between security and slope angle. In general, the piers are more efficient for gentler slopes, however, they give

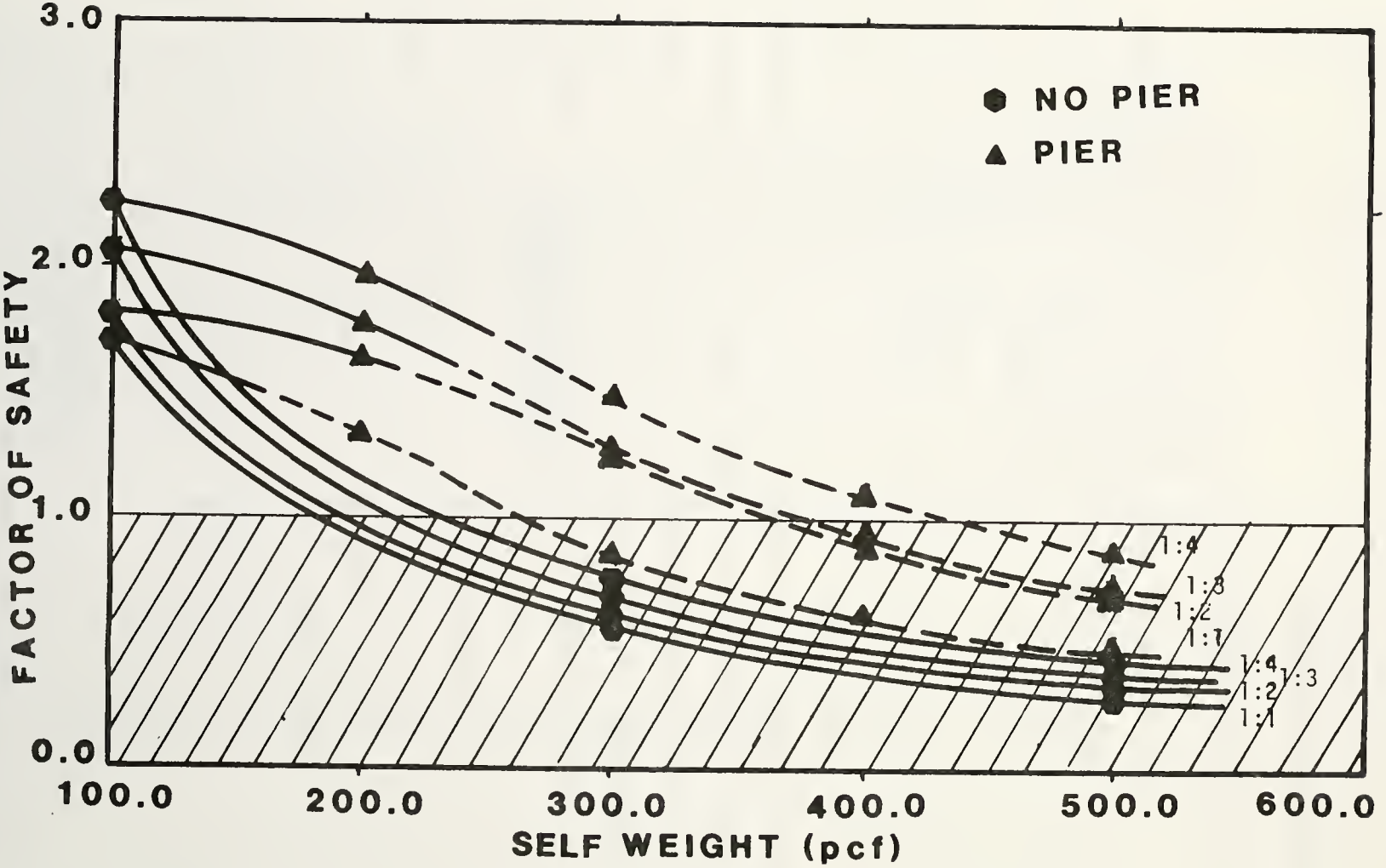

Figure 6.13: Factor of Safety as a Function of Slope Angle and Self Weight

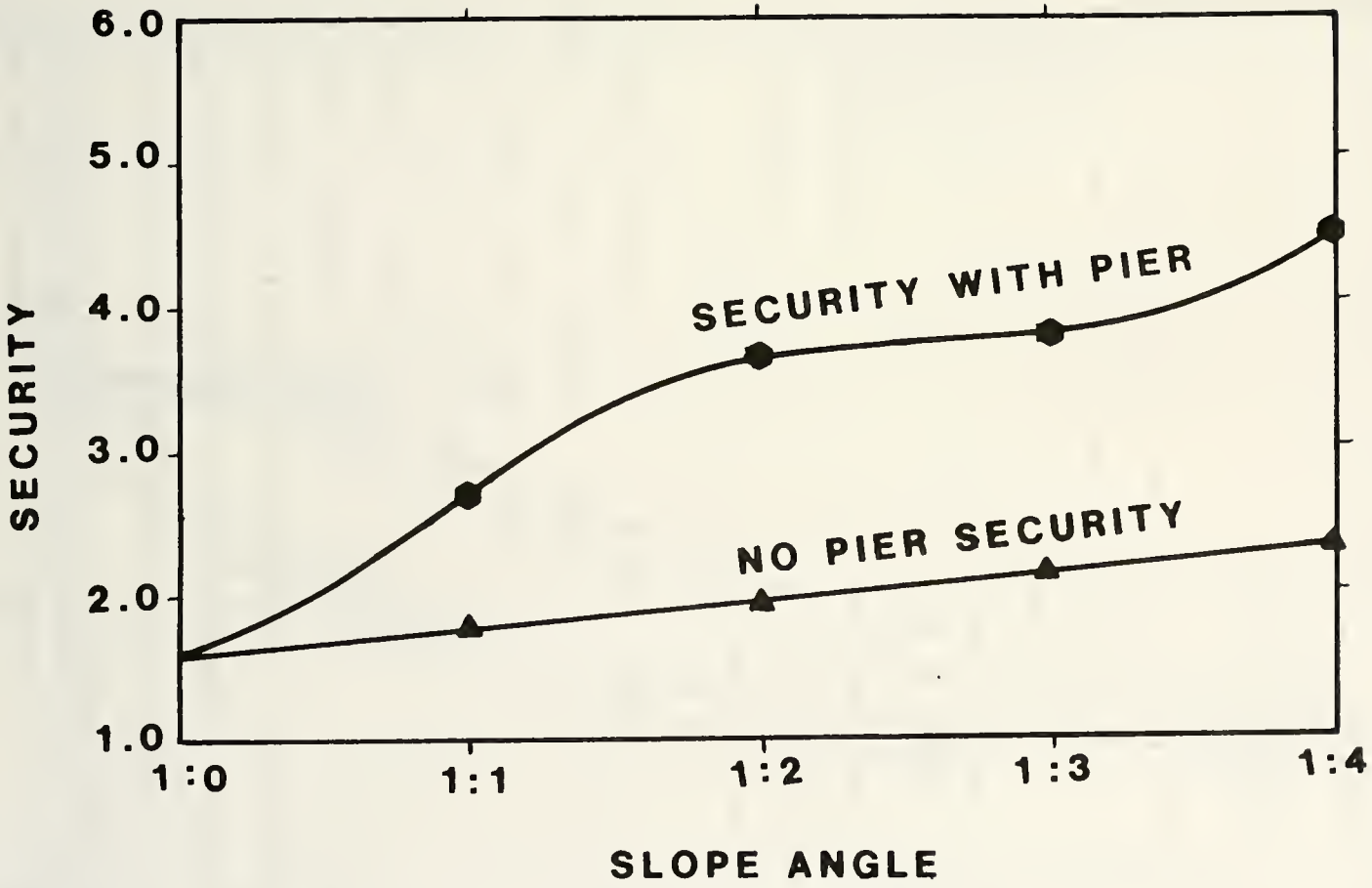

Figure 6.14: Security vs. Slope Angle

significant support in all cases. The efficiency of the piers does not increase significantly for slopes between 1:2 and 1:3. This again indicates a change in the mode of failure within this range of inclinations.

Effect of Depth to Bedrock

The depth to bedrock is an important factor in calculating the factor of safety, especially from the results of a finite element program such as is used in this study. In limiting equilibrium calculations, the depth to bedrock is important because it limits the extent of the failure surfaces. When computing the stresses and displacements in the finite element code, the bedrock is a boundary limiting both shear stresses and displacements.

Figure 6.15 shows the results of varying the depth to bedrock while keeping the other parameters given in figure 6.12 constant. In this example none of the surfaces reached the bedrock level, thus the bedrock did not limit the extent of the potential failure surfaces. A significant boundary effect did influence the stresses. For the cases involving no pier, when the foundation depth was 10 feet, there was a significant increase in the factor of safety. A foundation at 20 feet below the surface has no apparent effect on the stresses along the failure surface since its factor of safety curve is the same as the curve for a foundation depth of 30 feet. When a pier is added,

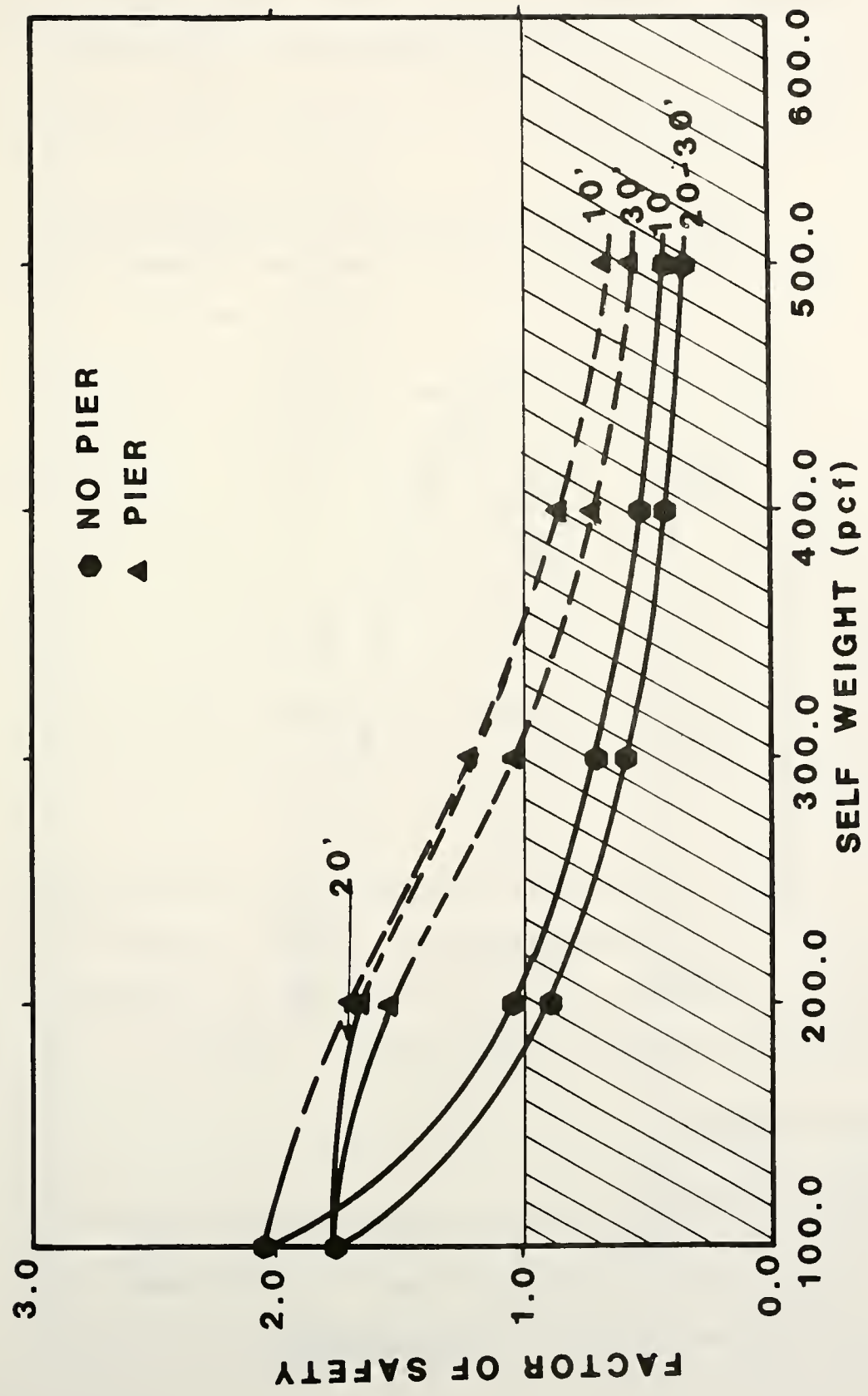

Figure 6.15: Factor of Safety as a Function of Foundation Depth and Self Weight

the foundation depth has an even more profound effect. In these cases, the curve representing the 20 foot depth quickly becomes asymptotic to the 10 foot curve indicating that a strong boundary effect is reducing the failure surface. Even at a depth of 30 feet, the boundary still has an effect on the failure surface shearing stresses as this curve is also convergent to the other two curves.

Figure 6.16 summarizes the securitys for this example. While the piers are highly efficient in all cases, the most effective situation is one where the boundary has little effect on the original slope, but becomes very important when a row of piers is added. This is an example of redirecting the stress field to actually increase the stability while also gaining stability through the effect of the piers. This occurs the case for the shallower depths.

It must be noted that only failure surfaces initiating from the toe where considered. Deeper failure surfaces initiating in front of the toe may have produced results more dependent on the depth to bedrock.

Soil Variables

Effect of Cohesion

In a linear elastic problem, the cohesion does not affect the determination of the stresses. Variations in

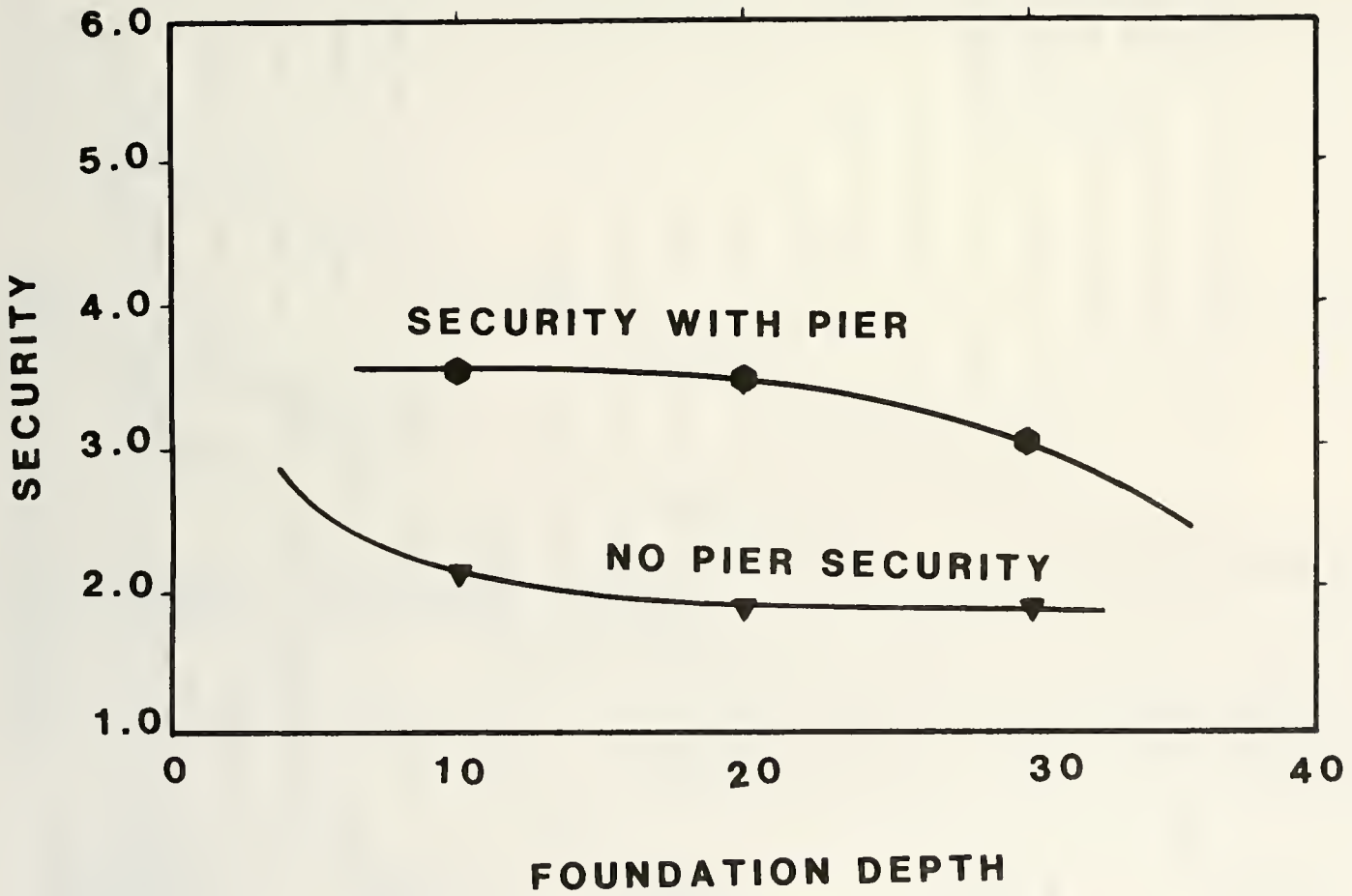

Figure 6.16: Security vs. Foundation Depth

the cohesion simply vary the numerator in the factor of safety calculations. The results of varying the cohesion are shown in figure 6.17. The efficiency is a constant for all cases.

Effect of Friction Angle

The effect of the frictional properties of the soil are primarily influenced by the confining pressure. For the case of a slope of purely frictional material, the confining pressure increases directly with the unit weight of the soil, thus the factor of safety is not influenced by the soil unit weight. The factor of safety is only a function of the friction angle and the slope angle in this case. In figure 6.18 the shape of the curves is a function of the cohesion. As the friction angle is increased, the relationship between the factor of safety and the load is proportionally increased. The curves become asymptotic to the ratio of the tangent of the friction angle over the tangent of the slope angle.

Piers used to reinforce slopes have a sharp reduction in efficiency with increasing friction angle. At some point, the piers may actually reduce the stability of the slopes. The reason for this decrease in effectiveness is the absorption of vertical loads by the piers which prevents the confining pressures from increasing at the same rate as the driving forces. A further problem when

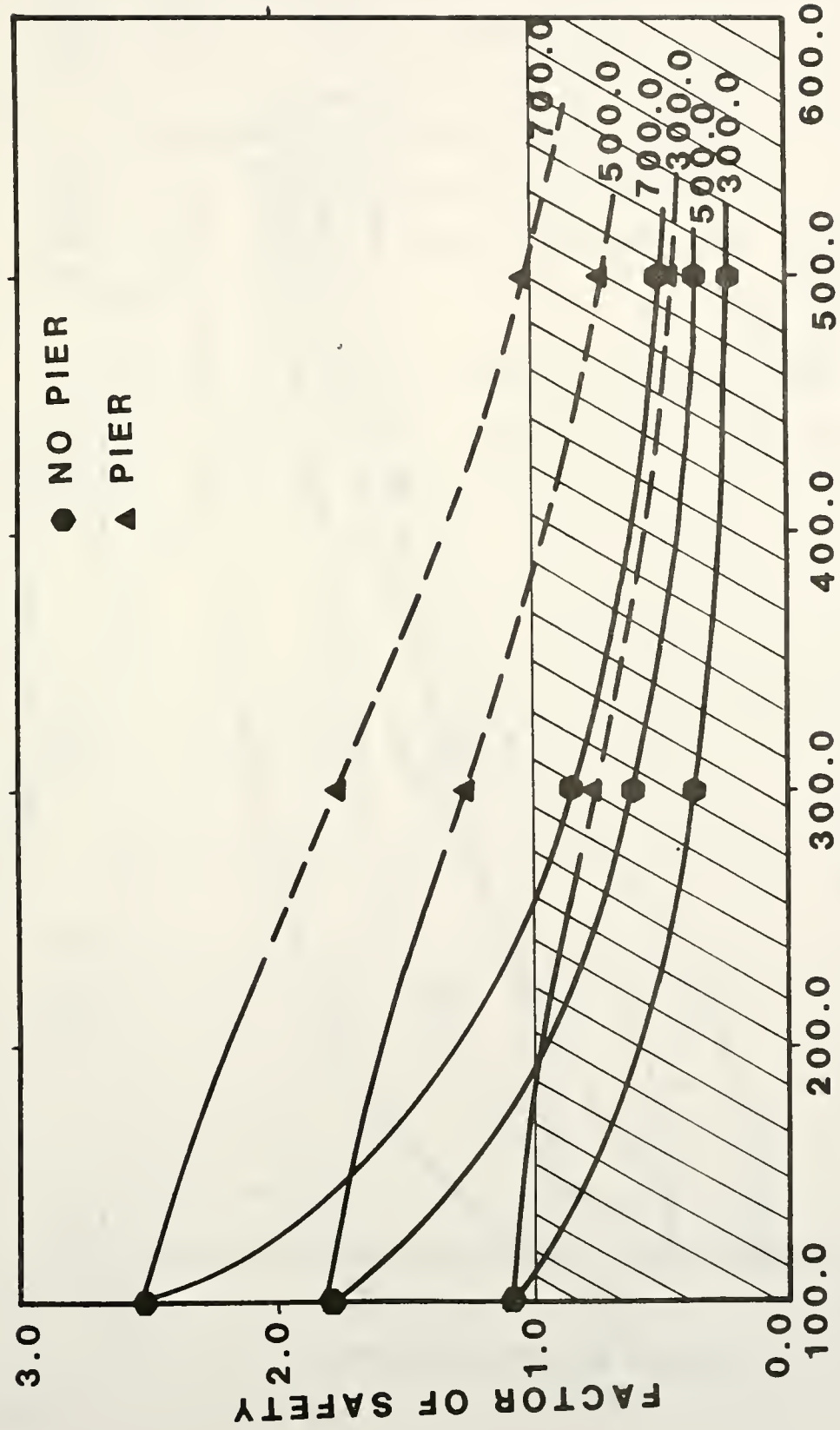

Figure 6.17: Factor of Safety as a Function of Cohesion and Self Weight

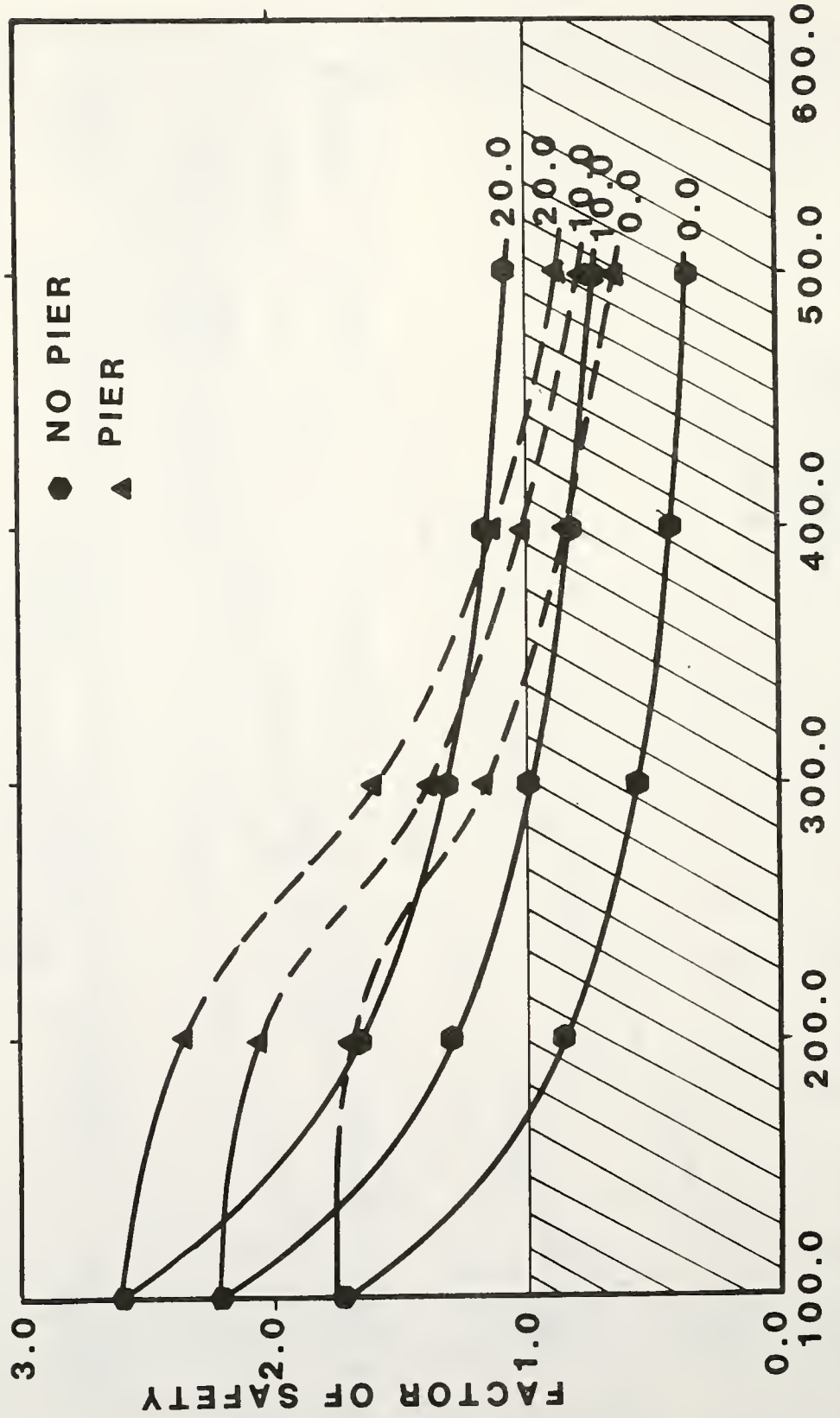

Figure 6.18: Factor of Safety as a Function of Friction Angle and Self Weight

trying to stabilize frictional materials with discontinuously spaced piers is that, for the soil arching effect to be maintained between the piers, the material within the arch must be in tension. Since frictional materials do not display much tensile strength, the soil will tend to "run" through the piers.

Piers used to stabilize material containing some component of friction should be placed such that they do not hinder the development of confinement on potential failure surfaces. This would indicate placing them in the lower portion for the slope. Piers used to support this type of material may also have application to cases of lateral and upward movement, such as an excavation, where the piers may actually retain some of the confinement.

Effect of the Modulus of Elasticity and Hyperbolic Soil Model

In the linear elastic case, the modulus value has little effect on the stability. Figure 6.19 shows the effect of using a non-linear elastic soil model instead of a linear elastic model. The parameters used where the same as used in the example in Chapter 5, K = 47.2, n = 0.5 and R_f = 1.0. A limiting value of 10% of the initial modulus was used as a lower bound. The factors of safety resulting from the finite element stress field are somewhat less for the case of the non-linear soil parameters.

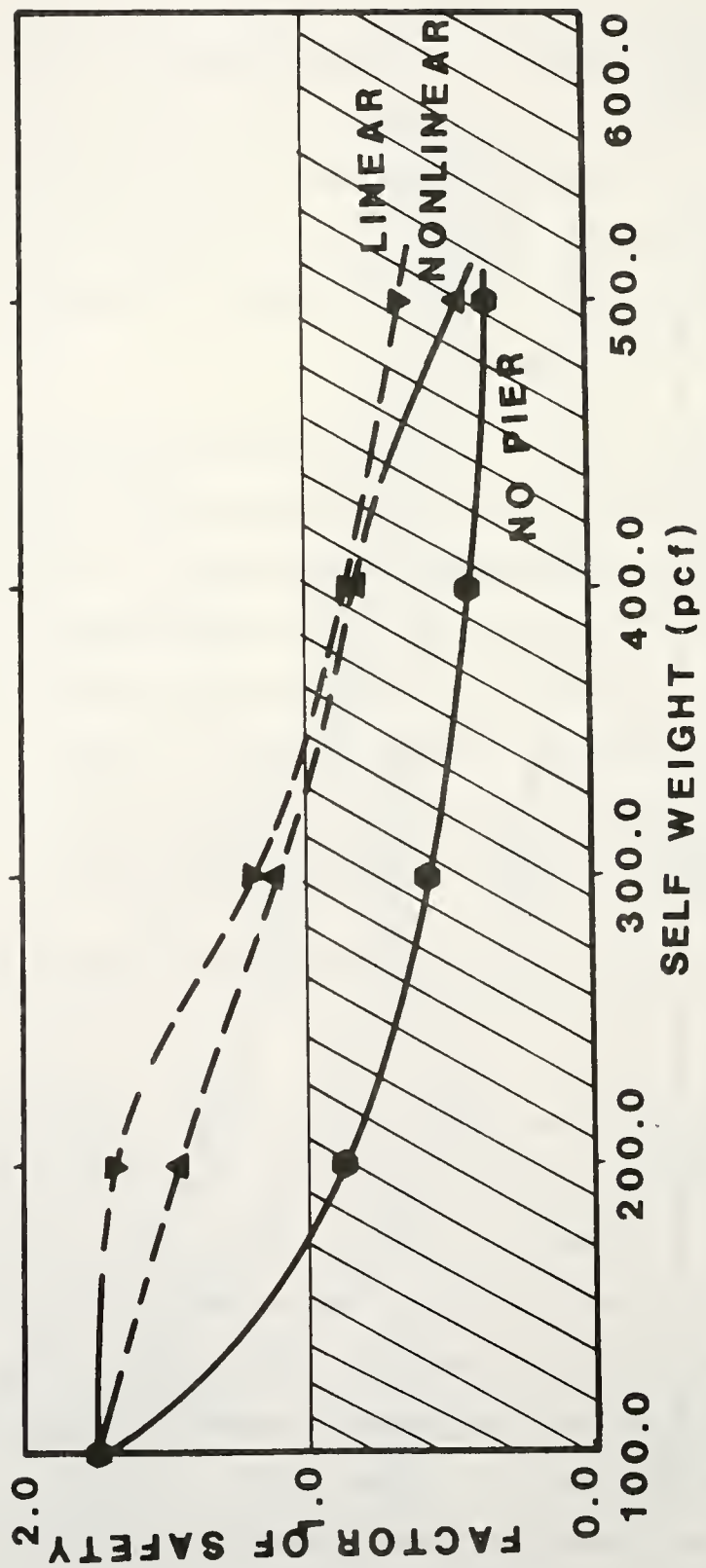

Figure 6.19: Factor of Safety as a Function of Soil Model and Self Weight

This is due to the fact that because of the higher confining pressures at these depths, the soil will be more deformable at greater depths. This creates the situation of a more rigid soil moving on top of a softer foundation. This alters the stress field, allowing the transition from a deep seated slide to a shallower slide to occur at a lower increment of load. The trend, however, reverses itself at very high levels of load, forcing the failure surface again into a deep seated mode. The factor of safety decreases rapidly at this point and eventually goes below that of the case with no pier.

These trends as well as the altered shape of the curve are very difficult to explain due to the complicating effect of the variable modulus on the stress field. In general, however, the curves tend to be similar, especially in the area around a factor of safety of unity. While more examples would be necessary to establish the effect of non-linearity, this example seems to indicate that the use of linear elastic modelling may be a suitable approximation in some cases. However, it should be understood that the use of linear elastic modelling yields unconservative results.

Weak Soil Layers

To model the effects of thin layers, the finite dimension slip elements developed by Desai, et al, (Desai

and Sargand, 1984; Desai and Lightener, 1985) are used. These elements, as described previously, have the advantage of having the same formulation as the typical soil elements. It is thus possible to assign soil parameters to the thin layers modelled by these elements. Two parameters, the shearing modulus and the cohesion of the layers are likely to have an effect on the factor of safety.

The finite dimension slip elements can be used to represent a thin layer of soil around the pier which has been disturbed by the drilling operation. This disturbance is modelled as a reduced modulus of elasticity. Using a reduced modulus of elasticity in a shell of elements four inches thick had a negligible effect on the factor of safety analysis. Negligible effect was found over a variety of reduced moduli up to a modulus reduction factor of 4.0. The limited width may restrict movement beyond the sensitivity of the study.

A lower modulus of elasticity may also be accompanied by a lower cohesion in the thin layer of elements around the pier. This again has a negligible effect on the factor of safety since only a very small portion of the failure extends through this weaker material.

The slip elements can also be used to model a weak seam within the soil mass. A case where a four inch weak seam is present along the soil/bedrock interface is tested

as an example. Similar to the case of using slip elements to model disturbed areas around the pier, lowering the modulus of elasticity has a negligible effect on the factor of safety. Again, this is due to the thinness of the layer. Figure 6.20 shows the results of decreasing both the modulus of elasticity and the cohesion of the material in the weak seam. This reduction in cohesion will not affect the factor of safety calculations unless the most probable failure surface extends through this material.

For the case with no pier, the weak seam is not a factor until its cohesion is less than one fourth that of the soil in the slope. Above this value, the most probable failure surface does not extend into the weak material. Even at a cohesion of one fourth that of the soil, the failure surface only extends a short distance in the weak material, causing only a small decrease in the factor of safety. Some of the decrease in the factor of safety is offset by the fact that the rest of the failure surface must follow a path which is kinematically more difficult than the path which would have been followed if no weak seam had been present.

The results are similar for the case of stabilizing piers added to the slope. Again, it is only when a cohesion reduction factor of four is used that the failure surface even extends into the weak seam. Even in this

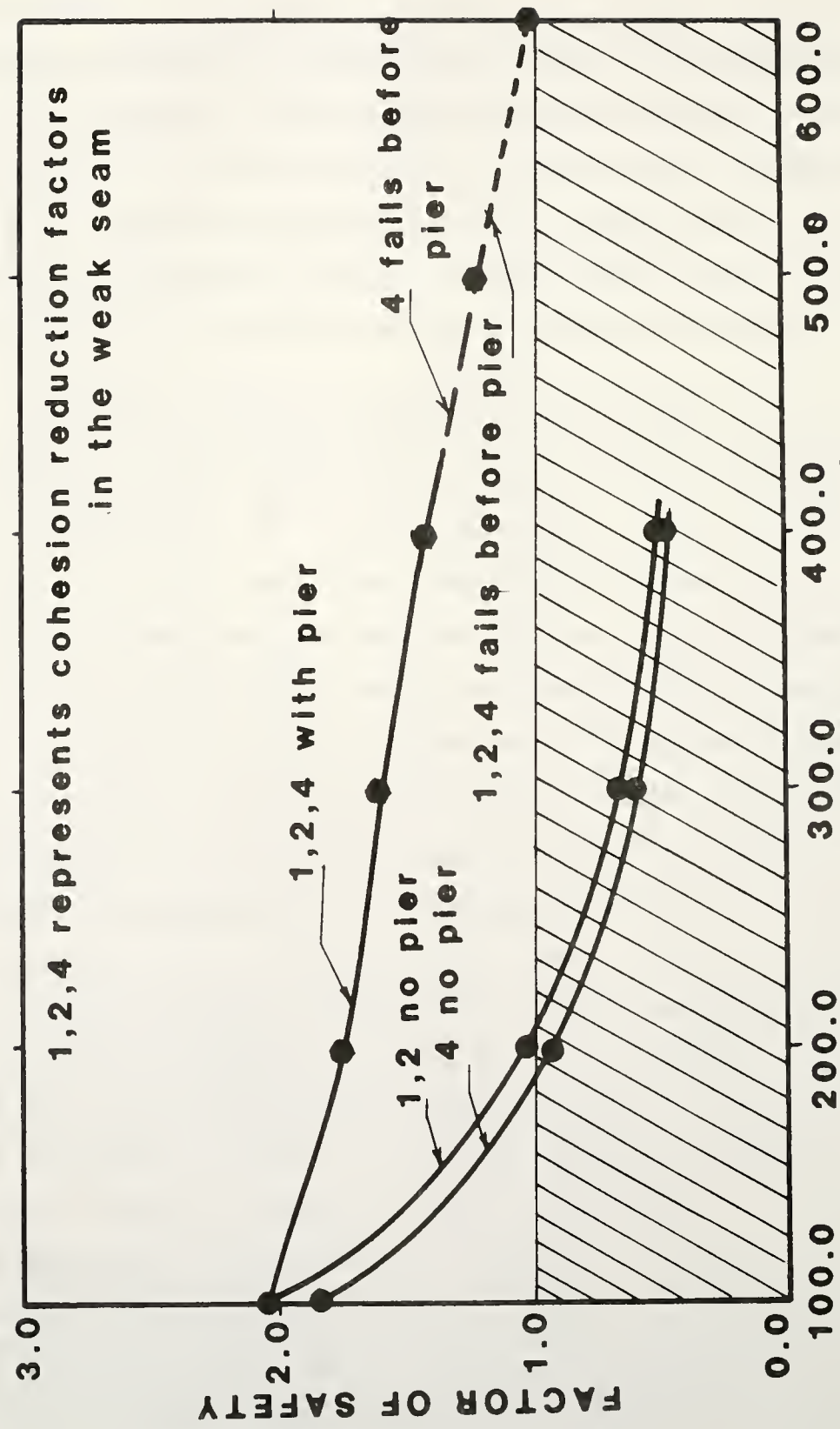

Figure 6.20: Factor of Safety as a Function of Cohesion Reduction Factor in the Weak Seam and Self Weight

case the reduction in the factor of safety is negligible. However, similar to the case of foundation depth, only failures initiating at the toe have been considered and deeper surfaces initiating before the toe may have a more profound effect.

Some effect on the variation of the cohesion reduction factor used is noticeable in the transition point between deep and shallow failures. When using a modulus reduction factor of four in the weak seam, the transition from a deep seated slide to a shallow slide is at a load of 430 pcf. These results are consistent with those from the effect of the hyperbolic soil model. The use of the hyperbolic model reduced the modulus of elasticity with depth which also allowed the transition to occur at a lower load.

Loading Variables

Surcharge at the crest of the slope was the main loading condition in the study by Oakland and Chameau (1982). One of the primary conclusions was that the piers should be placed as close as possible to the loading. This indicates placing them at the crest of the slope. This enables the piers to absorb the load before it is transmitted through the slope.

The case of self-weight loading, studied in this chapter, does not have the benefit of a finite loading area. In this case, it is not merely a matter of providing a barrier. The piers also act to absorb a substantial percentage of the additional vertical load. In this case there is a trade-off between the security against a shallow slide and a deep seated slide.

The application of a self loading scheme is to study the overall stability of cohesive slopes. Since there is a direct correlation between the conventional factor of safety and the security of an unreinforced slope under this loading condition, it is likely that a similar correlation exists for the reinforced slopes. The use of self weight also yields a generic case under which the effect of the piers can be studied. It is assumed that many of the principles displayed under these conditions will also be present (perhaps in a more subtle manner) for other loading conditions.

While parametric studies were not conducted in the case of an excavated or cut slope, a detailed example was presented in Chapter 5. This is a combination of the two previous cases. The loading is finite and restricted to the surface of the final slope, but, for cases where the pier is not at the crest, the load will be present on both sides of the pier so that a single optimum position may

not be possible. Similar to the case of self weight, a trade off between security, displacement control and potential failure size is present.

Summary

While only a limited number of examples were feasible to support this portion of the study and many of the variables could not be tested directly, conclusions on the stabilizing effect on the slope of the drilled piers are possible. These basic relationships are given in the following chapter. Using these general cases as a foundation to build upon, it is now possible to pursue the behavior of slopes under this complex boundary conditions on an individual level using specific slope geometries, soil parameters and loading conditions. Comparisons between to model and actual situations must be made to confirm these findings.

Guildlines for the Use of Drilled Piers

In general, under these generic conditions of self weight loading, the stability increases with increasing pier size and stiffness and decreasing pier spacing. The effect of pier position is complicated by a changing failure mode. Piers near the crest largely support vertical

loads, reducing the driving forces in the slope and guarding against deep seated slides. However, piers at this position may not adequately protect against shallow slides exiting before the pier row. Piers lower in the slope must sustain larger lateral loads, increasing the shearing resistance, and while providing better overall protection by preventing the less hazardous shallow slides, only marginally improve the stability against deep seated slides.

The performance of the piers in improving the slope stability is unconditionally favorable in frictionless materials. Both vertical and lateral support of the piers add to the stability. Caution is necessary when using the piers in materials containing a frictional component. While the lateral support improves the stability, vertical support may reduce the confining pressure along potential failure surfaces and reduce the resisting strength in the slope. Piers in these materials must be used lower in the slope the avoid possible lowering the stability.

CHAPTER 7: SUMMARY, CONCLUSIONS AND RECOMMENDATIONS

Summary of Work

The work accomplished in this study can be divided into two parts: modelling developments and typical analyzes. The modelling was accomplished through the development of the three dimensional finite element program "SPILES". Analysis of the stability of slopes with and without piers was performed by adapting a limiting equilibrium routine utilizing finite element stresses. A number of cases were tested to show the potential of the technique and help improve the understanding of the interaction between the piers and the slope.

Modelling Developments

The models of the slopes were created by mesh generators developed for this project. The generators are very specific to reduce the number of input parameters. However, by using several different generators, a wide variety of practical problems can be simulated. The generators utilize three dimensional isometric graphics for rapid visual inspection of the models.

The simulation of the slope's performance under loading was achieved through the three dimensional finite element program "SPILES". This program was specifically developed for this project to efficiently model static soil/structure interaction. The program develops a model for the relatively soft soil and stiff structure independently, balancing the forces and displacements transmitted between the two.

A three dimensional parallelepipedal block element with variable midside nodes has been developed following the approach outlined by Cook (1981) for the equivalent two dimensional element. The midside nodes offers the advantages of being able to model curved surfaces, to subdivide the mesh, and to provide better strain characteristics in critical areas. The advantage of using this variable node format instead of the conventional condensation of degrees of freedom is to minimize the matrix operations. The nodes which are not used are not carried though the calculations. For most elements, only the basic eight corner nodes are used reducing the matrix multiplications to build each element stiffness array by almost eight times.

A rotating, block by block, matrix solving routine has been developed for the program "SPILES". In typical block by block solving operations, 2 blocks must be held

in core at any given time. By rotating the lines in a block as it is being solved, only one block needs to be in core. To accomplish this, new lines are added to the top of the existing block, replacing already solved lines, instead of continuing downward into a new block.

The program incorporates an option to self establish the initial stress field in a generic manner. This generic manner is based entirely on the soil properties and gravity, it does not involve the history of the slope. This option is provided as an alternative if no other better information on the initial stresses is available. Initial stresses established by other means can be input into the model directly.

The program "SPILES" was developed as a practically oriented modelling tool. While able to model a wide variety of construction situations, the input necessary has been reduced to a minimum. The material stress-strain characteristics, which require the bulk of the parameters not self generated, can be obtained through standard testing procedures or correlations published in the literature.

The loading simulations have been simplified into three basic realms. The case of loading by increased self weight can be used to evaluate the general stability of a slope. The piers can be used as a corrective measure

against complete slope failure. Two other cases involve slope modification. The first is the case of a surcharge loading at the crest of the slope and the second is the case of an excavation, either from a horizontal ground surface or the steepening of a slope face. The piers in cases of slope modifications are installed as a retaining structure in advance of construction.

Finally, a post-processing limiting equilibrium program, "LOGFIND", was developed to convert the stress fields into a factor of safety. This program computes the ratio of soil strength to stress along potential circular or logspiral failure surfaces. A grid pattern of the circular or logspiral centers is used to form a searching routine to locate the most likely failure surfaces. The routine is also able to search for block type surfaces sliding along a weak seam in the soil profile.

The limiting equilibrium analysis program "LOGFIND" establishes a factor of safety similar to that obtained from commonly used slope stability programs. By utilizing the stress output from the finite element models, however, factors such as constitutive relations, construction sequences, and the effects of the drilled piers are included. A security factor can be established as a function of individual variables of the slope such as the unit weight of the soil, slope height, etc. The security is

defined as the allowable value of a variable (i.e. at a factor of safety of unity) divided by its normal value (i.e. working load). There are several advantages to defining the stability in this manner. First, this value has a linear relationship with the actual stability of the slope (i.e. a security of 4 indicates a slope twice as safe as a slope with a security of 2). Second, since a variability can be assigned to each of the variables used to establish securities, the securities can be used directly to estimate the stability in probabilistic terms. Third, the use of securities simplifies the analysis in complex situations, such as the use of piers to stabilize slopes, where the failure surface may have a complex shape as the soil shears around the piers. To assess the strength and stress fields over this complex surface would be difficult. By using the security, it only requires the load at which some critical surface fails. It can be assumed that the remainder of the complex surface has already failed. Even if it has not, the value remains conservative.

Typical Analyzes

Three general cases of drilled piers used to stabilize slopes have been explored. The case of added reinforcement for a slope which is to have a surcharge placed above its crest was studied by Oakland and Chameau (1984).

This paper was reviewed in this study. Drilled piers used to support an excavated slope and to confine a cut slope were used as specific examples in Chapter 5 of this study. Drilled piers used to support a slope under self weight was the subject of a parametric study in chapter 6.

There are several general conclusions concerning all three of these cases. The piers, even though not forming a continuous barrier, do effectively control lateral displacements and stress transfer. The arching action which occurs between the piers spans the clear spacing between the piers to act as a wall. The piers absorb induced soil stresses due to additional loading, transferring them directly to the more stable layers in the foundation. These stresses consist of lateral and vertical components. The ratio of these to components depends largely on the pier position and can have a great effect on the effectiveness of the piers. The piers also affect the induced stress patterns. The typical stress patterns in an unreinforced slope are circular in nature, conforming favorably to the formation of circular failure surfaces. The presence of the piers alters these pattern to a more random pattern. In order for a circular failure surface to form in this case, it would have to shear elements along planes other than the plane of maximum shear stress. More energy is required to form the latter surface.

Conclusions

A number of specific conclusions can be made from this study concerning the effect of drilled piers on the stabilization of slopes. These conclusions are drawn from three areas. First, several observations can be made from the limited number of case studies reviewed in the literature. Second, remarks can be made concerning the general behavior of the piers based on the numerical modelling of their use as stabilizing members. Finally, specific conclusions regarding the effect of the piers on the slope behavior can also be drawn from the analyzes performed in this study.

Observations From Case Studies

1) The piers are able to support small slopes with limited vertical relief very well, but they may not be able to develop adequate socketing strength to support large slides.

2) Although the piers work well as "dowels", pinning the failure surface and acting primarily as lateral supports, placing the piers near the top of the slope to support both vertical and lateral forces allows the piers to also utilize their greater axial capacity.

3) Pier top restraints, such as slab caps and tie-backs, can be used to ease the structural demands on the piers.

4) Large diameter piers seem to be able to control slope movement better than small diameter piers.

Forces on the piers

1) Socketing the piers provides additional stability improvement, but drastically increases the bending moments in the piers. As mentioned above, the addition of top restraints can alleviate some of these added stresses in the piers.

2) Increasing soil strength and stiffness with depth reduces the bending moments in the piers.

3) If the piers are placed near the upper boundary of the sliding mass, the lateral loads against the piers are reduced, however, the vertical loads absorbed by the piers are increased. While this can reduce the structural demands on the piers, the loss of additional confinement may reduce the overall security in frictional soils.

Effect of the Piers on the Slope

1) Drilled piers do improve the stability of cohesive slopes under a large number of conditions. Drilled piers must be used with caution when supporting slopes made of frictional materials. The vertical support which the piers provide may decrease the normal (confining) stress along potential failure surfaces below the pier.

2) With regard to pier variables, stability improves with:
   a) Decreased spacing,
   b) Increased diameter, and
   c) Increased pier stiffness (movements are controlled to a greater extent by this variable).

3) The stiffness of small diameter piers was found to be an extremely important variable in controlling movements by Rowe and Poulos (1979). They noticed that stability improved very little with stiffness. The present study found that the very high stiffnesses associated with large diameter piers in soft soils was not a significant factor.

4) The position of the drilled pier plays a large role in the stability. Piers towards the crest of the slope tend to absorb more vertical stresses and improve the stability against a deep seated slide. These piers do little to improve the stability against a shallow slide in front of the pier row. Piers closer to the toe of the slope absorb more horizontal loads while sharply decreasing the possibility of a shallow slide in front of the pier row and improve the deep seated stability only to a limited extent.

5) Piers are more effective in gentler slopes, at least for the cases studied, with the pier located halfway up the slope face.

6) The depth of the foundation level becomes an important factor in slopes reinforced by piers. The piers tend to redistribute the stress field over a larger area. Stress may be absorbed by the bedrock further stabilizing the slope.

7) The studies using nonlinear soil model show that the choice of the model may have a significant effect on the assessment of the overall stability of the reinforced slope. The differences between the linear and nonlinear cases were

not restricted to the magnitude of the displacement and stress fields, but have some effect on the mode of the failure. In the case tested, this involved the transition from a deep surface to a shallow one, then unexpectedly back to a deep surface as loading progressed.

8) The effect of a disturbed area around the piers was found negligible for the case studied.

9) A weak soil layer will have an effect on the shape and depth of the failure surface as well as the factor of safety only if it is within range of potential failure surfaces. The closer the weak seam is to the level of the failure surface for a case without weak seam, the greater its effect will be.

Relationship to Work by Hassiotis (1984)

The work done by Hassiotis (1984) determined the pressure distribution against the piers and used the resulting forces in a limiting equilibrium analysis of the slope. The strength of this approach is that the method used to determine the pressure distribution against the

piers has been developed exclusively for this purpose, based on elastic-plastic theory, and has been shown to give good results in model tests (Matsui, et al., 1982).

The finite element method provided two additional approaches to analyzing the problem of drilled piers used for slope stabilization. First, the displacement, stress and strain fields for the entire soil profile are represented. Second, the resulting stresses provide and alternate approach to finding the factor of safety in the slope. The primary concern is to find the stress distribution in the soil and observe how it is altered by the presence of the piers. A limiting equilibrium analysis is then made using these stresses to determine a factor of safety. This approach has inherent advantages over the approach taken by Hassiotis because the stress distribution in the soil is known. However, a disadvantage is that many assumptions must be made concerning the interaction between the piers and the soil. Assumptions, such as the gap forming behind the piers, the width and reduced modulus in the disturbed area around the pier, and the lack of vertical displacement of the piers, will influence the pressure distribution on the piers.

The approach used by Hassiotis (1984) and that of this study differ in their primary interest of concern. The approach of Hassiotis was dependent on the assessment

of the ultimate lateral load which the piers could carry, no concern was given to the changing stress distribution along the remainder of the failure surface. The approach used in this study was primarily concerned with the changing stress pattern in the soil (i.e. along the failure surface); it was assumed that the soil model will detect the yielding of the soil elements around the pier as the ultimate lateral load is reached. Each approach has strengths in the analysis of the problem of piers used to stabilize slopes.

The Hassiotis approach should be used to determine the following:

1) The lateral loads on the piers to be used for the structural design of the piers.

2) The factor of safety analysis of simple cases where piers are to primarily absorb lateral forces.

3) The parametric relations of pier size and spacing for specific cases of gentle slopes supported laterally. These factors are influenced by the lateral load on the piers.

The approach of the present should be used to determine the following:

1) The deformations, stresses and strains in the soil.

2) The slope factor of safety for cases where the piers strongly disrupt the soil stress distribution,

such as cases where vertical loads on the piers are significant, or cases involving construction sequences, or cases where an additional surface load is being applied.

3) The effect of the pier position in the slope and stiffness of the pier for specific cases. These factors are influenced by the absorption of the soil stress by the piers and by the pressure distributions which are created in the soil.

Recommendations for Further Work

Work which would be useful in continuing this study is comprised of confirmation and calibration of the work already established and expanding the model to explore new areas and include additional variables.

Some suggestions as to how the existing model could be verified include:

1) Scale model testing is needed to confirm the numerical models which have been created. The use of centrifugal modelling may be applicable to several aspects of this testing.

2) Monitoring of full scale construction using pressure transducers on the piers and slope inclinometers

in the soil are also needed to calibrate the numerical analyzes.

Physical testing, either through scale models or full scale construction, will best establish what revisions or improvements are needed in the existing model. Without this benefit, however, there are some points of the model which are worthy of further consideration.

1) More detailed distinction between the effect of the horizontal and vertical loads on the piers. During the development of the model little concern was initially given to the effect of the vertical support of the piers. During the analysis of the results, however the trend could only be explained by the changing modes of vertical and horizontal loading. Vertical degrees of freedom should be assigned to the piers to monitor vertical as well as lateral loading.

2) Throughout this project it has been assumed that the piers were firmly socketed into the bedrock to act as cantilevers. This may not be the case in some situations. Soft bedrock, poor construction, or high lateral loads may cause some rotation about the pier end. Free end rotation (no socketing) has

been shown to greatly reduce the capabilities of the piers (Poulos, et al., 1982; Hassiotis, 1984). The effect of a limited amount of rotation should also be explored. To accomplish this in the existing model either the foundation itself would need to be modelled or an elastic spring added to the base of the pier.

3) To duplicate the results of physical modelling, it may be necessary to implement a more complete soil model. A plasticity model would have the advantage of providing better estimates of the stress and displacement fields when loading is near failure. It may also be able to estimate pore pressures, and probably result in more accurate loads on the piers.

BIBLIOGRAPHY

BIBLIOGRAPHY

1. Andrews and Klasell (1964), "Cylinder Pile Retaining Wall," Highway Research Record, No. 56, Highway Research Board, pp. 83-97.

2. Bachus, R. C. and Barksdale, R. D. (1984), "Vertical and Lateral Behavior of Model Stone Columns," Proceeding, In Situ Soil and Rock Reinforcement, Paris, pp. 99-104.

3. Baguelin, F., Frank, R., and Guegaz, Y. (1976), "Calcul Sur Ordinateur Des Pieux Sollicites Horizontalement ou Subissant Des Poussees Parasites," Bulletin De Liaison Des Laboratoires des Ponts et Chaussees, No. 84, Juillet-Aout, pp. 113-120.

4. Barksdale, R. D. and Bachus, R. C. (1985), "Design and Construction of Stone Columns," Federal Highway Administration Report No. FHWA-RD-83-026, Georgia Institute of Technology, Atlanta, 194 pp.

5. Brown, C. B. and King, I. P. (1966), "Automatic Embankment Analysis: Equilibrium and Instability Conditions," Geotechnique, Vol. 16 No. 3, pp. 209-219.

6. Bulley, W. A. (1965), "Cylinder Pile Retaining Wall Construction - Seattle Freeway," Roads and Streets Conference, Seattle.

7. Chen, W. F., and Saleeb, A. F., (1982), Constitutive Equations for Engineering Materials, Vol. 1; Elasticity and Modeling, John Wiley and Sons, Inc., New York, 580 pp.

8. Clough, G. W. (1972), "Application of the Finite Element Method to Earth Structure Interaction," Proceedings, Application of the Finite Element Method in Geotechnical Engineering, Vicksburg, Vol. 3, pp. 1057-1116.

9. Clough, R. W., (1969), "Three Dimensional Finite Elements," Proceedings, ASCE Applications of the Finite Element Method in Civil Engineering, Nashville, pp. 1-20.

10. Clough, R. W. and Woodward, R. J. (1967), "Analysis of Embankment Stresses and Deformations," J. Soil Mech. Found. Div., ASCE, Vol. 93, No. SM4, July, pp. 529-550.

11. Cook, R. D., (1981), Concepts and Applications of Finite Elements Analysis, 2nd. ed., John Wiley and Sons, Inc., New York, 537 pp.

12. Christian, J. T., (1980), "Report on Working Group One," Proceedings of Workshop on Constitutive Modeling of Soils, McGill University, Montreal, Canada, May, pp. 93-101.

13. Dash U. and Jovino, P. L. (1980), "Root Piles at Monnesen Pen," Transportation Research Record, No. 749, Highway Research Board, pp 13-21.

14. De Paepe, R. and Wallays, M. (1984), "Stabilization of the Oudenberg Hill in Geraardsbergen," Proceedings, International Conference on Case Histories in Geotechnical Engineering, Edited by Shamsher Prakash, St. Louis, pp. 1345-1350.

15. Desai, C. S., (1968), "Solutions of Stress-Deformation Problems in Soil and Rock Mechanics Using the Finite Element Method," Ph.D. Dissertation, University of Texas, Austin, August, 266 pp.

16. Desai, C. S., (1971), "Nonlinear Analyses Using Spline Functions," J. Soil Mech. Found. Div., ASCE, Vol 97, No. SM10, October, pp. 1461-1479.

17. Desai, C. S., Eitani, I. M., and Haycocks, C. (1983), "An Application of Finite Element Procedure for Underground Structures with Nonlinear Materials and Joints," Proceedings, 5th. ISRM Congress, Melbourn, Aust, pp. 1-8.

18. Desai, C. S. and Lightner, J. G., (1985), "Mixed Finite Element Procedure for Soil-Structure Interaction and Construction Sequences," Intl. J. of Num. Methods in Eng., Vol. 21, No. 5, May, pp. 801-824.

19. Desai, C. S. and Sargard, S. (1984), "A Hybrid Finite Element Procedure for Soil-Structure Interaction," J. of Geotech. Eng. Div., ASCE, Vol. 110, No. 4, April 1984, pp. 473-486.

20. Desai, C. S., and Wu, T. H. (1976), "A General Function for Stress-Strain Curves," Proceedings, 2nd Intl. Conf. on Num. Methods in Geomechanics, Vol. 1, June, pp. 306-318.

21. Duncan, J. M. (1972), "Finite Element Analyses of Stress and Movements in Dams, Excavations and Slopes," Proceedings, Application of the Finite Element Method in Geotechnical Engineering, U.S. Army Eng. Waterways Experimentation Station, Vicksburg, MS, pp. 267-326.

22. Duncan, J.M. (1979), "Behavior and Design of Long-Span Metal Culverts," J. Geotech. Eng. Div., ASCE, Vol. 105, No. GT3, March, pp. 399-418.

23. Duncan, J. A. (1980), "Hyperbolic Stress-Strain Relationships," Proceedings of Workshop on Constitutive Modeling of Soils, McGill University, Montreal, Canada, May, pp. 443-460.

24. Duncan, J. M., and Chang, C. Y. (1970), "Nonlinear Analysis of Stress and Strain in Soils," J. of Soil Mech. Found. Div., ASCE, Vol. 96, No. SM5, p. 1629-1653.

25. Duncan, J. M., Byrne, P., Wong, K. S., and Mabry, P. (1978), "Strength, Stress-Strain and Bulk Modulus Parameters for Finite Element Analyses of Stresses and Movements in Soil Masses," Report No. UCB-GT-78-02, University of California, Berkeley, April, 70 pp.

26. Duncan, J. M. , and Dunlop, P. (1969), "Slopes in Stiff-figured Clays and Shales", J. of Soil Mech. Found. Div., ASCE, Vol. 95, No. SM2, March, pp. 467-492.

27. Dunlop, P. and Duncan, J. M. (1970), "Development of Failure Around Excavated Slopes," J. of Soil Mech. Found. Div., ASCE, Vol. 96, No. SM2, March, pp. 471-493.

28. Eisenstein, Z., and Krishnaya, A. U. G., and Morgenstern, N. R. (1972), "Analysis of Cracking at Duncan Dam," Proceedings, ASCE Conference on Performance of Earth Supported Structures, Purdue University, pp. 765-778.

29. Eringen, A. C. (1962), Nonlinear Theory of Continuous Media, McGraw-Hill Book Co., Inc., New York, 477 pp.

30. Evans, R. J., and Pister, K. S. (1966), "Constitutive Equations for a Class of Nonlinear Elastic Solids," Intl. J. of Solids and Structures, Vol. 2, No. 3, pp. 427-445.

31. Finn, L. W. D. (1980), "Evaluation of Critical State and Hyperbolic Stress-Strain Models: Working Croup Three," Proceedings of Workshop on Constitutive Modelling of Soils, McGill University, Montreal, Canada, May, pp. 132-150.

32. Feng, Y. C. (1965), Foundations of Solid Mechanics, Prentice-Hall, Inc., Englewood Cliffs, N.J., 525 pp.

33. Green, A. E., and Zerna, W. (1954), Theoretical Elasticity, Clarendon Press, Oxford, 442 pp.

34. Girijavallabhan, C. V. G., and Reese, L. C. (1968), "Finite Element Method Applied to Some Problem in Soil Mechanics," J. Soil Mech. Found. Div., ASCE, Vol. 94, No. SM2, March, pp. 473-496.

35. Goughnour and DiMaggio (1978), "Soil Reinforcement Methods on Highway Projects," Proceedings, Symposium on Earth Reinforcement, American Society of Civil Engineers Annual Convention, Pittsburgh, Pennsylvania, April, pp. 371-399.

36. Gould, J. D. (1970), "Lateral Pressures on Rigid Permanent Structures," Proceedings, Conference on Lateral Stresses in the Ground and Design of Earth Retaining Structures, Cornell University Press, Ithaca, pp. 219-269.

37. Gudehus, G. and Schwaz, W. (1985), "Stabilization of Creeping Slopes by Dowels," Proceedings of Conference on Soil Mechanics, San Franciso, pp. 1697-1700.

38. Hardin, B. O. (1970), "Constitutive Relations for Air Field Subgrade and Base Course Materials," Technical Report UKY 32-71-CE5, University of Kentucky.

39. Hardin, B. O., and Drnevich, V. P. (1972) "Shear Modulus and Damping in Soils: Measurement and Parameter Effect," J. Soil Mech. Found. Div., ASCE, Vol. 98, No. SM6, June, pp. 603-624.

40. Hassiotis (1984), "Stabilization of Slopes Using Piles," MSCE Thesis and Joint Highway Research Project No. JHRP-84-8, Purdue University, West Lafayette, Indiana, 181 pp.

41. Hellen, T. K. (1972), "Effective Quadrature Rules for Quadratic Solid Isoparametric Finite Elements," Intl. J. on Num. Method Eng., Vol. 4, No. 4, pp. 597-600.

42. Idriss, I. M., Dobry, R., and Singh, R. D. (1978), "Nonlinear Behavior of Soft Clays During Cyclic Loading," J. of Geotech. Div., ASCE, Vol. 104, No. GT12, December. pp. 1427-1447.

43. Irons, B. M. (1971), "Quadratic Rules for Brick Based Finite Elements," Short Communication, Intl. J. on Num. Method Eng., Vol. 3, No. 2, pp. 293-294.

44. Ito, T. and Matsui, T. (1975), "Discussion: Methods to Estimate Lateral Force Acting on Stabilizing Piles," Soils and Foundations, JMSSFE, Vol. 19, No. 4, April, pp. 43-57.

45. Jennings, P. C. (1964), "Periodic Response of a General Yielding Structure," J. Eng. Mech., ASCE, Vol. 90, No. EM2, April, pp. 131-166.

46. Kavazanjian, E., Jr., and Hadj-Hamou, T. (1980), "Determination of Dynamic Material Properties of Soils from the Results of Static Shear Tests," N.S.F. Earthquake Hazard Mitigation Program, Report No. 45, June, 36 pp.

47. Katona, M. G., Smith, J. M., Odello, R. S., and Allgood, J. R. (1976). "CANDE - A Modern Approach for Structural Design and Analysis of Buried Culverts," Report No. FHWA-RD-77-5, Naval Civil Engineering Laboratory, October, 470 pp.

48. Ko, H. -Y., and Masson, R. M. (1976), "Nonlinear Characterization and Analysis of Sand," Proceedings, 2nd Interbational Conference on Numerical Methods in Geomechanics, Vol. 1, June, pp. 294-305.

49. Kulhawy, F. H., Duncan, J. M., and Seed, H. B. (1969), "Finite Element Analysis of Stresses and Movements in Embankments During Construction," Report No. TE-69-4, University of California, Berkeley, 169 pp.

50. Kulhawy, F, and Duncan, J. M. (1972), "Stresses and Movements in Oroville Dam," J. of Soil Mech. Found. Div., ASCE, Vol. 98, No. SM7, July, pp. 653-665.

51. Leadbeater, A. D. (1985), "A57 Snake Pass Remedial Work to Slip Near Alport Bridge," Proceedings of Failures in Earthworks, London, March, pp. 26-38.

52. Lefebure, G., Duncan, J. M., and Wilson, E. L. (1973), Three Dimensional Finite Element Analysis of Dams," J. of Soil Mech. Found. Div., ASCE, Vol. 99, No. SM7, July, pp. 495-507.

53. Leonards, G. A., editor (1962), Foundation Engineering, McGraw-Hill Book Company, New York, 1136 pp.

54. Leonards, G. A., Wu, T. -H., and Juang, C. -H. (1982), "Predicting Performance of Buried Conduits," Joint Highway Research Project No. 81-3, Purdue University, West Lafayette, June, 213 pp.

55. Malvern, L. E. (1969), Introduction to Mechanics of a Continuous Medium, Prentice-Hall, Inc., Englewood Cliffs, N.J., 713 pp.

56. Mathis, H. (1981), "Temporary Landslide Corrective Techniques Avert Catastrophe," Proceedings of 32nd Annual Highway Geology Symposium, Gatlinburg, May, 1981, pp. 59-78.

57. Matsui, T., Hong, W. P., and Ito, T. (1982), "Earth Pressures on Piles in a Tow Due to Laterial Soil Movement," Soil and Foundations, JSSMFE, Vol. 22, No. 2, June, pp. 71-81.

58. Merriam, R. (1960), "Portuguese Bend Landslide, Palos Verdes Hills, California," Journal of Geology, Vol. 68, No. 2, March, pp. 140-153.

59. Meyers, V. J. (1981), Matrix Analysis of Structures, Harper and Row, New York, 497 pp.

60. Mizuno, E. and Chen, W. F. (1982), "Plasticity Analysis of Slope With Different Flow Rules," Structural Engineering Technical Report, No. CE-STR-82-3, Purdue University, West Lafayette, IN, 44 pp.

61. Muskhelishvili, N. J. (1963), Some Basic Problems of the Mathematical Theory of Elasticity, P. Nordoff, Ldt., Groningen, The Netherlands, 718 pp.

62. Naylor, D. J., Pande, G. N., Simpson, B., and Tabb, B. (1981), Finite Elements in Geotechnical Engineering, Pineridge Press, Swansea, U. K., 245 pp.

63. Oakland, M. W. and Chameau, J. A. (1984), "Finite-Element Analysis of Drilled Piers Used for Slope Stabilization," Laterally Loaded Deep Foundations: Analysis and Performance, ASTM Special Technical Publication No. 835, Kansas City, Mo., June, pp. 182-193.

64. Offenberger (1981), "Hillside Stabilization With Concrete Cylinder Pile Pile Retaining Wall," Public Works, September, pp. 82-86.

65. Ozawa, Y., and Duncan, J. M. (1976), "Elasto-Plastic Finite Element Analysis of Sand Deformations," Proceedings, 2nd Intl. Conf. on Numerical Methods in Geomechanics, Vol. 1, June, pp. 243-263.

66. Penman, A. D. M., Burland, J. B., and Charles, J. A. (1971), "Observed and Predicted Deformations in a Large Embankment Dam During Construction," Proceedings, I.C.E., Vol. 49, pp. 1-21.

67. Perloff, W. H., Baladi, G. K., and Harr, M. E. (1967), "Stress Distribution Within and Under Long Elastic Embankments," Highway Research Record, No. 181, Highway Research Board, pp. 12-40.

68. Poulos, H. G. (1973), "Analysis of Piles in Soil Undergoing Lateral Movement," J. of Soil Mech. and Found. Div., ASCE, Vol. 99, SM5, May, pp. 391-406.

69. Ramberg, W., and Osgood, W. R. (1943), "Description of Stress-Strain Curves by Three Parameters," Technical Note No. 902, National Advisory Committee for Aeronautics, Washington, D.C., 13 pp.

70. Richard, R. M. (1961), "A Study of Structural Systems Having Conservative Nonlinear Elements," Ph.D. Dissertation, Purdue University, West Lafayette, In., 78 pp.

71. Richard, R. M., and Abbott, B. J. (1975), "Versatile Elastic-Plastic Stress-Strain Formula," Technical Note, J. of Eng. Mech. Div., ASCE, Vol. 101, No. EM4, August, pp. 511-515.

72. Rowe, R. K. and Poulos, H. G. (1979), "A Method For Predicting the Effect of Piles on Slope Behavior," Proceedings, 3rd International Conference on Numerical Methods in Geomechanics, Vol 3, Aachen, April, pp. 1073-1085.

73. Saleeb, A. F., and Chen, W. F. (1980^1), "Nonlinear Hyperelastic (Green) Constitutive Models for Soils: Theory and Calibration," Proceedings of Workshop on Constitutive Modeling of Soils, McGill University, Montreal, Canada, May, pp. 492-538.

74. Saleeb, A. F., and Chen, W. F. (1980^2), "Nonlinear Hyperelastic (Green) Constitutive Models for Soils: Prediction and Comparison," Proceedings of Workshop on Constitutive Modeling of Soils, McGill University, Montreal, Canada, May, pp. 265-285.

75. Seigel, R. A. (1975), "Computer Analysis of General Slope Stability Problems," MSCE Thesis, Purdue University, West Lafayette, Indiana, 112 pp.

76. Silvestri, V. and Tabib, C. (1983^1), "Exact Determination of Gravity Stresses in Finite Elastic Slopes: Part I, Theoretical Considerations," Canadian Geotech Journal, Vol. 20, pp. 47-54.

77. Silvestri, V. and Tabib, C. (1983^2), "Exact Determination of Gravity Stresses in Finite Elastic Slopes: Part II," Applications," Canadian Geotech Journal, Vol. 20, pp. 55-60.

78. Singh, K. J., and Sandler, R. S. (1975), "A Computer Program for Finite Element Analysis of Nonlinear Elastic Incremental Soil System," Geotechnical Engineering Report, No. 2, Ohio State University, November.

79. Smith, I. M. (1982), Programming the Finite Element Method With Applications to Geomechanics, John Wiley and Sons, Chichester, 351 pp.

80. Smith, I. M., and Boorman, R. (1973), "The Analysis of Flexible Bulkheads in Sand," Proceedings, I.C.E., London, Vol. 57, pp. 413-436.

81. Snitbhan, N. and Chen, W. F. (1976), "Finite Element Analysis of Large Deformation in Slopes," Proceedings, A.S.C.E. Conference on Numerical Method in Geomech., Edited by C. S. Desai, Virginia Polytechnic Institute, pp. 744-756.

82. Snitbhan, N. and Chen, W. F. (1978), "Elastic-Plastic Large Deformation Analysis of Soil Slopes," Computers and Structures, Vol. 9, No. 4, April, pp. 567-577.

83. Taniguchi, T. (1967), "Landslides in Reservoirs," Proceedings of the 3rd Asian Regional Conference on Soil Mechanics and Foundation Engineering, Vol. 1, Southeast Asian Society of Soil Engineering, Bankok, Thailand, pp. 258-261.

84. Tesarik,D. R. and McWilliams, P. C. (1981), "Factor of Safety Charts for Estimating the Stability of Saturated and Unsaturated Tailings Pond Embankments," Bureau of Mines Report of Investigations, No. 8564, U. S. Department of the Interior, 74 pp.

85. Truesdell, C. (1955), "Hypoelasticity," J. Rational Mech. and Analysis, Vol. 4, No. 1, pp. 83-133.

86. Wilson, E. L. (1963), "Finite Analysis of Two Dimensional Structures," Report No. 63-2, Structures and Materials Research, Department of Civil Engineering, University of California, Berkeley, June.

87. Winter, H., Schwarz, W., Gudehus, G. (1983), "Stabilization of Clay Slopes by Piles," Proceedings, 8th European Conference on Soil Mechanics and Foundation Engineering, Vol. 2, Helsinki, May pp. 545-551.

88. Wong, F. S. (1984), "Uncertainties in F.E. Modeling of Slope Stability," Computers and Structures, Vol. 19, No. 56, pp. 777-791.

89. Wong, K. S. and Duncan J. M. (1974), "Hyperbolic Stress Strain Parameters for Nonlinear Finite Element Analysis of Streses and Movements in Soil Masses," Report No. TE-743, Berkeley, Ca., 90 pp.

90. Wright, S. G. (1974), "SSTAB1-A General Computer Program for Slope Stability Analyses," Research Report No. GE-74-1, Department of Civil Engineering, University of Texas, Austin, Texas.

91. Zienkiewicz, O. C. (1977), The Finite Elements Method, 3rd. Ed., McGraw-Hill Book Company (UK) Limited, London, 787 pp.

APPENDIX

Appendix: Stabilization of Surcharge Loading on Slopes

(Edited version of Oakland and Chameau (1984))

Introduction

During the past two decades innovative soil reinforcement techniques such as reinforced earth, stone column, soil anchors and cast-in-place piles and piers have been developed to answer many geotechnical problems. In particular these techniques can provide cost-effective solutions to many transportation design and construction problems. Laterally loaded piles and drilled piers have been used in several occasions to stabilize landslides and slopes. In Sweden timber piles are used to increase the slope stability of very soft clays (figure A.1a). Large diameter cast-in-place reinforced concrete piles have been used in the United States to stabilize active landslide areas in stiff clays and shales through dowel action (Merriam, 1960; Andrews and Klasell, 1964; Bulley, 1965; Gould, 1970; Offenberger, 1981). The diameter of the piles varied between 1.0 and 1.5 meters (figure A.1b) In Japan 300 mm diameter steel pipes have been used for the same purpose (Taniguchi, 1967). Other techniques, such as the Fondedile Reticulated Root Pile method (figure A.1c)

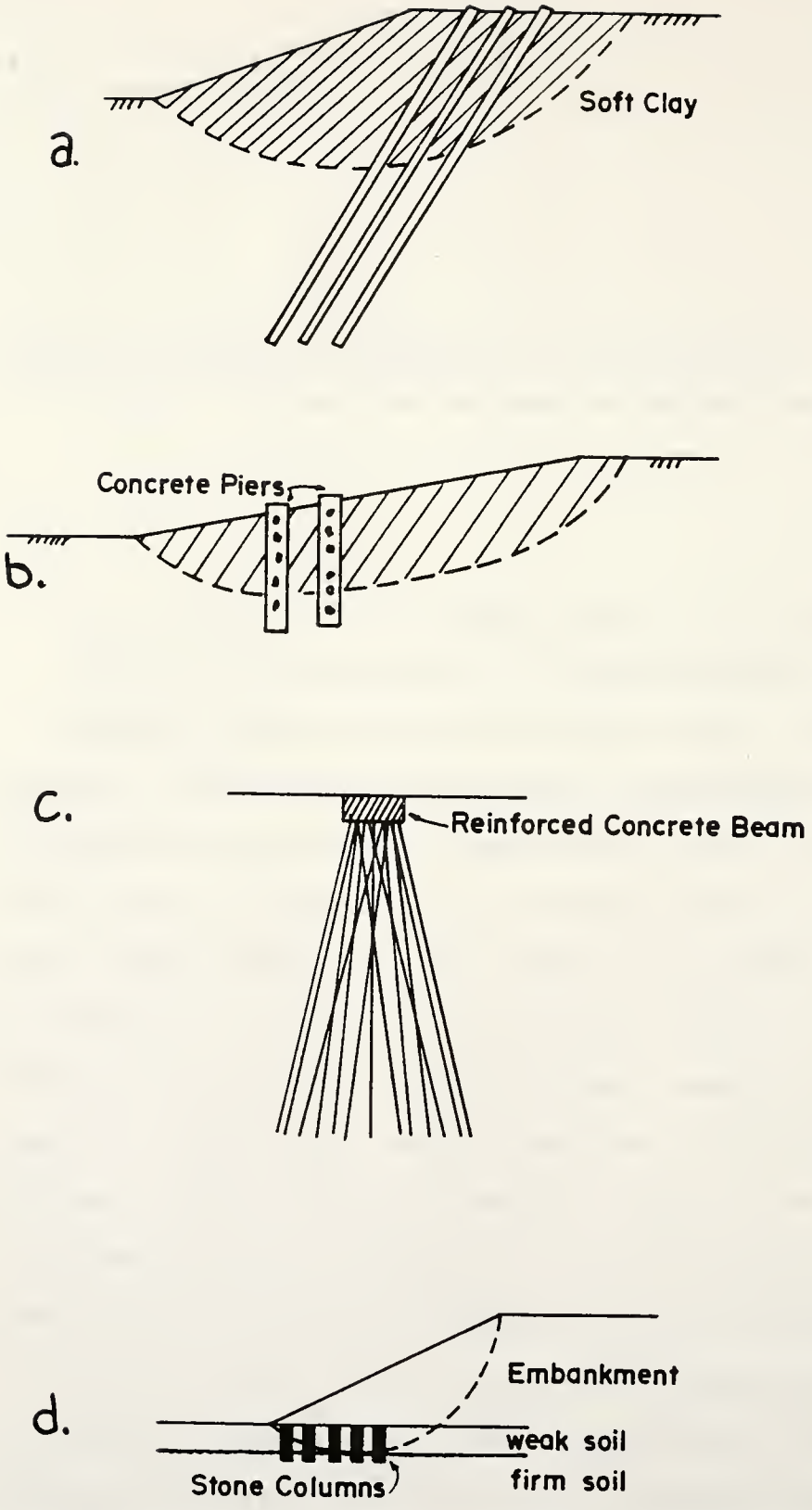

Figure A.1: Piles and Piers Used to Stabilize Slopes
a) Timber Piles
b) Concrete Piers
c) Reticulated Structure
d) Stone Columns

and stone columns (figure A.1d), although relatively new within the United States, have been proven to be quite effective techniques in Europe for a number of years (Goughnour and DiMaggio, 1978).

There are two major problems involved in the design of piers and piles used to correct and stabilize slopes. The first is to determine the load distribution along the axis of the pier in order to assess the shear forces and bending moments the pier has to restrain. The second is to evaluate the overall stability of the corrected slope. In this paper existing design methodologies are reviewed and a finite element based technique is proposed to analyze slopes stabilized with drilled piers.

Design Methodologies

Although the use of these reinforcing techniques is becoming more and more common, very little information is currently available regarding the pier and pile behavior under lateral loading induced by the movement of the surrounding soil. While literature is available for piles subjected to lateral loading (Broms, 1972; Davisson, 1970; Davisson and Gill, 1963; Reese and Cox, 1975; Poulos, 1971), most of it dealt with lateral loading imposed by a supported structure. Computer programs are currently available to assess the stability of drilled piers under such loads (Reese and Allen, 1977). The lateral loads

developed on a pier by a soil mass undergoing lateral movement are different from externally applied external loads from a structure. The major difficulties and differences are related to the location and distribution of the loading (lateral loads induced by the soil are nonuniform and distributed along the axis of the pier) and to the boundary conditions (head and tip restraints).

Thus, the problem of piles and piers subject to a soil induced lateral loading is unique and at present has not received particular attention and treatment. Several investigators have studied the problem of a single pile subjected to lateral soil movement, given certain simplifying assumptions with regard to the soil modes, soil-pile interface and repartition of the lateral loads (DeBeer and Wallays, 1972; Ito and Matsui, 1975; Ito et al, 1979 and 1981; Poulos, 1973; and Poulos and Davis, 1980). As an example, the model proposed by Poulos (1973) uses a finite difference technique to compute the displacements, shear forces and bending moments in a pile, assuming the soil to be elastic-plastic, no shear between pile and soil, and the distribution of horizontal movement with depth known from inclinometer data. Ito and Matsui (1975) derived a theoretical equation to determine the lateral force acting on piles used to stabilize soil movements. This is done by discretizing the soil into layers and assuming a Mohr-Coulomb plastic condition in the soil surrounding the

piles. Various end conditions can be considered for the pier tip and top. The computed values of lateral loads compared well with measured values. Later papers by Ito, et al. (1979, 1981) considered specific examples where these piles could be used.

The determination of the shear forces and bending moments along the axis of the pier is only the first aspect of the design of drilled-in piers used to increase slope stability. A second aspect is to make an estimate of the influence of piles or piers on the factor of safety against slope failure. A simplified procedure has been recently proposed to determine the additional resisting moment caused by the pile (Poulos and Davis, 1980). The added resistance is generated by the lower portion of the pile below the critical failure surface and can be assessed once the pile-soil pressure distribution has been discussed by Rowe and Poulos (1979), who have employed the technique for analyzing soil-structure interaction described by Rowe et al. (1978). The effect of piers upon slope deformation and stability is also a function of pier arrangement, pier stiffness and restrain condition as well as soil stiffness and strength.

Three-Dimensional Model

A finite element analysis of the stabilization of a slope should make allowance for soil-pier interaction and

three-dimensional effects such as arching between piers. The piers do not form a continuous barrier and soil movement occurs around the piers in the direction parallel to the slope (figure A.2). A three-dimensional finite element model can adequately model the geometry of the problems and the effects of piers position, size, spacing and stiffness on the amount of soil movement and on the stability of the slope.

Lines of symmetry exist in a slope containing a row of piers (figure A.2). Through the centerline of each pier and perpendicular to the slope is a line where the soil will not move parallel to the slope. A similar line exists at the midpoint between piers. The size of the model is drastically reduced by considering only the part of the slope between two of these lines. It is then assumed that the rest of the slope is a repetition of this part.

Currently, the program uses 8 node, 24 degrees of freedom, isoparametric parallelepipeds to model the soil (figure A.3a). These elements are among the simplest three-dimensional elements available, modeling geometry and displacements as linear functions. They are widely used in soil mechanics because the rectangular shape adapts itself well to typical slope and foundation problems (Desai and Christian, 1977). Although higher order

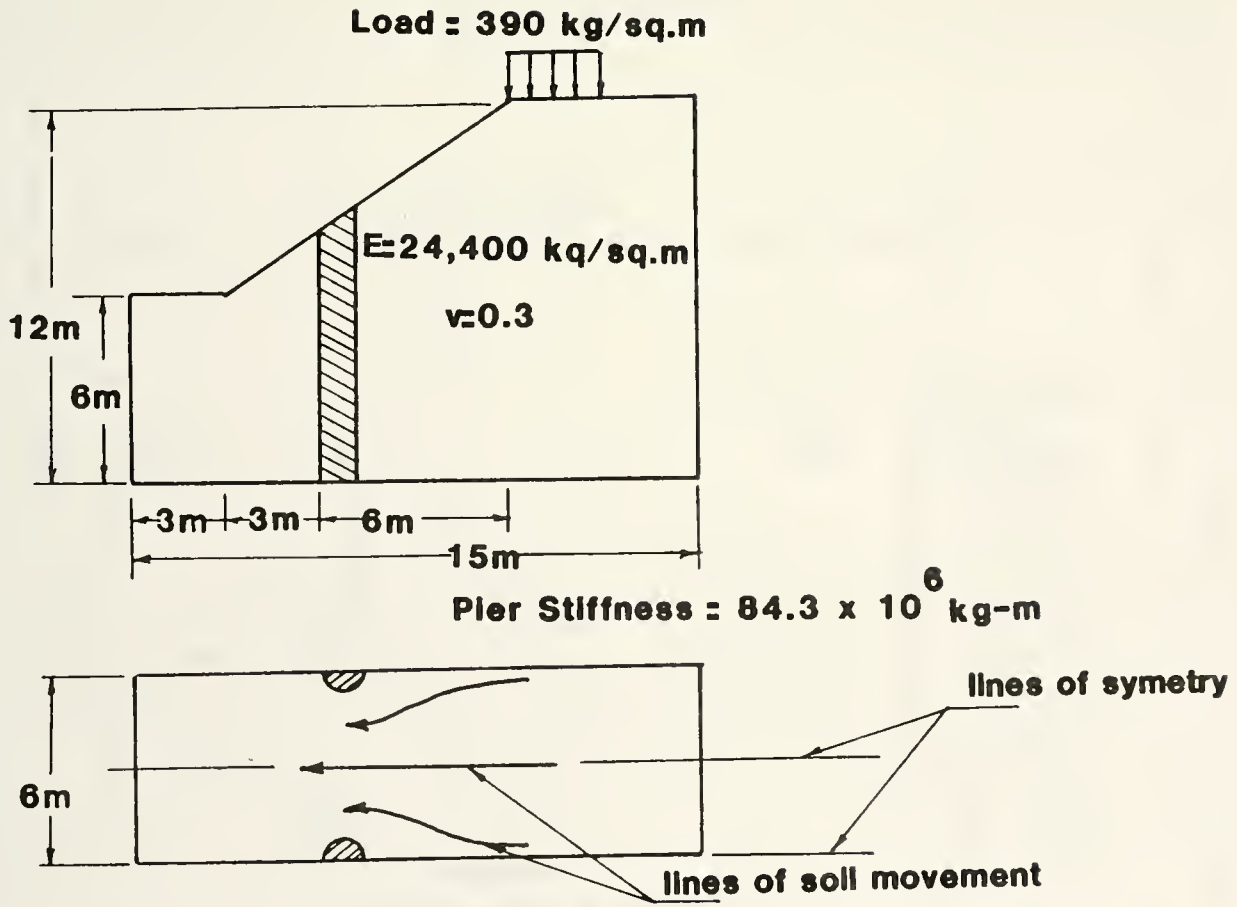

Figure A.2: General Problem

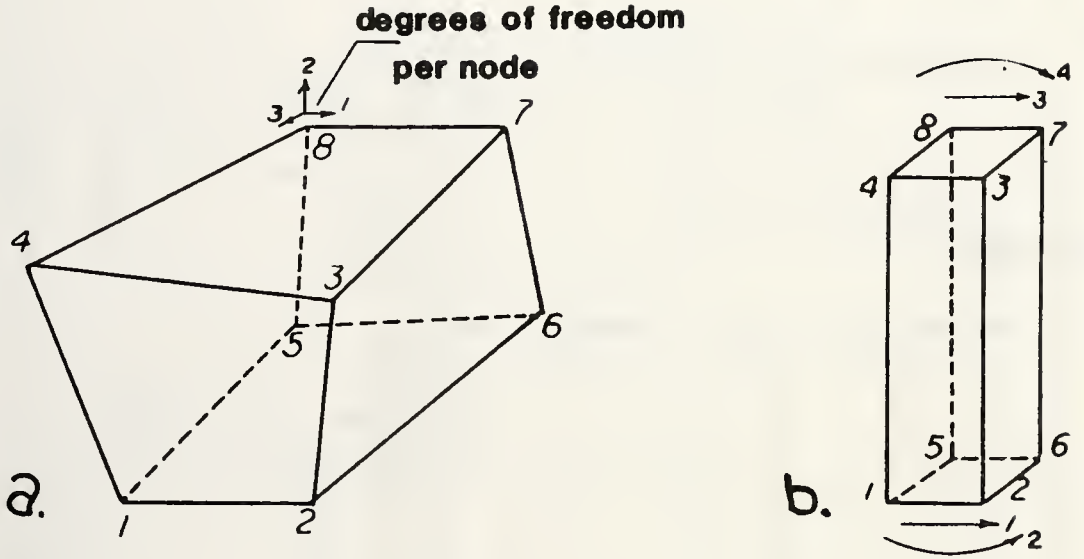

Figure A.3: Three Dimensional Finite Elements
a) Soil Element
b) Pier Element

elements provide a better model, the number of degrees of freedom increases so rapidly that computer space is often a problem. The pier is modeled by 8 node, 4 degree of freedom parallelepiped spar or bending elements (figure A.3b). The 8 node spar elements were chosen to be compatible with the 8 node soil element and to reduce the amount of computer space needed. The 24 degrees of freedom in the soil elements represent displacements in three dimensions at each corner. The 4 degrees of freedom in the pier elements represent displacements and rotations at the ends of the element in the direction perpendicular to the slope. It is assumed that the piers are incompressible and will not bend in any other direction. This assumption is not restrictive because of the high ratio of pier to soil moduli.

The boundaries of the problem are the two lines of symmetry which allow soil movement only in the direction perpendicular to the slope and an underlying rock layer which does not allow slip. The finite element mesh is assumed long enough in the direction perpendicular to the slope so that the end boundaries can be considered fixed. To simulate the piers being socketted in sedimentary bedrock, the tip of the pier is also fixed against displacement and rotation.

Three options are available in the program for the soil model: (1) linear elastic; (2) hyperbolic Duncan and Chang model (1970) with nonlinear modulus; and (3) Duncan and Chang model with both nonlinear modulus and Poisson`s ratio. The loads are applied in several increments, and an iteration technique is used within each increment to estimate the pier displacement. The basic operations of the program are:

1) Calculate principal soil stresses

2) Calculate soil parameters (hyperbolic model)

3) Apply a load increment with the piers held perfectly rigid

4) Generate the soil stiffness matrix and solve for the soil displacements

5) Determine loads on the rigid pier

6) Generate the pier stiffness matrix and compute the displacements of the pier

7) Iterate between pier displacements and soil nodal loads until convergence

8) Next cycle of loading (repeat 1 to 7)

The program is a conventional finite element program except for the interaction between pier and soil elements. There is a compatibility problem between the sides of the

soil elements which can only displace linearly and the pier elements which have cubic displacement functions. To circumvent this problem the soil and pier elements are treated separately. Since all of the transformations between the pier and soil are through the nodes, overlapping or separation of the two meshes will not affect the results. The stresses in the soil due to a loading increment are transformed into equivalent nodal loads. These nodal loads are then applied to the pier as if it were a cantilever beam in space. The resulting nodal displacements can be related to nodal forces and reapplied to the soil nodes. An iterative technique is necessary to assure compatibility of stresses between the soil and the pier. The rate of convergence of the iterative process is a function of the initial estimate of the pier displacements. If the difference between this estimate and the sought solution is too large, the forces on each side of the pier may be excessively unbalanced and result in large deflections causing adjacent soil elements to act in tension. Under these conditions tension and compression will act on opposite sides of the pier and the pier displacements will keep increasing. An initial estimate of about one third of the unreinforced slope displacements at the location of the pier has been found to achieve convergence.

Preliminary Results

The three-dimensional computer program described in the previous section is part of an on-going research project on the design of laterally loaded drilled-in-piers for landslide corrections. In its present state the program has a lot of deficiencies (to be discussed in a subsequent section) but can nevertheless be used to qualitatively assess the effect of drilled piers on slope movement and help give direction for further developments. As an example, the slope shown in figure A.2 was analyzed with the three-dimensional program for a uniform surcharge applied at the top of the slope. The horizontal and vertical movements induced by this loading condition in a typical cross-section of the non-stabilized slope (without piers) are shown in figure A.4. (Note the different scales for geometry and displacement in this figure.) The effectiveness of the piers will be based on reduction of this movement. Rectangular piers (.90 m x 1.80 m) with a center to center spacing of 6.0 m are installed at 3.0 m from the toe of the slope (figure A.2). The displacements along the cross-section at the centerline between the piers are given in figure A.4. Below the pier (with respect to the slope), the reduction in slope movement is very significant, ranging from 60 to 100 percent with an average reduction of about 70 percent. Above the pier the reduction is less but still significant, especially in the

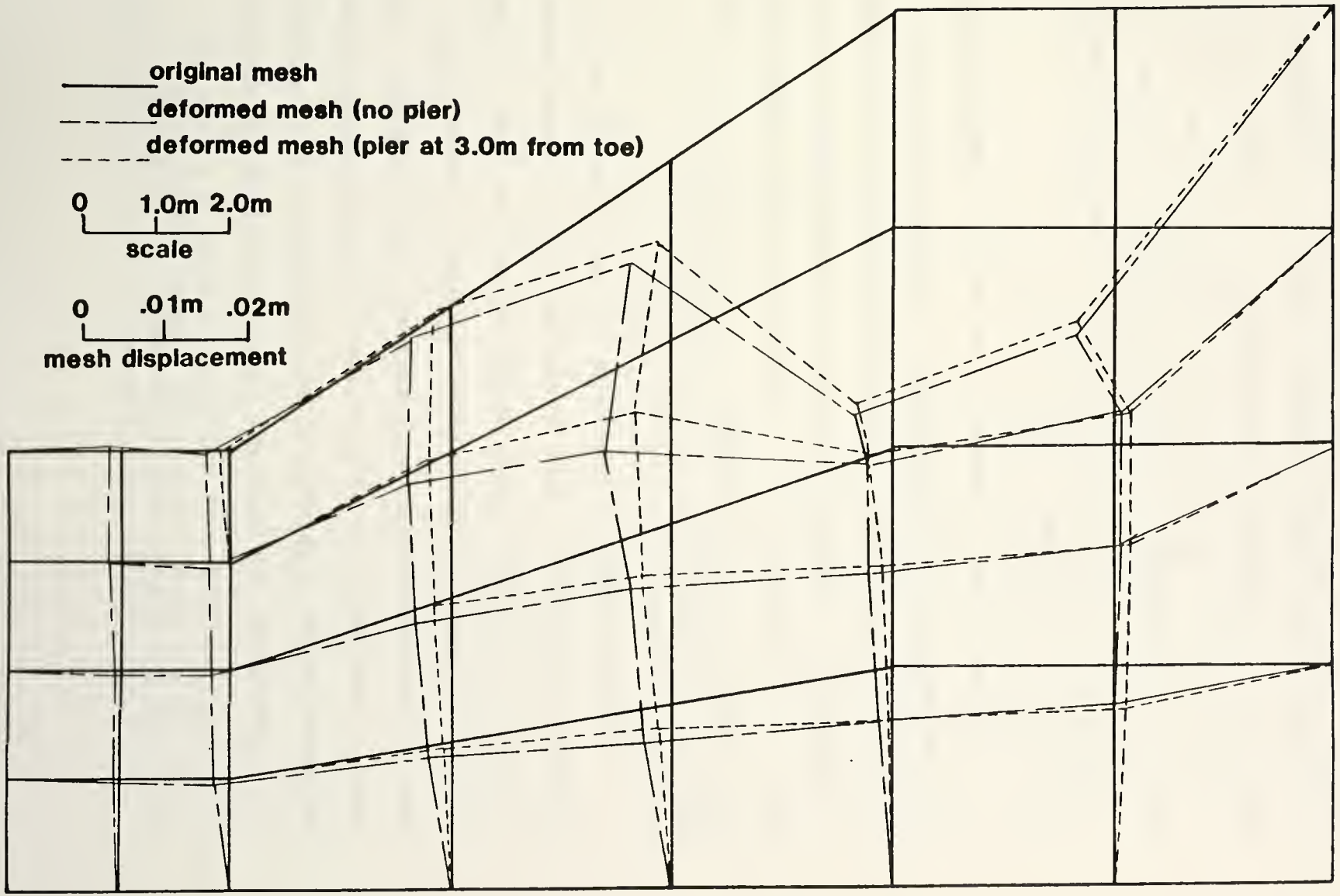

Figure A.4: Displacement at Center Plane between Piers

vertical direction. In the region of largest displacements the reduction in movement was less than 40 percent. As expected the largest movement reduction occurs next to the pier. The horizontal displacements obtained at 12 m from the toe are larger for the stabilized slope. This is due to the proximity of the fixed boundary. Further parametric studies will be necessary to determine how far the finite element mesh should extend.

The reduction in shear stress was also determined for each element along the cross-section between the piers. The reduction in shear stress was of the order of 80 percent for the elements located below the pier and 30 percent for the elements located above the pier. There is a very close correlation between the reduction in displacement and the reduction in shear stress.

In this example, the effect of the piers on the amount of movement is more significant for elements below than above the pier. This tends to indicate that the most effective design would require the piers to be near the top of the slope where the movements are largest for the case of loading at the top of the slope. The examine the influence of the position of the piers, two other cases are considered, one with the piers located at the toe to the slope, and one with the piers located 6 m from the toe. The horizontal surface movement at the center line

between the piers are given in figure A.5 for these two cases, together with the movements obtained in the previous case (piers at 3 m from the toe) and for the non-stabilized slope. For all three cases of stabilization the horizontal movements are reduced but the most efficient pier position is near the top of the slope, where the soil movements are the largest. Broms (1972) found that for distressed slopes, piers placed near the bottom were most effective. In his example however, the toe of the slope was the point of maximum soil movement. The results of the present study agree with Broms conclusion that the piers should be placed at the point of maximum soil movement.

As the spacing between piers is decreasing, the piers act more as a continuous barrier and the effect of soil arching becomes more significant and reduces the soil movements, especially below the pier. In figure A.6 the slope movements computed for a pier spacing of 3.9 m are compared to the movements obtained in the previous case (6.0 m center to center spacing). The displacements below the pier are reduced by about 50 percent, while the reduction above the piers are not significant. Similar results were found by Ito and Matsui (1975).

The piers placed near the top of the slope are the most efficient for the present case, despite the piers

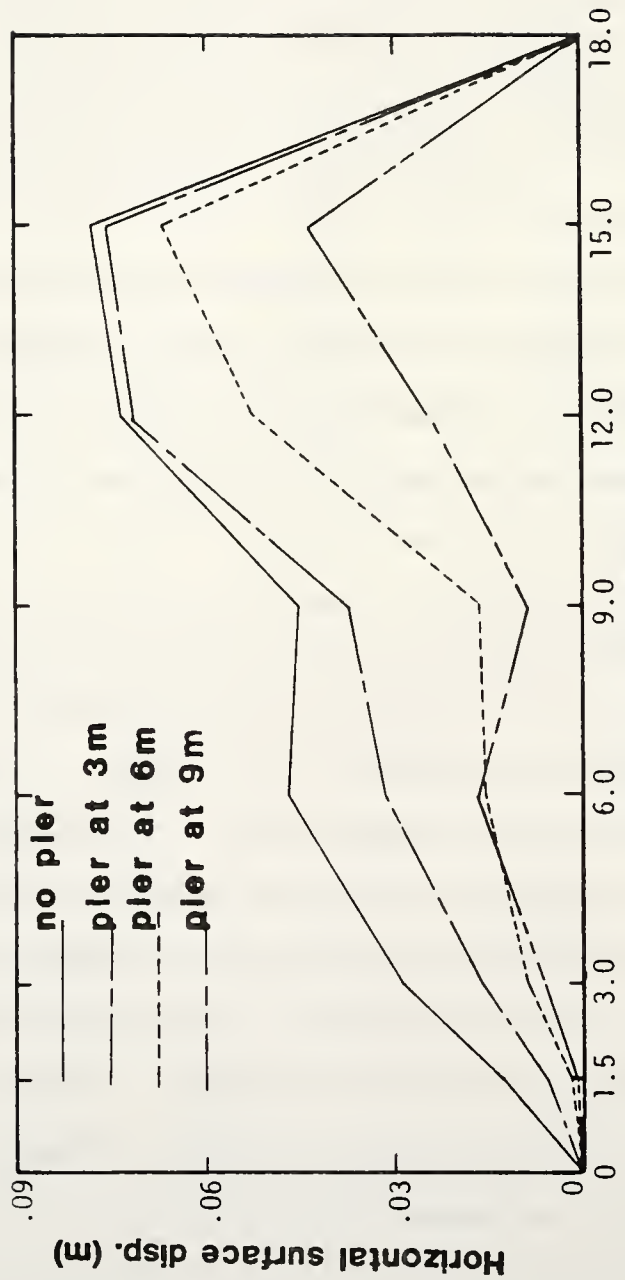

Figure A.5: Effect of Pier Position

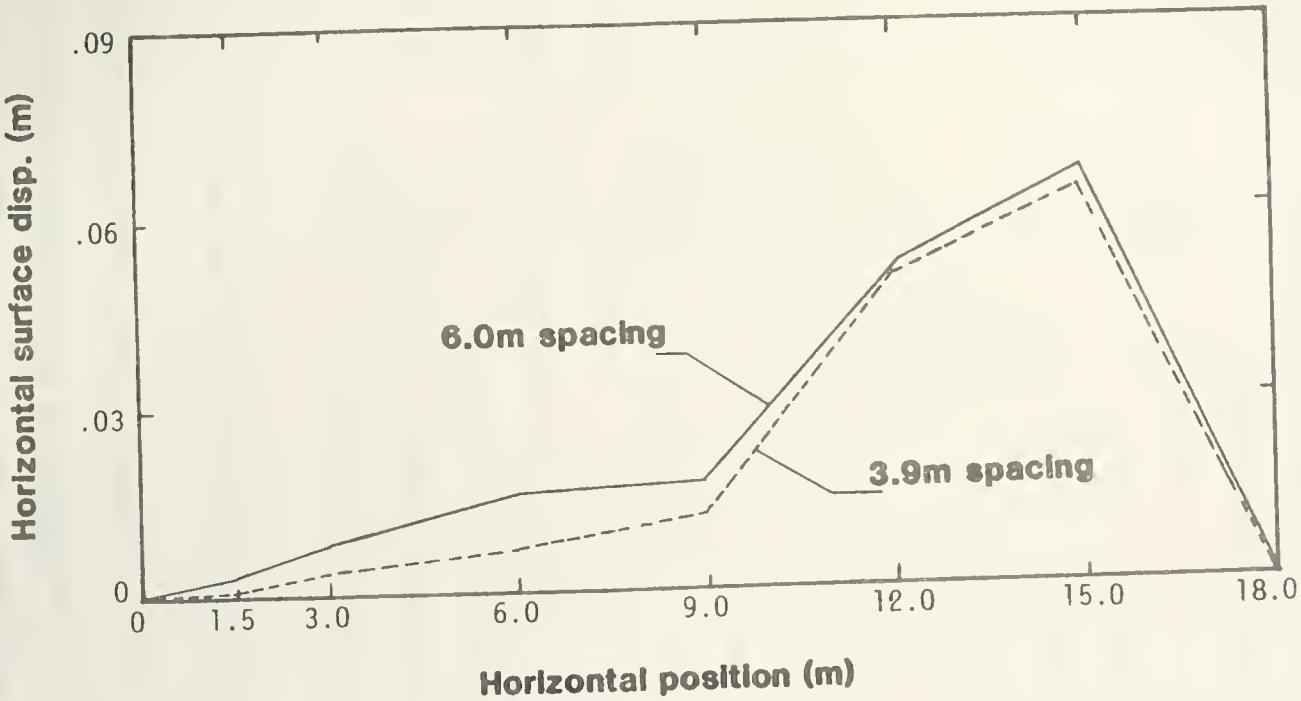

Figure A.6: Effect of Pier Spacing

larger flexibility due to their increased length. However, previous work by Rowe and Poulos (1979), showed that the stiffness of the piers has a significant effect on the soil movement. To evaluate the effect of pier stiffness, the previous cases were analyzed with completely rigid piers. Figure A.7 shows the horizontal surface movements along the center line between the piers for flexible and rigid piers at 3 m from the toe. The results from the other two cases were similar. In the case of rigid piers, the active pressure condition is not realized on the downslope face of the pier and the only soil movements below the pier are due to soil "flowing" around the pier. Consequently, the reduction in soil movement is more important for rigid piers than for flexible piers. However, the forces acting on the rigid piers are significantly increased, which may cause problems for the structural design of the piers. For the case studied, the effect of pier stiffness is not very significant and more parametric studies will be needed to define under which circumstances the stiffness of the piers or its ratio to the soil stiffness is an important parameter.

Present Limitations and Further Developments

Although the proposed three-dimensional finite element program is more general than conventional two-dimensional solutions, it is still limited by the

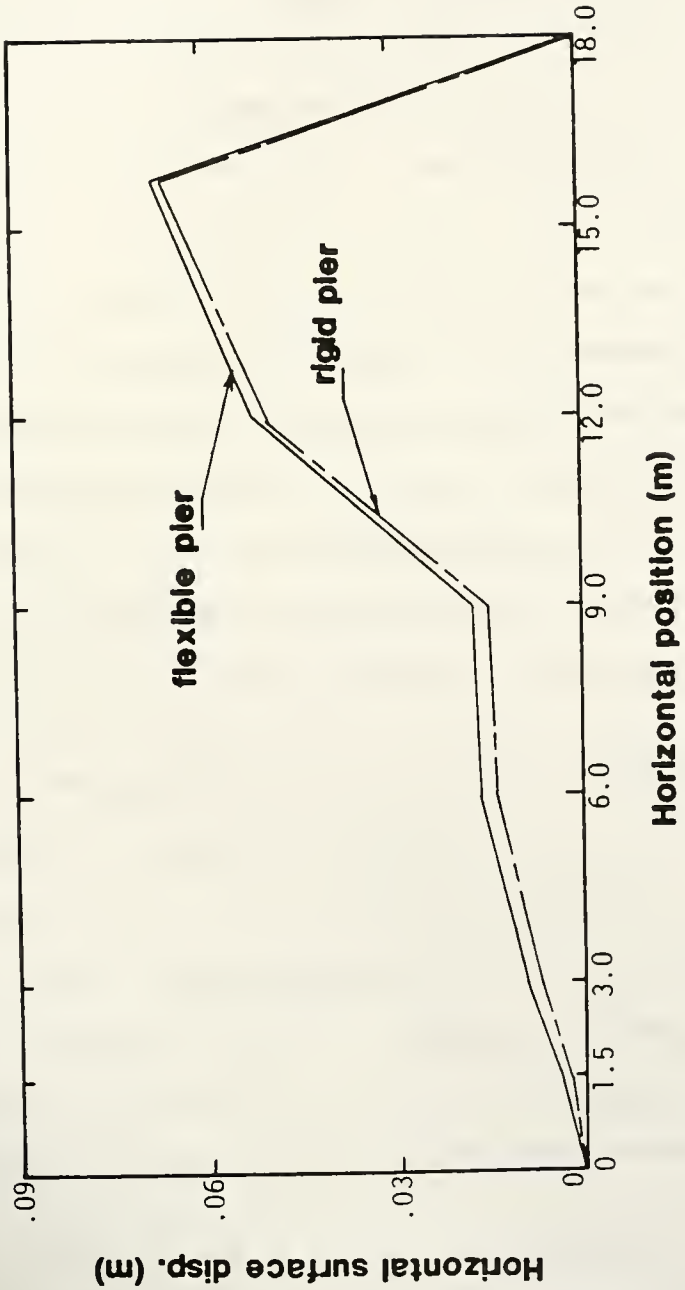

Figure A.7: Effect of Pier Stiffness

assumptions made regarding the boundary conditions, the geometry of the piers, the soil-pier interface and the soil model.

In the previous example, the nodes along all boundaries, except the lines of symmetry, were fixed. The boundaries limited the size of the problem and forced the nodes along the slope to displace downward rather than be pulled back towards the top. This was a good assumption for the boundary left of the toe because the amount of deformation was very limited for the elements located in this area. However, the elements at the upper boundary were distorted unrealistically as a result of this assumption. To model actual situations, more elements must be added to the upper portion and the optimum location of the fixed boundary must be determined or different boundary conditions (frictional boundary) have to be investigated.

In its present form, the 8 node spar elements used to model the piers is not sufficient because it limits the analysis to rectangular or square piers. The results can only be applied to the more conventional circular piers in a qualitative manner. Higher order interpolation functions will be introduced in the soil and pier elements to accommodate curved surfaces and model circular piers.

Relative displacements occur at the interface between soil and pier and play an important role in the soil-pier

interaction. The interface behavior will be represented using slip elements (Desai and Christian, 1977). Three-dimensional slip elements will be necessary to model the interface between the soil and the circular piers. The properties of the slip element depend on the roughness of the piers and the soil characteristics and can be determined from interface direct shear tests.

Conclusion

The effect of piles and piers upon slope deformation and stability is analyzed with a three-dimensional finite element program. The loads on the slope are applied incrementally and an iteration technique is used within each increment to model the soil-pier interaction. This technique can evaluate the effects of pier position, size, spacing and stiffness on the amount of slope movement. The piers can significantly reduce the movements, especially below the piers. The maximum pier efficiency is obtained by placing the piers where the largest movements are expected. Further improvements of this program are planned to release some of the assumptions made regarding the boundary conditions, the geometry of the piers, the soil-pier interface and the soil model.

References

1. Andrews and Klasell (1964), "Cylinder Pile Retaining Wall," Highway Research Record, No. 56, Highway Research Board, pp. 83-97.

2. Broms, B. B. (1972), "Stability of Flexible Structures (Piles and Pile Groups): General Report", Proceedings, 5th Europ. Conf. on Soil Mech. and Found. Eng., Vol. 2, Madrid, pp. 239-269.

3. Bulley, W. A. (1965), "Cylinder Pile Retaining Wall Construction - Seattle Freeway," Roads and Streets Conference, Seattle.

4. Davisson, M. T., (1970) "Lateral Load Capacity of Piles", Highway Research Record, No. 333, Highway Research Board, pp 104 -112.

5. Davisson, M. T. and Gill, H. L. (1963) "Field Testing and Analysis of Laterally Loaded Piers in Stiff Clay", J. of Soil Mech. Found. Div., ASCE, Vol. 89, No. SM3, May, pp. 63-94.

6. De Beer, E. E. and Wallays, M. (1972), "Forces Induced in Piles by Unsymmetrical Surcharges on the Soil Around the Pile", Proceedings, 5th Europ. Conf. on Soil Mech. and Found. Eng., Vol. 1, Madrid, pp. 325-332.

7. Desai, C. S. and Christian, J. T. (1977), Numerical Methods in Geotechnical Engineering, McGraw-Hill Book Co., New York, 781 pp.

8. Duncan, J. M., and Chang, C. Y. (1970), "Nonlinear Analysis of Stress and Strain in Soils," J. of Soil Mech. Found. Div., ASCE, Vol. 196, No. SM5, May, pp. 1629-1653.

9. Goughnour and DiMaggio (1978), "Soil Reinforcement Methods on Highway Projects," Proceedings, Symposium on Earth Reinforcement, American Society of Civil Engineers Annual Convention, Pittsburgh, Pennsylvania, April, pp. 371-399.

10. Gould, J. D. (1970), "Lateral Pressures on Rigid Permanent Structures," Proceedings, Conference on Lateral Stresses in the Ground and Design of Earth Retaining Structures, Cornell University Press, Ithaca, pp. 219-269.

11. Ito, T. and Matsui, T. (1975), "Discussion: Methods to Estimate Lateral Force Acting on Stabilizing Piles," Soils and Foundations, JMSSFE, Vol. 19, No. 4, Dec, pp. 43-57.

12. Ito, T., Matsui, T., and Hong, W. P. (1981) "Design Method for Stabilizing Piles Against Landslide - One Row of Piles", Soils and Foundations, JMSSFE, Vol. 21, No. 1, March, pp. 21-37.

13. Ito, T., Matsui, T., and Hong, W. P. (1979) "Design Method for the Stability Analysis of the Slope with Landing Pier", Soils and Foundations, JMSSFE, Vol. 19, No. 4, Dec. pp. 43-57.

14. Merriam, R. (1960), "Portuguese Bend Landslide, Palos Verdes Hills, California," Journal of Geology, Vol. 68, No. 2, March, pp. 140-153.

15. Oakland, M. W. and Chameau, J. A. (1984), "Finite-Element Analysis of Drilled Piers Used for Slope Stabilization," Laterally Loaded Deep Foundations: Analysis and Performance, ASTM Special Technical Publication No. 835, Kansas City, Mo., June, pp. 182-193.

16. Offenberger (1981), "Hillside Stabilization With Concrete Cylinder Pile Pile Retaining Wall," Public Works, September, pp. 82-86.

17. Poulos, H. G. (1973), "Analysis of Piles in Soil Undergoing Lateral Movement," J. of Soil Mech. Found. Div., ASCE, Vol. 99, SM5, May, pp. 391-406.

18. Poulos, H. G. (1971), "Behavior of Laterally Loaded Piles: II - Pier Groups", J. of Soil Mech. Found. Div., ASCE, Vol. 97, No. SM5, May, pp. 733-751.

19. Poulos, H. G. and Davis, E. H. (1980), Pile Foundation Analysis and Design, John Wiley and Sons, Inc., New York, 397 pp.

20. Reese, L. C. and Allen, J. D. (1977), "Drilled Shaft Design and Construction Guidelines Manual, Volume Two, Structural Analysis and Design for Lateral Loading", U.S. Dept. of Transportation, Fed. Highway Adm., Implementation Package 77-21, July, 360 pp.

21. Reese, L. C. and Cox, W. R., and Koop, F. D. (1975), "Field Testing and Analysis of Laterally Loaded Piles in Stiff Clay", Proc. 7th Annual Offshore Technology Conf., Vol. 2, Houston, Tex., pp. 672-690.

22. Rowe, R. K. and Poulos, H. G. (1979), "A Method For Predicting the Effect of Piles on Slope Behavior," Proceedings, 3rd International Conference on Numerical Methods in Geomechanics, Vol 3, Aachen, April, pp 1073-1085.

23. Rowe, R. K., Booker, J. R., and Balaam, N. P. (1978), "Application of the Initial Stress Method to Soil Structure Interaction", Intl. J. Num. Methods in Eng., Vol. 12, No. 5, pp. 873-880.

24. Taniguchi, T. (1967), "Landslides in Reservoirs," Proceedings of the 3rd Asian Regional Conference on Soil Mechanics and Foundation Engineering, Vol. 1, Southeast Asian Society of Soil Engineering, Bankok, Thailand, pp. 258-261.

COVER DESIGN BY ALDO GIORGINI